



HAL
open science

Plasticité, métaplasticité synaptique et neuronale dans le cortex somatosensoriel primaire chez le rat dans un modèle de douleur inflammatoire prolongée

Hien Luong Nguyen

► **To cite this version:**

Hien Luong Nguyen. Plasticité, métaplasticité synaptique et neuronale dans le cortex somatosensoriel primaire chez le rat dans un modèle de douleur inflammatoire prolongée. Santé. Université Clermont Auvergne [2017-2020], 2018. Français. NNT : 2018CLFAS027 . tel-02885400

HAL Id: tel-02885400

<https://theses.hal.science/tel-02885400>

Submitted on 30 Jun 2020

HAL is a multi-disciplinary open access archive for the deposit and dissemination of scientific research documents, whether they are published or not. The documents may come from teaching and research institutions in France or abroad, or from public or private research centers.

L'archive ouverte pluridisciplinaire **HAL**, est destinée au dépôt et à la diffusion de documents scientifiques de niveau recherche, publiés ou non, émanant des établissements d'enseignement et de recherche français ou étrangers, des laboratoires publics ou privés.

UNIVERSITE CLERMONT AUVERGNE

École doctorale des Sciences de la Vie, Santé, Agronomie, Environnement

THESE

pour le

DOCTORAT D'UNIVERSITE

Spécialité : Neurosciences

Soutenue publiquement le 14 Décembre 2018 par

NGUYEN Hien Luong

**Plasticité, metaplasticité synaptique et
neuronale dans le cortex somatosensoriel
primaire chez le rat dans un modèle de douleur
inflammatoire prolongée**

Membres du Jury

Jean-Christophe PONCER	DR, INSERM UMR-S 839, Paris	Rapporteur
Sylvia SOARES	MCU, Université de Paris 6	Rapporteur
Ipek YALCIN	CR, CNRS UPR 3212, Strasbourg	Rapporteur
Alain ARTOLA	PU, Université Clermont Auvergne	Directeur

A ma famille

La thèse, ça change ma vie !

REMERCIEMENTS

*En premier lieu, permettez-moi, chers Maîtres et membres du jury, de vous adresser ma sincère gratitude ; **Monsieur Jean-Christophe PONCER, Madame Sylvia SOARES et Madame Ipek YALCIN** d'avoir accepté d'apprécier mon travail me touche profondément.*

*Par la suite, je souhaiterais exprimer mes sentiments de reconnaissance envers notre directeur de laboratoire, **Pr Radouhane Dallel**. Je remercie particulièrement la confiance qu'il a porté envers moi et je suis consciente du risque qu'il a pu prendre en ayant accepté ma candidature alors que je n'avais aucune connaissance dans ce domaine.*

*Je voudrais également mentionner mon directeur de thèse, **Pr Alain Artola** sans qui ma thèse n'aurait aucune valeur et surtout sans qui je ne pourrais en arriver là. Vous m'avez guidée durant ces 3 longues et laborieuses années, avec une telle patience et persévérance que nul autre au monde n'en ferait preuve. Nous étions partis de zéro, sans même aucune compétence de ma part dans la matière ; pourtant, vous étiez toujours serein et déterminé et ne m'avez jamais abandonnée, même dans les périodes les plus difficiles, où j'étais dans l'angoisse et le désespoir total. Votre accompagnement et votre enseignement ont été pour moi non pas venant d'un professeur, mais d'un véritable mentor. Le travail n'en fût pas moins mental que technique. L'aventure se termine désormais mais je ne l'oublierai jamais.*

*Je remercie **Myriam** qui a joué un rôle déterminant dans ma montée en compétence en matière d'allocution. Nous savons tous que le travail d'un scientifique ne se restreint pas uniquement aux résultats qu'il parvient à décortiquer derrière la porte d'un laboratoire. En effet, le fruit de ses recherches doit se manifester à l'oral, donc au travers de séminaires, conférences et diverses soutenances. Et pour ce faire, Myriam a toujours été là pour affiner mon talent d'orateur.*

***Amélie, Karine**, vous avez sans doute été le duo de sages qui m'ont confié la clé d'accès à la toute première porte de ma thèse. Mon support de travail indispensable reste, comme pour la grande majorité de nos collègues, nos petits rats. Et dès les premiers jours, **Amélie**, tu m'as soigneusement montré la bonne pratique à adopter envers nos amis les rongeurs ; quant à toi **Karine**, tu m'as transmis tout le savoir-faire sur l'injection de substance ; et tout ceci m'a permis de faire passer mes résultats d'analyse, qui était au départ très prometteurs, en des données exceptionnelles.*

***Anne-Marie**, que dire de plus. Je ne suis sans doute que la simple doctorante n+1 qui vient s'ajouter à la liste des gens que tu vois arriver puis partir avec un mot de remerciement. Mais sache que pour moi, tu resteras THE secrétaire de notre laboratoire ; une Anne-Marie irremplaçable pour l'administratif certes mais surtout une Anne-Marie souriante, qui n'a jamais dit non à qui que ce soit et qui a toujours été présente pour nous soutenir dans toutes nos épreuves. Ton dévouement pour chacun d'entre nous est trop immense pour que l'on puisse se contenter d'un simple Merci ; il faudrait en faire un roman.*

***Cristina**, je voulais te remercier pour le temps que tu m'as accordée malgré ton planning chargé. Sans toi, ma thèse sera inachevée ; mes résultats déjà acquis au préalable resteraient en quelque sorte des corps sans âme. Et c'est ton expertise qui m'a permis d'aboutir à ce dénouement si ambitieux. De plus, on ne peut pas parler de toi sans évoquer ton leadership au laboratoire. Toutes ces soirées, ces événements qui ont contribué à la cohésion d'équipe, tu as joué un rôle primordial.*

***Philippe, Cédric, Lénaïc, François, Elric, Céline, Christelle, Jean-Louis**, nous n'avons pas eu l'occasion de travailler ensemble et je le regrette tout autant que vous. Votre gentillesse et votre sympathie que je ressens à chaque bonjour, à chaque conversation que nous avons pu entretenir en disent longuement sur votre agréabilité professionnelle. Et je suis sûre que les personnes qui ont la chance de travailler avec vous ressentent davantage de plaisir à venir au labo chaque matin.*

Marine, Sarah, nous y sommes donc. Pour commencer, un grand MERCI avec un énorme CALIN. Au-delà de simples collègues doctorantes, vous êtes d'incroyables copines de bureau, sans doute les meilleures que l'on puisse connaître. Cette thèse a pour moi été un véritable ascenseur émotionnel comme vous le savez et sans votre énergie et votre folie (je parle de façon positive bien entendu), j'aurais pu sombrer et tout arrêter. Nous nous sommes tellement amusées que le fardeau semblait parfois tellement léger ; je me suis tellement bien relâchées grâce à votre présence ; j'ai pu à plusieurs reprises m'échapper de mes prises de têtes grâce à nos potinages. Bref, si la thèse a duré 3 longues années, alors la collocation au bureau quant à elle, c'est passé tellement vite en votre compagnie. Je voulais donc vous dire merci encore une fois pour m'avoir supportée, soutenue et m'avoir fait rire. Maintenant, il ne me reste plus qu'à vous souhaiter à chacune de vous deux : bon courage, vous êtes sur la dernière ligne droite.

Je remercie également mon mari Hoang qui a su non pas me soutenir mais supporter mes caprices dans les moments les plus difficiles, où j'étais sur le point de sombrer. Ton aide n'a pas été que sentimental, il a aussi été très technique. En effet, c'est grâce à toi que j'ai pu me débloquent des dettes techniques qui contrariaient l'avancée de mes travaux en termes d'analyse des données. Ta petite application développée en une nuit a su faire renaître la lumière en moi, là où tous les autres outils me menaient vers l'obscurité. Merci également d'avoir été mon chauffeur en horaire imprévisible, surtout pendant la fin de thèse.

LISTE DES ABREVIATIONS

ACC :	Anterior Cingulate Cortex
AMPA :	α -amino-3-hydroxy-5-methyl-4-isoxazolepropionic acid
CFA :	Complete Freund's Adjuvant
CGRP :	calcitonin gene-related peptide
DLPFC :	cortex prefrontal dorsolateral
ERK1/2:	extracellular signal-regulated signal
fMRI :	functional magnetic resonance imaging
GDNF:	glial-cell derived neurotrophic factor
IASP:	International Association for Study of Pain
II _i :	couche II interne
II _e :	couche II externe
LTD:	long-term depression / dépression à long-terme
LTP:	long-term potentiation / potentialisation à long-terme
NGF :	nerve growth factor
NMDA:	N-methyl-D-aspartate
PET:	positron emission tomography
PKA:	protein kinase A
PFC:	cortex préfrontale
PKC γ :	protein kinase C γ
PKM ζ :	protein kinase M zeta
PM:	pain matrix
PPR :	paire pulse ratio

S1:	cortex somatosensorielles primaire
S2 :	cortex somatosensorielles secondaire
SP :	substance P
Sp5C :	sous-noyau caudal ou caudalis
Sp5O :	sous-noyau oral ou oralis
STP :	short-term potentiation
TrkA:	Récepteur tyrosine-kinase A
TrkB:	Récepteur tyrosine-kinase B
TRPV1 :	transient receptor potential vanilloïd1, receptor potential vanilloïd 1
VGLUT3 :	vesicular glutamate transporter type 3

TABLE DES MATIERES

INTRODUCTION GENERALE.....	12
1. LA DOULEUR, PLUSIEURS COMPOSANTES.....	13
2. LES DOULEURS.....	14
2.1. Les douleurs, leurs origines.....	14
<i>2.1.1. Douleurs « adaptées ».....</i>	<i>15</i>
<i>2.1.2. Douleurs « inadaptées ».....</i>	<i>15</i>
<i>2.1.3. Douleurs inflammatoires.....</i>	<i>15</i>
<i>2.1.4. Douleurs neuropathiques.....</i>	<i>16</i>
<i>2.1.5. Douleurs dysfonctionnelles ou idiopathiques.....</i>	<i>16</i>
2.2. Douleurs aiguës, douleurs chroniques.....	17
<i>2.2.1. Douleurs aiguës.....</i>	<i>17</i>
<i>2.2.2. Douleur chroniques.....</i>	<i>17</i>
3. LE SYSTEME TRIGEMINAL.....	18
3.1. Le système trigéminal périphérique.....	18
<i>3.1.1. Territoires d'innervation.....</i>	<i>18</i>
<i>3.1.2. Les fibres afférentes primaires.....</i>	<i>19</i>
<i>3.1.3. Les fibres afférentes primaires méningées.....</i>	<i>20</i>
3.2. Le complexe sensitif du trijumeau.....	20
<i>3.2.1. Organisation et afférences primaires.....</i>	<i>20</i>
<i>3.2.2. Rôle fonctionnel.....</i>	<i>21</i>
<i>3.2.3. Communication intratrigéminal.....</i>	<i>22</i>
3.3. Particularités du système trigéminal.....	23
3.4. Le sous-noyau caudal.....	25

3.4.1. Terminaisons centrales des afférences primaires	25
4. VOIES TRIGEMINALE ASCENDANTES.....	27
5. LA ‘PAIN MATRIX’.....	28
5.1. Thalamus.....	29
5.2. Anterior Cingulate Cortex (ACC)	30
5.3. Insula.....	32
5.4. Cortex somatosensoriels primaire (S1) et secondaire (S2).....	33
5.4.1. <i>Cortex somatosensoriel primaire (S1).....</i>	33
5.5. Cortex Préfrontal.....	34
5.6. Plusieurs cortex frontaux.....	35
5.7. Cervelet.....	35
6. DOULEURS CHRONIQUES ET PLASTICITE CORTICALE.....	35
6.1. Plasticité synaptique associée à la douleur dans le cortex cingulaire anté- rieur.....	36
6.2. Plasticités associées à la douleur dans le ‘Pain matrix’.....	38
6.2.1. <i>Thalamus.....</i>	38
6.2.2. <i>Amygdale.....</i>	39
6.2.3. <i>Cortex insulaire.....</i>	39
6.2.4. <i>Cortex préfrontal.....</i>	39
6.2.5. <i>Cortex somatosensoriel S1 et S2.....</i>	39
CHAPITRE 1.....	41
SYNAPTIC AND INTRINSIC PLASTICITIES AND METAPLASTICITIES AT VERTICAL INPUTS ONTO LAYER 2/3 PYRAMIDAL CELLS IN THE RAT PRIMARY SOMATOSENSORY CORTEX	

CHAPITRE 2.....	97
INFLAMMATORY PAIN-INDUCED NEURONAL PLASTICITIES AND METAPLASTICITIES IN SUPERFICIAL LAYERS ON THE RAT PRIMARY SOMATOSENSORY CORTEX	
CHAPITRE 3.....	144
RAPID DENDRITIC REMODELING IN THE RAT ADULT SOMATOSENSORY CORTEX FOLLOWING PERIPHERAL INFLAMMATION AND ITS ASSOCIATION WITH INFLAMMATORY PAIN	
CONCLUSION.....	157
REFERENCES.....	162
RESUME	

LISTE DES FIGURES

INTRODUCTION GENERALE

- Figure 1. Territoires cutanés innervés par le nerf trijumeau
- Figure 2. Organisation du complexe sensitif du trijumeau et ses connexions
- Figure 3. Communication intratrigéminal : organisation du sous-noyau spinal
- Figure 4. Diversité des tissus cranio-faciaux innervés par le nerf trijumeau
- Figure 5. Couches de Rexed au niveau C4 de la moelle épinière d'un rat adulte
- Figure 6. Schéma des voies ascendants et des structures subcorticales et corticales
- Figure 7. Models for the insular cortex (In) in pain transmission and chronic pain

CHAPITRE 1

- Figure 1. The level of postsynaptic depolarization determines the sign and magnitude of synaptic plasticity in S1 vertical input-L2/3 pyramidal neuron synapses.....89
- Figure 2. Pairing-induced synaptic plasticity, but not intrinsic plasticity, depends on NMDA receptor activation.....90
- Figure 3. Changes in intrinsic properties after pairing-induced synaptic LTD and LTP in naïve conditions.....91
- Figure 4. Changes in intrinsic properties and in synaptic strength are not correlated.....92
- Figure 5. Synaptic plasticity rule in potentiated conditions.....93
- Figure 6. Synaptic plasticity rule in depressed conditions.....94
- Figure 7. Intrinsic plasticity rule in potentiated conditions.....95
- Figure 8. Intrinsic plasticity rule in depressed conditions.....96

CHAPITRE 2

- Figure 1. Experimental design and behavioral testing.....136
- Figure 2. Facial inflammation is associated with LTP of synaptic transmission in superficial layers of the somatosensory cortex (S1).....137
- Figure 3. LTP of synaptic transmission in superficial layers of the somatosensory cortex (S1) is stable over the first 3 days after pain onset.....138

Figure 4. Voltage-response curves for the induction of synaptic LTD/LTP in CFA- and NaCl-injected rats, 1 hour after injection.....	139
Figure 5. Voltage-response curves for the induction of synaptic LTD/LTP in CFA- and NaCl-injected rats, 3 days after injection.....	140
Figure 6. Time course of synaptic metaplasticity decay.....	141
Figure 7. Facial inflammation is associated with LTP of the intrinsic excitability of L2/3 pyramidal neurons within the somatosensory cortex (S1).....	142
Figure 8. LTP of intrinsic excitability of S1 L2/3 pyramidal neurons is stable over the first 3 days after pain onset.....	143

CHAPITRE 3

Figure 1. Methodology for morphological analysis.....	153
Figure 2. Morphometric analysis and morphologic classes of S1 L2/3 pyramidal neurons 1 hour and 3 days after CFA injection.....	154
Figure 3. CFA-induced facial inflammation produces reversible structural modifications in vertical S1 L2/3 pyramidal neurons.....	155
Figure 4. The morphological features of control and post-CFA injection day 3 horizontal S1 L2/3 pyramidal neurons are similar.....	156

LISTES DES TABLEAUX

Table 1. Electrophysiological features of S1 L2/3 pyramidal neurons, before and after pairing induction of intrinsic plasticity in naïve conditions	86
Table 2. Electrophysiological features of S1 L2/3 pyramidal neurons, before and after pairing induction of intrinsic plasticity in potentiated conditions	87
Table 3. Electrophysiological features of S1 L2/3 pyramidal neurons, before and after pairing induction of intrinsic plasticity in depressed conditions	88

INTRODUCTION GENERALE

LA DOULEUR est la compagne de toujours de l'Homme dès son origine – pensons à la douleur liée à l'accouchement chez la femme ou celle due aux blessures de guerre chez l'homme. En fait, il n'existe pas une douleur, mais des douleurs.

1. LA DOULEUR, PLUSIEURS COMPOSANTES

Selon l'Association Internationale pour l'Etude de la Douleur (International Association for the Study of Pain, IASP), la douleur est une « *expérience sensorielle et émotionnelle désagréable associée à un dommage corporel réel ou potentiel ou bien décrite en de tels termes* ». Ainsi on distingue plusieurs composantes à la douleur : (i) une composante sensorielle ou sensorio-discriminative, consistant en la détection du stimulus et l'analyse de son intensité, (ii) une composante affectivo-émotionnelle exprimant le caractère pénible, déplaisant de la douleur, et (iii) une composante cognitivo-évaluative. En effet, la douleur n'est pas seulement un stimulus mais un ressenti. Qu'un stimulus donné soit perçu comme douloureux ou pas, dépend bien entendu de sa nature mais encore de l'état physiologique, émotionnel, cognitif et de l'expérience du sujet qui reçoit ce stimulus (Merskey et Bogduk, 1994). Douleur et Nociception ne sont pas synonymes.

Ainsi :

- *La nociception*

En 1906, Sherrington développe le concept de stimulus nociceptif (Sherrington, 1906). Ces stimuli, dangereux pour l'intégrité du corps, activent des récepteurs spécifiques : les nocicepteurs. Le terme nociception, introduit par Sherrington au début du siècle dernier, caractérise donc la perception d'un stimulus intense entraînant des réactions de défense afin de sauvegarder l'intégrité de l'organisme. La nociception ne fait pas intervenir de mécanisme conscient.

- *La perception*

Selon le Larousse, il s'agit d'un « *événement cognitif dans lequel un stimulus ou un objet, présent dans l'environnement immédiat d'un individu, lui est représenté dans son activité psychologique interne, en principe de façon consciente* ». La perception douloureuse, elle, fait donc intervenir la cognition, mettant en jeu des fonctions telles que l'attention, l'anticipation ou la mémoire. Stimulus nociceptif et perception douloureuse sont donc dissociés : on peut par exemple, se blesser mais être trop concentré par ailleurs pour le percevoir.

- *La sensation*

Toujours selon le Larousse, c'est un « *état psychologique découlant des impressions reçues et à prédominance affective ou physiologique* ». La sensation douloureuse est ici aussi subjective. Elle peut même être déclenchée par une émotion forte, en l'absence de tout stimulus nociceptif.

- *La réaction*

Cette composante fait intervenir de multiples réactions comportementales : motrices (frottement de la zone douloureuse), verbales (cris) et végétatives (tachycardie, malaise, nausées) ... Chez l'animal, seules ces réactions sont observables. On ne peut que supposer qu'elles expriment la perception de sensations désagréables chez l'animal à la suite de l'activation des nocicepteurs.

2. LES DOULEURS

La douleur aiguë est essentielle à la survie ; elle joue un rôle d'alerte. En fait, il existe plusieurs douleurs en fonction de leur caractère spontané ou provoqué, de leurs caractéristiques : séquence (prolongée, continue, intermittente), durée (douleur aiguë, douleur chronique), qualité (pulsatile, brûlure, piqûre, décharge électrique, crampe), intensité, localisation (localisée, diffuse, projetée).

On distingue les douleurs en fonction (i) de leur origine et (ii) de leur durée, aiguë ou chronique.

2.1. Les douleurs, leurs origines

2.1.1. Douleurs « adaptées »

Adaptées ou nociceptives, ces douleurs sont déclenchées par la stimulation de récepteurs spécifiques au niveau des extrémités périphériques des fibres afférentes primaires nociceptives amyélinisées, de type C, ou peu myélinisées, de type A δ . Ces récepteurs périphériques sont activés par des stimuli mécaniques, thermiques ou chimiques de forte intensité (Woolf et Ma, 2007).

La douleur nociceptive est nécessaire à la survie : elle joue un rôle d'alarme et a valeur d'information. Elle induit des réactions pour en éliminer la cause et éviter, autant que possible, ses conséquences. Cette douleur survient donc en réponse à un stimulus nociceptif et cesse dès que ce stimulus disparaît.

2.1.2. Douleurs « inadaptées »

Elles sont dues à des modifications ou plasticité du système nerveux, périphérique ou central. On distingue trois types de douleurs inadaptées en fonction de leur cause : inflammatoire, neuropathique ou fonctionnelle.

Cependant, quel que soit leurs causes, ces douleurs se caractérisent toutes par des symptômes douloureux identiques : douleurs spontanées et douleurs évoquées, traduisant une hypersensibilité à la douleur : réduction des seuils douloureux, diffusion spatiale et sommation temporelle. Ainsi, cette hypersensibilité douloureuse se manifeste par deux symptômes douloureux : (i) exagération de la sensation douloureuse à un stimulus normalement déjà douloureux, i.e. au-dessus des seuils nociceptifs – c'est l'hyperalgésie – et (ii) sensation douloureuse évoquée par un stimulus normalement non douloureux, i.e. au-dessous des seuils nociceptifs – c'est l'allodynie.

Cette hypersensibilité douloureuse peut non seulement se manifester au niveau de la zone lésée – on parle alors d'hyperalgésie primaire – mais aussi diffuser dans la zone non lésée, autour de la lésion – on parle alors d'hyperalgésie secondaire. A noter ici que le terme hyperalgésie inclue ici à la fois une hyperalgésie et une allodynie.

La sommation temporelle (phénomène de 'wind-up') se caractérise par une augmentation de la sensation douloureuse à la suite d'une stimulation répétée de fréquence 0,3-2 Hz, l'intensité de la stimulation restant constante. Le wind-up traduit une potentialisation de la réponse des neurones nociceptifs non spécifiques de la corne dorsale. A noter que cette potentialisation de la sensation douloureuse/réponse neuronale n'est pas durable : elle disparaît dès que la stimulation s'arrête.

Réduction des seuils douloureux, diffusion spatiale et sommation temporelle traduisent des phénomènes de plasticité sur les voies de la douleur – on parle ici de sensibilisation – périphérique et/ou centrale.

2.1.3. Douleurs inflammatoires

Elles apparaissent en réponse à une lésion tissulaire et à la libération locale des médiateurs de l'inflammation. Ce sont des douleurs par excès de nociception. Elle ne s'agit plus d'informer mais d'adapter le comportement afin de protéger la zone lésée et faciliter sa cicatrisation : cette douleur diminue le risque de contacts, de nouveaux traumatismes, au niveau – hyperalgésie

primaire – et autour de la zone lésée – hyperalgésie secondaire. Si l'hypersensibilité douloureuse primaire peut mettre en jeu des phénomènes de sensibilisation périphérique et/ou centrale, l'hypersensibilité douloureuse secondaire – elle survient en territoire non lésé – ne peut être due qu'à une sensibilisation centrale (Juhl et al., 2008 ; Vardeh et al., 2009).

La douleur inflammatoire régresse normalement avec la disparition du processus inflammatoire sauf dans les cas de maladies inflammatoires chroniques, telle la polyarthrite rhumatoïde où la douleur devient « inadaptée » (Michaud et al., 2007).

2.1.4. Douleurs neuropathiques

Les douleurs neuropathiques sont secondaires à une lésion du système nerveux périphérique ou central.

Elles apparaissent dans le territoire d'innervation correspondant à la lésion. La particularité de ces douleurs est d'être associées à des symptômes sensitifs : positifs (paresthésies, dysesthésies) et/ou déficitaires (diminution ou perte de la sensibilité).

Périphériques, ces douleurs neuropathiques sont secondaires à une lésion mécanique (compression, étirement lors de fractures, envahissement par des tumeurs, section lors de chirurgies), métabolique (diabète), neurotoxique (chimiothérapies : vincristine, taxotère...) ou infectieuses (zona) des fibres nerveuses.

Centrales, elles sont liées à une lésion du système nerveux central : traumatismes de la moelle épinière (para- ou tétraplégique), accidents vasculaires cérébraux, ou pathologies telle que la sclérose en plaque ou la maladie de Parkinson (Dworkin et al., 2003).

2.1.5. Douleurs dysfonctionnelles ou idiopathiques

Ces douleurs idiopathiques sont totalement inadaptées : elles ne jouent aucun rôle, ni informatif, ni protecteur. Elles sont présentes dans des pathologies telles que la fibromyalgie, le syndrome de l'intestin irritable ou migraine. Elles surviennent en l'absence de tout stimulus nociceptif ou de lésion inflammatoire ou nerveuse.

Pourtant, il est maintenant clair que ces douleurs résultent d'un processus pathologique ou dysfonctionnement du système somatosensoriel. Dans les cas de l'intestin irritable et de la fibromyalgie, la douleur pourrait être liée à une amplification des signaux nociceptifs lors de leur traitement par le système nerveux central, notamment dans la corne dorsale suite à un déséquilibre entre contrôles descendants excitateurs et inhibiteurs (Feng et al., 2009).

Comme pour les douleurs précitées, on retrouve réduction des seuils douloureux, diffusion spatiale et sommation temporelle (wind-up : voir ci-dessus).

2.2. Douleurs aiguës, douleurs chroniques

2.2.1. Douleurs aiguës

Les douleurs aiguës sont transitoires. Elles ont un rôle d'alarme : elles protègent l'organisme contre une lésion potentielle, en entraînant une modification comportementale – réaction – de retrait, par exemple, pour éviter la lésion (Woolf et Ma, 2007). Elles régressent une fois le stimulus nociceptif disparu ou la lésion cicatrisée.

2.2.2. Douleur chroniques

La douleur chronique est définie par le IASP comme « *une douleur qui persiste au-delà du délai normal de cicatrisation. En dehors d'une douleur cancéreuse, 3 mois est considéré comme le point de bascule entre la douleur aiguë et la douleur chronique, mais dans le cadre de la recherche un délai supérieur à 6 mois est préféré* ». (Merskey et Bogduk, 1994).

Ces douleurs perdurent après que le stimulus nociceptif a disparu, la cicatrisation est terminée et le traitement symptomatique et étiologique a été bien mené. Elles ont bien évidemment perdu toute valeur protectrice. C'est devenu une '*maladie en soi*', associant douleur chronique avec des manifestations physiques, psychologiques, comportementales et sociales. Ce '*syndrome douloureux*' s'observe dans des situations extrêmement variées : migraines, lombalgies, affections neurologiques et douleurs psychogènes.

Cette distinction douleur aiguë/chronique semble bien artificielle (Von Korff et al., 2008). En fait, douleurs aiguës, persistantes et chroniques constituent un continuum, tant sur le plan physiopathologique que clinique ; et le passage d'une douleur aiguë à un syndrome douloureux chronique peut-être évité par un traitement correct de la douleur aiguë (Juhl et al., 2008).

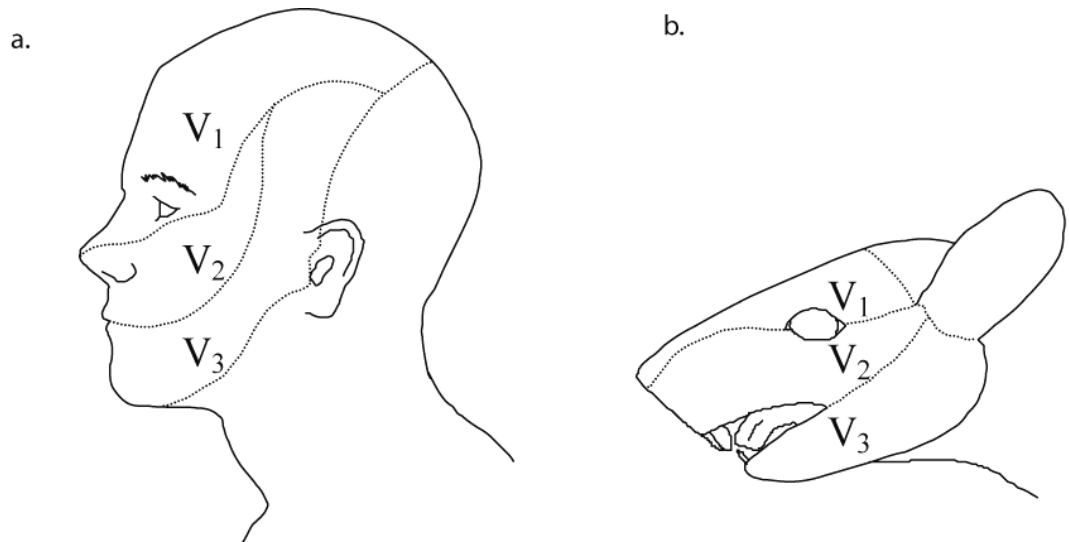


Figure 1 : Territoires cutanés innervés par le nerf trijumeau. Schémas illustrant (a) chez l'homme et (b) chez le rat les territoires cutanés innervés par les trois branches sensibles du nerf trijumeau (V1, ophtalmique, V2, maxillaire et V3, mandibulaire). (D'après Kandel et Schwart, 1985 et Waite et Tracey, 1995).

3. LE SYSTEME TRIGEMINAL

3.1. Le système trigéminal périphérique

3.1.1. Territoires d'innervation

Le nerf trijumeau rejoint le/émerge du tronc cérébral au niveau de la protubérance annulaire par deux racines : sensitive, volumineuse et motrice grêle, innervant les muscles masticateurs, du marteau et tenseur du voile.

La racine sensitive draine l'information périphérique par l'intermédiaire de trois branches (Figure 1) :

- Nerf ophtalmique ou V1 : Il innerve un territoire cutané incluant la partie antérieure de la région temporale, le front, les paupières supérieures, et le dos du nez, et un territoire muqueux incluant les fosses nasales, les sinus éthmoïdal et frontal. Cette branche draine aussi l'information sensitive en provenance de la cornée et des méninges. Ces afférences méningées sont particulièrement importantes dans le contexte de la physiopathologie de la migraine
- Nerf maxillaire ou V2 : Il assure l'innervation sensitive de la partie moyenne de la face : (i) le nerf infra-orbitaire innerve la paupière inférieure, l'aile du nez, la lèvre supérieure et la joue, (ii) le nerf alvéolaire supérieur, les dents et le vestibule maxillaire et (iii) le nerf ptérygopalatin, les muqueuses de l'amygdale, du voile du palais, de la voûte palatine ainsi que celles des sinus maxillaires et des fosses nasales.
- Nerf mandibulaire ou V3 : Il assure l'innervation sensitive du territoire mandibulaire : à la fois une région cutanée temporale, jugale, labiale et mentonnière, la partie antérieure du pavillon de l'oreille et le conduit auditif externe, et une région muqueuse linguale (2/3 antérieur), labiale et vestibulaire mandibulaire. Il innerve aussi les dents mandibulaires et les articulations temporo-mandibulaires.

Il faut noter que d'autres nerfs contribuent à l'innervation sensitive de la tête et du cou : (i) le plexus cervical supérieur (C2) pour le cou, la partie postérieure du crâne et l'angle de la mandibule, (ii) les nerfs facial (VII), glossopharyngien (IX) et vague (X) pour la région cutanée autour du conduit auditif externe et les 2/3 antérieurs de la langue (VII), (iii) le IX pour le 1/3 postérieur de la langue et le pharynx et enfin (iv) le X, pour le larynx, une partie du pharynx et l'épiglotte.

3.1.2. Les fibres afférentes primaires

Les fibres afférentes primaires sont classées selon leur origine périphérique (cutanée, musculaire, articulaire ou viscérale), leur vitesse de conduction (fonction de leur diamètre et du degré de myélinisation), leur modalité sensorielle et leur phénotype neurochimique (expression ou pas de peptides). En fonction de leur vitesse de conduction : on distingue les fibres afférentes primaires :

- de type A β : Elles possèdent une gaine de myéline épaisse (diamètre 6-20 μm) et ont une conduction rapide (30-60 m.s^{-1} chez l'homme). Elles codent et transmettent les informations tactiles et proprioceptives (Koltzenburg & Scadding, 2001). Les fibres A β d'origine cutanée sont connectées à des récepteurs périphériques différenciés, spécifiques d'une modalité tactile: pression, vibration et frottement (Iggo & Andres, 1982).

- de type A δ et C : Elles recueillent les informations nociceptives et thermiques, le prurit et aussi la sensibilité à la pression non douloureuse (Koltzenburg & Scadding, 2001) par l'intermédiaire de terminaisons libres. Les fibres A δ sont recouvertes d'une gaine de myéline fine et ont un diamètre (1-5 μm) et une vitesse de conduction intermédiaires (4-30 m.s^{-1} chez l'homme) entre les fibres A β (ci-dessus) et les fibres, C, dépourvues de myéline, de petit diamètre (0,3-1,5 μm) et, par conséquent, de conduction lente (0,4-2,0 m.s^{-1}).

En fait, il existe plusieurs types de fibres afférentes de type C : en fonction de leur modalité et de leurs caractéristiques neurochimiques. Ainsi, en plus des fibres C répondant aux stimuli mécaniques douloureux et thermiques, il existe des fibres C activées par l'histamine, à l'origine de démangeaisons (Schmelz, 2001; Schmelz et al., 1997; Andrew & Craig, 2001). Ces deux types de fibres C, qui véhiculent douleur et prurit, interagissent entre elles dans la corne dorsale, les premières inhibant la transmission des secondes (Liu et al., 2010; Lagerström et al., 2010). D'autres afférences de type C véhiculent des informations tactiles agréables (Löken et al., 2009), informations ne contribuant pas à la sensibilité tactile épicrotique et aboutissant plutôt aux régions limbiques qu'au cortex somatosensoriel (Craig, 2003). Leur activation provoque une sensation agréable et pourrait expliquer les réponses hormonales et émotionnelles suscitées par les caresses (Olausson et al., 2003; Wessberg et al., 2003; McGlone et al., 2007). Ces afférences expriment spécifiquement le transporteur vésiculaire de type 3 (*vesicular glutamate transporter 3* ou VGLUT3; Seal et al., 2009) Enfin, certaines afférences primaires de type C ne sont actives que dans des conditions pathologiques (inflammation tissulaire) et sont donc normalement silencieuses (Lynn, 1991; R. Schmidt et al., 1995). Elles représentent 10 à 20% de l'ensemble des fibres C (Cervero, 1994).

En fonction de leurs caractéristiques neurochimiques (Snider & McMahon, 1998), on distingue principalement deux sous-populations de fibres C nociceptives.

- « peptidergiques », synthétisant et utilisant des peptides – substance P (SP) et *calcitonin gene related peptide* (CGRP) – comme neurotransmetteur. Elles sont sensibles au *nerve growth factor* (NGF) dont elles expriment le récepteur tyrosine-kinase, TrkA. Enfin, elles portent le récepteur *transient receptor potential vanilloïde 1* (TRPV1), activé à des températures supérieures à 42°C (Caterina et al., 1997).

- « non peptidergiques », n'exprimant pas de neuropeptide, elles se reconnaissent à la présence à leur surface du récepteur à l'isolectine B4. Elles portent également la sous unité P2X3 du récepteur ionotropique de l'ATP et le récepteur tyrosine-kinase, TrkB, spécifique du *glial derived neurotrophic factor* (GDNF).

3.1.3. Les fibres afférentes primaires méningées

Seuls, deux types d'afférences primaires méningées, A δ et C, ont été identifiés en fonction de leur vitesse de conduction (Strassman et al., 1996 ; Schepelmann et al., 1999 ; Burstein et al., 1998 ; Levy & Strassman, 2002 ; Pantelev et al., 2005). Ainsi, la réponse des neurones trigéminaux à la stimulation électrique des méninges comprend le plus souvent deux composantes, correspondant à des fibres ayant des vitesses de conduction dans les gammes A δ (Burstein et al., 1998 : > 2,0 m.s⁻¹; Pantelev et al., 2005: 1,5–3,5 m.s⁻¹) et C (Burstein et al., 1998: 0,5–2,0 m.s⁻¹; Pantelev et al., 2005: 0,5–1 m.s⁻¹). Cependant, il pourrait exister des fibres afférentes méningées beaucoup plus rapides (Strassman et al., 1996 : 11,6 \pm 4,1 m.s⁻¹ ; Levy & Strassman, 2002 : >5 m.s⁻¹) et de gros diamètre (Strassman et al., 2004), à limite supérieure des A δ .

3.2. Le complexe sensitif du trijumeau

3.2.1. Organisation et afférences primaires

Les informations somesthésiques d'origine oro-faciales et méningé (douleur, température, proprioception et tact) font relai dans le complexe sensitif du trijumeau dans le tronc cérébral. Ce complexe va des premiers segments cervicaux jusqu'à l'extrémité caudale du mésencéphale. Il comporte deux noyaux : le noyau principal, rostral (plus spécifiquement dédié aux messages non nociceptifs) et le noyau spinal, caudal. Ce dernier comprend lui-même trois sous-noyaux : dans le sens rostro-caudal, les sous-noyaux oral (Sp5O), interpolaire et caudal (Sp5C) (Figure 2).

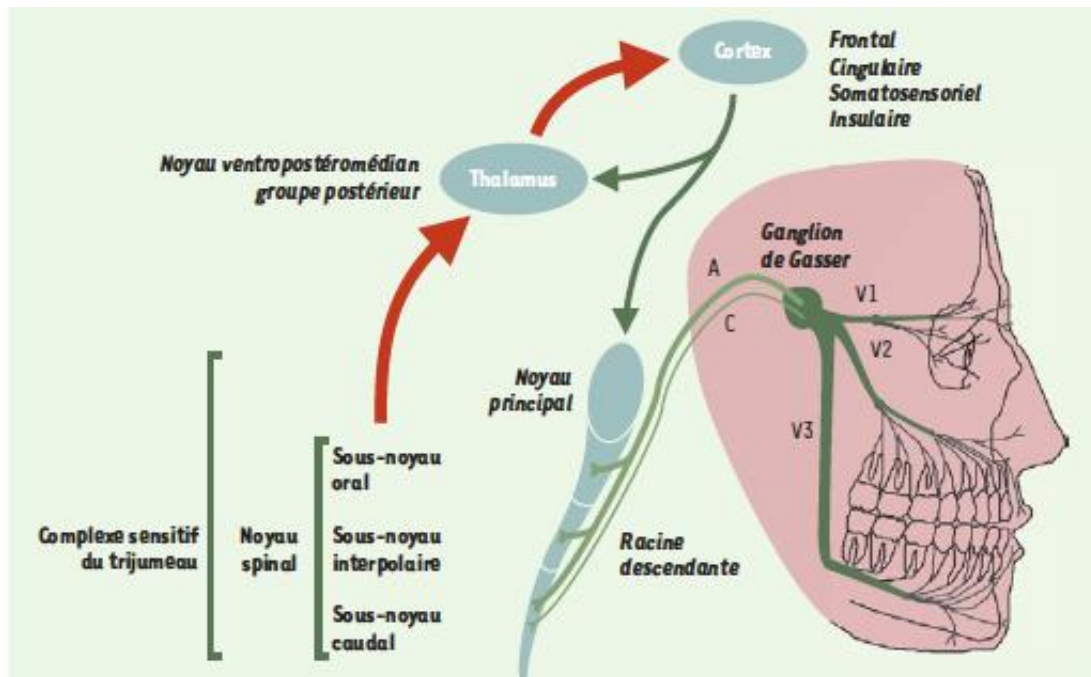


Figure 2 : Organisation du complexe sensitif du trijumeau et ses connexions. Les flèches rouges illustrent les voies ascendantes issues du complexe sensitif du trijumeau ou du thalamus, et les flèches vertes les voies descendantes issues du cortex. A : fibres A ; C : fibres C ; V1 : nerf ophtalmique ; V2 : nerf maxillaire ; V3 : nerf mandibulaire (D'après Dallel, 2003).

Dans le tronc cérébral, les fibres afférentes primaires se divisent en deux branches : l'une, ascendante vers le noyau principal et l'autre descendante. Cette dernière abandonne de nombreuses collatérales dans les différents sous-noyaux du noyau spinal. Les projections des afférences primaires diffèrent en fonction de leur modalité et des tissus qu'elles innervent.

- les afférences cutanées A β se projettent sur l'ensemble du complexe sensitif du trijumeau; les afférences musculaires ou articulaires (groupes I et II) – dont le corps cellulaire est au niveau du ganglion mésencéphalique – aboutissent essentiellement au niveau du noyau principal et du sous-noyau oral (Shigenaga et al., 1988; Capra & Wax, 1989).

- Les afférences A δ d'origine cutanées se terminent sur les trois sous-noyaux du noyau spinal ; celles en provenance des tissus profonds (groupe III) ne se projettent que sur le Sp5C.

- Enfin, toutes les fibres C aboutissent exclusivement au niveau Sp5C (Nishimori et al., 1986).

A noter que le complexe sensitif du V reçoit des afférences d'autres paires de nerfs crâniens (VII, IX et X), ainsi que de nerfs cervicaux supérieurs.

3.2.2. Rôle fonctionnel

On considère le noyau principal et le sous-noyau interpolaire comme les relais de la sensibilité tactile discriminative et de la proprioception. Le Sp5C et le Sp5O sont les relais de la nociception.

En effet, les patients souffrant d'une lésion bulbaire, qui a détruit le noyau spinal mais a préservé la partie rostrale du complexe trigéminal, voient une réduction ou une perte de leur sensibilité thermique et algique mais pas de leur sensibilité tactile (Gérard, 1923). De plus, chez l'homme comme chez l'animal, la section chirurgicale de la racine descendante du trijumeau (tractotomie à l'obex), qui entraîne une déafférentation du seul Sp5C, produit seulement une anesthésie thermo-algique du côté lésé (Gérard, 1923).

Or, une telle tractotomie ne soulage pas les patients souffrant de douleurs spécifiques de la cavité buccale. Seules une section plus rostrale ou la destruction du Sp5O est efficace (Graham et al., 1988). De même, chez le rat, une tractotomie de l'obex n'abolit ni les comportements algiques oraux (Pajot et al., 2000; Dallel et al., 1989), ni la réponse des neurones du thalamus ventrobasal à une stimulation douloureuse oro-faciale (Raboisson et al., 1989). On reconnaît les deux types de neurones nociceptifs – spécifiques et non spécifiques – dans le Sp5O comme dans le Sp5C. En fait, les neurones de type nociceptifs non spécifiques ou à convergence représentent la grande majorité des neurones nociceptifs du SpO : ils sont activés par des stimulations à la fois non-douloureuses tactiles et nociceptives de nature mécanique, thermique,

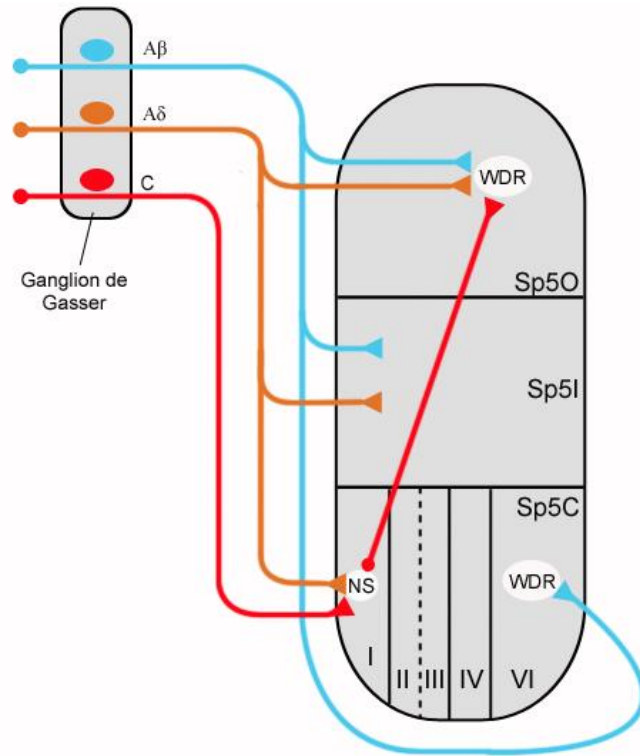


Figure 3 : Communication intratrigéminal : organisation du sous-noyau spinal. Sp5C : sous-noyau caudal ; Sp5I : sous-noyau interpolaire ; Sp5O : sous-noyau oral ; NS : neurone nociceptif spécifique ; WDR : neurone « wide dynamic range »

chimique ou électrique de la région orale ou péri-orale. Ils codent l'intensité des stimulations électriques ou mécaniques (Dallel et al., 1999). De plus, leurs réponses sont facilitées par l'inflammation (Hu et al., 1992), une désafférentation (Hu et al., 1999) ou encore lors du phénomène de wind-up (voir ci-dessus) (Dallel et al., 1999). Les propriétés des neurones à convergence du Sp5O sont semblables à celles des neurones de la couche V de la corne dorsale de la moelle épinière (Besson & Chaouch, 1987), ce qui a conduit à considérer le Sp5O comme l'équivalent fonctionnel d'une couche V spinale (Dallel et al., 1998), dans l'intégration et la transmission des messages douloureux de la région orale. algiques oraux (Pajot et al., 2000; Dallel et al., 1989), ni la réponse des neurones du thalamus ventrobasal à une stimulation douloureuse oro-faciale (Raboisson et al., 1989). On reconnaît les deux types de neurones nociceptifs – spécifiques et non spécifiques – dans le Sp5O comme dans le Sp5C. En fait, les neurones de type nociceptifs non spécifiques ou à convergence représentent la grande majorité des neurones nociceptifs du SpO : ils sont activés par des stimulations à la fois non-douloureuses tactiles et nociceptives de nature mécanique, thermique, chimique ou électrique de la région orale ou péri-orale. Ils codent l'intensité des stimulations électriques ou mécaniques (Dallel et al., 1999). De plus, leurs réponses sont facilitées par l'inflammation (Hu et al., 1992), une désafférentation (Hu et al., 1999) ou encore lors du phénomène de wind-up (voir ci-dessus) (Dallel et al., 1999). Les propriétés des neurones à convergence du Sp5O sont semblables à celles des neurones de la couche V de la corne dorsale de la moelle épinière (Besson & Chaouch, 1987), ce qui a conduit à considérer le Sp5O comme l'équivalent fonctionnel d'une couche V spinale (Dallel et al., 1998), dans l'intégration et la transmission des messages douloureux de la région orale.

3.2.3. Communication intratrigéminal

Les différents noyaux du complexe sensitif du trijumeau ne sont pas isolés les uns des autres mais fortement interconnectés par des voies intratrigéminales ascendantes et descendantes.

Il existe par exemple des connexions ascendantes du Sp5C vers le Sp5O. En effet, les réponses des neurones non nociceptifs du Sp5O sont inhibées par un blocage du Sp5C par le froid ou une tractotomie à l'obex (Sessle & Greenwood, 1976) et, au contraire, facilitées par une micro-injection de strychnine dans le Sp5C (Khayyat et al., 1975). Le Sp5C jouerait donc un rôle facilitateur tonique sur les neurones non nociceptifs du Sp5O. De plus la micro-injection de morphine dans le Sp5C déprime les réponses des neurones à convergence Sp5O à l'activation, spécifiquement, des fibres C (Dallel et al., 1998). Le Sp5C servirait donc aussi de relais pour

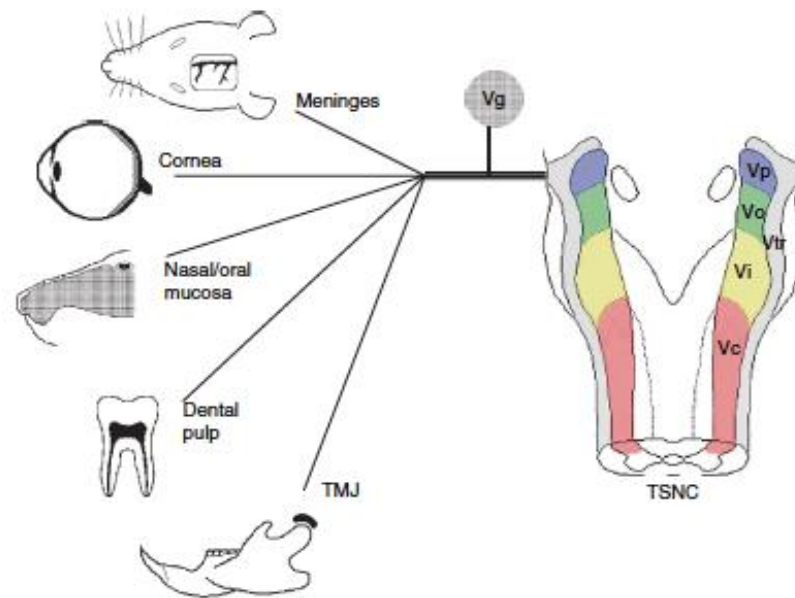


Figure 4 : Diversité des tissus cranio-faciaux innervés par le nerf trijumeau. (Bereiter, 2008).

les informations véhiculées par les fibres C. Par contre, une tractotomie à l'obex n'a pas ou peu d'effet sur la réponse à une stimulation nociceptive, orale ou péri-orale, transmise par fibres afférentes primaires de type A δ , par exemple, la stimulation de la pulpe dentaire (Pajot et al., 2000; Dallel et al., 1989). Ces résultats indiquent que le Sp5O reçoit (i) directement des messages nociceptifs dus à la mise en jeu des fibres A δ et (ii) indirectement des messages dus à la mise en jeu des fibres C via des interneurons des couches superficielles du Sp5C (Woda et al., 2004; Coste et al., 2008).

Une telle redondance de la nociception n'existe pas au niveau spinal. Sa signification cependant demeure inconnue.

3.3. Particularités du système trigéminal

Une première particularité du trijumeau est d'innervé une grande diversité de tissus spécialisés. Il assure l'innervation de tissus aussi différents que la peau, les muqueuses, les méninges, la pulpe dentaire, les articulations temporo-mandibulaires (Figure 4). Certains de ces tissus tels la pulpe dentaire, la cornée ou la dure-mère ne possèdent pas de fibre afférente A β , et toutes stimulations, nociceptives ou non, de ces tissus provoquera une douleur (Feindel et al., 1960; Kenshalo, 1960; Beurman & Tanelian, 1979; Trowbridge et al., 1980). Les afférences sensorielles innervant les muqueuses oculaires, nasales et orales sont très sensibles aux agents chimiques volatiles (Cometto-Muñiz & Cain, 1995). La cornée est le tissu le plus innervé de notre corps (Rózsa & Beurman, 1982) et le seul où les fibres nerveuses pénètrent jusque dans les couches épithéliales externes (Müller et al., 1996) : d'infimes variations de température et d'humidité ou un corps étranger seront ainsi immédiatement détectés à la surface de l'œil. De plus, le trijumeau innerve cette partie unique de notre corps où se concentrent les récepteurs sensoriels ultra-spécialisés de nos cinq sens. Il innerve spécifiquement des récepteurs sensoriels dans les muqueuses buccale (papilles gustatives) et nasale. Le Sp5C est donc un lieu de grande convergence pour des afférences de différents tissus, régions anatomiques et modalités. Cela signifie qu'un même neurone peut être activé indifféremment par des stimuli appliqués sur des tissus éloignés les uns des autres tels que la peau, les muqueuses, la pulpe dentaire, les articulations temporo-mandibulaires, les muscles ou les méninges. Selon Sessle et collaborateurs (Sessle et al., 1993), 70% des neurones enregistrés dans le Sp5C ont un champ récepteur cutané pur, 20% à la fois des champs récepteurs cutanés et profonds et seulement 10% un champ récepteur profond. Il s'ensuit que la majorité des neurones dits « profonds » ont aussi un champ récepteur cutané.

Une seconde particularité est de présenter une proportion de fibres afférentes primaires de type A et C différente de celle des autres nerfs sensitifs. En effet, les fibres C ne représentent que 40% des afférences trigéminales (Lazarov, 2002), mais 70% des afférences spinales (Millan, 1999). De même, la proportion de fibres sympathiques semble bien moindre dans le nerf trijumeau que dans les nerfs spinaux (Hoffmann & Matthews, 1990). Cela pourrait expliquer l'incidence moindre de syndromes douloureux régionaux complexes au niveau cranio-facial que dans les autres parties du corps (Matthews, 1989).

Les corps cellulaires des afférences primaires somatosensorielles trigéminales sont situés dans le ganglion de Gasser et ceux des fibres proprioceptives de gros diamètre, musculaires et articulaires, sont situés dans un autre noyau, le noyau mésencéphalique. Alors que les ganglions de la moelle ne présentent aucune organisation apparente, le ganglion de Gasser et la racine sensitive présentent une somatotopie : les afférences mandibulaires sont en position dorsale alors que les afférences ophtalmiques sont en position ventrale et celles maxillaires entre les deux (Aigner et al., 2000; Arvidsson et al., 1992; Marfurt, 1981).

Les neurones du trijumeau pourraient enfin être particulièrement sensibles aux oestrogènes. En effet, les oestrogènes provoquent dans les neurones trigéminaux une augmentation de l'expression de neuropeptides, tels la prolactine, capables de sensibiliser les réponses neuronales à la capsaïcine ou à la chaleur douloureuse (Diogenes et al., 2006). Lors du test au formol, une injection de formol dans la face chez des rates femelles ovariectomisées provoque une plus grande hyperalgésie que si cette injection est pratiquée au niveau de la patte postérieure (Pajot et al., 2003). Une surexpression des récepteurs oestrogéniques spécifiquement dans le Sp5C suite à l'ovariectomie serait la cause de cette hypersensibilité spécifique de la face. Ces résultats suggèrent que la sensibilité à la douleur spécifiquement au niveau céphalique est modulée par les oestrogènes : d'où, peut-être la différence de prévalence, en fonction du sexe, dans la plupart des douleurs chroniques de l'extrémité céphalique (migraine : 2-4 femmes pour 1 homme (Stewart et al., 1992; Steiner et al., 2003); stomatodynie 3-20 femmes pour 1 homme (Gorsky et al., 1991; Lamey & Lewis, 1989; Tammiala-Salonen et al., 1993). Cependant, il faut noter que la présence comme l'absence d'oestrogènes pourrait augmenter la sensibilité à la douleur céphalique. Ainsi la prévalence de la migraine et des dysfonctions temporo-mandibulaires est plus importante chez les femmes en période pubertaire que chez les femmes ménopausées ou prépubertaires (Stewart et al., 1992; Steiner et al., 2003; Gonçalves et al., 2010). Par contre la plupart des patientes qui présentent une stomatodynie sont ménopausées ou en cours de ménopause (Gorsky et al., 1991).

3.4. Le sous-noyau caudal

Le Sp5C est le seul, dans le complexe sensitif trigéminal, à recevoir l'ensemble des fibres afférentes primaires, de types A β , A δ et C, et notamment les fibres C. Il présente une structure laminaire identique à celle de la corne dorsale de la moelle épinière (Rexed, 1952). Ainsi les cinq couches du Sp5C sont-elles identiques aux couches les plus superficielles, I à V, de la corne dorsale de la moelle épinière.

3.4.1. Terminaisons centrales des afférences primaires

Les modalités sensorielles sont associées à cette structure laminaire. Ainsi, les fibres afférentes primaires d'origine cutanée de type A β , qui transmettent l'information mécanique à bas seuil, se distribuent globalement dans les couches profondes III-V. On a montré chez le rat que des collatérales de ces afférences primaires A β contactent directement des neurones particuliers de la couche II interne (II_i) qui concentrent la sous-unité γ de l'enzyme protéine kinase C (PKC γ ; Hughes et al., 2003; Neumann et al., 2008). Ces neurones jouent un rôle clé dans l'activation du circuit allodymique dans la corne dorsale et donc dans la manifestation de l'allodynie mécanique (Malmberg et al., 1997; Miraucourt et al., 2006; 2007; Peirs et al., 2015; Phan Dang et al., 2016).

Il existe deux types de fibres afférentes primaires A δ . Les premières, ayant un seuil mécanique bas, non nociceptives, innervent les follicules pileux (D-hair afferents) et se projettent dans la partie la plus superficielle de la couche III et de façon extensive dans la couche II interne (Light & Perl, 1979). Les secondes, nociceptives, se distribuent dans les couches I et II externes.

La localisation des terminaisons des fibres afférentes primaires nociceptives de type C est fonction de leur modalité et de leur nature neurochimique (Hunt & Rossi, 1985; Nagy & Hunt, 1982; Hunt & Mantyh, 2001; Julius & Basbaum, 2001; McMahon, 1998). Chez le rat, les fibres C nociceptives peptidergiques se terminent dans les couches I et II externe (II_e), et les fibres C nociceptives non-peptidergiques quasi exclusivement dans la couche II_i (Ribeiro-Da-Silva et al., 1986; Guo et al., 1999; Silverman & Kruger, 1988; Bennett et al., 1998). Les fibres C, exprimant le VGLUT3, sont fonctionnellement des mécanorécepteurs à bas seuil (toucher plaisant, voir ci-dessus), se terminent à la partie ventrale de la couche II_i, là où se concentrent les neurones PKC γ (Seal et al., 2009).

En résumé, les afférences nociceptives cutanées, se terminent dans les couches les plus superficielles (I-II), tandis que afférences qui transmettent l'information tactile, quelques soit

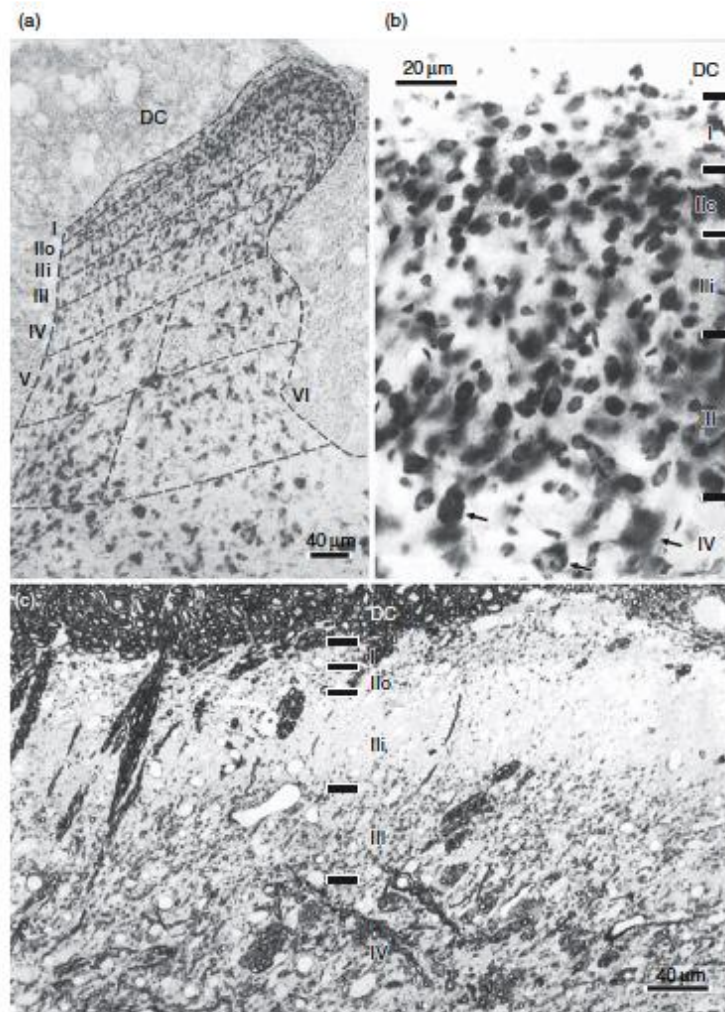


Figure 5 : Couches de Rexed au niveau C4 de la moelle épinière d'un rat adulte. (a) et (b) Coupes microscopiques de 50 μ m d'épaisseur, colorées au bleu de toluidine comme décrit par Rexed (1952) (a) représente l'ensemble de l'organisation laminaire de la corne dorsale. (b) La couche I montre une faible densité de cellules, alors que la couche II externe (II_e) se démarque par un amas de petits neurones, qui la différencie de la couche II interne (II_i). Les couches II_i et II_e ont de nombreux petits neurones de taille relativement uniforme. La présence de quelques neurones légèrement plus larges sépare la couche II_i de la couche III, alors que la couche IV se distingue facilement de la couche III par une plus faible densité de cellules et la présence de quelques larges neurones. (c) représente une coupe microscopique de 2 μ m d'épaisseur de section transversale de corne dorsale de rat au niveau de C4, colorée au bleu de toluidine et Azur II, pour montrer que les couches de Rexed peuvent être identifiées sur coupes et peuvent être utilisées comme référence.

leur nature anatomique, se terminent dans les couches plus profondes (II_i-V), la couche des neurones PKC γ formant la limite entre les terminaisons des afférences ventrales, tactiles, et dorsales, douloureuse et thermique.

D'un point de vue fonctionnel, l'entrée synaptique des fibres nociceptives dans les couches superficielles doit être considérée schématiquement selon deux régions différentes. Dans la couche I, les contacts interviennent sur des neurones de projection participant aux voies spino-réticulaire et spino-thalamique impliquées dans la nociception et la thermoception (Craig & Kniffki, 1985; Ikeda et al., 2003; Perl, 1984). Dans la couche II, les entrées activent un circuit polysynaptique local (Szentagotai, 1964; Pearson, 1952; Light, 1992). Cette ségrégation suggère que les processus ayant lieu dans la couche II permettent un traitement concomitant de l'information sensorielle et une modulation du message (Lu & Perl, 2005). Plus récemment, il a été montré, que la corne dorsale présente aussi une structure modulaire (Lu & Perl, 2005). En effet, il a été noté une répétition de connexions excitatrices entre des neurones spécifiques de différentes couches et recevant des afférences primaires de différents types. La corne dorsale serait ainsi constituée de la juxtaposition de modules, comme d'autres régions du cerveau (Lorente de No, 1938; Mountcastle, 1957; Leise, 1990). Ces modules serviraient une fonction commune : combiner des informations de modalités différentes provenant d'une même région du corps et transmettre aux neurones de projection de la couche I, et donc au cerveau, une synthèse du traitement de ces différentes informations.

Les fibres afférentes primaires d'origine profonde (viscérale, méningée), elles, ne sont que nociceptives. Les fibres A δ se terminent dans les couches I, IV et V et les fibres C, toutes peptidergiques, dans les couches I, II, V et X.

Les projections vers les régions suprasegmentaires partent de la :

- couche I, de neurones nociceptifs spécifiques, qui répondent uniquement à des stimulations nociceptives
- couche V, de neurones nociceptifs non-spécifiques, ou à convergence qui reçoivent à la fois des afférences nociceptives et non nociceptives, somatiques et viscérales.

4. VOIES TRIGEMINALE ASCENDANTES

Les informations nociceptives véhiculées par le système trigéminal aboutissent au cortex cérébral, l'amygdale et l'hypothalamus par l'intermédiaire du thalamus, la formation réticulée bulbaire, le noyau parabrachial ou le noyau du faisceau solitaire (Villanueva et Nathan, 2000). L'ensemble de ces structures participent au traitement de l'information douloureuse.

La plupart des neurones de projection du complexe sensitif du trijumeau croisent la ligne médiane, constituant la voie trigémino-thalamique qui rejoint la voie ascendante spinothalamique au niveau du bulbe et du pont. Comme pour la voie spino-bulbo-thalamique, les projections trigémino-bulbo-thalamiques contiennent des afférences de tous types : mécaniques à bas seuils nociceptives spécifiques et nociceptives non spécifiques (ou à convergence).

La voie trigémino-thalamique est divisée en deux : une voie latérale appelée néo-trigémino-thalamique et une voie médiale appelée paléo-trigémino-thalamique.

- La voie trigémino-thalamique latéral va du Sp5C au noyau thalamique ventro-postérieur latéral (VPL) controlatéral et se termine au niveau du cortex somatosensoriel primaire (S1). C'est une voie rapide chargée de l'analyse sensori-discriminative de la douleur : intensité, localisation.

- La voie trigémino-thalamique médiale va du Sp5C, chemine dans le tronc cérébral au niveau de la substance réticulée jusqu'au noyau thalamique ventral postérieur médian homolatéral pour se terminer au niveau de structures limbiques (cortex cingulaire antérieur et insula). Les projections du complexe sensitif du trijumeau pour le noyau ventral postérieur médian proviennent essentiellement de neurones nociceptifs spécifiques et des neurones à convergence des Sp5C droit et gauche avec des champs récepteurs larges. Ils répondent préférentiellement aux stimuli nociceptifs ipsilatéraux (Craig 2004, Krout et al. 2000). Ce système médian lent et mal systématisé est responsable de la composante affectivo-motivationnelle de la douleur : il est impliqué dans l'intégration émotionnelle et comportementale de la douleur. Ces projections n'effectuent pas un codage sensori-discriminatif mais sont impliqués dans les réactions d'éveil ou de défense face à un stimulus douloureux

C'est en fait une description très simplifiée des voies trigémino-thalamique. En effet, tout au long de leur ascension vers le thalamus, les axones croisent et recroisent la ligne médiane, émettant des collatérales du tronc cérébral au thalamus (Figure 6).

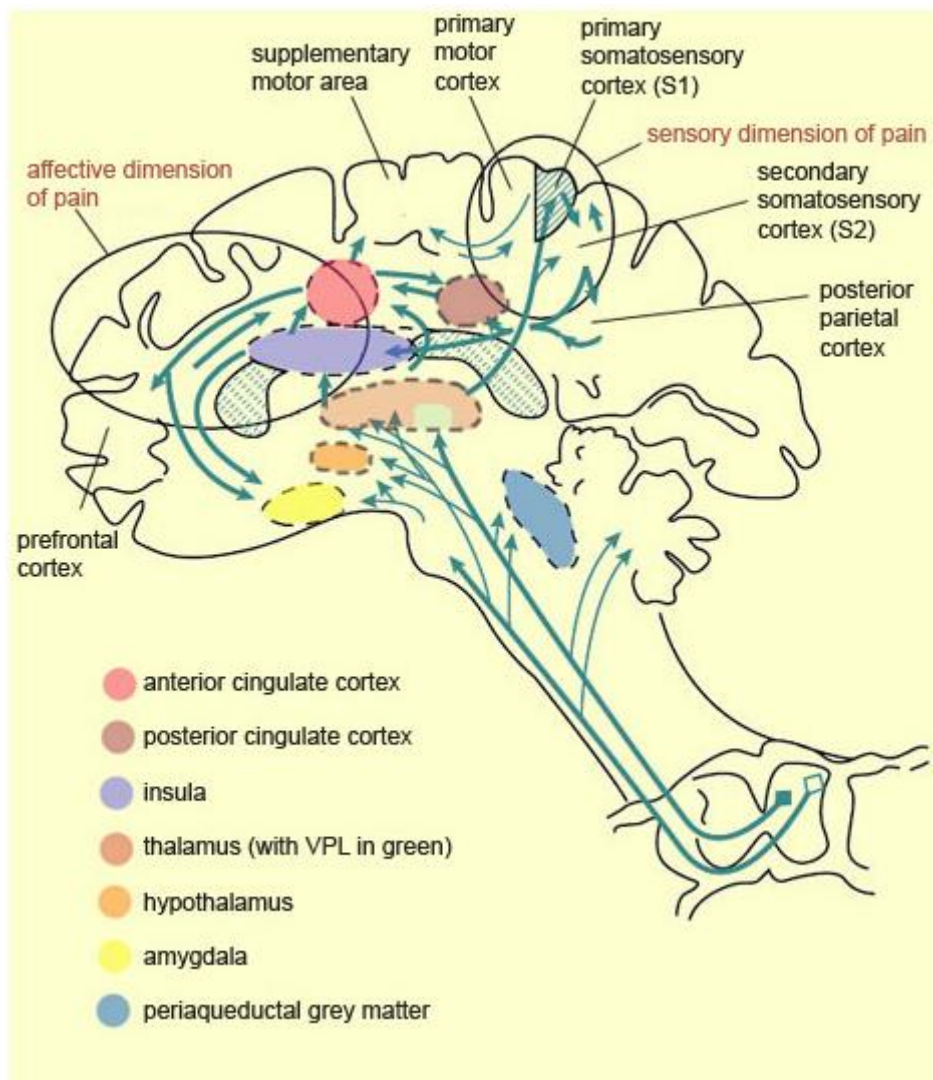


Figure 6 : Schéma des voies ascendants et des structures subcorticales et corticale (cérébrales) impliquée dans le traitement de l'information douloureuse PAG, periaqueductal gray; PB, parabrachial nucleus of the dorsolateral pons; VMpo, ventromedial part of the posterior nuclear complex; MDvc, ventrocaudal part of the medial dorsal nucleus; VPL, ventroposterior lateral nucleus; ACC, anterior cingulate cortex; PCC, posterior cingulate cortex; HT, hypothalamus; S-1 and S-2, first and second somatosensory cortical areas; PPC, posterior parietal complex; SMA, supplementary motor area; AMYG, amygdala; PF, prefrontal cortex. (Price, 2000).

5. LA 'PAIN MATRIX'

Alors qu'au niveau périphérique et dans la corne dorsale, un système dédié détecte et traite l'information nociceptive (voir ci-dessus), il n'existe pas de centre de la douleur à proprement parler dans le cerveau (sauf peut-être l'insula ; voir ci-dessous). La douleur implique au contraire un réseau de régions, corticales et sous corticales, disséminées dans le cerveau ; ce réseau est désigné sous le terme de 'Pain Matrix' (PM) (Figure 6). Ces régions régulent, traitent l'information nociceptive et peuvent même déclencher la perception d'une douleur en l'absence de toute stimulation. Cette pluralité est responsable des composantes sensori-discriminative, affectivo-motivationnelle et cognitivo-évaluative de la douleur. Aussi, l'implication de ces différentes aires du cerveau dans la sensation douloureuse dépend-elle du contexte (Peyron et al., 2000a,b ; Tracey et Mantyh, 2007).

L'utilisation de virus trans-synaptique montre que les principales cibles corticales du système spinothalamique chez le primate sont le cortex insulaire antérieur (~40%), l'opercule medio-pariétal (~30%) et le cortex cingulaire médian (*mid-cingulate* ; ~24%) (Dum et al., 2009). Chez l'homme, ces régions sont bien le site de la réponse la plus rapide à un stimulus douloureux (Frot et al., 1999 ; 2013 ; Lenz et al., 1998_{a,b} ; Ohara et al., 2006). Mais l'utilisation de l'imagerie cérébrale a permis d'identifier en plus d'autres aires corticales activées lors de différents types de douleur. En fonction de la constance de leur activation lors de douleurs :

- activées régulièrement : les aires insulaires moyennes et antérieures, cingulaire antérieure (CCA), somatosensorielles primaire (S1) et secondaire (S2), préfrontales (Prefrontal Cortex ou PFC) et pariétales postérieures (Bushnell et al., 2013 ; Apkarian et al., 2005 ; Talbot et al., 1991) ;
- activées moins régulièrement : le striatum, l'aire motrice supplémentaire, l'hippocampe, le cervelet, et la jonction temporopariétale.

Il faut noter que ces aires de 'second ordre' partagent certaines caractéristiques communes : (i) aucune n'est une cible directe du système spinothalamique ; (ii) leur stimulation directe ne provoque pas de douleur ; (iii) inversement leur destruction n'induit pas d'analgésie ; (iv) elles peuvent être activées dans un tout autre contexte que la douleur ; et (v) leur contribution à la PM, nulle ou, au contraire prédominante, dépend du contexte dans lequel le stimulus nociceptif est appliqué. Parce que les projections spinothalamiques renseignent le cerveau sur la nature/localisation des stimuli, le cerveau détecte tout d'abord l'approche d'un

stimulus menaçant. Puis cette information est transférée aux régions du PM qui, activées secondairement, procurent une référence à la perception.

Cette organisation en réseau est particulièrement adaptée au traitement de la douleur – complexe, subjective, multidimensionnelle – par le cerveau. On a l’habitude de considérer que (i) le thalamus latéral et SI sont responsables de la composante sensori-discriminative ou nociception (localisation, qualité, et intensité) et que (ii) le thalamus médian, l’insula, le CCA, et le cortex préfrontal cortex, sont responsables des composantes affectivo-motivationale et cognitivo-évaluative de la douleur. Cependant, bien que la PM ait bien une composante latérale (sensorielle) et médiane (affective) (Tracey et Mantyh, 2007), certains trouvent trop simple d’attribuer une aire du cerveau à une dimension spécifique de la douleur (Coghill et al., 1999 ; Neugebauer et Li, 2003).

5.1. Thalamus

Le groupe latéral et le groupe médian du thalamus sont importants pour le traitement des informations nociceptives (Kandel et al., 2000). Ceci est confirmé par les études en imagerie fonctionnelle chez des patients (Tracey et Mantyh, 2007).

- Le groupe latéral inclue les noyaux ventropostérieurs médian et latéral et le noyau postérieur, qui projettent dans SI pour coder la composante sensori-discriminative – intensité et localisation – de la sensation douloureuse (Cruccu et al., 2008). Ce groupe reçoit les projections spinothalamiques de neurones nociceptifs spécifiques et non-spécifique/à convergence des couches I et V, respectivement, de la corne dorsale (Tracey et Mantyh, 2007). Ces neurones thalamiques, comme les neurones afférents spinaux, possèdent des champs récepteurs de petite taille, compatibles avec leur rôle dans la localisation de la douleur. Une lésion spécifique de ce groupe latéral provoque chez le patient des difficultés à localiser un stimulus douloureux mais n’a aucun effet sur la composante affective – caractère désagréable – de cette douleur (Lundy-Ekman, 2007). De même, une telle lésion ne provoque pas d’analgésie (Casey, 1999).

- Le groupe médian du thalamus se compose du noyau central latéral et du complexe intralaminaire (Jones, 2012). La stimulation de ce groupe médian du thalamus déclenche une réaction de peur et un comportement de fuite. Chez l’homme, une lésion à ce niveau peut provoquer un soulagement en cas de douleur intractable (Melzack, 1999).

Le thalamus semble jouer un rôle majeur dans la manifestation d’une douleur chronique.

Une des modifications les plus reproductibles chez les patients neuropathiques est une hypoperfusion du thalamus contralatérale à la lésion douloureuse (pour revue voir Garcia-Larrea et Peyron, 2013). Il existe aussi une hypoperfusion thalamique chez des patients fibromyalgiques comparés à des individus en bonne santé (Mountz et al., 1995 ; Kwiatek et al., 2000). Au contraire, l'activité du thalamus augmente avec l'analgésie (Wik et al., 1999). L'association d'un symptôme 'positif' – la douleur – à une hypoactivité (et donc un hypométabolisme) est paradoxale. Il est possible que parce que la douleur neuropathique survient dans une zone d'hypoesthésie, l'hypoactivité thalamique résulte d'une déafferentation sensorielle. Cette hypoactivité devenue autonome, participerait à l'initiation de la douleur neuropathique (voir discussion dans Garcia-Larrea et Peyron, 2013).

5.2. Anterior Cingulate Cortex (ACC)

Comme son nom l'indique, l'ACC forme la partie antérieure du cortex cingulaire. Il fait partie système limbique. Il reçoit l'information nociceptive somatique et viscérale de trois sources indirectes : (i) du thalamus médian (Shyu et Vogt, 2009 ; Dum et al., 2009) et donc des afférences spinothalamiques, (ii) de l'amygdale, notamment le noyau central, qui elle-même la reçoit du noyau parabrachial (Ma et Peschanski, 1988 ; Han et al., 2015) et enfin (iii) d'autres aires corticales de la PM comme S1 (Eto et al., 2011) et le cortex insulaire. Les cellules pyramidales de la couche V de l'ACC projettent dans des régions subcorticales telles que l'hypothalamus et la substance grise périaqueducule (Bragin et al., 1984), cette dernière donnant naissance à une voie descendante modulant la transmission sensorielle dans la corne dorsale.

Lésions de l'ACC et imagerie cérébrale indiquent que l'ACC code pour des fonctions neurovégétatives et cognitives dont l'empathie, les émotions, et l'anticipation d'une récompense (Figure 7) (Jensen et al., 2012). En conséquence, l'activité de l'ACC est associée plutôt aux composantes affectivo-motivationale et cognitivo-évaluative de la douleur incluant aussi l'attention et l'anticipation à la douleur et même l'initiation de comportements pour faire face à cette douleur (Jensen et al., 2012 ; Neugebauer et Li, 2003). L'analyse des effets d'une lésion de l'ACC, aussi bien expérimentale chez l'animal (Foltz et White, 1962) qu'accidentelle chez le patient (Hurt et Ballantine, 1973), indique que cette lésion n'a aucun effet sur les fonctions nociceptives discriminatives mais provoque un déficit dans l'identification des qualités du stimulus, la perception de cette douleur.

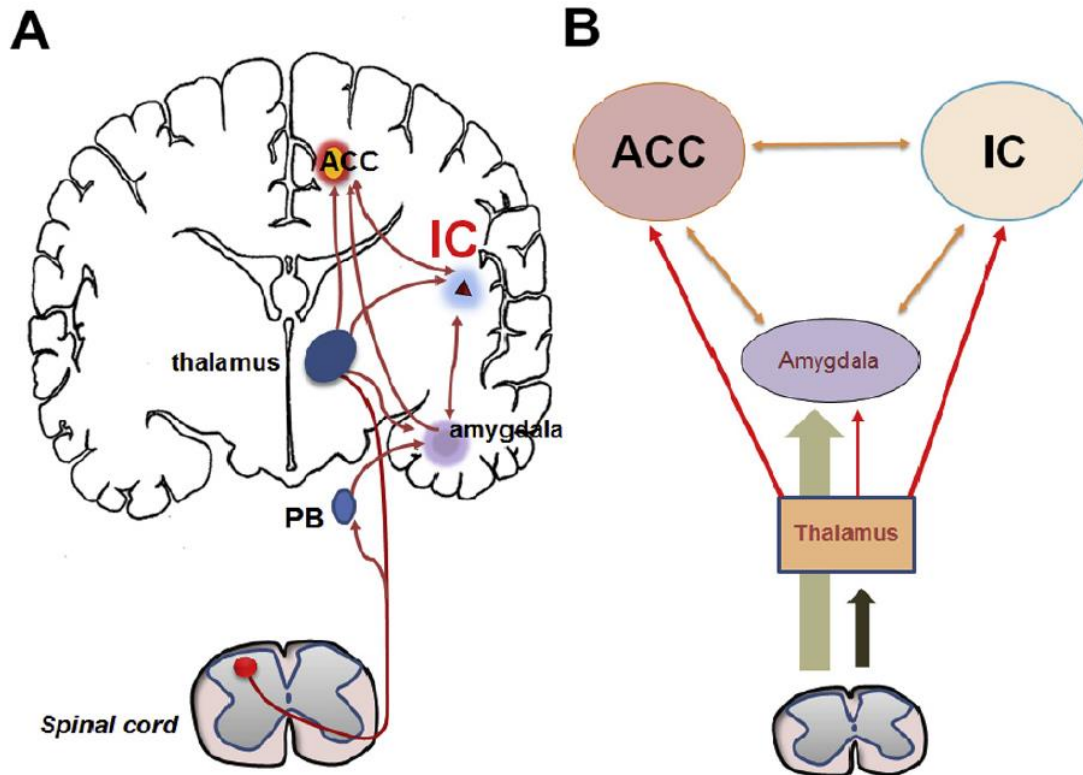


Figure 7 : *A*, Modélisation du rôle du cortex insulaire dans le traitement de l'information douloureuse et la douleur chronique. Dans ce diagramme (très simplifié), le cortex insulaire reçoit l'information nociceptive en provenance de la corne dorsale par l'intermédiaire du thalamus et de l'amygdale. Il est aussi connecté avec le cortex cingulaire antérieur et d'autres régions du cerveau (non montrées). Abréviations : ACC, anterior cingulate cortex ; IC, insular cortex ; PB, parabrachial area. **B**, Les neurones de l'ACC et du cortex insulaire sont impliqués dans le codage de la douleur; en particulier, dans son caractère déplaisant. Ils reçoivent l'information soit nociceptive soit émotive déplaisante par l'intermédiaire du thalamus et de l'amygdale. Les interactions entre ACC/cortex insulaire et amygdale sont bi-directionnelles, propices à des mécanismes de réenforcement comme de compensation au niveau subcortical et cortical. Une lésion ou une inhibition du seul ACC ou cortex insulaire pourrait ne pas être suffisante pour bloquer complètement l'induction d'une douleur chronique. Réduire la plasticité neuronale dans ces deux régions pourrait être plus efficace pour soulager la douleur chez les patients. (Zhuo, 2016)

En accord avec leur rôle limité dans le codage de l'information spatiale, les neurones de l'ACC ont des champs récepteurs bilatéraux et étendus (Sikes et Vogt, 1992).

L'imagerie fonctionnelle et la Positron Emission Tomography (PET), chez l'homme, montrent l'existence d'une hyperactivité de l'ACC lors de douleurs, qu'elles soient provoquées chez un sujet sain (Howland et al., 1995 ; Derbyshire et al., 1997 ; Rainville et al., 1997 ; Svensson et al., 1997) ou chroniques chez un patient (Derbyshire et al., 2002 ; Svensson et al., 1997). L'ACC est impliqué dans la mémoire de la peur occasionnée par la douleur et l'anticipation à cette douleur (Lorenz et Casey, 2005 ; Jensen, 2010).

Chez le rongeur, l'activation par optogénétique dans l'ACC (i) des cellules pyramidales excitatrices est suffisante pour provoquer une hypersensibilité (à la douleur) (Kang et al., 2015 ; même effet avec une stimulation du MCC : Tan et al., 2017), mais celle (ii) des neurones inhibiteurs réduit au contraire les comportements douloureux lors du test à la formaline (Gu et al., 2015) et l'hypersensibilité mécanique dans le modèle CFA (Kang et al., 2015). Dans ce dernier cas, c'est l'activation spécifique des interneurons inhibiteurs à parvalbumine, mais pas de ceux à somatostatine, qui est responsable de cette antalgie (Kang et al., 2015). Ces résultats inhibiteurs réduit au contraire les comportements douloureux lors du test à la formaline (Gu et al., 2015) et l'hypersensibilité mécanique dans le modèle CFA (Kang et al., 2015). Dans ce dernier cas, c'est l'activation spécifique des interneurons inhibiteurs à parvalbumine, mais pas de ceux à somatostatine, qui est responsable de cette antalgie (Kang et al., 2015). Ces résultats suggèrent que l'activation des neurones pyramidaux de l'ACC est nécessaire à la manifestation d'une hypersensibilité douloureuse.

Il est intéressant de noter que l'activation de l'ACC a été aussi associée à la douleur émotionnelle ou psychique. Ainsi, le déclenchement expérimental d'un sentiment triste, une exclusion ou un rejet social peuvent provoquer une augmentation de l'activité dans cette aire (Eisenberger et al., 2003 ; Yoshino, et al., 2010). Ceci est en accord avec l'hypothèse que l'ACC code le caractère déplaisant de la douleur.

Enfin chez l'homme, Rainville et collaborateurs (Rainville et al., 1997) montrent que l'hypnose peut réduire le désagrément provoqué par la douleur et que cette réduction est associée à une diminution de la réponse de l'ACC à une douleur. Ainsi une représentation de l'information nociceptive pourrait être modifiée par la cognition.

5.3. Insula

L'insula est divisée en deux parties : postérieure et antérieure. L'insula est connectée à des régions impliquées dans la régulation neurovégétative (Lévesque et al., 2003), aux lobes frontal, temporal, et pariétal, à l'amygdale, au gyrus cingulaire et au thalamus. De plus des études chez l'animal indiquent que l'insula antérieure se projette dans le tronc cérébral, sur la substance grise périaqueducale, l'aire rostro-ventro médullaire et le noyau parabrachial (Tracey et Mantyh, 2007). L'insula intègre donc des multiples informations en provenance des aires sensorielles, motrices, somatosensorielles, vestibulaires et du langage, et joue un rôle essentiel dans de multiples fonctions dont les émotions, l'homéostasie (contrôle respiratoire), la perception, le contrôle moteur, la cognition, les fonctions d'exécution (Augustine, 1985 ; 1996) (Figure 7).

Des études en PET chez l'homme montrent que l'activation de l'insula est associée aux émotions – tristesse, joie, peur, et colère (Lane et al., 1997 ; Damasio et al., 2000) – et à l'anxiété (Curtis et al., 1992) et à son anticipation (Reiman et al., 1997 ; Chua et al., 1999).

L'Insula postérieure participe aussi à l'expérience multidimensionnelle de la douleur (Neugebauer et Li, 2003). Elle reçoit des projections directes du thalamus et, par son intermédiaire, du système spinothalamique (voir ci-dessus). L'insula postérieure présente une organisation somatotopique. Avec la partie interne de l'opercule interne, c'est la seule région du cerveau humain où (i) une stimulation électrique déclenche une douleur aiguë (Mazzola et al., 2006 ; 2012) et (ii) une lésion cérébrale incluant cette aire produit une élévation des seuils nociceptifs (Biernacki, 1956 ; Greenspan et al., 1999 ; Garcia-Larrea et al., 2010) associée à une douleur neuropathique (Biernacki, 1956, revue voir Garcia-Larrea, 2012). Stimuler une région thalamique projetant dans l'insula postérieure et l'opercule (Lenz et al., 1995) ou disséquer la région operculoinsulaire lors de chirurgies (Pereira et al., 2005) provoque une douleur intense. Une activité épileptique localisée dans l'insula postérieure peut déclencher des crises d'épilepsie douloureuses et, inversement, une thermocoagulation focalisée de l'insula postérieure a pu supprimer de telles crises chez un patient pendant deux ans (Isnard et al., 2011).

Une lésion de l'insula conduit à un comportement de négligence pour la douleur ou asymbolie à la douleur (Berthier et al., 1988) : l'individu identifie un stimulus comme douloureux mais n'exprime pas la réponse émotionnelle appropriée. L'insula postérieure est donc essentielle au traitement de la composante émotionnelle de la douleur comme elle est impliquée dans l'évaluation du caractère pénible des informations sensorielles, cognitives et interoceptives (Chua et al., 1999). Elle est d'autant plus active qu'il y a menace pour la vie

même de l'individu et joue donc un rôle dans les aspects neurovégétatifs de la douleur (Jensen, 2010). L'insula s'active aussi par anticipation (Ploghaus et al., 1999) ou empathie (Singer et al., 2004) à la douleur.

Lorsque la douleur devient chronique, l'activation de l'insula se déplace rostralement vers sa partie antérieure (Tracey et Mantyh, 2007). L'insula moyenne et antérieure participe aussi à la PM. Son activation pourrait être le signe d'un flux postéro-antérieur d'informations le long de l'insula (Pomares et al., 2013), transformant des événements sensoriels en des réactions végétatives associées à des sentiments (Caruana et al., 2011 ; Craig, 2009 ; Wicker et al., 2003).

5.4. Cortex somatosensoriels primaire (S1) et secondaire (S2)

Situés dans le lobe Pariétal, S2 derrière S1, en arrière de la scissure de Rolando ou scissure centrale, le cortex somatosensoriel code pour la composante sensori-discriminative (nociception) de la douleur : intensité et localisation du stimulus (Dong et al., 1994 ; Bromm et al., 2000 ; Hari et al., 1997). A noter cependant que les réponses des neurones de S2 sont très influencées par le niveau de vigilance (Casey et al., 1996 ; Petrovic et al., 2000) : l'activation de S2 diminue chez des individus distraits (Petrovic et al., 2000) mais augmente chez des individus concentrés (Mima et al., 1998).

5.4.1. Cortex somatosensoriel primaire (S1)

S1 joue un rôle primordial dans le traitement de l'information somatosensorielle, à la fois sa détection et sa discrimination (Sessle et al., 2005 ; Neugebauer et Li, 2003). Mais S1 est aussi activé en cas de douleur (Ploner et al., 2000). S1 est responsable du codage des caractéristiques sensorielles de la douleur, notamment son intensité, sa localisation (Bushnell et al. 1999 ; Gross et al., 2007).

Le rôle de S1 semble aussi très important dans un contexte de douleur chronique. Ainsi, si S1 est constamment activé en réponse à une douleur aiguë, il l'est encore plus en cas de douleur chronique inflammatoire ou neuropathique (imagerie chez l'homme : Seifert and Maihöfner, 2009 ; Peyron et al., 2004 ; Seminowicz et al., 2009 ; microscopie multiphotonique chez le rongeur : Eto et al., 2011 ; 2012).

Il semble que cette potentialisation de l'activation de S1 lors de douleurs chroniques soit due à des phénomènes de plasticité (voir ci-dessous). Chez des individus présentant une douleur

du membre fantôme, l'activation de S1 est corrélée avec la douleur (Flor et al., 1995). Or, une stimulation de l'avant-bras, chez ces même individus, déclenche une sensation dans la main fantôme (Melzack et al., 2001). Comme les représentations de la main et de l'avant-bras sont voisines dans S1, la douleur du membre fantôme résulterait d'un réarrangement de ces deux représentations ou plasticité dans ce cortex. En accord avec cette hypothèse, des stratégies visant à réduire cette hyperexcitabilité ou réorganisation de S1 tendent à réduire le développement de douleurs chroniques (Flor et al., 2001 ; Lotze et al., 1999 ; De Ridder et al., 2007).

5.5. Cortex Préfrontal

Le cortex préfrontal (prefrontal cortex ou PFC) s'étend dans le lobe Frontal en avant des aires motrices et prémotrices (aire de Brodmann 9-12 et 44-47). Ce cortex intervient dans des fonctions cognitives dites 'supérieures' dont l'attente d'une récompense, un comportement dirigé vers un but, la personnalité, la prise de décision, le comportement social (Jensen, 2010). Il n'a pas de rôle immédiat dans le traitement de l'information somatosensorielle mais intervient dans son traitement 'supérieur' ; il est en relation avec les systèmes moteur et limbique (Cruccu et al., 2008 ; Romo et al., 2002).

Le PFC est activé lors de douleurs évoquées (Neugebauer et Li, 2003) par exemple après injection sous-cutanée de capsaïcine (Lorenz et Casey, 2005). Le PFC code la composante cognitivo-évaluative de la douleur (Jensen, 2010).

Le PFC mettrait en jeu des contrôles descendants inhibiteurs issus du tronc cérébral, et notamment de la substance grise périaqueducale, réduisant ainsi la perception douloureuse (Lorenz et Casey, 2005 ; Jensen, 2010). Plusieurs résultats confirment cette hypothèse d'un rôle inhibiteur du PFC sur la douleur : (i) l'activation du PFC et la perception de la sévérité de la douleur sont anti-corrélées (Jensen, 2010), (ii) le PFC est désactivé chez des patients souffrant de douleurs chroniques – réduisant ainsi la capacité à réduire la douleur (Neugebauer et Li, 2003), (iii) la douleur chronique du bas du dos et fibromyalgie sont corrélées avec une réduction de l'épaisseur de la substance grise dans le PFC (Jensen, 2010).

5.6. Plusieurs cortex frontaux

Le cortex frontal postero-médian (Posterior medial frontal cortex ou pmFC) est activé lors de l'anticipation d'une douleur (Porro et al., 2002), et lors de cette douleur en fonction de son intensité (Lorenz et Casey, 2005).

Le cortex préfrontal dorsolatéral (Dorsolateral prefrontal cortex ou DLPFC), jouerait un rôle dans l'inhibition de l'information nociceptive (Dias et al., 1996).

5.7. Cervelet

L'imagerie par résonance magnétique fonctionnelle (Functional Magnetic Resonance Imaging ou fMRI) démontre clairement que le cervelet est activé lors d'une stimulation douloureuse (Apkarian et al., 2005 ; Borsook, 2007). Cependant la fonction de cette activation reste inconnue.

Le cervelet reçoit des informations en provenance des afférences primaires (Marfurt et Rajchert, 1991), dont des informations douloureuses (Almeida, 2004 ; Saab et Willis, 2001). Chez l'animal, l'information véhiculée par les nocicepteurs peut gagner les cellules de Purkinje par l'intermédiaire de la voie spino-olivo-cérébelleuse et des fibres grimpantes (Yang, et al., 1993 ; Hagains et al., 2011). Cependant on ne sait pas comment cette information est codée à ce niveau.

Le cervelet jouerait un rôle modulateur. Ainsi une stimulation électrique du cervelet élève les seuils de douleurs (Siegel et Wepsic, 1974) peut être en réduisant la réponse des neurones de la corne dorsale à une stimulation périphérique (Hagains et al., 2011).

6. DOULEURS CHRONIQUES ET PLASTICITE CORTICALE

Bien que douleurs aiguës et chroniques partagent les mêmes voies, le passage de la première à la seconde passe par une transformation durable des propriétés de ces voies. Il est donc primordial de découvrir les mécanismes cellulaires et moléculaires qui sont responsables spécifiquement de ce passage en vue de prévenir l'installation d'une douleur chronique

Les résultats obtenus sur des modèles de douleur chronique chez le rongeur suggèrent que la plasticité synaptique et neuronale – on parle ici de sensibilisation (pour revue voir Latremoliere et Woolf, 2009 ; Costigan et al., 2009 ; Zhuo, 2008 ; 2014 ; Sandkuhler, 2007) – périphériques – au niveau des terminaisons et fibres nerveuses – et centrale – impliquant des

phénomènes de plasticité à long-terme au niveau de la corne dorsale et des aires sous corticale et corticales – contribuent à l’installation d’une douleur chronique.

Dans la corne dorsale de la moelle épinière, les synapses entre fibres afférentes primaires C et neurones de projection dans la corne dorsale, et notamment ceux qui projettent vers l’aire parabrachiale, sont capables de potentialisation à long-terme (long-term potentiation ou LTP ; Ikeda et al., 2003 ; 2006 ; Ruscheweyh et al., 2011). Or cette transmission synaptique excitatrice entre afférences primaires et neurones de la corne dorsale est potentialisée chez des animaux neuropathiques (Sandkuhler et Liu, 1998) ou inflammatoires (Ikeda et al., 2006).

Les différentes aires du PM sont aussi le site de transformations à long-terme qui participent à la manifestation de la douleur chronique. Cette plasticité a été très étudiée au niveau de l’ACC, en particulier par le groupe de Min Zhuo à Toronto (Canada).

6.1. Plasticité synaptique associée à la douleur dans le cortex cingulaire antérieur

L’utilisation de marqueurs anatomiques d’activation neuronale, tels que l’expression de la protéine Fos ou la phosphorylation de l’extracellular signal-regulated kinase’ (ERK1/2) montrent que les douleurs chroniques chez le rat, qu’elles soient neuropathiques (Li et al., 2010 ; Chen et al., 2014) inflammatoire (Wei et al., 2001), ou viscérale (Wei et al., 1999) s’accompagnent toutes d’une activation de l’ACC.

Des enregistrements intracellulaires (technique du patch-clamp, configuration cellule entière) de **neurones pyramidaux des couches 2/3** de l’ACC sur des tranches *ex vivo* prélevées sur des rongeurs douloureux chronique révèlent que les synapses excitatrices sur ces neurones sont potentialisées, que ce soit à la suite de la lésion d’un nerf périphérique ou une lésion inflammatoire cutanée.

Les mécanismes responsables de cette potentialisation sont à la fois :

- presynaptiques (augmentation de la libération de neurotransmetteur) (animaux neuropathiques Xu et al., 2008 ; Shen et al. 2015 ; Koga et al., 2015 ; animaux inflammatoires-modèle CFA : Zhao et al. 2006 ; Koga et al., 2015)

- postsynaptiques, que cela se manifeste par une augmentation de l’amplitude des potentiels synaptiques (animaux neuropathiques : Xu et al., 2008 ; Shen et al. 2015 ; Koga et al., 2015 ; animaux inflammatoires-modèle CFA : Koga et al., 2015), une augmentation de la phosphorylation de la sous-unité GluR1 des récepteurs au glutamate de type α -amino-3-

hydroxy-5-methyl-4-isoxazole propionic acid (AMPA) (animaux neuropathiques : Xu et al., 2008) ou du nombre de récepteurs AMPA contenant cette sous-unité GluR1 dans la membrane postsynaptique (animaux neuropathiques : Xu et al., 2008 ; Li et al., 2010 ; animaux inflammatoires-modèle CFA : Bie et al., 2011). Il faut noter ici que le groupe de Min Zhuo (Wu et al. 2005) observe aussi une augmentation de l'expression de la sous-unité NR2B des récepteurs au glutamate de type N-méthyl-D-aspartate (NMDA), 1 jour après une injection de CFA dans la patte. Or des souris, chez lesquelles l'expression de cette sous-unité NR2B est génétiquement augmentée, présentent une plus grande sensibilité à la douleur de type inflammatoire (modèles formol et CFA : Wei et al., 2001).

Lorsque les auteurs comparent les propriétés membranaires des neurones enregistrés dans des tranches *ex vivo* d'animaux douloureux chroniques et témoins, ils notent aucune différence dans le potentiel de membrane de repos, la résistance membranaire, le seuil des potentiels d'action et la réponse à un courant dépolarisant (animaux neuropathiques : Ning et al. 2013 ; animaux inflammatoires-modèle CFA : Wu et al., 2005 ; mais voir Li et al., 2014). Cependant, chez l'animal vivant, les oscillations du potentiel membranaire sont plus rapides et l'activité spontanée plus élevée chez le rat neuropathique que chez l'animal indemne (Ning et al., 2013).

Des enregistrements identiques dans des tranches *ex vivo* mais de **neurones pyramidaux de la couche 5** de l'ACC révèlent une même potentialisation des synapses excitatrices mais ici seulement sur les neurones qui envoient leurs projections vers la moelle épinière (Chen et al., 2014). A nouveau, il n'y a pas de modification des propriétés membranaires de ces neurones (Xu et al., 2008).

Des résultats récents (Koga et al., 2015) suggèrent que les deux potentialisations, pre- et postsynaptique, de la transmission synaptique excitatrice sur les neurones pyramidaux de la couche 2/3 de l'ACC jouent un rôle différent : la potentialisation presynaptique pour l'anxiété et la potentialisation postsynaptique pour la douleur chronique. Cette convergence des deux types de potentialisation sur la même synapse excitatrice expliquerait le rôle de l'ACC dans la composante affectivo-motivationnelle de la douleur. Il est intéressant de noter que, chez des souris ayant subi une lésion nerveuse, cette potentialisation de la transmission synaptique, associée à une augmentation de la contribution des récepteurs NMDA, dans les couches superficielles de l'ACC perdure au-delà de la période d'hypersensibilité douloureuse et est plutôt corrélée avec le comportement anxio-dépressif de l'animal déclenché par la douleur neuropathique (Sellmeijer et al., 2018). Etant donné que l'inhibition optogénétique de l'hyperactivité dans l'ACC soulage l'aspect aversif de la douleur et l'anxiété-dépression, cela

soulève la question : l'ACC code-t-il pour la douleur, sa composante affectivo-motivationale ou seulement pour ses conséquences anxio-dépressives ?

Pourtant, il est important de noter ici que toutes les manœuvres visant à prévenir cette potentialisation de la transmission synaptique excitatrice sur les neurones pyramidaux de la couche 2/3 de l'ACC réduisent de façon significative l'hypersensibilité douloureuse. Ainsi l'administration bilatérale dans l'ACC, d'antagonistes des récepteurs NMDA, de la calmoduline, de la protéin kinase A (PKA ; Wei et al., 2002), des récepteurs NMDA contenant la sous-unité NR2B (Wu et al., 2005), de la protéin kinase M zeta (PKM ζ ; Li et al., 2010) et de la connexin 36 (Chen et al., 2016) et l'élimination génétique de la calmodulin-stimulated adenylyl cyclase (Wei et al., 2002 ; Zhao et al., 2006 ; Xu et al., 2008 ; Li et al., 2010) – tous mécanismes impliqués dans la LTP des synapses excitatrice sur les neurones pyramidaux de la couche 2/3 de l'ACC – réduisent (i) l'hypersensibilité **mécanique** (Wei et al., 2002 ; Wu et al., 2005 ; Xu et al., 2008 ; Li et al., 2010 ; Eto et al., 2011 ; Shen et al., 2015 ; Chiou et al., 2016), (ii) l'hypersensibilité **thermique** (Shen et al., 2015), (iii) la **douleur tonique** (douleur neuropathique : Li et al., 2010) et (iv) le **comportement douloureux** (test au formol: Gu et al., 2015), que cette douleur chronique soit d'origine (i) **inflammatoire** (modèle CFA dans la patte: Wei et al., 2002; Wu et al., 2005; Eto et al., 2011; test au formol: Gu et al., 2015), (ii) **neuropathique** (Xu et al., 2008; Li et al., 2010; Shen et al., 2015; Chen et al., 2016) ou (iii) **cancéreuse** (Chiou et al., 2016),

6.2. Plasticités associées à la douleur dans le 'Pain matrix'

On a aussi observé une plasticité dans d'autres aires du PM.

6.2.1. *Thalamus*

Bien qu'une augmentation de la fréquence de décharge des neurones thalamiques ait été notée dans des modèles de douleurs neuropathique (Guilbaud et al., 1990 ; Zhao et al., 2006) et inflammatoire (Guilbaud et al., 1986) chez le rongeur, on ignore toujours si les projections spinothalamiques sur les neurones thalamiques sont capables de dépression à long-terme (long-term depression ou LTD) et LTP.

6.2.2. Amygdale

La transmission excitatrice entre les afférences parabrachiales et le noyau central de l'amygdale est augmentée dans les modèles animaux de douleurs inflammatoire (Gereau, 2003) et neuropathique (Ikeda et al., 2007 ; Nakao et al., 2012).

6.2.3. Cortex insulaire

Des enregistrements *ex vivo* sur tranches de cortex insulaire révèlent que les synapses peuvent être potentialisées ou déprimées durablement (Liu et al., 2013a, b). La transmission excitatrice, est potentialisée, aussi bien celle impliquant les récepteurs NMDA que celle des récepteurs AMPA, dans un modèle d'animal neuropathique (Qiu et al., 2013; 2014). De même, dans un modèle neuropathique trigéminal, l'expression de l'allodynie mécanique est associée à une phosphorylation de ERK1/2 dans la zone de projection du cortex insulaire postérieur (Alvarez et al., 2008).

6.2.4. Cortex préfrontal

La douleur neuropathique entraîne une potentialisation de la transmission excitatrice NMDA et des modifications morphologiques – allongement, augmentation du nombre de branches et augmentation de la densité des épines dendritiques des/sur les dendrites basaux – des neurones pyramidaux des couches 2/3 (Metz et al., 2009). Paradoxalement, la douleur inflammatoire s'accompagne d'une diminution de l'excitabilité de ces mêmes neurones (Wang et al., 2015).

6.2.5. Cortex somatosensoriel S1 et S2

Des études chez le rat neuropathique (Eto et al., 2011 ; 2012) confirme qu'il existe bien une hyperexcitation de S1 comme chez les patients douloureux chroniques (Seifert and Maihöfner, 2009 ; Peyron et al., 2004 ; Seminowicz et al., 2009). L'augmentation de l'excitation excède celle de l'inhibition (Eto et al., 2012). Il y aurait un shift de l'activité des réseaux neuronaux inhibiteurs en faveur de l'activité neuronale pyramidale : ainsi l'activité des neurones inhibiteurs à somatostatine et à parvalbumine est réduite chez des souris neuropathiques (Cichon et al., 2017 ; mais voir Eto et al., 2012). Cette augmentation de l'activité dans les cortex S1 et S2 paraît contribuer à l'augmentation de l'excitation de l'ACC par l'intermédiaire de connections des cortex S1 et S2 vers l'ACC (Eto et al., 2011).

Cependant Kim et Nabekura dès 2011 (Kim et Nabekura, 2011), montrent que cette hyperactivité s'accompagne d'un réarrangement rapide (< 1 semaine) des épines dendritiques sur les neurones pyramidaux des couches 2/3, suggérant qu'il y a plasticité.

Mais on ignore toujours s'il existe bien une plasticité dans le cortex S1. Ce travail a pour but de répondre à la question :

**L'induction d'une douleur chronique est-elle associée
à une plasticité dans le cortex somatosensoriel primaire (S1) ?**

Quelles plasticités ? Nous avons mesuré simultanément plusieurs types de plasticité : (i) plasticité à long-terme de la transmission synaptique, **LTD et LTP**, (ii) **métoplasticité** (ou altération de la capacité pour une synapse de générer une plasticité synaptique à long-terme, LTD ou LTP, en fonction de son activité passée), (iii) **plasticité de l'excitabilité neuronale** et (iv) **plasticité anatomique**.

Quel modèle de douleur chronique ? Nous avons utilisé le modèle de douleur inflammatoire : injection de CFA dans l'aire des vibrisses (**modèle CFA de la face** ; voir Alba-Delgado et al., 2018).

Quelles techniques ? Après avoir vérifié que cette injection de CFA entraîne bien une allodynie mécanique (**Comportement**), nous avons enregistré (**Electrophysiologie** : enregistrements **intracellulaires** – technique du patch-clamp, configuration cellule entière) des neurones pyramidaux des couches 2/3 dans l'aire de projection des afférences de la face dans le cortex S1 sur des tranches *ex vivo* chez ces rats. A la fin des enregistrements, les tranches sont fixées et traitées pour une étude morphologique des neurones remplis avec de la biocytine lors de l'enregistrement (**Anatomie**).

Chapitre 1: **Synaptic and Intrinsic Plasticities and Metaplasticities at Vertical Inputs onto Layer 2/3 Pyramidal Cells in the Rat Primary Somatosensory Cortex**

Chapitre 2: **Inflammatory Pain-induced Neuronal Plasticities and Metaplasticities in Superficial Layers on the Rat Primary Somatosensory Cortex**

Chapitre 3: **Rapid dendritic remodeling in the adult somatosensory cortex following peripheral inflammation and its association with inflammatory pain**

CHAPITRE 1:

SYNAPTIC AND INTRINSIC PLASTICITIES AND METAPLASTICITIES AT VERTICAL INPUTS ONTO LAYER 2/3 PYRAMIDAL CELLS IN THE RAT PRIMARY SOMATOSENSORY CORTE

**Synaptic and Intrinsic Plasticities and Metaplasticities
at Vertical Inputs onto Layer 2/3 Pyramidal Cells in the Rat Primary Somatosensory
Cortex**

Abbreviated title: Synaptic-Intrinsic Plasticity Rules in Neocortex

Hien Luong Nguyen¹, Radhouane Dalle^{1,2}, Myriam Antri¹ and Alain Artola^{1*}

¹ Université Clermont Auvergne, Inserm, Neuro-Dol, F-63000 Clermont-Ferrand, France;

² CHU Clermont-Ferrand, Service d'Odontologie, F-63000 Clermont-Ferrand, France.

*** Correspondence:**

Alain ARTOLA, Inserm/UCA , U1107, Neuro-Dol, Trigeminal Pain and Migraine

Faculté de Chirurgie Dentaire, 2 rue de Braga, F-63100 CLERMONT-FERRAND, FRANCE

Phone + (33) 4 73 17 73 67

Mail : alain.artola@uca.fr

Number of pages (entire manuscript): 57

Number of Figures: 8

Number of Tables: 3

Abstract: 250 words

Introduction: 650 words

Discussion: 1480 words

Acknowledgements:

ABSTRACT

Synaptic activity can trigger multiple plasticity processes. At the synaptic level, it induces bidirectional synaptic plasticity (long-term potentiation [LTP], long-term depression [LTD]) as well as lasting changes in the ability of synapses to subsequently express such plasticity (metaplasticity). At the neuronal level, it also produces bidirectional lasting changes in the postsynaptic intrinsic neuronal excitability (LTP/LTD-IE). It is critical to know how such plasticity processes relate to synaptic activity to determine their contribution to memory engram formation. Using *ex vivo* whole-cell patch clamp recordings and a brief (<1min) pairing to trigger plasticity, we assessed simultaneously synaptic and intrinsic plasticities and their activity-dependent in superficial layers of the rat primary somatosensory (S1) cortex. Synaptic and intrinsic changes were mostly parallel (synergistic) and depended on both the postsynaptic membrane potential during pairing (V_m) and initial synaptic/intrinsic state. In naïve conditions, there was no synaptic/intrinsic modification at $V_m < 30\text{mV}$, synaptic/intrinsic LTD at $-30\text{mV} < V_m < -10\text{mV}$, and, finally, synaptic/intrinsic LTP at $V_m > -10\text{mV}$. In depressed conditions, the synaptic/intrinsic LTD threshold, Θ^- , was shifted toward more depolarized V_m s and the synaptic/intrinsic LTP threshold, Θ^+ , toward more polarized V_m s, occluding the window for synaptic/intrinsic LTD and facilitating synaptic/intrinsic LTP. Conversely in potentiated conditions, Θ^- was shifted toward more polarized V_m s and Θ^+ , to more depolarized V_m s, opening the window for synaptic/intrinsic LTD and inhibiting synaptic/intrinsic LTP. Unexpectedly, pairings to $V_m > \Theta^+$ induced synaptic LTP but non-synergistic (homeostatic) LTD-IE. Therefore, the synaptic and intrinsic plasticity rules in S1 are mostly parallel, the synaptic and intrinsic LTD and LTP thresholds exhibiting similar activity-dependent shifts.

SIGNIFICANCE STATEMENT

INTRODUCTION

The ability of neurons to modify their structure and function as a result of activity is critical for normal development, learning and responding to brain damage and neurological disease. Synaptic activity can concomitantly trigger several plasticities. At the synaptic level, it generates bidirectional persistent changes in synaptic strength, such as LTP and LTD. Factors that have the demonstrated ability to control the magnitude and sign of synaptic plasticity include the level of postsynaptic depolarization (Artola et al., 1990), the rate of synaptic inputs (Dudek and Bear, 1992), the phase of synaptic input relative to ongoing theta frequency network oscillations (Huerta et al., 1995; Holscher et al., 1997; Hyman et al., 1997) or gamma frequency oscillations (Wespatat et al., 2004) and EPSP/spike timing (Markram et al., 1997; Bi and Poo, 1998; Debanne et al., 1998). The key variable governing the polarity of synaptic change was proposed to be the amplitude in post-synaptic calcium signal ($[Ca^{2+}]_i$): a modest rise triggering LTD, a more substantial or prolonged one triggering LTP (Lisman, 1989; Artola and Singer, 1993; Malenka and Nicoll, 1993). Consistent with such synaptic plasticity rule, low and high $[Ca^{2+}]_i$ are associated with voltage- (Bröscher et al., 1992; Hansel et al., 1997), frequency- (Cummings et al., 1996) and spike-timing-dependent induction (Koester and Sakmann, 1998) of LTD and LTP, respectively.

Synaptic activity also modulates subsequent induction of synaptic plasticity. This phenomenon, or “metaplasticity” (Abraham and Bear, 1996; Abraham and Tate, 1997), manifests as modifications in the direction or degree of activity-dependent synaptic changes. In hippocampus, low-frequency stimulation (LFS) has no effect on naïve synapses but depresses them if they were previously activated, whether such prior activity induces LTP (Barrionuevo et al., 1980; Staubli and Lynch, 1990; Fujii et al., 1991; Larson et al., 1993; Bortolotto et al., 1994; O’Dell and Kandel, 1994;

Norris et al., 1996; Wagner and Alger, 1995; Ngezahayo et al., 2000), short-term potentiation (STP) (Wexler and Stanton, 1993), or no synaptic modification (Christie and Abraham, 1992; Wang et al., 1998). Repeated STPs also inhibit subsequent tetanus-induced LTP (Huang et al., 1992). Thus, the same synaptic activity concomitantly facilitates subsequent LTD induction and inhibits subsequent LTP induction. Conversely, a synaptic activation which induces LTD, concomitantly inhibits subsequent LTD induction and facilitates subsequent LTP induction (Ngezahayo et al., 2000).

At the neuronal level, synaptic activity can also induce persistent changes in the intrinsic excitability of postsynaptic neurons (cerebellum: Aizenman & Linden, 2000; hippocampus: Abraham et al., 1987; Daoudal et al., 2002). Intrinsic and synaptic plasticities may occur in parallel: LTP of intrinsic excitability (LTP-IE) with synaptic LTP (hippocampus: Abraham et al., 1987; Daoudal et al., 2002; Campanac and Debanne, 2008; Campanac et al., 2013; Lopez-Rojas et al., 2016; cerebellum: Armano et al., 2000; Belmeguenai et al., 2010) and LTD of intrinsic excitability (LTD-IE) with synaptic LTD (hippocampus: Daoudal et al., 2002; Campanac and Debanne, 2008; cerebellum: Shim et al., 2017). But they can also be non-synergistic (i.e. homeostatic) in hippocampal CA1: LTP-IE with synaptic LTD (Brager & Johnston, 2007) and *vice versa* (Narayanan & Johnston, 2006; Fan et al., 2005); raising the question as to how synergistic and homeostatic intrinsic plasticities are related to synaptic activity (see Gasselín et al., 2017 for an intrinsic plasticity rule).

Surprisingly, little is known about intrinsic plasticity in neocortex. Since it was previously induced in the presence of ionotropic glutamate receptor antagonists (Sourdet et al., 2003; Cudmore et al., 2004; Paz et al., 2009), we still ignore how synaptic activity regulates neuronal intrinsic excitability—i.e. the intrinsic plasticity rule. Moreover, how does activity-dependent intrinsic plasticity modulate subsequent induction of plasticity? Although intrinsic plasticity is

certainly an important plasticity mechanism on its own, it can modulate the subsequent induction of synaptic plasticity, through regulating the postsynaptic depolarization and Ca^{2+} signal, thus having metaplastic effects. We addressed these issues by simultaneously assessing synaptic and intrinsic plasticities/metaplasticities at vertical inputs onto layer 2/3 pyramidal cells in the rat S1 cortex.

MATERIALS AND METHODS

Animals

Male Sprague-Dawley rats (Charles River, France), weighing about 50-75 g at their arrival, were housed 3–4 per cage at 22°C under 12h light/dark cycles (lights on 8 am) with *ad libitum* access to food and water. All efforts were made to minimise the number of animals used. All the experimental procedures followed the ethical guidelines of the International Association for the Study of Pain and the European Community Council directive of November 24, 1986 (86/609/EEC) and were approved by the local institutional animal care and use committee (UFR d'Odontologie, Université de Clermont-Auvergne).

Ex vivo electrophysiological recordings

Slices. Slices were prepared using a method adapted from Agmon and Connors (1991). Briefly, rats were deeply anesthetized by an intraperitoneal injection of chloral (7%; 70 mg.kg⁻¹), decapitated and their brain were quickly removed. The tissue was placed with the ventral face down into ice-cold (0-4°C) sucrose-based artificial cerebrospinal fluid (aCSF) containing (in mM): sucrose (205), KCl (2), MgCl₂ (7), CaCl₂ (0.5), NaHCO₃ (26), NaH₂PO₄.H₂O (1.2) and D-glucose (11). A vertical cut was made through the tissue at an angle of 55° to the right of the posterior-to-anterior axis of the brain, intersecting this axis at about its anterior one-third point. The tissue caudal to the cut was then glued onto the stage of a Vibratome (VT 1200S,

Leica Microsystems, Wetzlar, Germany) with the cut surface down and the pial surface toward the blade. A small cube of agar was glued to the stage at the back of the tissue to prevent its movements due to blade pressure. Then the tissue was totally immersed into an ice-cold solution containing (in mM): K-gluconate (135), NaCl (5), MgCl₂·6H₂O (2), EGTA (0.2), HEPES (10), and sucrose (10). This solution was designed to mimic the intracellular medium and thus to limit the entry of extracellular ions into the cells during the slicing procedure (Dugué et al., 2005). Two or three (depending on brain size) slices 800- μ m-thick were cut and discarded until the blade started to cut the left hemisphere. Then, 350 μ m-thick slices were cut until the lateral ventricle (recognized by its pink tint) could no longer be seen on the surface of the tissue. Only the right hemispheres containing the primary somatosensory cortex (S1) were collected and suspended into normal aCSF containing (in mM) NaCl (125), KCl (2.5), CaCl₂ (2), MgSO₄ (2), NaHCO₃ (26), NaH₂PO₄·H₂O (1.25) and D-glucose (25) at 30°C for a 20-min recovery period and then maintained at room temperature (20-23°C) (Sessolo et al., 2015). All cutting, holding and recording external solutions were saturated with 5% CO₂/95% O₂ (pH 7.4; 310–320 mOsm).

Patch-clamp whole cell recordings. One slice was transferred into the recording chamber where it was continuously perfused at 2.0 mL·min⁻¹ with normal aCSF at room temperature (20-23°C). Neurones were visualized using an upright Zeiss Axioskop2 FS plus (Germany) fitted with infrared differential interference contrast (DIC) optics and a CCD video camera (Hamamatsu, Japan). Patch-clamp whole-cell recordings were obtained from S1 layer 2/3 pyramidal neurones using double patch clamp EPS 10 amplifier (HEKA, Germany) and a Patchmaster acquisition software (HEKA, Germany). Signals were low-pass filtered at 10 kHz with a Bessel filter and sampled at 1 kHz. Electrodes were pulled from thin-wall borosilicate capillaries (outer diameter: 1.5 mm, inner diameter: 1.12 mm, WPI, Sarasota, FL, USA) using a horizontal puller (Model P-97, Sutter Instruments, Navato, CA, USA). Recording electrodes had resistances ranging 5-

7 M Ω , being filled with an internal solution containing (in mM) K-gluconate (135), NaCl (5), MgCl₂ (2), sucrose (10), HEPES (10), ethylene glycol-bis-(o-aminophenoxy)-ethane-N,N,N',N'-tetraacetic acid (EGTA) (0.2), Na₂ATP (2.5), NaGTP (0.3), pH adjusted to 7.3, and osmolality of 300 ± 5 mOsm.

Excitatory postsynaptic currents (EPSC), recorded in voltage clamp mode from layer 2/3 pyramidal neurons, were evoked by 0.1-ms current pulses, using a monopolar glass stimulating electrode (filled with normal aCSF, 2-3 Mohm) placed in layer 4/5 of S1. In most of the experiments, stimuli were paired within a delay of 50 msec. During conditioning, afferent stimulation at 2 Hz for 50 sec was paired with various postsynaptic membrane depolarization. *Analysis.* Resting membrane potential (RPM) was measured as the mean baseline potential during 80 ms in current-clamp mode just after break-in. During the course of the experiments, input (R_i) and series resistances (R_s) were periodically monitored using a 500-ms-long, 10-pA-hyperpolarizing current pulse. Cells were included in the analysis if they met the following criteria: RPM < -60 mV, and $R_s < 40$ M Ω . To evaluate intrinsic excitability, neurons were injected with depolarizing current pulses (500-ms-long, ranging from 350 to 770 pA, with 30 pA increments) in current-clamp mode measured from about $V_m = -70$ mV at which the neuron was kept. Curves of the number of action potential firing as a function of injected current were constructed. Rheobase [the minimal depolarizing current amplitude injected at the soma in order to make the cell fire an action potential (AP)] was measured as the first of three consecutive current pulses of the same intensity able to generate at least one AP. A ramp of current (from 0 pA to 2 times the rheobase, in 1 s) was used to assess AP voltage threshold: it was the voltage at which the value of dV/dt exceeded 20 mV/ms. AP characteristics were obtained from the first spike evoked by the minimal depolarizing current pulse in every S1 pyramidal neuron recorded. AP amplitude was measured from its threshold to its peak and AP duration at half maximum amplitude. After-hyperpolarization (AHP) represented the difference

between spike threshold and post AP hyperpolarization. Paired pulse ratio (PPR) was the ratio of the amplitude of the second EPSC to that of the first one.

All the above analyses were performed using Fitmaster (HEKA, Germany).

Drugs

Acide 2-amino-5-phosphonovalérique (APV) was purchased from Tocris

Statistical analysis

One-way repeated measures analysis of variance (ANOVA) was conducted. Significant interactions were followed up with the Tukey or Tukey's HSD (honestly significant difference) *post hoc* test. All data are presented as mean \pm SEM. In each group, n is for the number of recorded neurons and N is for the number of rats.

RESULTS

The level of postsynaptic depolarization determines the direction and magnitude of synaptic plasticity at vertical inputs to S1 L2/3 pyramidal neurons.

To address these issues, we first established the reference voltage-response curve for the induction of LTD/LTP in naïve excitatory synapses onto S1 L2/3 pyramidal neurons of young adult rats (Fig. 1). Pairing brief low-frequency afferent stimulation (2 Hz for 50 s) with postsynaptic depolarization ≤ -30 mV, referred to as pairing to $V_m \leq -30$ mV in the remainder of the paper, produced no lasting change in synaptic transmission (pairing to -40 mV: $101.6 \pm 2.6\%$ of baseline; One way ANOVA for repeated measures: $P=0.9309$; $n=3$; $N=3$; pairing to -30 mV: $100.2 \pm 1.4\%$ of baseline; $P=0.5677$; $n=6$; $N=6$). On the other hand, pairing to -20 mV induced a robust LTD ($66.9 \pm 1.2\%$ of baseline; $P<0.0001$; $n=10$; $N=10$). Finally, pairing to $V_m \geq -10$ mV produced LTP (pairing to -10 mV: $128.8 \pm 2.1\%$ of baseline; $P<0.0001$; $n=12$; $N=12$; pairing to 0 mV: $161.7 \pm 3.3\%$ of baseline; $P<0.0001$; $n=16$; $N=15$; pairing to 10 mV: $188.5 \pm 2.4\%$

of baseline; $P < 0.0001$; $n = 6$; $N = 6$; pairing to 20 mV: $215.2 \pm 7.7\%$ of baseline; $P < 0.0001$; $n = 8$; $N = 8$). These results demonstrate that the induction of synaptic LTD and LTP in naïve S1 vertical input-L2/3 pyramidal neuron synapses of young adult rats depends on the level of post-synaptic depolarization. The voltage–response function for the induction of synaptic LTD/LTP, or synaptic plasticity rule, in naïve S1 synapses describes a two-voltage threshold curve (Fig. 1F), similar to those in the hippocampal CA1 (Ngezahayo *et al.*, 2000; Artola *et al.*, 2005) and anterior cingulate cortex (Toyoda *et al.*, 2005) with a synaptic LTD threshold (between -30 mV and -20 mV) and a synaptic LTP threshold (between -20 mV and -10 mV), referred to as Θ^- and Θ^+ , respectively, in the remainder of the paper. Of note, in naïve synapses, the V_m range for inducing synaptic LTD was rather narrow, only 10-15 mV large. Moreover, the magnitude of synaptic LTP increased linearly with membrane depolarization within the -10 to +20 mV V_m range.

Paired-pulse ratio (PPR; pulse interval: 50 ms) was measured to assess whether pairing-induced LTD or LTP were, at least in part, presynaptically expressed through a change in transmitter release. Indeed, over such time scales, short-term plasticity is typically due to a presynaptic mechanism (Zucker and Regehr, 2002). Neither pairings inducing LTD nor pairings inducing LTP altered PPR, consistent with a postsynaptic site of expression for synaptic changes in both directions (Fig. 1G).

The induction of homosynaptic LTD as well as LTP of S1 vertical input-L2/3 pyramidal neuron synaptic transmission was previously shown to require NMDA receptor (NMDAR) activation (Castro-Alamancos *et al.*, 1995; Feldman, 2000). To determine whether NMDA receptor activation is also needed for inducing synaptic LTD or LTP with our pairing protocol, we bath-applied the NMDA receptor antagonist DL-AP-5 (200 μ M) during pairings to -20 mV or 0 mV, which induce synaptic LTD and LTP, respectively, in control conditions. Blocking NMDARs completely prevented the induction of both synaptic LTD (pairing to -20 mV in the

presence of AP5: $99.6 \pm 3.5\%$ of baseline; One way ANOVA for repeated measures: $P=0.4624$; $n=5$; $N=5$) and synaptic LTP (pairing to 0 mV in the presence of AP5: $101.4 \pm 1.2\%$ of baseline; $P=0.8218$; $n=5$; $N=5$) (Fig. 2, A, B).

The level of postsynaptic depolarization determines the direction of intrinsic plasticity in S1 L2/3 pyramidal neurons

The above results above demonstrate that the level of postsynaptic depolarization during a brief afferent stimulation determines the direction as well as the magnitude of the change in S1 vertical input-L2/3 pyramidal neuron synaptic strength. Since synaptic activation was shown to also produce long-term changes in intrinsic neuronal excitability in various brain areas, including the cerebellum (Aizenman & Linden, 2000) and hippocampal CA1 (Daoudal et al., 2002), we investigated whether the intrinsic excitability of the post-synaptic pyramidal neurons was also altered after the various pairings.

Intrinsic excitability was measured in current-clamp mode by injecting brief depolarizing currents (350 to 770 pA, with 30 pA increments) from a baseline potential of -70 mV. The number of depolarization-evoked action potentials (AP) was taken as a measure of neuronal excitability. Comparison of the input–output curves, relating the number of evoked APs or firing response to the injected depolarizing current, referred to as F-I curve, before and 30 min after pairing, shows that neuronal excitability was stable ($n=6$, $N=6$; One-way ANOVA for repeated measures, $P=0.9876$; Fig. 3A) when pairings produced no change in synaptic efficacy (pairings to -40 mV or -30 mV). On the other hand, the same comparison reveals that F-I curves were shifted to the right after pairing to -20 mV; that is, less APs were elicited by depolarizing current steps after synaptic LTD had been induced (Fig. 3B). Intrinsic excitability was decreased over the whole range of suprathreshold currents ($n=12$; $N=11$; $P<0.05$), the response to a 770-pA-step, 30 min after pairing, being $71.9 \pm 3.1\%$ of baseline. Conversely, F-I curves were shifted

to the left after pairings to $V_m \geq -10$ mV, which reliably induced synaptic LTP; that is, more APs were elicited by depolarizing current steps after synaptic potentiation (Fig. 3C). Again, intrinsic excitability was increased over the whole range of suprathreshold currents ($n=34$; $N=25$; $P < 0.0001$) and the response to a 770-pA-step, 30 min after pairing, was $148.8 \pm 2.9\%$ of baseline. Of note, no change in R_{in} was observed in all groups (Table 1). These results thus demonstrate that S1 L2/3 pyramidal neurons undergo intrinsic plasticity—LTD-IE or LTP-IE—and that changes in synaptic efficacy and intrinsic excitability are synergistic. The intrinsic plasticity vs. postsynaptic depolarization function (or intrinsic plasticity rule) in naïve synapses describes a two voltage-thresholds curve, these thresholds being similar to those of the voltage-response curve for the induction of synaptic plasticity.

As previously observed in the visual neocortex (Cudmore and Turrigiano, 2004), depolarization-evoked increases in firing rates scaled linearly with input current amplitude in S1 L2/3 pyramidal neurons. Interestingly, the gains of the firing responses (slope of the F-I curves) in baseline conditions and after induction of either LTD-IE or LTP-IE were similar (0.0279 ± 0.0012 and 0.0263 ± 0.0014 and 0.0273 ± 0.0006 and 0.0273 ± 0.0004 number of AP.pA⁻¹, before and after LTD-IE and LTP-IE, respectively; One way ANOVA, $P=0.6819$; Fig. 3, B, C). Therefore, there was no change in the gain of the firing response. Altogether, these results indicate that LTD-IE and LTP-IE in naïve S1 L2/3 pyramidal neurons result from simple rightward and leftward shifts in the F-I curves, respectively.

To further examine changes in the intrinsic properties, we analyzed the properties of APs (Table 1). We found that the LTD-IE after pairings to -20mV was associated with a 2-mV depolarizing shift in the voltage threshold and an enhanced rheobase, AP amplitude and AHP, indicating that, after induction of LTD-IE, neurons fail to respond to previously suprathreshold inputs. Conversely, the increase in intrinsic excitability after pairings to ≥ -10 mV was associated with a ≈ 5 mV polarizing shift in the voltage threshold, and a reduced rheobase, AP amplitude

and AHP, indicating that, after LTP-IE, neurons become responsive to previously subthreshold inputs. In addition, AP duration was enhanced. Importantly, the observation that the level of postsynaptic depolarization during pairing determined the direction of the changes in AP properties strongly suggest that these changes did not merely reflect alteration in the microelectrode or general health of the impaled cell.

Given that L2/3 pyramidal neurons integrate tremendous input from subcortical regions and generate output signals to lamina V output neurons, we questioned whether the strategy for the information processing would be changed during LTD-IE and LTP-IE. To answer this question, we investigated spike frequency adaption (SFA), which operates to filter the output signal by attenuating unnecessary firing (Benda and Herz, 2003; Pozzorini et al., 2013). To determine SFA, all interspike intervals (ISIs) of the firing responses to 770-pA-steps were calculated and normalized to the first ISIs. Despite the reduction or increase in the firing rates corresponding to LTD- and LTP-IE, there was no significant change in calculated SFA compared with baseline (Fig. 3 D, E). We concluded that LTD- or LTP-IE do not manifest as changes in the strategy of information process, but only modify the gain of the firing rates.

We also assessed whether blocking NMDAR during pairing could prevent LTD- and LTP-IE (Fig. 2). Interestingly, bath-applied DL-AP-5 (200 mM) prevented synaptic but not intrinsic plasticity. Following pairings to -20mV in the presence of AP5, F-I curves were still shifted to the right, intrinsic excitability being decreased over the whole range of suprathreshold currents ($n=5$; $N=5$; One-way ANOVA for repeated measures, $P<0.001$) (Fig. 2C). The response to 770-pA-steps, 30 min after pairing, were $71.1 \pm 1.7\%$ of baseline (not different from that in control conditions; One-way ANOVA, $P=0.7693$). Following pairings to 0mV in the presence of AP5, F-I curves were shifted to the left (Fig. 2D). As in control conditions, intrinsic excitability was decreased over the whole range of suprathreshold currents ($n=5$; $N=5$; One-way ANOVA for repeated measures, $P<0.05$), and the firing response to 770-pA-steps, 30 min after pairing,

were $146.9 \pm 6.7\%$ of baseline (not different from that in control conditions; One-way ANOVA, $P=0.5170$).

The level of postsynaptic depolarization does not determine the magnitude of intrinsic plasticity in S1 L2/3 pyramidal neurons

Since pairings to the four Vms, -10, 0, +10 and +20 mV, produced increasing levels of synaptic potentiation, we questioned whether they also induced increasing levels of LTP-IE. To address this issue, we plotted the four pairs of F-I curves, before and after pairing to -10, 0, +10 and +20 mV (Fig. 4A). There was no difference in the four baseline F-I curves: both in the firing responses to 770-pA-steps (6.5 ± 0.2 , 5.6 ± 0.1 , 6.3 ± 0.4 and 6.5 ± 0.5 APs before pairing to -10, 0, +10 and +20 mV, respectively; One-way ANOVA, $P=0.3303$) and the slopes of F-I curves (0.0269 ± 0.0010 , 0.0274 ± 0.0009 , 0.0274 ± 0.0013 and 0.0272 ± 0.0025 AP.pA⁻¹ before pairing to -10, 0, +10 and +20 mV, respectively; $P=0.9855$). Importantly, there was also no difference in the four F-I curves after pairing: neither in the firing responses to 770-pA-steps (770 pA: $143.2 \pm 4.9\%$, $150.5 \pm 2.5\%$, $150.9 \pm 11.5\%$ and $150.3 \pm 7.6\%$ APs after pairing to -10, 0, +10 and +20 mV, respectively; $P=0.7821$) nor the slopes of F-I curves (0.0273 ± 0.0007 , 0.0263 ± 0.0009 , 0.0277 ± 0.0008 and 0.0273 ± 0.0009 AP.pA⁻¹ after pairing to -10, 0, +10 and +20 mV, respectively; $P=0.3320$). Therefore, whereas the magnitude of synaptic LTP continuously increased with the level of post-synaptic depolarization within the -10 to +20 mV Vm range, that of LTP-IE stayed constant once post-synaptic polarization had reached Θ^+ .

Moreover, as LTP-IE, the changes in AP properties were similar after pairings to -10, 0, +10 and +20 mV (Fig. 4 B-E). That changes in intrinsic excitability were correlated with changes in AP properties but not with those of synaptic efficacy, strongly suggests that LTP-IE was derived from altered intrinsic properties and not from increased synaptic weight.

The two voltage-response curves, for synaptic and intrinsic plasticity, in naïve conditions

(synapses and postsynaptic neuron) are displayed in Fig. 4F. LTD- and LTP-IE were found to occur concomitantly with synaptic LTD and LTP, respectively, but their magnitudes were not correlated. Of note, the magnitude of LTP-IE was already maximum after pairing to -10 mV, even larger than that of synaptic LTP.

Synaptic plasticity rule in potentiated conditions

Having established that synaptic and intrinsic plasticities synergistically vary in S1 L2/3 pyramidal neurons, we then explored how the induction of synaptic LTD/LTP was altered by prior induction of synaptic/intrinsic plasticity.

The evidence in adult hippocampal CA1 that LFS can depress potentiated responses while producing little or no depression in naïve synapses (Barrionuevo et al., 1980; Staubli and Lynch, 1990; Fujii et al., 1991; Larson et al., 1993; Bortolotto et al., 1994; O'Dell and Kandel, 1994; Norris et al., 1996; Wagner and Alger, 1995) suggests that, in potentiated synapses, induction of synaptic LTD requires a lower level of postsynaptic depolarization. Consistently, it was shown in CA1, using a pairing protocol, that the LTD threshold or Θ^- is shifted to the left in potentiated synapses (Ngezahayo *et al.*, 2000). Therefore, in a first series of experiments, we tested whether pairings at V_{ms} which had no effect in naïve conditions could depress synapses in potentiated conditions, i.e. potentiated synaptic strength and intrinsic excitability. We applied a first, or conditioning, pairing to 0 mV to potentiate synaptic strength and intrinsic excitability and a second, or test pairing, to various V_{ms} , 30 min later, that is once synaptic transmission had stabilized after the first pairing. The second pairing could occur late after the beginning of the recording as, whereas factors required for LTP induction dialyze out of the recorded neuron, those for LTD induction do not (Stevens and Wang, 1994; Ngezahayo *et al.*, 2000). While a test pairing to -40 mV had no net effect (compared with values before the test pairing), test pairings to -30 and -20 mV induced a significant relative depression (test pairing to -30mV: $80.2 \pm 1.3\%$

of baseline before this test pairing; One way ANOVA for repeated measures: $P < 0.0001$; $n = 4$; $N = 4$; test pairing to -20 mV: $49.2 \pm 1.8\%$ of baseline before the test pairing; $P < 0.0001$; $n = 7$; $N = 7$) (Fig. 5 A, B). Normalizing EPSC amplitudes to baseline before the test pairings, revealed that the range for LTD-inducing V_m in potentiated conditions—synaptic strength and intrinsic excitability—had not only a lower limit, between -40 mV and -30 mV, but also an upper one, at 0 mV, indicating that LTD can only be induced within a limited V_m range, even when LTP cannot be obtained.

These results show that in S1 vertical input-L2/3 pyramidal neuron synapses, too, the voltage threshold for LTD induction, or Θ^- , is shifted, about 10 mV, to the left: from between -30 mV and -20 mV to between -40 mV and -30 mV in potentiated conditions. But they also suggest that the voltage threshold for LTP induction, or Θ^+ , is concomitantly shifted to the right, that is in opposite direction. However, it is not possible to conclude from the above experiments that there is an actual rightward shift in Θ^+ since mechanisms required for LTP induction have dialyzed out of the recorded neuron. Therefore, in a second series of experiments, the second (test) pairing was applied less than 10 min after the first (conditioning) pairing to 0 mV. Serial ordered pairings to $0/0$ mV, $0/10$ mV and $0/20$ mV produced LTP. Nevertheless, only pairings to $0/10$ mV and 0 mV/ 20 mV serials produced a larger LTP than that after a single pairing to 0 mV (pairings to $0/10$ mV: $233.2 \pm 11.5\%$ of baseline before pairings to $0/10$ mV serial, $n = 3$, $N = 3$; One way ANOVA for repeated measures: $P < 0.0001$; pairings to $0/20$ mV: $288.1 \pm 9.1\%$ of baseline before pairings to $0/20$ mV serial, $n = 4$, $N = 4$; $P < 0.0001$; pairings to $0/10$ mV and 0 mV/ 20 mV serials vs. single pairing to 0 mV, One way ANOVA, $P < 0.0001$) (Fig. 5 C). To assess the net effect of the test pairing to 0 mV, 10 mV and 20 mV in these potentiated conditions, we normalized synaptic changes after serial conditioning/test pairings to that of a single pairing to 0 mV. This confirmed that the voltage threshold for LTP induction, or Θ^+ , was at 0 mV. Altogether, the comparison of the two voltage-response curves for the induction of synaptic plasticity (synaptic plasticity rules) in naïve and potentiated conditions (obtained by combining

the results from the two series of experiments, before and after washout of LTP mechanisms; Fig. 5 D, E) shows that the latter exhibits: (i) a larger range of LTD-inducing Vms, (from between -40 mV and -30 mV to 0 mV) due to opposite shifts in Θ^- and Θ^+ , (ii) a larger maximum magnitude of LTD (pairing to -20 mV in potentiated and naïve conditions: $-50.8 \pm 1.8\%$ and $-33.1 \pm 1.2\%$ of baseline before the test pairing, respectively; One way ANOVA, $P < 0.0001$) (iii) smaller magnitude of synaptic LTP at intermediate (pairing to 10 mV in potentiated and naïve conditions: $+66.5 \pm 11.5\%$ and $+88.5 \pm 5.9\%$ of baseline before the test pairing, respectively; $P < 0.0001$) but not very depolarized Vms (pairing to 20 mV in potentiated and naïve conditions: $+126.1 \pm 9.1\%$ and $+115.2 \pm 17.7\%$ of baseline before the test pairing, respectively; $P = 0.0941$) (Fig. 5F).

Synaptic plasticity rule in depressed conditions

To assess changes in the voltage-response curve for the induction of synaptic plasticity in depressed conditions—synaptic strength and intrinsic excitability—, we applied two successive pairings, a first or conditioning pairing to -20mV to depress synapses and less than 10 min later a second or test pairing to various Vms. Serial ordered pairings to -20/-40mV, -20/-30mV and -20/-20mV produced the very same depression as a single pairing to -20mV (pairings to -20/-30 mV: $68.7 \pm 1.4\%$ of baseline before pairings to -20/-30 mV serial; One way ANOVA for repeated measures: $P < 0.0001$; $n=3$; $N=3$; pairing to -20/-20 mV: $67.3 \pm 2.0\%$ of baseline before pairings to -20/-20 mV serial; $P < 0.0001$; $n=4$; $N=4$; compared with the effect of a single pairing to -20 mV: $66.9 \pm 1.2\%$ of baseline; see above; pairings to -20/-30 mV and -20/-20 mV serials vs. single pairing to -20 mV: One way ANOVA, $P = 0.2355$) (Fig. 6A, B), suggesting that test pairings to -40, -30 and -20mV had no effect on synaptic transmission in depressed conditions—synaptic strength and intrinsic excitability. On the other hand, serial ordered pairings to -20/-10mV and -20/0mV produced a potentiation (pairings to -20/-10mV: $119.8 \pm$

10.0% of baseline before pairings to -20/-10 mV serial; One way ANOVA for repeated measures: $P < 0.0001$; $n=4$; $N=4$; compared with the effect of a single pairing to -20mV: $66.9 \pm 1.2\%$ of baseline; pairings to -20/-30 mV and -20/-20 mV serials vs. single pairing to -20 mV: One way ANOVA, $P=0.2355$) (Fig. 6A, B), suggesting that pairings to $V_{ms} \geq -10\text{mV}$ could potentiate synaptic transmission in depressed conditions—synaptic strength and intrinsic excitability. To assess the net effect of the test pairing in depressed conditions, we normalized synaptic changes after the different serial ordered conditioning/test pairings to that after a single pairing to -20 mV. The resulting voltage-response curve for the induction of synaptic plasticity (or synaptic plasticity rule) in depressed conditions—synaptic strength and intrinsic excitability—exhibited a single voltage threshold curve, for LTP induction: there was no longer V_m range for inducing LTD and test pairing to -10mV produced larger synaptic potentiation than in naïve conditions (pairing to -10mV in depressed and naïve conditions: $+66.1 \pm 4.8\%$ and $+28.8 \pm 2.1\%$, respectively; One way ANOVA, $P < 0.0001$; pairing to 0 mV in depressed and naïve conditions: $+85.2 \pm 0.1\%$ and $+61.7 \pm 3.3\%$, respectively; $P < 0.0001$).

Intrinsic plasticity rule in potentiated conditions

The above results show how prior synergistic synaptic and intrinsic changes modulate the ability of S1 vertical input-L2/3 pyramidal neuron synapses to exhibit synaptic LTD and LTP. They demonstrate that changes in synaptic efficacy can be reversed—previously potentiated synapses can be subsequently depressed and previously depressed synapses subsequently potentiated—provided that synaptic activation is paired with the right level of post-synaptic depolarization. These findings raise the question as to whether prior synergistic synaptic and intrinsic changes also modulate the ability of S1 L2/3 pyramidal neurons to undergo LTD-IE and LTP-IE.

We first addressed this question after prior induction of synaptic and intrinsic LTP by a first

(conditioning) pairing to 0mV. The intrinsic excitability of S1 L2/3 pyramidal neurons was assessed 30 min after the second, test pairing of serial ordered pairings to 0mV/test Vm. The net effect of the test pairings on F-I curves – compared with that of a single pairing to 0 mV – depended on the level of postsynaptic depolarization during pairing. Test pairings to -40 mV had no net effect on F-I curves, that is pairings to 0/-40mV serials produced the same rightward shift as a single pairing to 0 mV (Fig. 7 A). On the other hand, intrinsic excitability was strongly decreased after pairings to 0/-30mV, 0/-20mV and 0/-10mV serials. Importantly, not only the firing response to a 770-pA-step ($40.1 \pm 7.8\%$ of pre-pairings to 0/test Vm serials; $n=5, N=5$; One way ANOVA, $P<0.05$), but also the gain of the firing response (slope of F-I curve: 0.0095 ± 0.0012 after compared with 0.0267 ± 0.0017 AP.pA⁻¹ before pairings to 0/test Vm serials; $n=5, N=5$; $P<0.05$) were reduced (Fig. 7 C, E). Of note, intrinsic changes after pairings to 0/-30mV, 0/-20mV and 0/-10mV serials were the very same (Fig. 7C). Thus, test pairings to -30 mV, -20 mV or -10 mV, which reversed synaptic LTP, did not simply reverse the leftward shift in F-I curve of LTP-IE but strongly depressed the whole firing response of S1 L2/3 pyramidal neurons. Test pairings to 0 mV had no net effect on F-I curves, whether they were applied soon or later after the conditioning pairing to 0 mV, as they produced the same rightward shift as a single pairing to 0 mV (Fig. 7 B). Finally, unexpectedly, intrinsic excitability was also strongly decreased after pairings to 0/10mV and 0/20mV serials ($46.9 \pm 4.0\%$; of pre-pairings to 0/test Vm serials; $n=7, N=7$; One way ANOVA, $P<0.0001$; slope of the F-I curve: 0.0126 ± 0.0025 after compared with 0.0265 ± 0.0013 AP.pA⁻¹ before pairings to 0/test Vm serials; $n=7, N=7$; $P<0.0001$) (Fig. 7 D, E). As previously, there was no difference in the intrinsic changes produced by pairings to 0/10mV and 0/20mV serials (Fig. 7 D). Finally, comparison of F-I curves after pairings to 0/-30mV, 0/-20mV and 0/-10mV serials and after pairings to 0/10mV and 0/20mV serials (Fig. 7 E) shows that changes in the neuronal intrinsic excitability were the same. Importantly, they were also associated with a similar ~27% increase in Rin (Table 2). Of

note, for the sake of simplicity, we compared intrinsic excitability after versus before pairings to 0/test Vm serials. Test pairing-induced LTD-IE was therefore underestimate as intrinsic excitability after pairings to test Vm serial should have been compared with that, potentiated, after pairing to 0mV.

The two voltage-response curves, for synaptic and intrinsic plasticity (or synaptic and intrinsic plasticity rules), in potentiated–synaptic and intrinsic–conditions are displayed in Fig. 7F. Importantly, whereas the very same LTD-IE occurred concomitantly with both synaptic LTD and LTP, there was no intrinsic plasticity in between, at the synaptic LTP threshold. As previously, there was no correlation between the magnitudes of synaptic and intrinsic plasticity.

Intrinsic plasticity rule in depressed conditions

We also examined the changes in intrinsic excitability of S1 L2/3 pyramidal neurons after prior induction of synaptic and intrinsic LTD by a first, conditioning pairing to -20mV. The intrinsic excitability of S1 L2/3 pyramidal neurons was assessed 30 min after the second, test pairing of serial ordered pairings to -20 mV/test Vm. Again, the net effect of test pairings on F-I curves—compared with that of a single pairing to -20mV—depended on the level of postsynaptic depolarization during pairing. Pairings to -20/-40mV, -20/-30mV and -20/-20mV serials produced the very same rightward shift as a single pairing to -20 mV: the response to a 770-pA-step was reduced ($-77.3 \pm 5.3\%$ of baseline before pairings to -20 mV/test Vm serials; $n=9$, $N=9$; One way ANOVA, $P<0.005$; compared with that $-71.9 \pm 3.1\%$ —after a single pairing to -20mV: $P=0.84$) but the gain of the firing response was not changed (slope of the F-I curve: 0.0254 ± 0.0010 AP.pA⁻¹ after compared with 0.0256 ± 0.0008 AP.pA⁻¹ before pairings to -20 mV/test Vm serials; $n=9$, $N=9$; $P=0.7695$) (Fig. 8 A). Again, changes in intrinsic excitability were the same after pairings to -20/-40mV, -20/-30mV and -20/-20mV serials (not shown). This suggests that test pairings to -40, -30 and -20mV, which have no net effect of synaptic strength, have also no net effect on the intrinsic excitability of postsynaptic S1 L2/3 pyramidal neurons

(compare figures 8 A and 2C and 3B). On the other hand, pairings to -20/-10mV and -20/0mV serials produced no rightward shift: neither the response to a 770-pA-step ($+105.9 \pm 5.0\%$ of baseline before pairings to -20 mV/test Vm serials; One way ANOVA, $P=0.7911$; compared with that $-71.9 \pm 3.1\%$ of a single pairing to -20mV: $P<0.0001$) nor the gain of the firing response were changed (slope of the F-I curve: 0.0265 ± 0.0013 AP.pA⁻¹ after compared with 0.0256 ± 0.0008 AP.pA⁻¹ before pairings to -20 mV/test Vm serials; $n=7$, $N=7$; $P=0.9789$) (Fig. 8 B). There was also no difference in the properties of APs and after-hyperpolarization before and after pairings to -20/-10mV and -20/0mV serials (Table 3). This suggests that test pairings to -10mV or 0mV could reverse pairing to -20 mV-induced both (i) rightward shift in the F-I curves and (ii) changes in the properties of APs and after-hyperpolarization.

The two voltage-response curves, for synaptic and intrinsic plasticity (synaptic and intrinsic plasticity rules, in depressed-synaptic and intrinsic-conditions are displayed in Fig. 8C. LTP-IE was found to occur concomitantly with synaptic LTP. Again, there was no correlation between the magnitudes of synaptic and intrinsic plasticity.

DISCUSSION

Brief (<1 min), low frequency (2 Hz) stimulation of vertical inputs to S1 L2/3 pyramidal neurons induces bidirectional synaptic and intrinsic plasticity. Their direction depends on both the level of post-synaptic depolarization and initial synaptic/neuronal state. In most cases, intrinsic changes occur in parallel with synaptic modifications (synergistic changes). In naïve conditions, pairing to low Vms—below Θ^- ($-30\text{mV} > \Theta^- > -20$ mV)—has no effect, to higher Vms—over Θ^- but below Θ^+ ($-20\text{mV} > \Theta^+ > -10$ mV)—induces synaptic/intrinsic LTD and to even higher Vms—over Θ^+ —induces synaptic/intrinsic LTP. In depressed conditions, Θ^- is shifted toward more depolarized Vms and Θ^+ toward more polarized Vms, occluding the window for synaptic/intrinsic LTD—further synaptic/intrinsic LTD cannot be obtained—while

synaptic/intrinsic LTP is facilitated. Conversely, in potentiated conditions, Θ^- is shifted toward more polarized Vms and Θ^+ toward more depolarized Vms, opening the window for synaptic/intrinsic LTD. But, then, pairings to $V_{ms} > \Theta^+$ induce synaptic LTP but homeostatic LTD-IE.

Synaptic plasticity rule

Our description of the synaptic plasticity rule for naïve S1 vertical input-L2/3 pyramidal neuron synapses involves two voltage-dependent thresholds, for LTD and LTP induction, as defined in the Artola, Bröcher and Singer (ABS) rule of synaptic plasticity (Artola et al., 1990; Artola and Singer, 1993). There are multiple evidence for a voltage-threshold for NMDAR-dependent LTD: (i) pairing-induced LTD always requires a postsynaptic depolarization (S1: Feldman, 2000; Sjöström et al., 2004; anterior cingulate cortex: Toyoda et al., 2005; entorhinal/perirhinal cortex: Griffiths et al., 2008; CA1; Ngezahayo et al., 2000; Artola et al., 2005), and (ii) hyperpolarizing postsynaptic hippocampal neurons during LFS prevents synaptic LTD (Mulkey and Malenka, 1992; Deisseroth et al., 1996). That the level of postsynaptic depolarization determines the direction of NMDAR-dependent synaptic plasticity was demonstrated by selectively varying the (i) rate of presynaptic stimulation (CA1: Dudek and Bear, 1992; visual cortex: Kirkwood et al., 2003; Kirkwood and Bear, 2004; S1: Aroniadou-Anderjaska and Keller, 1995; Castro-Alamancos et al., 1995; Kitagawa et al., 1997) or (ii) postsynaptic current injection during presynaptic stimulation (CA1: Ngezahayo et al., 2000; anterior cingulate cortex: Toyoda et al., 2005; S1 cortex: Feldman, 2000).

Activity-dependent changes in the synaptic plasticity rule for S1 vertical input-L2/3 pyramidal neuron synapses involve concomitant opposite shifts in the LTD and LTP voltage-thresholds. In the Bienenstock, Cooper, and Munro (BCM) model (Bienenstock et al., 1982), a single threshold—the modification threshold, θ_m , or LTP threshold—slides as a function of the recent integrated postsynaptic activity—: θ_m is reduced in weakly active neurons whereas it is raised

in hyperactive neurons. The shifts in our Θ^+ match the predicted θm shifts assuming that active synapses are depressed on weakly active neurons and potentiated on hyperactive neurons. But our experimental data demonstrate that activity-dependent changes in the synaptic plasticity rule in S1 neocortex involve, as in hippocampal CA1 (Ngezahayo et al., 2000), the concomitant shifts in the second voltage-threshold, Θ^- . Consistent with the conclusion that when Θ^- slides toward more polarized Vms, facilitating LTD induction, Θ^+ concomitantly slides toward more depolarized Vms, inhibiting LTP induction, stimulation patterns that facilitate subsequent LTD induction also inhibit subsequent LTP induction (Fujii et al., 1991; Christie and Abraham, 1992; Christie et al., 1995). Furthermore, both LFS, which has little or no effect (Barrionuevo et al., 1980; Staubli and Lynch, 1990; Fujii et al., 1991; Larson et al., 1993; Wexler and Stanton, 1993; Bortolotto et al., 1994; O'Dell and Kandel, 1994; Wagner and Alger, 1995; Norris et al., 1996), and tetani, which produce LTP (Yang and Faber, 1991), can subsequently induce LTD (see Abraham, 2008).

There are several issues to be noted. First, there is a limited Vm range for inducing LTD. The voltage window for LTD induction—assessed in isolation after washout of LTP mechanisms—in potentiated conditions extends from -40/-30 mV to 0 mV. Second, this voltage window for LTD induction varies with the synapse/neuron state. In depressed conditions, it even closes. This is not due to saturation but to inhibition of LTD induction: the capacity of inducing LTD in depressed conditions can be recovered by increasing postsynaptic depolarization at levels at which LTP is normally induced (Ngezahayo et al., 2000). Finally, synaptic activity can produce similarly large LTP in potentiated as in naïve conditions, provided that the level of postsynaptic depolarization is increased.

Intrinsic plasticity rule

In naïve conditions, LTD-IE and LTP-IE manifested as rightward and leftward shifts, respectively—with changes in neither the slope of F-I curves nor R_{in} . Moreover, synaptic and

intrinsic plasticity rules were parallel, exhibiting the very same two voltage-thresholds. Synergistic synaptic and intrinsic changes were already observed in CA1 pyramidal neurons (Daoudal *et al.*, 2002; Wang *et al.*, 2003; Xu *et al.*, 2005; Campannac and Debanne, 2008; Gosselin *et al.*, 2017) and cerebellar granule (Armano *et al.*, 2006; ± Rizwan *et al.*, 2016) and Purkinje cells (Belmeguenai *et al.*, 2010; Ohtsuki *et al.*, 2012; Shim *et al.*, 2017; but see Yang and Santamaria, 2016). Moreover, parallel frequency-dependent (Daoudal *et al.*, 2002) or spike-timing-dependent (Campannac and Debanne, 2008) synaptic and intrinsic plasticity rules were observed in hippocampal CA1. Of note, in cerebellar granule cells, LTP-IE required a weaker input than synaptic LTP (Armano *et al.*, 2000).

The present results also provide evidence for activity-dependent changes in the intrinsic plasticity rule. In depressed conditions, synaptic and intrinsic plasticity rules underwent parallel changes, exhibiting the same single voltage-threshold for synaptic LTP and LTP-IE. LTP-IE manifested as a reversal of the rightward shift in the F-I curve, or LTD-IE, produced by the first, conditioning pairing to -20mV. Such reversibility does not occur in Purkinje cells (Shim *et al.*, 2017).

In potentiated conditions, only LTD-IE was observed, manifested as a strong decrease in the gain of the F-I curve associated with enhanced R_{in} . Of great interest, the same LTD-IE occurred with both synaptic LTD (synergistic) and LTP (homeostatic). Experimental artifacts cannot account for such reduced F-I gain: it occurred only when test pairings induced net synaptic LTD or LTP—F-I gain was unchanged after pairings below Θ^- or at Θ^+ —and whether synaptic LTP mechanisms were washed out, or not. Importantly, homeostatic LTD-IE was associated with large synaptic LTP as in CA1 (Fan *et al.*, 2005; Narayanan & Johnston, 2006; Campannac *et al.*, 2008).

That the synaptic and intrinsic plasticity rules undergo parallel activity-dependent changes raises the question as to whether their expressions are correlated. This is unlikely. First,

blocking NMDAR prevented synaptic but not intrinsic plasticity. High frequency stimulation-induced LTP-IE in cerebellar deep nuclear neurons (Aizenman and Linden, 2000) and granule cells (Armano *et al.*, 2000; Rizwan *et al.*, 2016) and in CA1 pyramidal cells (Campanac *et al.*, 2008) requires NMDAR activation. Such discrepancy might stem from the different areas. Yet, another possibility is that, here, we used a pairing protocol, artificially depolarizing the postsynaptic neuron during afferent stimulation. Since, both LTD-IE (Shim *et al.*, 2017) and LTP-IE (Aizenman and Linden, 2000; Belmeguenai *et al.*, 2010) depend on $[Ca^{2+}]_i$ signaling, postsynaptic depolarization during pairing might help provide enough Ca^{2+} influx to trigger LTD-IE and LTP-IE. Consistently, directly depolarizing postsynaptic neurons can induce LTP-IE (Aizenman and Linden, 2000; Sourdet *et al.*, 2003; Cudmore and Turrigiano, 2004; Belmeguenai *et al.*, 2010; Paz *et al.*, 2009) and LTD-IE: Paz *et al.*, 2009; Shim *et al.*, 2017). Voltage-dependent thresholds for LTD-IE and LTP-IE might thus reflect thresholds in $[Ca^{2+}]_i$ signaling as for synaptic plasticity.

Second, intrinsic changes appear to be ‘all or none’, not correlated with synaptic ones. Intrinsic plasticity results from modifications of voltage- or calcium-dependent ion channels including A-type K channels (Frick *et al.*, 2004), large-conductance, calcium-dependent K channels (Nelson *et al.*, 2005), small conductance, calcium-dependent K channels (Sourdet *et al.*, 2003; Lin *et al.*, 2008; Belmeguenai *et al.*, 2010), as well as hyperpolarization-activated and cyclic nucleotide-gated (HCN) channels (*I_h*; Nolan *et al.*, 2003; Fan *et al.*, 2005; Brager and Johnston, 2007; Campanac *et al.*, 2008; Gasselin *et al.*, 2017). We did not address the mechanisms of intrinsic plasticity in S1. However, in CA1, R_{in} increase is associated with down-regulated *I_h* and LTP-IE (Brager *et al.*, 2007; Campanac *et al.*, 2008; Gasselin *et al.*, 2017). Here, enhanced R_{in} was associated with LTD-IE, suggesting that *I_h* are not involved.

Intrinsic plasticity and synaptic metaplasticity

That activity-induced changes in the synaptic plasticity rule involves concomitant shifts in

opposite directions of the two thresholds, for LTD and LTP, put constraints on their mechanisms. Intrinsic plasticity, through regulating postsynaptic depolarization, certainly modulates subsequent induction of synaptic plasticity. For instance, reduced AHPs facilitates LTP induction (Sah and Bekkers, 1996). But, LTP-IE and LTD-IE, whereas they can account for a facilitation and inhibition, respectively, of a synaptic change, cannot explain the inhibition and facilitation, respectively, of the other one.

Altogether, our results suggest that synaptic activity triggers several processes which can modulate subsequent induction of synaptic plasticity. They include homeostatic metaplasticity, restricted to activated synapses (see Abraham et al., 2008) and synergistic/homeostatic intrinsic plasticity involving all, activated and non-activated, inputs synapsing on the postsynaptic neuron.

REFERENCES

- Abraham WC (2008) Metaplasticity: tuning synapses and networks for plasticity. *Nat Rev Neurosci.* 9:387-399.
- Abraham WC, Bear MF (1996) Metaplasticity: the plasticity of synaptic plasticity. *Trends Neurosci* 19:126–130.
- Abraham WC, Gustafsson B, Wigstrom H (1987) Long-term potentiation involves enhanced synaptic excitation relative to synaptic inhibition in guinea-pig hippocampus. *J Physiol* 394, 367–380.
- Abraham WC, Huggett A (1997) Induction and reversal of long-term potentiation by repeated high-frequency stimulation in rat hippocampal slices. *Hippocampus* 7:137–145.
- Abraham WC, Tate WP (1997) Metaplasticity: a new vista across the field of synaptic plasticity. *Prog Neurobiol* 52:303–323.
- Agmon A, Connors BW (1991) Thalamocortical responses of mouse somatosensory (barrel) cortex in vitro. *Neuroscience* 41:365-380.
- Aizenman CD, Linden DJ (2000) Rapid, synaptically driven increases in the intrinsic excitability of cerebellar deep nuclear neurons. *Nat Neurosci* 3:109-111.
- Armano S, Rossi P, Taglietti V, D'Angelo E (2000) Long-term potentiation of intrinsic excitability at the mossy fiber-granule cell synapse of rat cerebellum. *J Neurosci.* 20:5208-5216.
- Aroniadou-Anderjaska V, Keller A (1995) LTP in the barrel cortex of adult rats. *Neuroreport* 6:2297–2300.
- Artola A, Singer W (1993) Long-term depression of excitatory synaptic transmission and its relationship to long-term potentiation. *Trends Neurosci* 16:480–487.

- Artola A, Bröcher S, Singer W (1990) Different voltage-dependent thresholds for inducing long-term depression and long-term potentiation in slices of rat visual cortex. *Nature* 347:69 – 72.
- Artola A, Kamal A, Ramakers GM, Biessels GJ, Gispen WH (2005) Diabetes mellitus concomitantly facilitates the induction of long-term depression and inhibits that of long-term potentiation in hippocampus. *Eur J Neurosci* 22:169-178.
- Barrionuevo G, Schottler F, Lynch G (1980) The effects of repetitive low frequency stimulation on control and “potentiated” synaptic responses in the hippocampus. *Life Sci* 27:2385–2391.
- Bienenstock EL, Cooper LN, Munro PW (1982) Theory for the development of neuron selectivity: orientation specificity and binocular interaction in visual cortex. *J Neurosci* 2:32– 48.
- Belmeguenai A, Hosy E, Bengtsson F, Pedroarena C, Piochon C, Teuling E, He Q, Ohtuski G, De Jeu MT, Elgersma Y, De Zeeuw CI, Jorntell H, Hansel C (2010) Intrinsic plasticity complements long-term potentiation in parallel fiber input gain control in cerebellar Purkinje cells. *J Neurosci* 30:13630 –13643.
- Benda J, Herz AV (2003) A universal model for spike-frequency adaptation. *Neural Comput* 15:2523–2564.
- Bi GQ, Poo MM (1998) Synaptic modifications in cultured hippocampal neurons: dependence on spike timing, synaptic strength, and postsynaptic cell type. *J Neurosci.* 18:10464-10472.
- Bortolotto ZA, Bashir ZI, Davies CH, Collingridge GL (1994) A molecular switch activated by metabotropic glutamate receptors regulates induction of long-term potentiation. *Nature* 368:740 –743.

- Brager DH, Johnston D (2007) Plasticity of intrinsic excitability during long-term depression is mediated through mGluR-dependent changes in I(h) in hippocampal CA1 pyramidal neurons. *J Neurosci* 27:13926–13937.
- Bröcher S, Artola A, Singer W (1992) Intracellular injection of Ca²⁺ chelators blocks induction of long-term depression in rat visual cortex. *Proc Natl Acad Sci U S A.* 89:123-127.
- Campanac E, Daoudal G, Ankri N, Debanne D (2008) Downregulation of dendritic I(h) in CA1 pyramidal neurons after LTP. *J Neurosci.* 28:8635-8643.
- Campanac E, Debanne D (2008) Spike timing-dependent plasticity: a learning rule for dendritic integration in rat CA1 pyramidal neurons. *J Physiol* 586:779–793.
- Campanac E, Gasselin C, Baude A, Rama S, Ankri N, Debanne D (2013) Enhanced intrinsic excitability in basket cells maintains excitatory-inhibitory balance in hippocampal circuits. *Neuron* 77:712–722.
- Castro-Alamancos, M.A., Donoghue, J.P., and Connors, B.W. (1995) Different forms of synaptic plasticity in somatosensory and motor areas of the neocortex. *J. Neurosci.* 15, 5324– 5433.
- Christie BR, Abraham WC (1992) Priming of associative long-term depression in the dentate gyrus by theta frequency synaptic activity. *Neuron* 8:79–84.
- Christie BR, Stellwagen D, Abraham WC (1995) Evidence for common expression mechanisms underlying heterosynaptic and associative long-term depression in the dentate gyrus. *J Neurophysiol* 74:1244 –1247.
- Coan EJ, Irving AJ, Collingridge GL (1989) Low frequency activation of the NMDA receptor system can prevent the induction of LTP. *Neurosci Lett* 105:205–210.
- Cudmore RH, Turrigiano GG (2004) Long-term potentiation of intrinsic excitability in LV visual cortical neurons. *J Neurophysiol* 92:341-348.
- Cummings JA, Mulkey RM, Nicoll RA, Malenka RC (1996) Ca²⁺ signaling requirements for long-term depression in the hippocampus. *Neuron* 16:825– 833.

- Daoudal G, Hanada Y, Debanne, D (2002) Bidirectional plasticity of excitatory postsynaptic potential (EPSP)-spike coupling in CA1 hippocampal pyramidal neurons. *Proc Natl Acad Sci USA* 99:14512–14517.
- Debanne D, Gähwiler BH, Thompson SM (1998) Long-term synaptic plasticity between pairs of individual CA3 pyramidal cells in rat hippocampal slice cultures. *J. Physiol. (Lond.)* 507: 237–247.
- Deisseroth K, Bito H, Tsien RW (1996) Signaling from synapse to nucleus: postsynaptic CREB phosphorylation during multiple forms of hippocampal synaptic plasticity. *Neuron* 16:89–101.
- Dudek SM, Bear MF (1992) Homosynaptic long-term depression in area CA1 of hippocampus and effects of N-methyl-D-aspartate receptor blockade. *Proc Natl Acad Sci USA* 89:4363–4367.
- Dugué GP, Dumoulin A, Triller A, Dieudonné S (2005) Target-dependent use of co-released inhibitory transmitters at central synapses. *J Neurosci* 25:6490-6498.
- Fan Y, Fricker D, Brager DH, Chen X, Lu HC, Chitwood RA, Johnston D (2005) Activity-dependent decrease of excitability in rat hippocampal neurons through increases in I(h). *Nat Neurosci* 8:1542–1551.
- Feldman DE (2000) Timing-based LTP and LTD at vertical inputs to layer II/III pyramidal cells in rat barrel cortex. *Neuron* 27:45-56.
- Frick, A., Magee, J., and Johnston, D. (2004) LTP is accompanied by an enhanced local excitability of pyramidal neuron dendrites. *Nat. Neurosci.* 7:126–135.
- Fujii S, Saito K, Miyakawa H, Ito K, Kato H (1991) Reversal of longterm potentiation (depotential) induced by tetanus stimulation of the input to CA1 neurons of guinea pig hippocampal slices. *Brain Res* 555:112–122.

- Gasselín C, Inglebert Y, Ankri N, Debanne D (2017) Plasticity of intrinsic excitability during LTD is mediated by bidirectional changes in h-channel activity. *Sci Rep* 7(1):14418.
- Griffiths S, Scott H, Glover C, Bienemann A, Ghorbel MT, Uney J, Brown MW, Warburton EC, Bashir ZI (2008) Expression of long-term depression underlies visual recognition memory. *Neuron* 58(2):186-194.
- Hansel C, Artola A, Singer W (1997) Relation between dendritic Ca²⁺ levels and the polarity of synaptic long-term modifications in rat visual cortex neurons. *Eur J Neurosci* 9:2309-2322.
- Huang Y-Y, Colino A, Selig DK, Malenka RC (1992) The influence of prior synaptic activity on the induction of long-term potentiation. *Science* 255:730–733.
- Huerta PT, Lisman JE (1995) Bidirectional synaptic plasticity induced by a single burst during cholinergic theta oscillation in CA1 in vitro. *Neuron* 15:1053–1063.
- Hölscher C, Anwyl R, Rowan MJ (1997) Stimulation on the positive phase of hippocampal theta rhythm induces long-term potentiation that can be depotentiated by stimulation on the negative phase in area CA1 in vivo. *J Neurosci.* 17:6470-6477.
- Hyman JM, Wyble BP, Goyal V, Rossi CA, Hasselmo ME (2003) Stimulation in hippocampal region CA1 in behaving rats yields long-term potentiation when delivered to the peak of theta and long-term depression when delivered to the trough. *J. Neurosci.* 23:11725–11731.
- Kitagawa H, Nishimura Y, Yoshioka K, Lin M, Yamamoto T (1997). Long-term potentiation and depression in layer III and V pyramidal neurons in the cat sensorimotor cortex in vitro. *Brain Res* 751, 339–343.
- Kirkwood A, Bear MF (1994) Homosynaptic long-term depression in the visual cortex. *J Neurosci* 14:3404-3412.
- Kirkwood A, Dudek SM, Gold JT, Aizenman CD, Bear MF (1993) Common forms of synaptic plasticity in the hippocampus and neocortex in vitro. *Science* 260:1518 –1521.

- Koester HJ, Sakmann B (1998) Calcium dynamics in single spines during coincident pre- and postsynaptic activity depend on relative timing of back-propagating action potentials and subthreshold excitatory postsynaptic potentials. *Proc Natl Acad Sci U S A* 95:9596-9601.
- Larson J, Xiao JP, Lynch G (1993) Reversal of LTP by theta frequency stimulation. *Brain Res* 600:97–102.
- Lin MT, Lujan R, Watanabe M, Adelman JP, Maylie J (2008) SK2 channel plasticity contributes to LTP at Schaffer collateral-CA1 synapses. *Nat. Neurosci.* 11:170–177.
- Lisman J (1989) A mechanism for the Hebb and the anti-Hebb processes underlying learning and memory. *Proc Natl Acad Sci U S A.* 86:9574-9578.
- Markram H1, Lübke J, Frotscher M, Sakmann B (1997) Regulation of synaptic efficacy by coincidence of postsynaptic APs and EPSPs. *Science* 275:213-215.
- Malenka RC, Nicoll RA (1993) NMDA-receptor-dependent synaptic plasticity: multiple forms and mechanisms. *Trends Neurosci* 16:521-527.
- Narayanan R, Johnston D (2007) Long-term potentiation in rat hippocampal neurons is accompanied by spatially widespread changes in intrinsic oscillatory dynamics and excitability. *Neuron* 56:1061–1075.
- Nelson, A.B., Gittis, A.H., and du Lac, S. (2005). Decreases in CaMKII activity trigger persistent potentiation of intrinsic excitability in spontaneously firing vestibular nucleus neurons. *Neuron* 46:623–631.
- Ngezahayo A, Schachner M, Artola, A (2000) Synaptic activity modulates the induction of bidirectional synaptic changes in adult mouse hippocampus. *J. Neurosci.* 20:2451–2458.

- Nolan MF, Malleret G, Lee KH, Gibbs E, Dudman JT, Santoro B, Yin D, Thompson RF, Siegelbaum SA, Kandel ER, Morozov A (2003). The hyperpolarization-activated HCN1 channel is important for motor learning and neuronal integration by cerebellar Purkinje cells. *Cell* 115:551–564.
- Norris CM, Korol DL, Foster TC (1996) Increased susceptibility to induction of long-term depression and long-term potentiation reversal during aging. *J Neurosci* 16:5382–5392.
- O'Dell TJ, Kandel ER (1994) Low-frequency stimulation erases LTP through an NMDA receptor-mediated activation of protein phosphatases. *Learn Mem* 1:129–139.
- Ohtsuki G, Piochon C, Adelman JP, Hansel C (2012) SK2 channel modulation contributes to compartment-specific dendritic plasticity in cerebellar Purkinje cells. *Neuron* 75:108-120.
- Paz JT, Mahon S, Tiret P, Genet S, Delord B, Charpier S (2009) Multiple forms of activity-dependent intrinsic plasticity in layer V cortical neurones in vivo. *J Physiol* 587(Pt 13):3189-205.
- Pozzorini C, Naud R, Mensi S, Gerstner W (2013) Temporal whitening by power-law adaptation in neocortical neurons. *Nat Neurosci* 16:942–948.
- Sessolo M, Marcon I, Bovetti S, Losi G, Cammarota M, Ratto GM, Fellin T, Carmignoto G (2015) Parvalbumin-Positive Inhibitory Interneurons Oppose Propagation But Favor Generation of Focal Epileptiform Activity. *J Neurosci* 35:9544-9557.
- Rizwan AP, Zhan X, Zamponi GW, Turner RW (2016) Long-Term Potentiation at the Mossy Fiber-Granule Cell Relay Invokes Postsynaptic Second-Messenger Regulation of Kv4 Channels. *J Neurosci* 36:11196-11207.
- Sah P, Bekkers JM (1996) Apical dendritic location of slow afterhyperpolarization current in hippocampal pyramidal neurons: implications for the integration of long-term potentiation. *J Neurosci*. 16:4537-4542.

- Shim HG, Jang DC, Lee J, Chung G, Lee S, Kim YG, Jeon DE, Kim SJ (2017) Long-Term Depression of Intrinsic Excitability Accompanied by Synaptic Depression in Cerebellar Purkinje Cells. *J Neurosci* 37:5659–5669.
- Sjöström PJ, Turrigiano GG, Nelson SB (2004) Endocannabinoid-dependent neocortical layer-5 LTD in the absence of postsynaptic spiking. *J Neurophysiol* 92:3338-3343.
- Sourdet V, Russier M, Daoudal G, Ankri N, Debanne D (2003) Long-term enhancement of neuronal excitability and temporal fidelity mediated by metabotropic glutamate receptor subtype 5. *J Neurosci* 23:10238-10248.
- Staubli U, Lynch G (1990) Stable depression of potentiated synaptic responses in the hippocampus with 1–5 Hz stimulation. *Brain Res* 513:113–118.
- Stevens CF, Wang Y (1994) Changes in reliability of synaptic function as a mechanism for plasticity. *Nature* 371:704 –707.
- Toyoda H1, Zhao MG, Zhuo M (2005) Roles of NMDA receptor NR2A and NR2B subtypes for long-term depression in the anterior cingulate cortex. *Eur J Neurosci* 22:485-494.
- Wagner JJ, Alger BE (1995) GABAergic and developmental influences on homosynaptic LTD and depotentiation in rat hippocampus. *J Neurosci* 15:1577–1586.
- Wang Y, Wu J, Rowan MJ, Anwyl R (1998) Role of the protein kinase C in the induction of homosynaptic long-term depression by brief low frequency stimulation in the dentate gyrus in the rat hippocampus in vitro. *J Physiol (Lond)* 513.2:467– 475.
- Wang Z, Xu NL, Wu CP, Duan S, Poo MM (2003) Bidirectional changes in spatial dendritic integration accompanying long-term synaptic modifications. *Neuron* 37:463-472.
- Wespatat V, Tennigkeit F, Singer, W (2004) Phase sensitivity of synaptic modifications in oscillating cells of rat visual cortex. *J. Neurosci* 24:9067–9075.
- Wexler EM, Stanton PK (1993) Priming of homosynaptic long-term depression in hippocampus by previous synaptic activity. *NeuroReport* 4:591–594

- Xu J, Kang N, Jiang L, Nedergaard M, Kang J (2005) Activity-dependent long-term potentiation of intrinsic excitability in hippocampal CA1 pyramidal neurons. *J Neurosci* 25:1750-1760.
- Yang X-D, Faber DS (1991) Initial synaptic efficacy influences induction and expression of long-term changes in transmission. *Proc Natl Acad Sci USA* 88:4299–4303.
- Yang Z, Santamaria F (2016) Purkinje cell intrinsic excitability increases after synaptic long-term depression. *J Neurophysiol.* 116(3): 1208–1217.

LEGENDS TO TABLES

Table 1: Electrophysiological features of S1 L2/3 pyramidal neurons, before and after pairing induction of intrinsic plasticity in naïve conditions

Data represent the mean \pm S.E.M from n S1 L2/3 pyramidal neurons. *P<0.05, **P<0.01 and ***P< 0.001, comparing values after versus before pairing by one-way ANOVA.

Table 2: Electrophysiological features of S1 L2/3 pyramidal neurons, before and after pairing induction of intrinsic plasticity in potentiated conditions

Data represent the mean \pm S.E.M from n S1 L2/3 pyramidal neurons. *P<0.05, **P<0.01 and ***P< 0.001, comparing values after versus before pairings to 0mV/Vm serials: 0/-40mV and 0/0mV (No change), 0/-30mV, 0/-20mV and 0/-10mV (induction of LTD by the test pairing) and 0/10mV and 0/20mV (induction of LTP by the test pairing) by one-way ANOVA. Importantly, values before pairing are those before any pairing. Therefore, changes in electrophysiological properties of neurons in the 'No change' column are those produced by the first conditioning pairing to 0mV (compare this column with the LTP one in Table 1. Note the same ~27% increase in the input resistance following induction of LTD-IE or LTP-IE in potentiated synapses.

Table 3: Electrophysiological features of S1 L2/3 pyramidal neurons, before and after pairing induction of intrinsic plasticity in depressed conditions

Data represent the mean \pm S.E.M from n S1 L2/3 pyramidal neurons. *P<0.05 and **P<0.01, comparing values after versus before pairings to -20mV/Vm serials: -20/-40mV, -20/-30mV and -20/-20mV (No change) and -20/-10mV and -20/0mV (induction of LTP by the test pairing) by one-way ANOVA. Importantly, values before pairing are those before any pairing. Therefore,

changes in electrophysiological properties of neurons in the 'No change' column are those produced by the first conditioning pairing to -20mV (compare this column with the LTD one in Table 1). Note that all electrophysiological changes are reversed following induction of LTP-IE by the test pairing to -10mV or 0mV, consistent with our conclusion that this is a true reversal of pairing to -20mV-induced LTD-IE.

LEGENDS TO FIGURES

Figure 1. The level of postsynaptic depolarization determines the sign and magnitude of synaptic plasticity in S1 vertical input-L2/3 pyramidal neuron synapses. **A–D**, Summary graphs of whole-cell recordings in which synaptic stimulation (2 Hz, 50 sec) was paired to 0 mV (**A**; $n = 16$, $N = 16$), -10 mV (**B**; $n = 12$, $N = 12$), -20 mV (**C**; $n = 10$, $N = 10$) and -30 mV (**D**; $n = 6$, $N = 6$). Superimposed averages of 10 successive evoked EPSCs recorded before (thin trace) and 30 min after (thick trace) pairing in representative cells. Calibration bars: 20 msec, 50 pA. **E**, Cumulative histograms showing the effect of a pairing to -40mV ($n = 3$, $N = 3$), -30mV ($n = 6$, $N = 6$; same as 1D), -20mV ($n = 12$, $N = 11$; same as Fig. 1C), -10mV ($n = 12$, $N = 12$; same as Fig. 1B), 0mV ($n = 16$, $N = 16$; same as Fig. 1A), +10mV ($n = 6$, $N = 6$), and +20mV ($n = 8$, $N = 8$), in every neuron before the LTP mechanisms had dialyzed out of the recorded neuron. **F**, Voltage–response function for the induction of LTD/LTP (synaptic plasticity rule) in naive synapses. **G**, Bar histograms of the averaged paired-pulse ratios (+ S.E.M) measured before (black bars) and 30 min after (grey bars) pairings to -40 to +20 mV (from left to right). None of the pairings produced any change in PPF. Same numbers of neurons/rats as in E. In **A**, **B**, **C**, **D**, **F** and **G**, values are presented as mean \pm S.E.M.

Figure 2: Pairing-induced synaptic plasticity, but not intrinsic plasticity, depends on NMDA receptor activation. **A**, **B**, Summary graphs of whole-cell recordings in which synaptic stimulation (2 Hz, 50 sec) was paired in control conditions (filled symbols) and in the presence of DL-APV (200 mM; empty symbols) to -20mV (**A**) ($n=10$, $N=10$, same as Fig. 1, C, and $n=5$, $N=5$, respectively) and to 0mV (**B**) ($n=16$, $N=16$, same as Fig. 1, A and $n=5$, $N=5$, respectively). Bath applied DL-APV prevents the induction of pairing-induced synaptic plasticity. **C**, **D**, Relationships between injected current and evoked firing rate (F-I curves) prior to (open symbols) and 30 min after (filled symbols) application of the pairings to -20mV (**C**; $n=5$, $N=5$)

and 0mV (**D**; n=5, N=5) in the presence of DL-APV. **C, D insets**, Examples of firing responses to 500, 590 and 770 pA current pulses recorded before (left) and after (right) pairings to -20mV (**C, Inset**) and 0mV (**D, Inset**) in representative pyramidal neurons. Bath applied DL-APV does not prevent the induction of pairing-induced intrinsic plasticity. Scale bars for **C** and **D insets**, 20 mV (vertical) and 100 ms (horizontal). In **C** and **D**, *p≤0.05, **p≤0.01 after versus before pairings by Tukey's HSD post test following one-way ANOVA for repeated measures. Values are presented as mean ± S.E.M.

Figure 3: Changes in intrinsic properties after pairing-induced synaptic LTD and LTP in naïve conditions. **A**, Averaged relationships between injected current and evoked firing rate (F-I curve) prior to (open symbols) and 30 min after (filled symbols) application of a pairings to -40mV or -30mV (n=6; N=6). **B**, Averaged F-I curves prior to (open symbols) and 30 min after (filled symbols) application of pairings to -20mV (n=12; N=12). **C**, Averaged F-I curves prior to (open symbols) and 30 min after (filled symbols) application of pairing to -10, 0, 10 and 20mV (n=34; N=34). Note that LTD-IE and LTP-IE manifest as rightward and leftward, respectively, shifts in the F-I curves. **A, B, C insets**, Examples of firing responses to 500, 590 and 770 pA current pulses recorded before (left) and after (right) pairings to -40mV (**A, Inset**), -20mV (**B, Inset**) and 0mV (**C, Inset**) in representative pyramidal neurons. Scale bars for **A, B** and **C insets**, 20 mV (vertical) and 100 ms (horizontal). In **C** and **D**, *p≤0.05, **p≤0.01, ***p≤0.001 after versus before pairings by Tukey's HSD post test following one-way ANOVA for repeated measures. **D, E**, Normalized instantaneous frequency prior to (open symbols) and 30 min after (filled symbols) pairings to -20mV (**D**) and to -10, 0, 10 and 20mV (**E**). The power of frequency adaptation was not changed in both LTD-IE (**D**) and LTP-IE (**E**). Values are presented as mean ± S.E.M.

Figure 4: Changes in intrinsic properties and in synaptic strength are not correlated. *A*, Relationship between injected current and evoked firing rate (F-I curve) prior to (open symbols) and 30 min after (filled symbols) application of a pairings to -10mV (n=6; N=6; circles), 0mV (n=12; N=12; squares), 10mV (n=6; N=6; triangles) and 20mV (n=8; N=8; diamonds). Note that the F-I curves both before and after pairings are superimposed suggesting that the four pairings produce similar leftward shifts in the F-I curves. *B*, *C*, *D*, *E*, Individual values (and mean (\pm S.E.M.) of the threshold (*B*), rheobase (*C*) and amplitude (*D*) of action potentials and amplitude of after-hyperpolarizations (*E*) before (empty symbols) and 30 min after (filled symbols) pairings to -10mV (circles), 0mV (squares), 10mV (triangles) and 20mV (diamonds) (same as in *A*). Note that the four pairings produce the very same changes in the properties of action potentials and after-hyperpolarization. *F*, Superimposed voltage–response functions for the induction of synaptic LTD/LTP (empty circles) and LTD-IE/LTP-IE (empty squares) (synaptic and intrinsic plasticity rules) in naive conditions. Note that the two rules of plasticity display the very same voltage-thresholds but that the magnitude of synaptic and intrinsic changes are not correlated. Intrinsic changes appear to occur ‘all-or-none’. Values are presented as mean \pm S.E.M.

Figure 5: Synaptic plasticity rule in potentiated conditions. *A*, Summary graphs of whole-cell recordings in which synaptic stimulation (2 Hz, 50 sec) was paired to 0mV (conditioning pairing) and 30 min later, to 40mV (filled symbols; (n = 3, N = 3) or -30mV (empty symbols; n = 4, N = 4) (test pairing). Only test pairings to -30 mV could depress the potentiated transmission. *Inset*, Superimposed averages of 10 successive evoked EPSCs recorded before (thin trace) and 30 min after the test pairing to -40mV (left) and to -30mV (right) in representative pyramidal neurons. *B*, Summary graph of whole-cell recordings in which synaptic stimulation (2 Hz, 50 sec) was paired to -20mV, 30 min after pairing to 0mV (n=7,

N=7). EPSC amplitudes are normalized to EPSC amplitude before the second, test pairing to -20 mV. It is superimposed with the summary graph of pairing to -20 mV in naïve synapses (same as Fig. 1C; filled symbols). Pairing to -20 mV produces a larger LTD in potentiated synapses than in naïve ones. ***Inset***, Superimposed averages of 10 successive evoked EPSCs recorded before (thin trace) and 30 min after pairing to -20mV in naïve (left) and potentiated synapses (right) in representative pyramidal neurons. **C**, Summary graphs of whole-cell recordings in which synaptic stimulation (2 Hz, 50 sec) was paired to 0mV and, less than 10 min later, to +20mV, that is, before the LTP mechanisms had dialyzed out of the recorded neuron (n=4, N=4). Combined pairings to 0mV/20mV produced a huge potentiation. ***Inset***, Superimposed averages of 10 successive evoked EPSCs recorded: left, before any pairing (1; thin trace) and immediately after pairing to 0mV (2, thick trace) and right, after pairings to 0mV (2, thin trace) and to 20mV (3, thick trace) in a representative neuron. **A, B, C Insets**, Calibration bars: 20 msec, 50 pA. **D**, Cumulative histograms showing the net effect of the second, test pairing to -40mV (n=3, N=3), -30mV (n = 4, N = 4), -20 mV (n = 7, N = 7), -10 mV (n = 4, N = 4), 0 mV (n = 5, N =5), +10 mV (n=3, N=3) and +20mV (n=4, N=4) (normalized amplitude measured 30 min after test pairing) in every neuron. **E**, Voltage–response functions for the induction of LTD/LTP in depressed synapses before (empty circles) and after LTP mechanisms had dialyzed out of the recorded neuron (filled squares). The effect of test pairings to 0mV assessed before and after washout of LTP mechanisms were averaged together. Note that when synaptic LTD is assessed in isolation, it is only obtained within a voltage window: $-40\text{mV} < V_m < 0\text{mV}$. In **D, E**, the net effect of test pairings was measured as following: (i) when test pairings (to -40, -30, -20, -10, 0, 10 and 20 mV) were applied 30 min after the conditioning pairing to 0mV—after pairing to 0mV-induced synaptic LTP had stabilized—synaptic responses after test pairings were directly normalized to pre-test pairing baseline, (ii) when test pairings (to 0, 10 and 20 mV) were applied less than 10 min after conditioning pairing to 0mV—before

pairing to 0mV-induced synaptic LTP had stabilized—synaptic responses after test pairing were computed by subtracting the effect of a single pairing to 0mV (+61.7% potentiation) from normalized values to pre-pairings 0mV/Vm serial baseline. **F**, Superimposed voltage–response functions for the induction of synaptic LTD/LTP (synaptic plasticity rules) in potentiated (empty symbols, same n and N as in D) and naïve conditions (filled symbols). Values are presented as mean \pm S.E.M.

Figure 6: Synaptic plasticity rule in depressed conditions. **A**, Superimposed summary graphs of whole-cell recordings in which synaptic stimulation (2 Hz, 50 sec) was first paired to -20mV (conditioning pairing) and subsequently to -30 mV (n = 3, N = 3), -20 mV (n=4, N=4) or -10 mV (n = 4, N = 4) (test pairing). Note that whereas test pairing to neither -30mV nor -20mV produces any change compared to pre-test pairing baseline, test pairing to -10 mV produces a strong LTP, even compared to pre-pairings to -20 mV/-10 mV serial. **B**, Cumulative histograms showing the net effect of a test pairing to -40 mV (n=2, N=2), -30 mV (D; n=3, N=3), -20 mV (n=4, N=4), -10 mV (n=4, N=4), 0 mV (n=3, N=3) in every neuron before the LTP mechanisms had dialyzed out of the recorded neuron. The amplitude of synaptic responses 30 min after the test pairing were computed by subtracting the effect of a single pairing to -20mV (-33.1% depression) from normalized values to pre-pairings -20mV/Vm serial baseline. **C**, Superimposed voltage–response functions for the induction of synaptic LTD/LTP (synaptic plasticity rules) in depressed (empty symbols, same n and N as in B) and naïve conditions (filled symbols). Note that voltage window for the induction of synaptic LTD is totally occluded. Values are presented as mean \pm S.E.M.

Figure 7: Intrinsic plasticity rule in potentiated conditions. **A**. Relationship between injected current and evoked firing rate (F-I curve) prior to (open symbols) and 30 min after (filled

symbols) application of the pairings to 0/-40mV serials (n=2; N=2). *p≤0.05, **p≤0.01 after versus before pairings to 0/-40mV serials by Tukey's HSD post test following one-way ANOVA for repeated measures. **B**, F-I curves prior to (open symbols) and 30 min after (filled symbols) application of pairings to 0/0mV serials (n=4; N=4). *p≤0.05, **p≤0.01 after versus before pairings to 0/0mV serials by Tukey's HSD post test following one-way ANOVA for repeated measures. Note in **A** and **B** the same leftward shift in the F-I curves after pairings to 0/-40mV and 0/0mV, as after a single pairing to 0 mV (see Fig. 3C). **C**, F-I curves prior to (open symbols) and 30 min after (filled symbols) application of pairings to 0/-30mV (n=3; N=3; circles), 0/-20mV (n=1; N=1; squares) and 0/-10mV (n=1; N=1; triangles) serials. &p≤0.05 after versus before pairings to 0/-30mV serials by Tukey's HSD post test following one-way ANOVA for repeated measures. **D**, F-I curves prior to (open symbols) and 30 min after (filled symbols) application of pairings to 0/10mV (n=3; N=3; circles) and 0/20mV (n=4; N=4; squares) serials. ⁺p≤0.05, ⁺⁺p≤0.01 after versus before pairings to 0/10mV serials and [§]p≤0.05, ^{§§}p≤0.01 after versus before pairings to 0/-30mV, 0/-20mV and 0/-10mV serials by Tukey's HSD post test following one-way ANOVA for repeated measures. Note in **C** and **D**, the strong reduction in the gain of F-I curves, indicating that LTD-IE after pairings to 0/-30mV, 0/-20mV and 0/-10mV serials is not a simple reversal of LTP-IE. **A, C, D insets**, Examples of firing responses to 500, 590 and 770 pA current pulses recorded before (left) and after (right) pairings to 0/-40mV (**A, Inset**), 0/-30mV (**C, Inset**) and 0/10mV (**D, Inset**) serials, in representative pyramidal neurons. Scale bars for **A, C** and **D insets**, 20 mV (vertical) and 100 ms (horizontal). **E**, Averaged F-I curves prior to (open symbols) and 30 min after (filled symbols) application of pairings to 0/-30mV, 0/-20mV and 0/-10mV serials (n=5; N=5; circles) and pairings to 0/10mV and 0/20mV (n=7; N=7; squares). [§]p≤0.05, ^{§§}p≤0.01 after versus before pairings to 0/-30mV, 0/-20 mV and 0/-10mV serials, [#]p≤0.05, ^{##}p≤0.01 after versus before pairings to 0/10mV and 0/20mV serials by Tukey's HSD post test following one-way ANOVA for repeated measures. Note that the two

F-I curves after pairings to 0/Vm serials, are superimposed and thus do not depend on the direction, depression or potentiation, of test pairing-induced synaptic plasticity. **F**, Superimposed voltage–response functions for the induction of synaptic LTD/LTP (empty circles) and LTD-IE/LTP-IE (empty squares) (synaptic and intrinsic plasticity rules) in potentiated conditions. Note that (i) the two rules of plasticity display the very same voltage-thresholds, (ii) the direction of intrinsic plasticity (LTD-IE) does not depend on that of synaptic plasticity and (iii) the magnitude of synaptic and intrinsic changes are not correlated. Intrinsic changes appear to occur ‘all-or-none’. Values are presented as mean \pm S.E.M.

Figure 8: Intrinsic plasticity rule in depressed conditions. **A**, Averaged (n=9; N=9) relationship between injected current and evoked firing rate (F-I curve) prior to (open symbols) and 30 min after (filled symbols) application of the pairings to -20/-40mV (n=2; N=2), -20/-30mV (n=3; N=3) and -20/-20mV (n=4; N=4) serials. F-I curves before and after pairings to -20/Vm serials were averaged since they were overlapping. Note, after pairings to -20/Vm serials, the same rightward shift in the F-I curve as after a single pairing to -20 mV (Fig. 3B). *p \leq 0.05 after versus before pairings by Tukey’s HSD post test following one-way ANOVA for repeated measures. **B**, Averaged (n=7; N=7) F-I curves prior to (open symbols) and 30 min after (filled symbols) application of the pairings to -20/-10mV (n=4; N=4) and -20/0mV (n=3; N=3) serials. F-I curves before and after pairings to -20/Vm serials were averaged since they were overlapping. Note that the two F-I curves, before and after pairing to -20/Vm serials, are now superimposed, suggesting that LTD-IE after the conditioning pairing to -20mV was reversed by LTP-IE. **A, B Insets**, Examples of firing responses to 500, 590 and 770 pA current pulses recorded before (left) and after (right) pairings to -20/-20mV (**A, inset**) and -20/-10mV (**B, Inset**) serials, in representative pyramidal neurons. Scale bars for **A** and **B** insets, 20 mV (vertical) and 100 ms (horizontal). **C**, Superimposed voltage–response functions for the induction of synaptic

LTD/LTP (empty circles) and LTD-IE/LTP-IE (empty squares) (synaptic and intrinsic plasticity rules) in potentiated conditions. Note that (i) the two rules of plasticity display the very same LTP-threshold, and (ii) the window for LTD-IE, as that for synaptic LTD, is totally occluded. Values are presented as mean \pm S.E.M.

Table 1: Electrophysiological features of S1 L2/3 pyramidal neurons, before and after pairing-induced intrinsic plasticity in naïve conditions

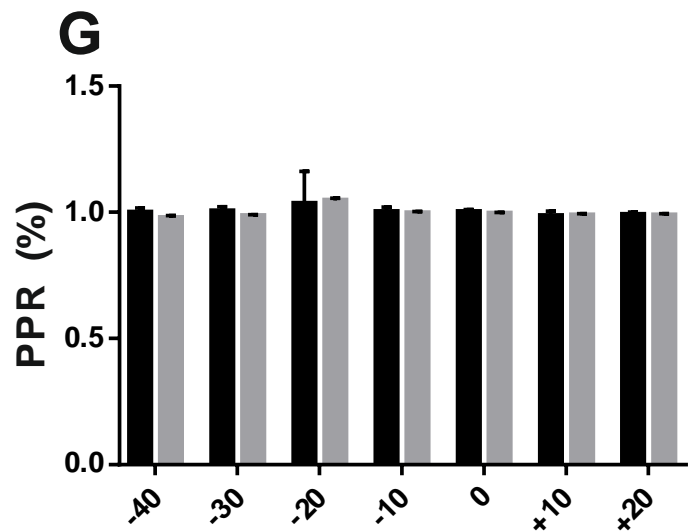
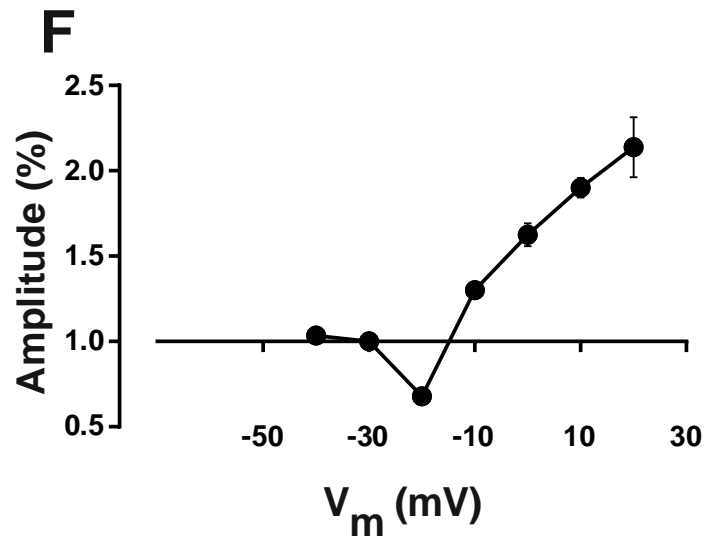
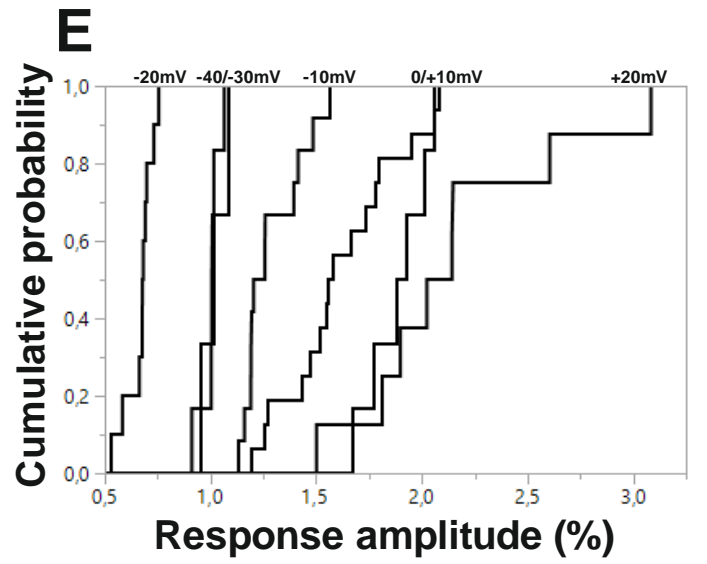
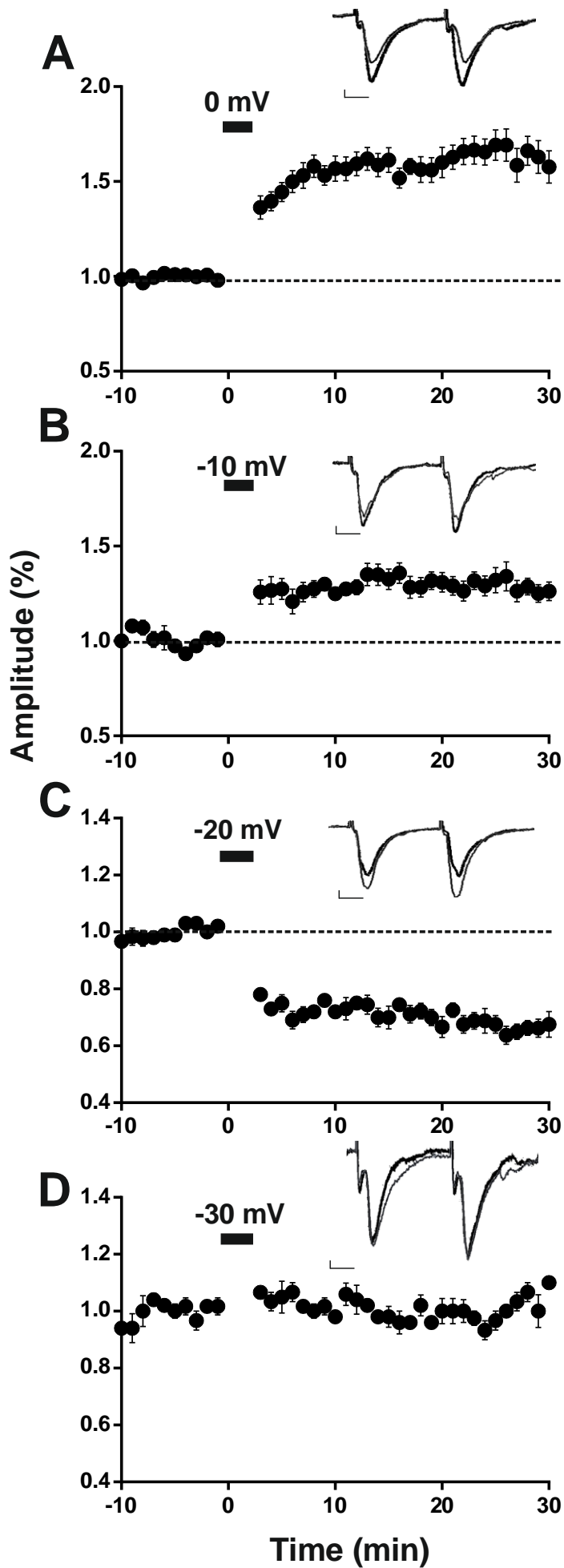
Membrane properties						
	No change		LTD-IE		LTP-IE	
	Before pairing	After pairing	Before pairing	After pairing	Before pairing	After pairing
n	6	6	12	12	37	34
Resting membrane potential (RMP), mV	-91.8 ± 0.6	-92.3 ± 0.4	-93.3 ± 0.5	-94.3 ± 0.5	-92.0 ± 0.5	-93.3 ± 0.7
Input Resistance (R _{in}), M	157.5 ± 14.7	169.7 ± 31.8	-156.1 ± 11.9	145.8 ± 11.7	160.9 ± 7.1	154.1 ± 6.3
Action potential characteristics						
Threshold, mV	-42.9 ± 0.5	-42.6 ± 0.7	-44.3 ± 0.7	-42 ± 0.6*	-43.4 ± 0.4	-48.7 ± 0.6***
Rheobase, pA	542.5 ± 11.5	543.5 ± 11.4	582.5 ± 11.6	639.9 ± 15.3**	552.7 ± 8.8	434.9 ± 8.8***
Amplitude, mV	85.4 ± 1.6	84.7 ± 1.1	84.71 ± 0.9	88.1 ± 1.0*	87.3 ± 0.6	80.4 ± 0.7***
Duration, ms	2 ± 0.1	2 ± 0.1	1.9 ± 0.0	1.8 ± 0.1	1.9 ± 0.0	2.3 ± 0.0***
After hyperpolarization, mV	6.8 ± 0.2	6.6 ± 0.2	6.5 ± 0.2	8.6 ± 0.3**	6.8 ± 0.1	5.6 ± 0.1**

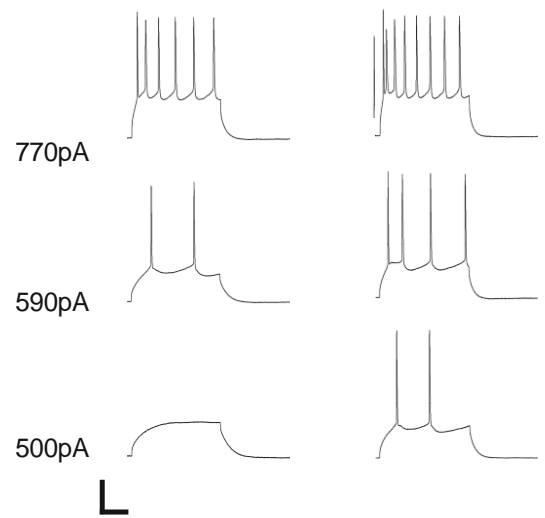
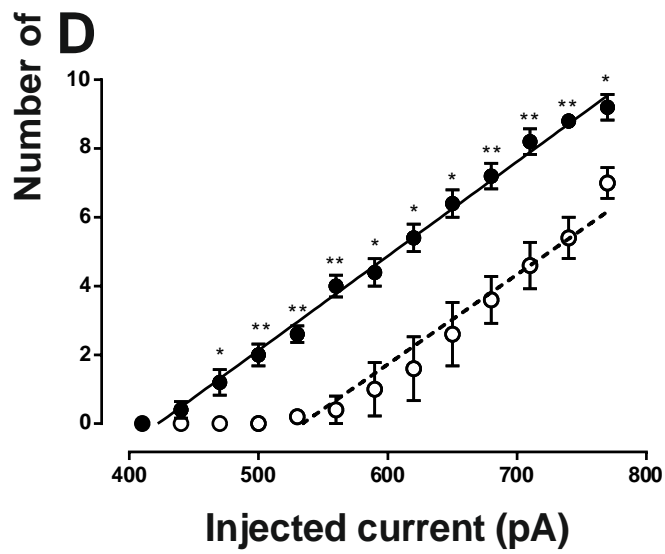
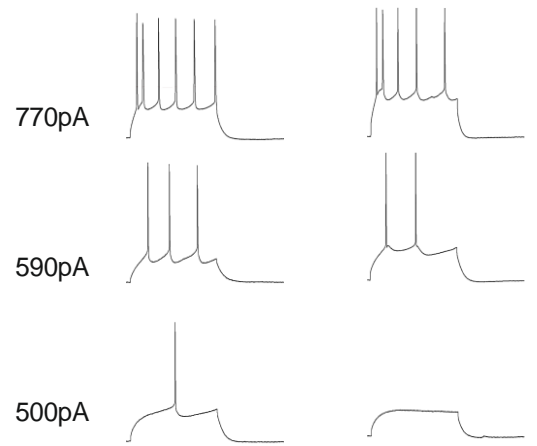
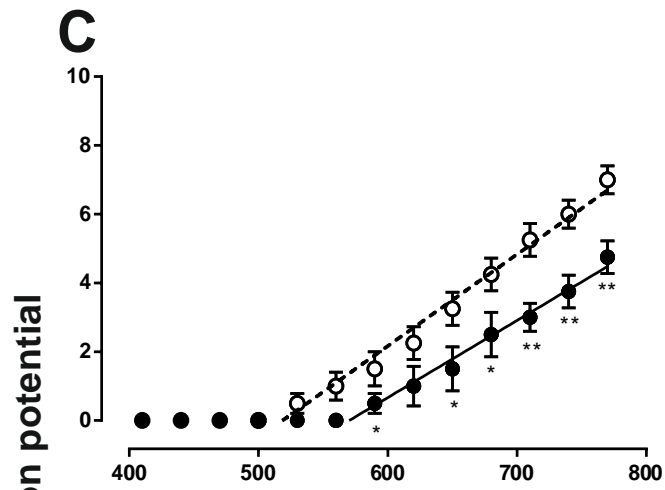
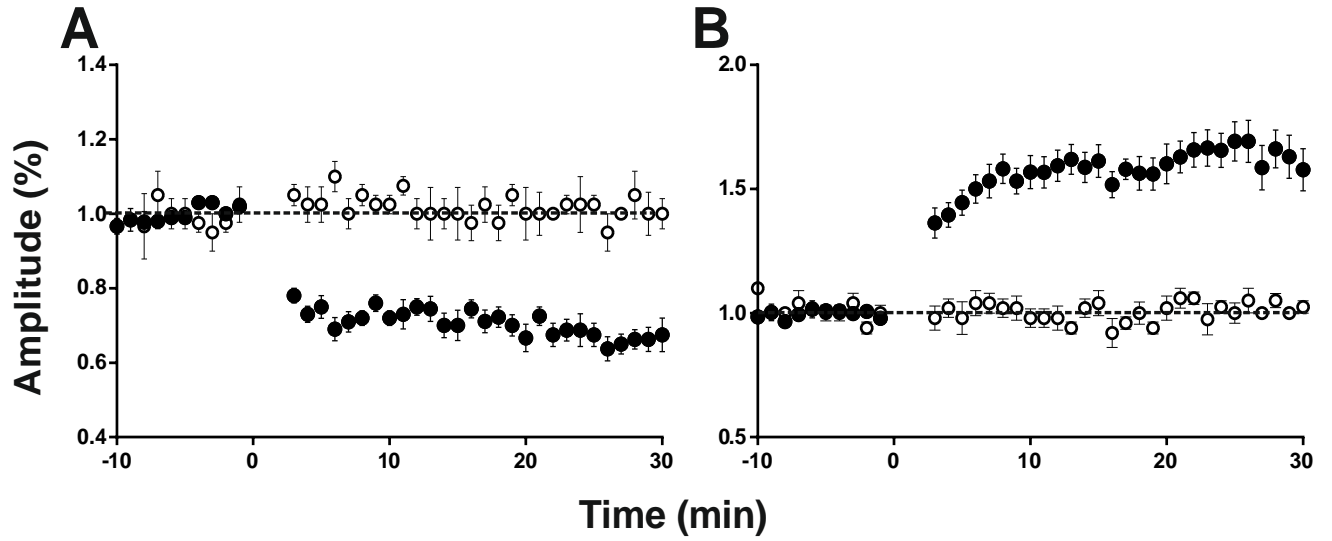
Table 2: Electrophysiological features of S1 L2/3 pyramidal neurons, before and after pairing-induced intrinsic plasticity in potentiated conditions

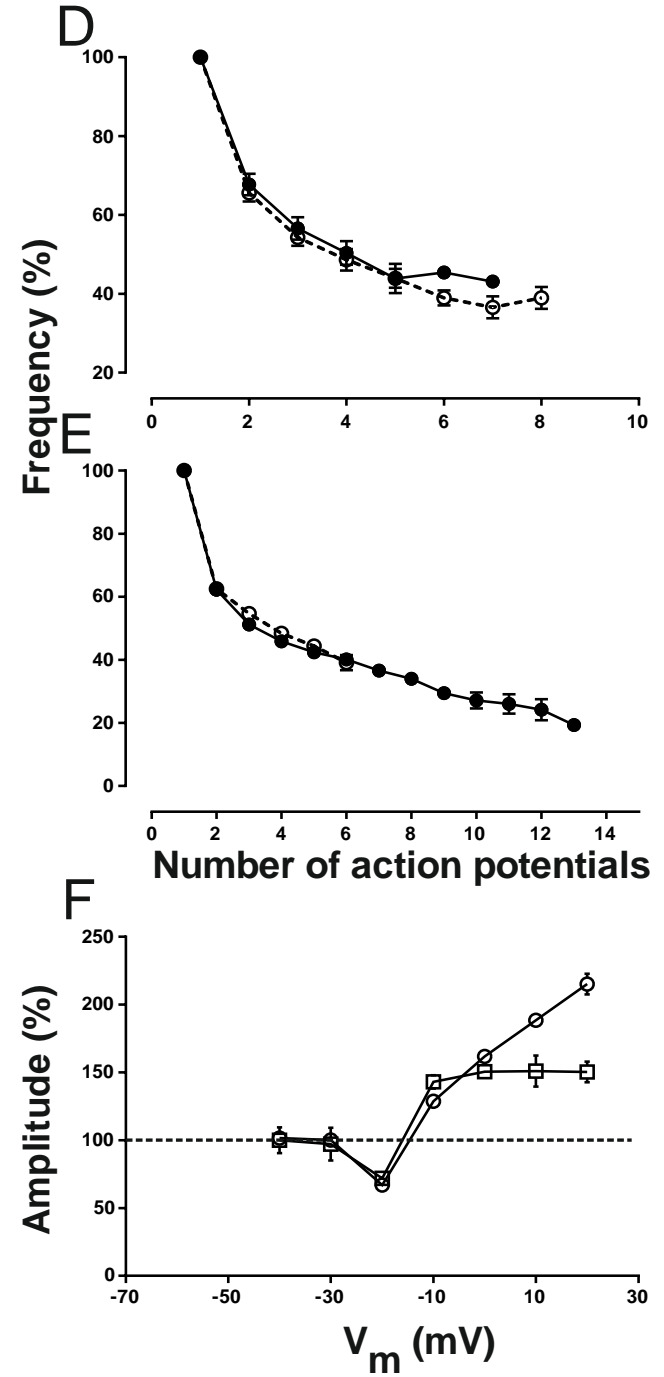
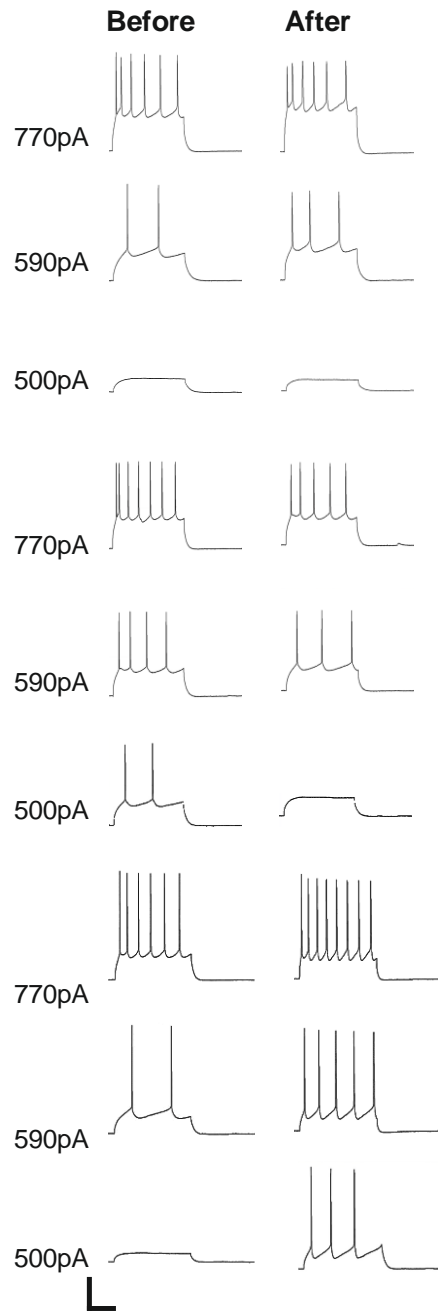
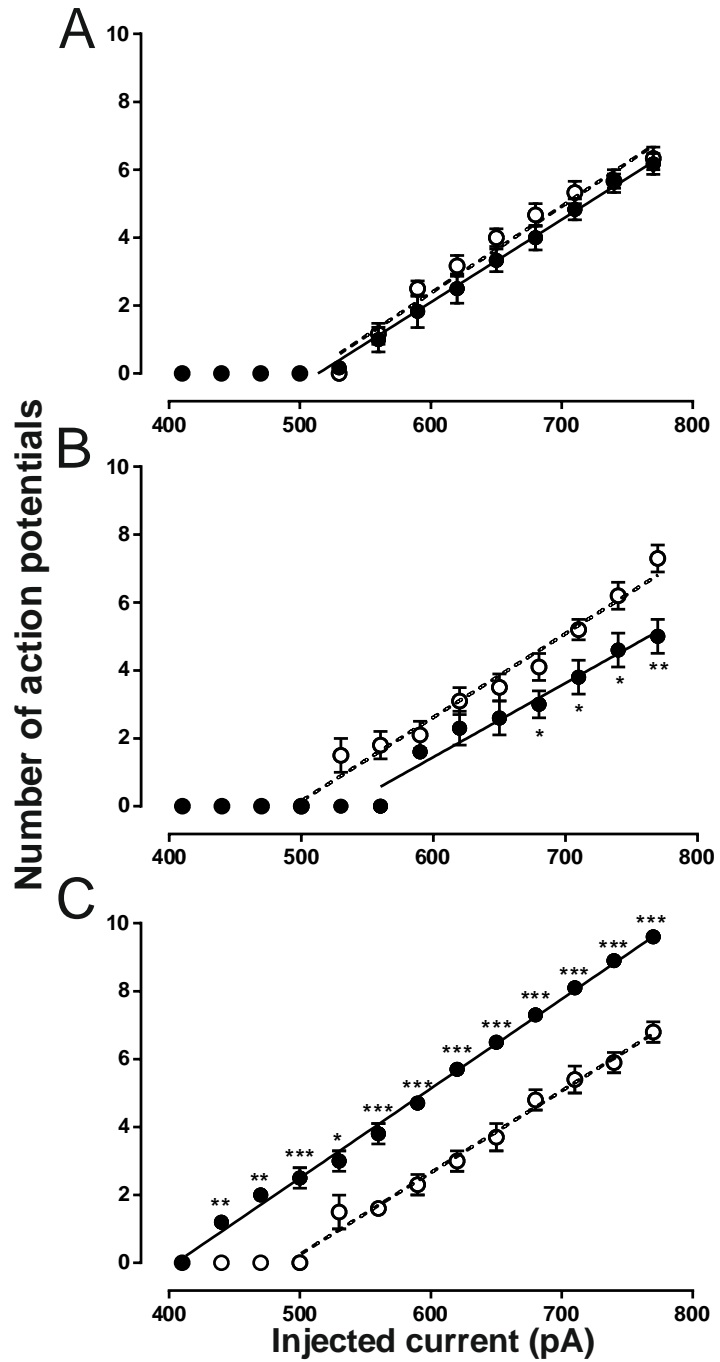
Membrane properties						
	No change		LTD-IE		LTP-IE	
	Before pairing	After pairing	Before pairing	After pairing	Before pairing	After pairing
n	6	6	5	5	7	7
Resting membrane potential (RMP), mV	-91.3 ± 0.6	-92.7 ± 1.0	-91.4 ± 0.5	-92.3 ± 0.8	-93.0 ± 0.4	-92.43 ± 0.4
Input Resistance (R_{in}), M	139.5 ± 10.4	144.2 ± 16.3	140.6 ± 8.4	178.7 ± 13.1*	149.5 ± 9.6	189.3 ± 13.5*
Action potential characteristics						
Threshold, mV	-41.1 ± 0.5	-45.9 ± 1.0**	-43.7 ± 0.5	-41.32 ± 0.8*	-42.32 ± 0.6	-40.3 ± 0.5*
Rheobase, pA	597.0 ± 18.3	504.2 ± 27.15*	546.0 ± 31.2	647.0 ± 32.9 (<i>p</i> =0.0591)	581.4 ± 18.1	655.7 ± 23.0*
Amplitude, mV	85.4 ± 1.3	80.8 ± 1.1*	85.2 ± 1.8	79.2 ± 2.5 (<i>p</i> =0.0856)	84.3 ± 1.3	80.3 ± 0.9*
Duration, ms	1.83 ± 0.06	2.18 ± 0.06**	1.86 ± 0.02	2.04 ± 0.05*	1.77 ± 0.05	2.03 ± 0.05**
After hyperpolarization, mV	7.2 ± 0.4	5.3 ± 0.3**	7.0 ± 0.1	7.4 ± 0.9	6.9 ± 0.2	7.8 ± 0.8

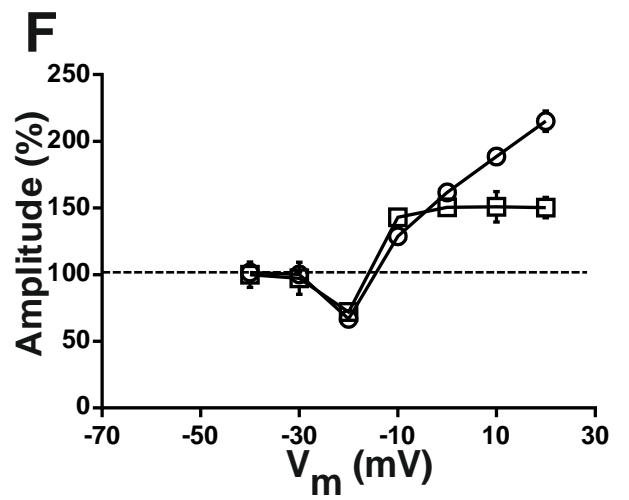
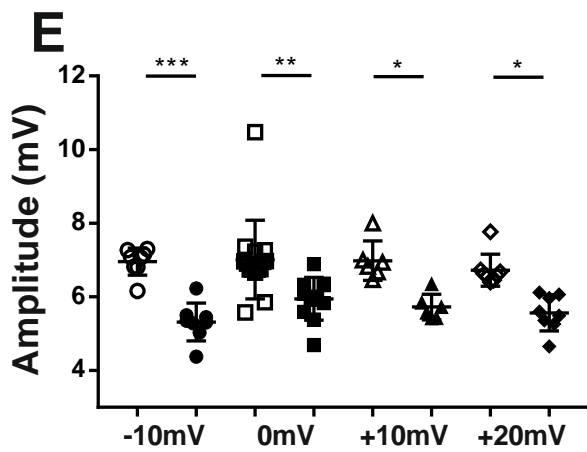
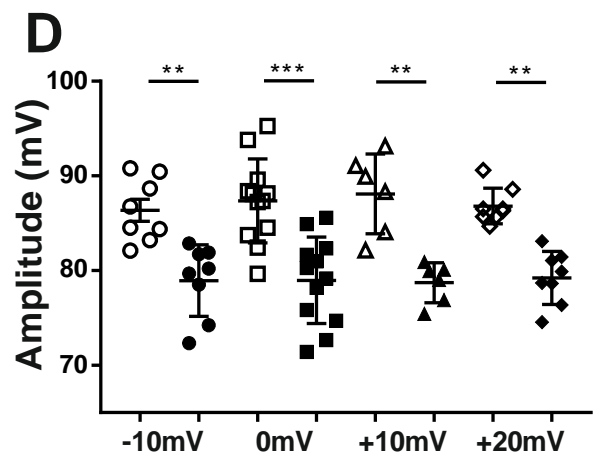
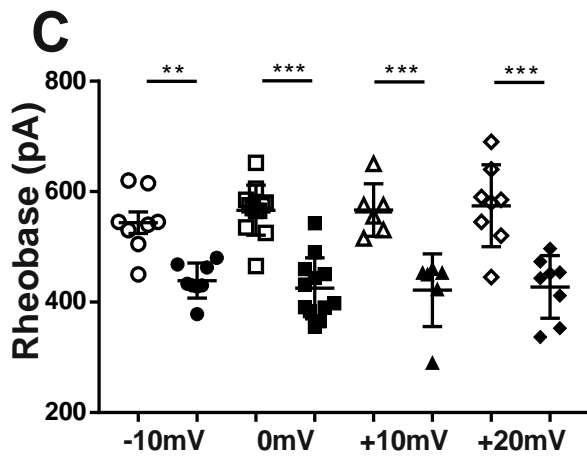
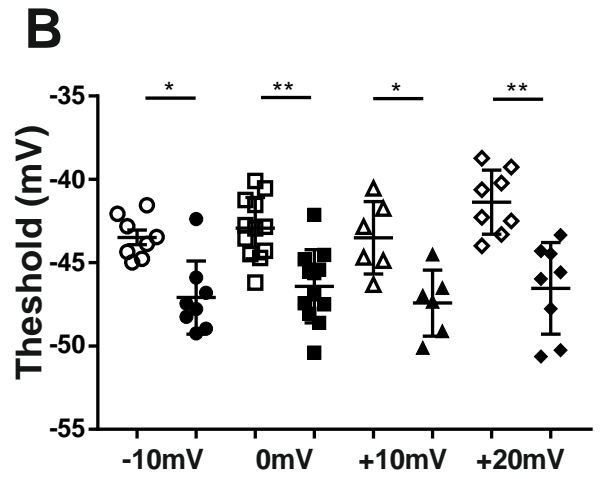
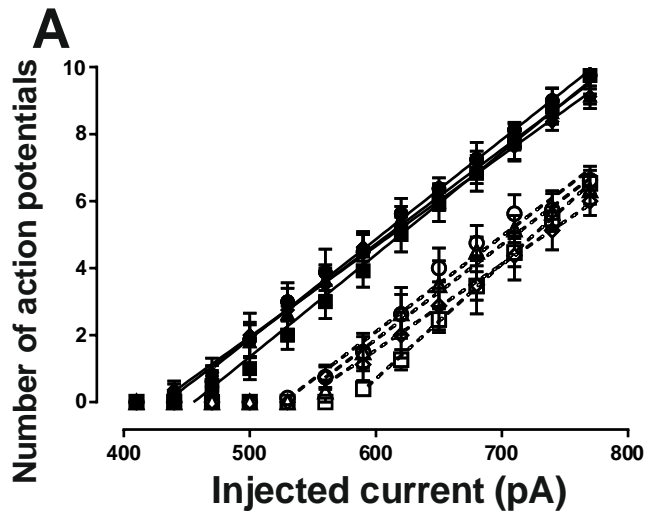
Table 3: Electrophysiological features of S1 L2/3 pyramidal neurons, before and after pairing-induced intrinsic plasticity in depressed conditions

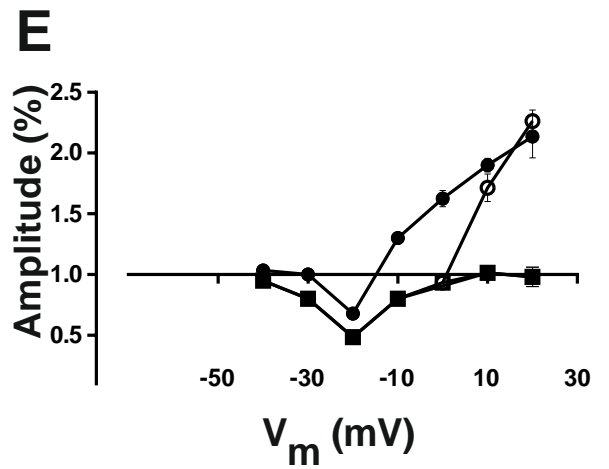
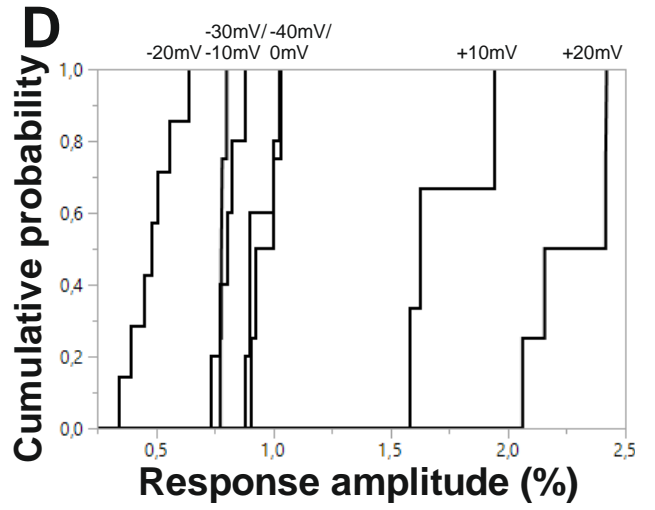
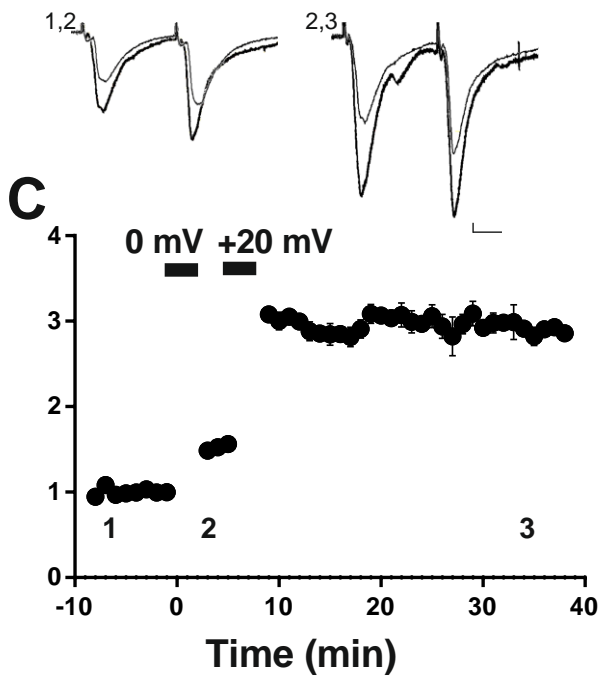
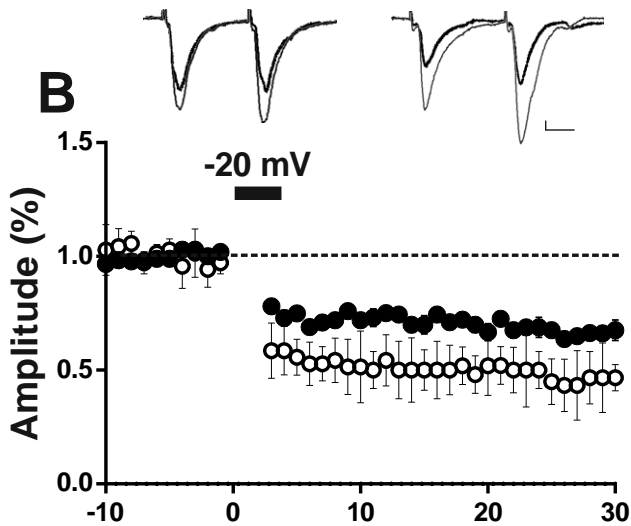
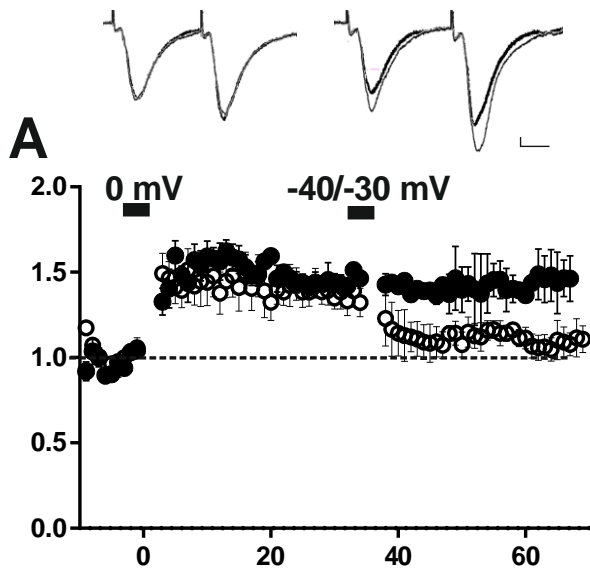
Membrane properties				
	No change		LTP-IE	
	Before pairing	After pairing	Before pairing	After pairing
n	9	9	7	7
Resting membrane potential (RMP), mV	-92.2 ± 0.6	91.1 ± 0.6	-91.3 ± 0.5	-91.9 ± 0.8
Input Resistance (R _{in}), M	186.3 ± 13.24	170.2 ± 13.7	176 ± 18.7	193 ± 17.6
Action potential properties				
Threshold, mV	-41.8 ± 0.7	-39.0 ± 0.6**	-42.6 ± 0.1	-42.8 ± 1.7
Rheobase, pA	535.6 ± 13.3	597.8 ± 14.0**	545 ± 10.1	561.4 ± 29.3
Amplitude, mV	80.7 ± 1.2	84.7 ± 1.5*	81.5 ± 1.6	79.8 ± 2.4
Duration, ms	2.17 ± 0.07	1.93 ± 0.06*	2.19 ± 0.15	2.21 ± 0.15
After hyperpolarization, mV	6.4 ± 0.1	7.9 ± 0.2*	6.8 ± 0.2	6.9 ± 0.2

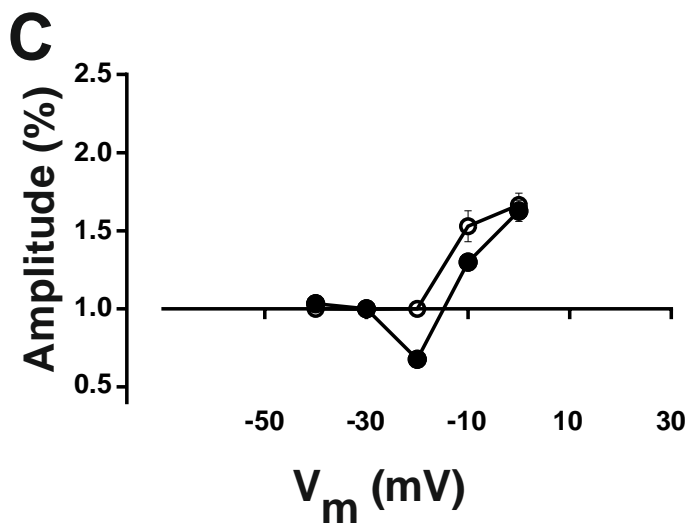
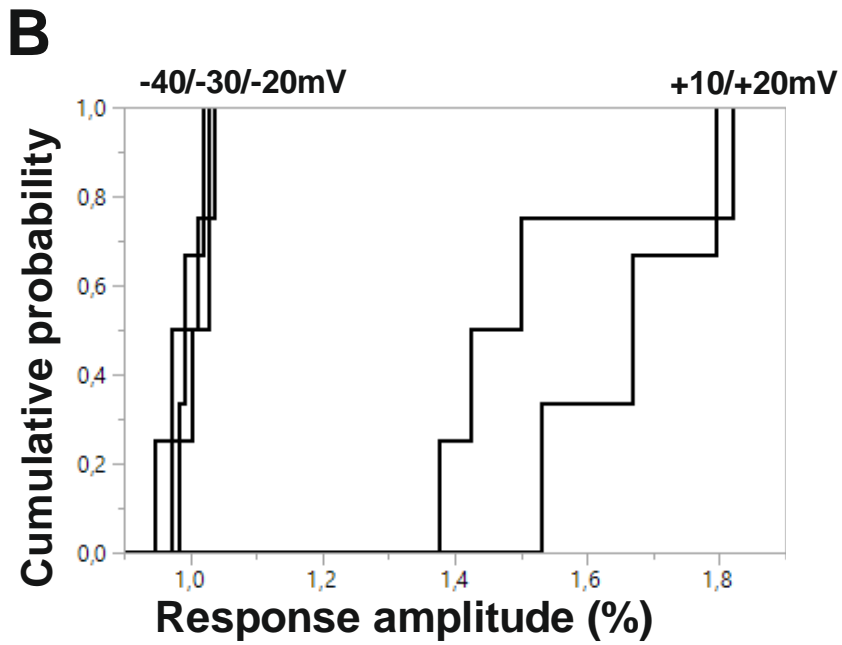
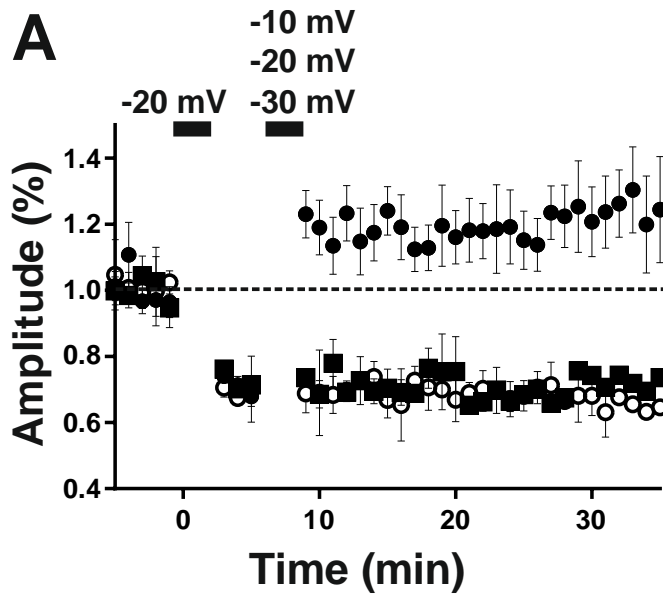


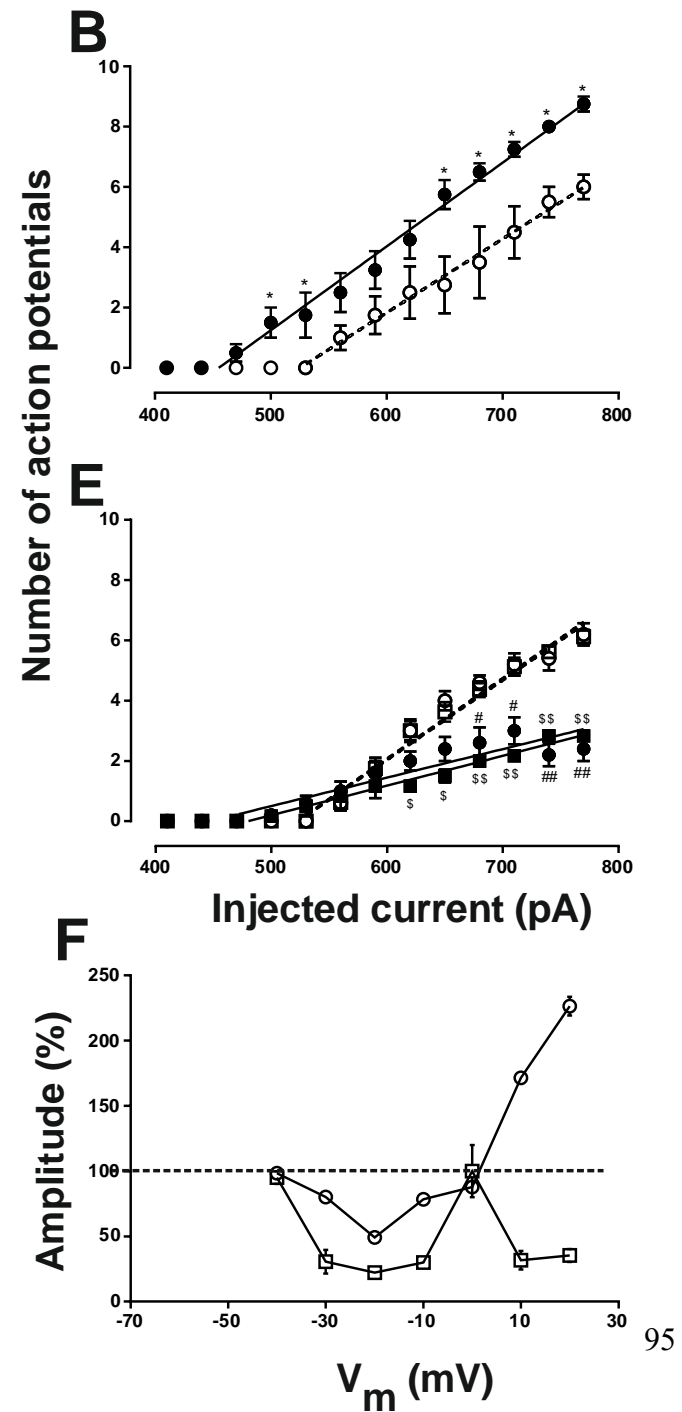
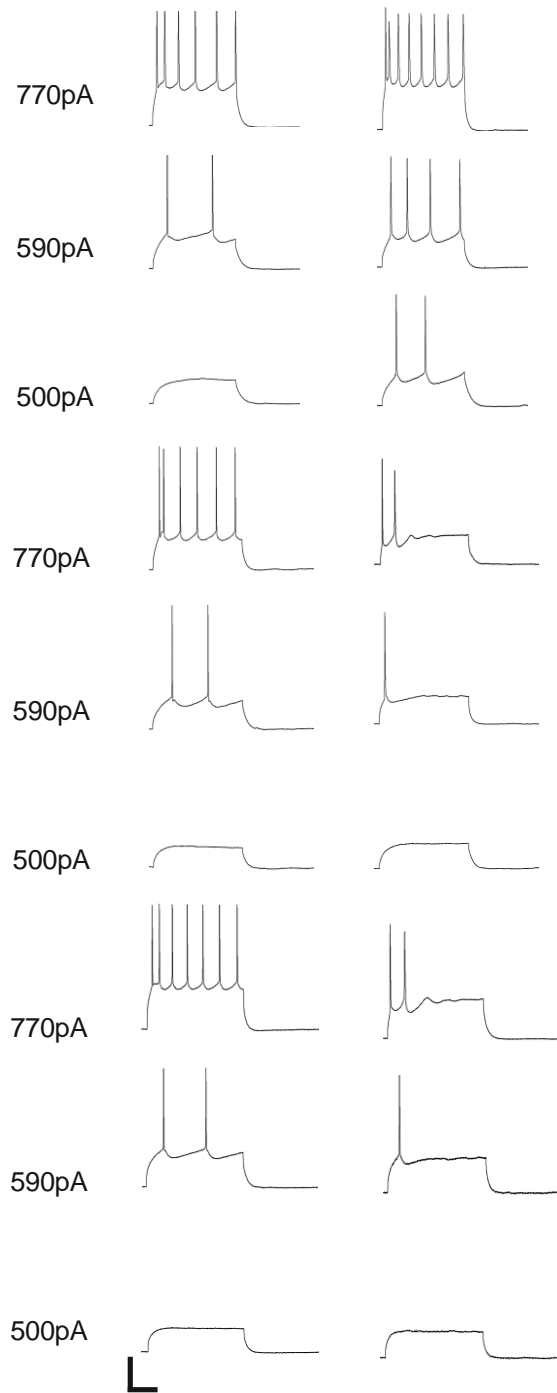
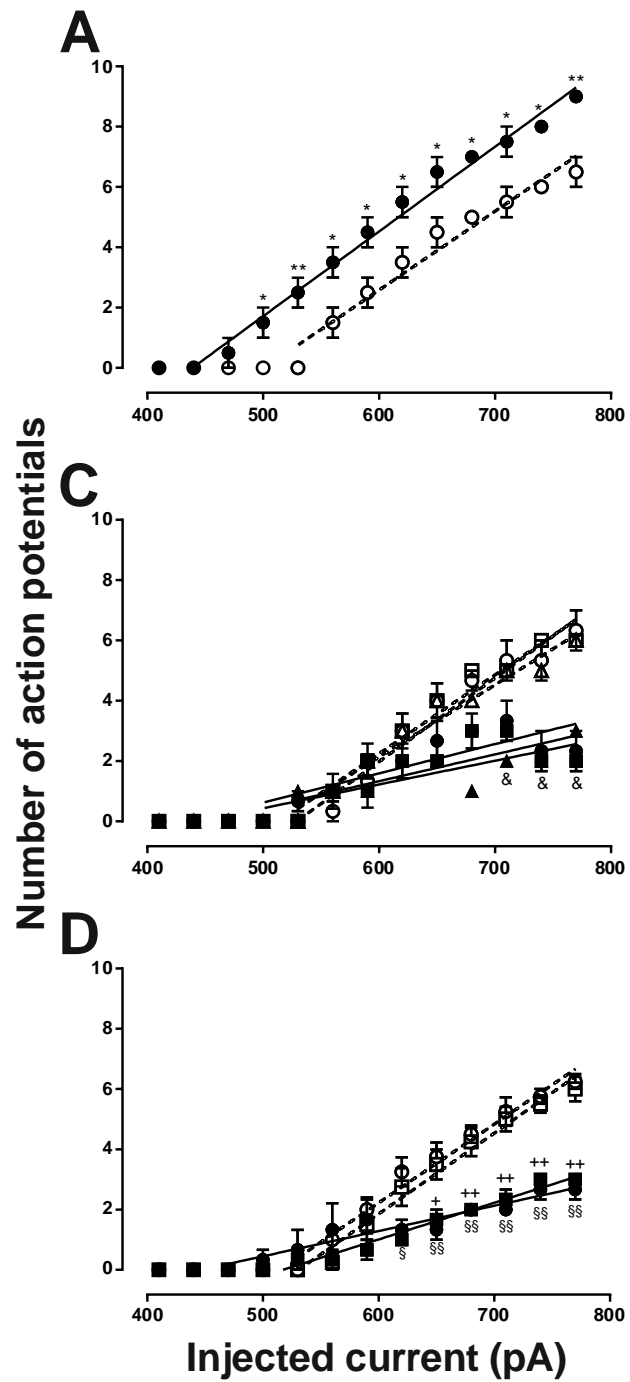


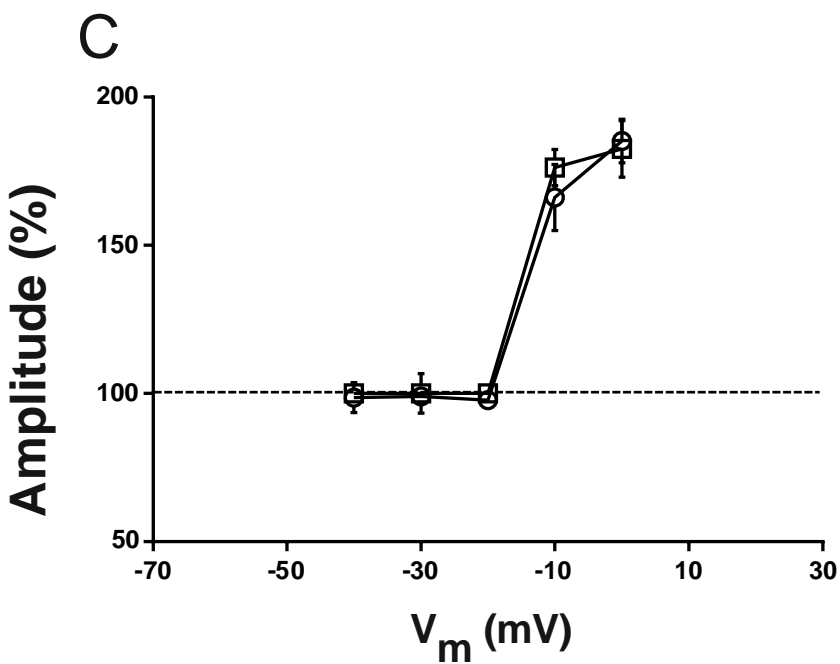
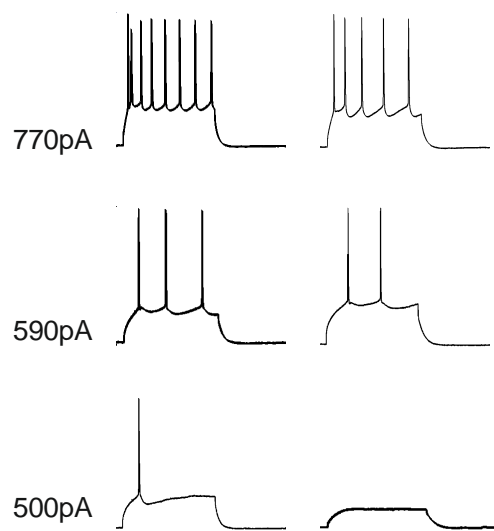
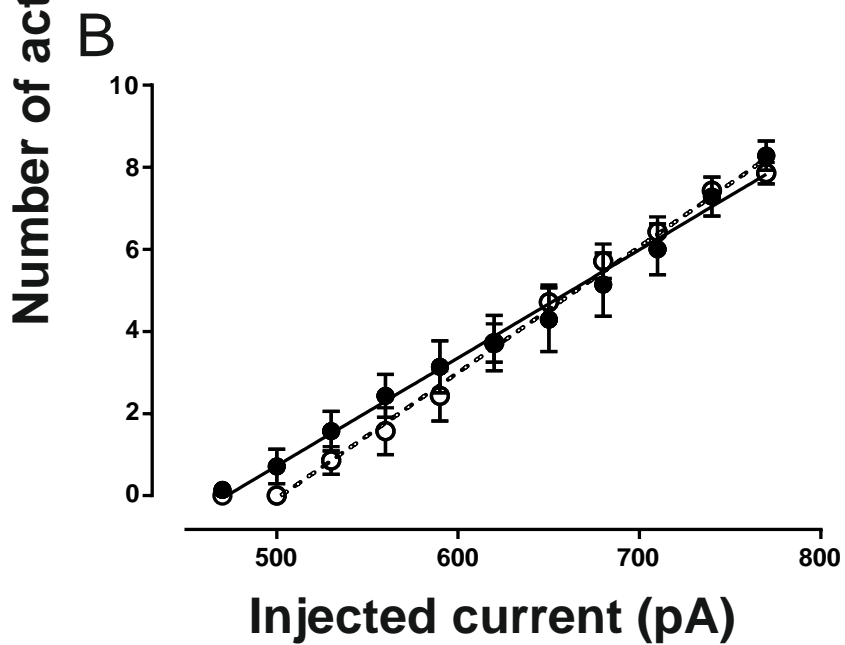
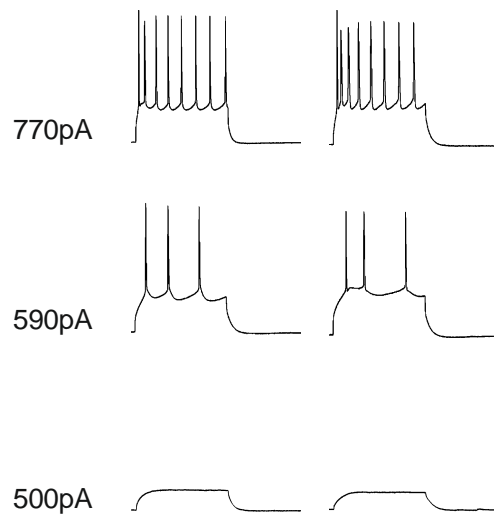
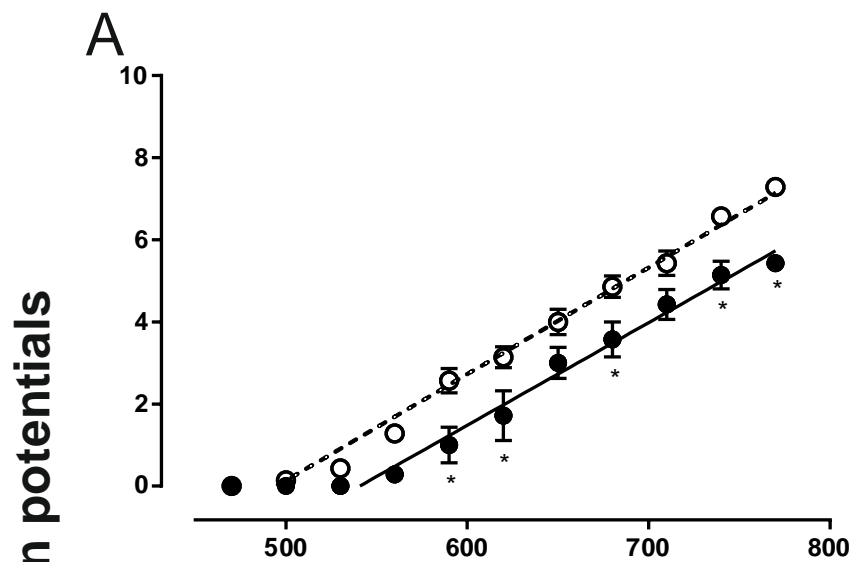












L

CHAPITRE 2:

INFLAMMATORY PAIN-INDUCED NEURONAL PLASTICITIES AND METAPLASTICITIES IN SUPERFICIAL LAYERS ON THE RAT PRIMARY SOMATOSENSORY CORTEX

**Inflammatory pain-induced neuronal plasticities and metaplasticities in superficial
layers on the rat primary somatosensory cortex**

Abbreviated title: Pain-induced plasticities in the rat S1 cortex

Hien Luong Nguyen¹, Cristina Alba-Delgado¹, Radhouane Dallel^{1,2}, Myriam Antri¹
and Alain Artola^{1*}

¹ Université Clermont Auvergne, Inserm, Neuro-Dol, F-63000 Clermont-Ferrand, France;

²CHU Clermont-Ferrand, Service d'Odontologie, F-63000 Clermont-Ferrand, France.

*** Correspondence:**

Alain ARTOLA, Inserm/UCA , U1107, Neuro-Dol, Trigeminal Pain and Migraine

Faculté de Chirurgie Dentaire, 2 rue de Braga, F-63100 CLERMONT-FERRAND, FRANCE

Phone + (33) 4 73 17 73 67

Mail : alain.artola@uca.fr

Number of pages (entire manuscript):

Number of Figures:

Number of Tables: 0

Abstract: 250

Introduction: 618

Discussion: 1486

Acknowledgements:

ABSTRACT

The development of chronic neuropathic or inflammatory pain hypersensitivity is believed to result from long-lasting changes in synaptic and neuronal functions in pain transmission pathways, from peripheral nociceptors to cortical areas, including the primary somatosensory cortex (S1). S1 cortex, coding sensory aspects—intensity, location—of pain, is consistently activated during nociception and becomes hyperactive under chronic pain states. How does S1 become hyperactive? Using *ex vivo* electrophysiological recordings from S1 layer 2/3 pyramidal neurons in a rat model of chronic facial inflammatory pain (Complex Freund Adjuvant—CFA— injection into the vibrissa pad), we assessed synaptic and neuronal plasticities at 1 hour and 3 days after injection. CFA injection produced facial mechanical allodynia: strong at 1 hour, still increasing at 3 days after injection. Facial mechanical allodynia was associated, at 1 hour, with, at the synaptic level, (i) long-term potentiation (LTP) of excitatory synapses onto pyramidal neurons and (ii) an inhibition to generate further synaptic LTP but a facilitation to generate synaptic long-term potentiation (LTD) (metaplasticity), and, at the neuronal level, (iii) LTP of the intrinsic excitability of postsynaptic pyramidal neurons. Whereas synaptic and intrinsic LTP, as behavioural mechanical allodynia, stayed constant over 3 days, LTP inhibition and LTD facilitation slowly decayed to control levels; that is metaplasticity reversed. These results suggest that both synaptic and intrinsic LTP underlie S1 hyperactivity during chronic pain states. Homeostatic metaplasticity which prevents too large synaptic potentiation right after CFA injection slowly decays at the time when activity in pain transmission pathways is likely decreased.

SIGNIFICANCE STATEMENT

INTRODUCTION

Persistent, chronic pain is initiated by peripheral tissue damage and inflammation (inflammatory pain) or peripheral and/or central nerve injury (neuropathic pain). It is characterized by persistent pain hypersensitivity, including spontaneous pain (pain experienced in the absence of any obvious peripheral stimulus), hyperalgesia (exacerbated response to noxious stimuli), and allodynia (pain in response to normally innocuous stimuli).

The development of such pain hypersensitivity is believed to be due to long-lasting changes in synaptic and neuronal functions in the pain transmission pathways, from the peripheral nociceptors and spinal dorsal horn to supraspinal and cortical areas including the primary somatosensory cortex (S1) and the anterior cingulate cortex (ACC) (Latremoliere and Woolf, 2009; Basbaum et al., 2009; Kuner, 2010; Saab, 2012; Bushnell et al., 2013).

Increasing evidence from rodent studies indicates that ACC activation contributes to chronic pain states and synaptic plasticity may underlie this effect. Imaging studies in humans (Vogt et al., 2003; Vogt, 2005; Shackman et al., 2011; Wager et al., 2013) and rodents (Wei et al., 2001; Li et al., 2010; Chen et al., 2014) have revealed the ACC to be consistently activated during pain perception. *Ex vivo* electrophysiological recordings in rodent models of inflammatory and neuropathic pain have demonstrated LTP of synaptic transmission onto from L2/3 (Wu et al., 2005; Zhao et al. 2006; Xu et al., 2008; Li et al., 2010; Bie et al. 2011; Ning et al. 2013; Koga et al., 2015; Chen et al. 2016) as well as L5 pyramidal neurons (Chen et al., 2014). Preventing such inflammatory (Wei et al., 2002; Wu et al., 2005; Eto et al., 2011; Gu et al., 2015), neuropathic (Xu et al., 2008; Li et al., 2010; Shen et al., 2015; Chen et al., 2016) or cancer (Chiou et al., 2016) pain-induced synaptic plasticity significantly attenuates pain hypersensitivity. Finally, silencing ACC reduces or prevents mechanical hypersensitivity (Xu et al., 2008; Eto et al., 2011; Chiou et al., 2016; Tan et al., 2017) whereas its activation can

induce and maintain nociceptive hypersensitivity in the absence of conditioned peripheral noxious drive (Chiou et al., 2016; Tan et al., 2017).

S1 cortex is responsible for the sensory aspects of pain, including the intensity and location of pain (Bushnell et al. 1999; Gross et al., 2007). It is consistently activated during nociception and becomes hyperactive under both chronic inflammatory and neuropathic pain states, both human (Seifert and Maihöfner, 2009; Peyron et al., 2004 ; Seminowicz et al., 2009) and rodent (Eto et al., 2011; 2012). Furthermore, strategies to reduce S1 hyperexcitability and reorganization demonstrate benefits against chronic pain development (Flor et al., 2001; Lotze et al., 1999; De Ridder et al., 2007).

How S1 cortex becomes hyperactive during the development of chronic inflammatory and neuropathic pain states remains unclear. There is evidence, under neuropathic pain conditions, for a shift in the activity of local inhibitory interneuron networks in favour of pyramidal neuron hyperactivity: local somatostatin-expressing and parvalbumin-expressing inhibitory neurons reduce their activity, while vasoactive intestinal polypeptide-expressing ones increase their activity (Cichon et al., 2016; but see Eto et al., 2012). But the postsynaptic efficacy of synaptic inhibition can also be decreased. Thus, under inflammatory pain conditions, the expression and function of the potassium–chloride cotransporter KCC2 is reduced (Eto et al., 2012), and thus anion homeostasis resulting disrupted (Coull et al., 2003). Release of the brain-derived neurotrophic factor (BDNF) could be one possible trigger of such KCC2 reduction (Coull et al., 2005). Under inflammatory conditions, BDNF is upregulated in the S1 cortex (Thibault et al., 2014).

Surprisingly, though, whether synaptic and/or neuronal plasticity also accounts chronic pain-induced S1 hyperactivity is still unknown. We addressed these issues by simultaneously assessing synaptic and intrinsic plasticities/metaplasticities in the superficial layers of the rat S1 cortex.

MATERIALS AND METHODS

Animals

Male Sprague-Dawley rats (Charles River, France), weighing about 50-75 g at their arrival, were housed 3–4 per cage at 22°C under 12h light/dark cycles (lights on 8 am) with *ad libitum* access to food and water. All efforts were made to minimise the number of animals used. All the experimental procedures followed the ethical guidelines of the International Association for the Study of Pain and the European Community Council directive of November 24, 1986 (86/609/EEC) and were approved by the local institutional animal care and use committee (UFR d'Odontologie, Université de Clermont-Auvergne).

Inflammation

Rats were anaesthetised (for 4-5 min) with halothane and quickly injected with 20µL of either NaCl 0.9% (control rats) or Complex Freund's Adjuvant (CFA rats) subcutaneously between the 1st and the 2nd line of vibrissae at the right side. CFA was obtained by diluting 100 mg of dried *Mycobacterium butyricum* (Difco Laboratories, Detroit, MI, USA) in: Tween 80 (1.66 mL) paraffin oil (10 mL), NaCl 0.9% (6.66 mL). CFA was stored at 4°C until use and kept 30 min at room temperature before injection. The success of CFA injection was confirmed by the development of an oedema (diameter: 0.8 to 1.2 cm) immediately after injection.

Facial sensitivity

A modified up-down method with a series of ten von Frey filaments (0.008, 0.02, 0.04, 0.07, 0.16, 0.4, 0.6, 1.0, 1.4 and 2.0 g; 2.0-g cut-off; Bioseb, France) was used. In this method, stimuli

were presented following an up-down sequence, each filament being applied 5 times with at least 5 s intervals. The experimenter held the rat gently with minimal restraint, and the first von Frey filament (see below) was presented perpendicular to the surface of the right vibrissa pad with sufficient strength to cause slight buckling. Behavioural features as eye winking, turning of the head away, attacking the tip of the filament and body freezing were considered as positive detection responses. If this filament was detected three or more times by the rat (3 to 5 positive responses), the next weaker stimulus was applied again 5 times; in the absence of detection (0, 1 or 2 positive responses), conversely, the next stronger stimulus was applied 5 times. The facial mechanical sensitivity threshold (in g) was the weaker von Frey filament to which the rat responded three times or more. When positive or negative responses were continuously observed until 0.008 g or 2.0 g filaments, we assigned these respective values as threshold to the session. In each session, rats were tested with at least 2 filaments and up to 4 filaments.

For behavioural testing, animals were first habituated to filaments, experimental room and researcher for five consecutive days. At the end of such habituation, none of the rats showed aversive response to 2 g filament. The day of drug injection, rats were first habituated for 30 min in the experimental room. Facial sensitivity to non-nociceptive mechanical stimuli was then measured before (baseline) and at 10-20 min intervals after drug administration, up to a maximum of 180-210 min. Baseline sessions started with 1.4 g filament and that following drug administration with 0.4 g filament. According to the responses, the next stronger or weaker von Frey filament was tested to determine the facial mechanical sensitivity threshold. Once the sensitivity threshold was determined, the next detection session (20 minutes later) started from this filament.

Ex vivo electrophysiological recordings

Slices. Slices were prepared using a method adapted from Agmon and Connors (1991). Briefly,

rats were deeply anesthetized by an intraperitoneal injection of chloral (7%; 70 mg.kg⁻¹), decapitated and their brain were quickly removed. The tissue was placed with the ventral face down into ice-cold (0-4°C) sucrose-based artificial cerebrospinal fluid (aCSF) containing (in mM): sucrose (205), KCl (2), MgCl₂ (7), CaCl₂ (0.5), NaHCO₃ (26), NaH₂PO₄.H₂O (1.2) and D-glucose (11). A vertical cut was made through the tissue at an angle of 55° to the right of the posterior-to-anterior axis of the brain, intersecting this axis at about its anterior one-third point. The tissue caudal to the cut was then glued onto the stage of a Vibratome (VT 1200S, Leica Microsystems, Wetzlar, Germany) with the cut surface down and the pial surface toward the blade. A small cube of agar was glued to the stage at the back of the tissue to prevent its movements due to blade pressure. Then the tissue was totally immersed into an ice-cold solution containing (in mM): K-gluconate (135), NaCl (5), MgCl₂.6H₂O (2), EGTA (0.2), HEPES (10), and sucrose (10). This solution was designed to mimic the intracellular medium and thus to limit the entry of extracellular ions into the cells during the slicing procedure (Dugué et al., 2005). Two or three (depending on brain size) slices 800-µm-thick were cut and discarded until the blade started to cut the left hemisphere. Then, 350 µm-thick slices were cut until the lateral ventricle (recognized by its pink tint) could no longer be seen on the surface of the tissue. Only the left hemispheres containing the primary somatosensory cortex (S1) were collected and suspended into normal aCSF containing (in mM) NaCl (125), KCl (2.5), CaCl₂ (2), MgSO₄ (2), NaHCO₃ (26), NaH₂PO₄.H₂O (1.25) and D-glucose (25) at 30°C for a 20-min recovery period and then maintained at room temperature (20-23°C) (Sessolo et al., 2015). All cutting, holding and recording external solutions were saturated with 5% CO₂ / 95% O₂ (pH 7.4; 310–320 mOsm).

Patch-clamp whole cell recordings. One slice was transferred into the recording chamber where it was continuously perfused at 2.0 mL.min⁻¹ with normal aCSF at room temperature (20-23°C). Neurones were visualized using an upright Zeiss Axioskop2 FS plus (Germany) fitted with

infrared differential interference contrast (DIC) optics and a CCD video camera (Hamamatsu, Japan). Patch-clamp whole-cell recordings were obtained from S1 layer 2/3 pyramidal neurones using double patch clamp EPS 10 amplifier (HEKA, Germany) and a Patchmaster acquisition software (HEKA, Germany). Signals were low-pass filtered at 10 kHz with a Bessel filter and sampled at 1 kHz. Electrodes were pulled from thin-wall borosilicate capillaries (outer diameter: 1.5 mm, inner diameter: 1.12 mm, WPI, Sarasota, FL, USA) using a horizontal puller (Model P-97, Sutter Instruments, Navato, CA, USA). Recording electrodes had resistances ranging 5-7 M Ω , being filled with an internal solution containing (in mM) K-gluconate (135), NaCl (5), MgCl₂ (2), sucrose (10), HEPES (10), ethylene glycol-bis-(o-aminophenoxy)-ethane-N,N,N',N'-tetraacetic acid (EGTA) (0.2), Na₂ATP (2.5), NaGTP (0.3), pH adjusted to 7.3, and osmolality of 300 ± 5 mOsm.

Excitatory postsynaptic currents (EPSC), recorded in voltage clamp mode from layer 2/3 pyramidal neurons, were evoked by 0.1-ms current pulses, using a monopolar glass stimulating electrode (filled with normal aCSF, 2-3 Mohm) placed in layer 4/5 of S1. In most of the experiments, stimuli were paired within a delay of 50 msec. During conditioning, afferent stimulation at 2 Hz for 50 sec was paired with various levels of postsynaptic membrane depolarization. Spontaneous excitatory postsynaptic currents (sEPSCs) were recorded in voltage-clamp mode at a holding potential of -70 mV. Frequency and amplitude of sEPSCs were analysed over a 5-minute duration data segment.

Analysis. Resting membrane potential (RPM) was measured as the mean baseline potential during 80 ms in current-clamp mode just after break-in. During the course of the experiments, input (R_{in}) and series resistances (R_s) were periodically monitored using a 500-ms-long, 10-pA-hyperpolarizing current pulse. Cells were included in the analysis if they met the following criteria: RPM < -60 mV, and R_s < 40 M Ω . To evaluate intrinsic excitability, neurons were injected with depolarizing current pulses (500-ms-long, ranging from 350 to 770 pA, with 30 pA

increments) in current-clamp mode measured from about $V_m = -70$ mV at which the neuron was kept. Curves of the number of action potential firing as a function of injected current were constructed. Rheobase [the minimal depolarizing current amplitude injected at the soma in order to make the cell fire an action potential (AP)] was measured as the first of three consecutive current pulses of the same intensity able to generate at least one AP. A ramp of current (from 0 pA to 2 times the rheobase, in 1 s) was used to assess AP voltage threshold: it was the voltage at which the value of dV/dt exceeded 20 mV/ms. AP characteristics were obtained from the first spike evoked by the minimal depolarizing current pulse in every S1 pyramidal neuron recorded. AP amplitude was measured from its threshold to its peak and AP duration at half maximum amplitude. After-hyperpolarization (AHP) represented the difference between spike threshold and post AP hyperpolarization.

Paired pulse ratio (PPR) was the ratio of the amplitude of the second EPSC to that of the first one.

All the above analyses were performed using Fitmaster (HEKA, Germany).

Statistical analysis

One-way analysis of variance (ANOVA) for repeated measures or not was conducted. Significant interactions were followed up with the Tukey or Tukey's HSD (honestly significant difference) *post hoc* test. Spontaneous EPSC were analysed using the Kolmogorov–Smirnov test. All the data are presented as mean \pm SEM. In each group, n is for the number of recorded neurons and N is for the number of rats.

RESULTS

In a rat model of facial chronic inflammatory pain (CFA injection into the vibrissa pad), we examined whether mechanical allodynia is associated with plasticity within superficial layers (layers 2/3) of the projection area of the right vibrissa pad afferents (barrel cortex) into the left

primary somatosensory cortex (S1). Behavioural mechanical sensitivity and plasticity were examined at two delays after CFA injection: 1 hour and 3 days (Fig. 1A). We simultaneously assessed several types of plasticities: changes in synaptic strength and in postsynaptic intrinsic neuronal excitability and (synaptic) metaplasticity. Experiments in CFA- and NaCl-injected rats (controls) were intermingled for comparison.

CFA injection into the vibrissae pad induces a facial mechanical allodynia

The mechanical sensitivity of rats after subcutaneous injection of CFA (2.5 mg/kg) into the right vibrissa pad was measured using von Frey filaments (Fig. 1B). Compared with controls, CFA injection led to a profound decrease in thresholds for evoking facial withdrawal to mechanical stimuli at 1 h (1.92 ± 0.04 g, N=34 and 4.25 ± 0.17 g, N=16 in CFA- and NaCl-injected rats, respectively; One-way ANOVA, $P < 0.0001$) and 3 days after injection (1.36 ± 0.06 g, N=21 and 4.19 ± 0.13 g, N=13 in CFA- and NaCl-injected rats, respectively; One-way ANOVA, $P < 0.0001$). Of note, mechanical allodynia was already very strong at 1 hour after CFA injection (1.92 ± 0.04 g compared with baseline 4.06 ± 0.06 g, N=34; One-way ANOVA, $P < 0.0001$) but still increased at post-injection day 3 (3 days vs 1 hour after CFA injection, N=34 and 21, respectively, One-way ANOVA, $P < 0.0001$).

CFA injection induces a lasting potentiation of synaptic transmission onto S1 L2/3 pyramidal neurons

To assess excitatory synaptic transmission in S1 superficial layers, we recorded sEPSCs at -70 mV (holding potential) from L2/3 pyramidal neurons in *ex vivo* S1 slices from CFA- and NaCl-injected rats (Fig. 2).

At 1 hour after injection (Fig. 2, left), compared with NaCl-injected rats (n=5, N=5), the cumulative amplitude distribution of sEPSCs in CFA-injected rats (n=19, N=19) was shifted to

the right (Kolmogorov–Smirnov test: $P < 0.0001$) (Fig. 2 B, left and their amplitudes were larger by a factor of ~50% (mean amplitude: 27.9 ± 0.9 pA and 21.2 ± 0.8 pA, in CFA- and NaCl-injected rats, respectively; One-way ANOVA, $P < 0.0001$) (Fig. 2 C, left). On the other hand, there was no change in sEPSC frequency (mean frequency: 2.5 ± 0.1 Hz and 2.6 ± 0.1 Hz, in CFA- and NaCl-injected rats, respectively; One-way ANOVA, $P = 0.7272$) (Fig. 2 D, left). These results suggest that, in CFA-injected rats, synaptic transmission onto S1 L2/3 pyramidal neurons is potentiated and that such potentiation involves postsynaptic mechanisms as sEPSC amplitudes, but not frequencies, are enhanced. To further test this hypothesis, we compared sEPSCs in naïve synapses in CFA-injected rats (see above) with those in NaCl-injected rats after LTP of vertical input-L2/3 pyramidal neuron synapses had been induced by a pairing to 0mV ($n=5$, $N=5$). The cumulative amplitude distribution of potentiated sEPSCs in control animals became superimposed with that of CFA-injected rats (Kolmogorov–Smirnov test: $P > 0.05$) and their amplitude similar (mean amplitude: 27.9 ± 0.9 pA and 29.6 ± 1.6 pA, in CFA- and NaCl-injected rats, respectively; One-way ANOVA, $P = 0.6490$) (Fig. 2 B, C, left). There was still no difference in sEPSC frequency (mean frequency: 2.5 ± 0.1 Hz and 2.6 ± 0.1 Hz, in CFA- injected rats and NaCl-injected ones after pairing to 0mV, respectively; One-way ANOVA, $P = 0.8089$) (Fig. 2 D, left). These results confirm that excitatory synapses onto L2/3 pyramidal neurons within S1 cortex have undergone LTP as early as 1 h after CFA injection.

Comparison of sEPSCs in CFA- and NaCl-injected rats, at post-injection day 3 (Fig. 2, right), led to the same conclusion as at 1 h after injection. Compared with NaCl-injected rats ($n=4$, $N=4$), CFA-injected ones ($n=17$, $N=17$) exhibited a rightward shift in the cumulative amplitude distribution (Kolmogorov–Smirnov test: $P < 0.0001$) (Fig. 2 B, right) and ~50% larger sEPSCs (mean amplitude: 28.0 ± 0.7 pA and 19.3 ± 0.9 pA, in CFA- and NaCl-injected rats, respectively; One-way ANOVA, $P < 0.0001$) (Fig. 2 C, right). Moreover, both cumulative

amplitude distribution and mean sEPSC amplitude were the same in CFA-injected (see above) rats and NaCl-injected rats after LTP of vertical input-L2/3 pyramidal neuron ($n=4$, $N=4$) (Kolmogorov–Smirnov test: $P>0.05$; mean amplitude: 28.0 ± 0.7 pA and 27.4 ± 0.3 pA, in CFA- and NaCl-injected rats, respectively; One-way ANOVA, $P=0.9167$) (Fig. 2 B, C, right).

There was still no difference in sEPSC frequency (mean frequency: 2.4 ± 0.1 Hz, 2.5 ± 0.1 Hz, and 2.5 ± 0.5 Hz in CFA-injected rats and NaCl-injected ones before and after pairing to 0mV, respectively; One-way ANOVA, $P=0.8968$) (Fig. 2 D, right).

Finally, comparison of sEPSCs at 1 hour and 3 days after CFA injection (Fig. 3) shows that they were equivalently potentiated: the cumulative amplitude distributions were overlapping (Kolmogorov–Smirnov test: $P>0.05$) and their mean amplitudes similar (27.9 ± 0.9 pA and 28 ± 0.7 pA, 1 h and 3 days after injection, respectively; One-way ANOVA, $P>0.9999$). Altogether, these results indicate that CFA injection triggers LTP of excitatory synaptic transmission within superficial layer of the S1 cortex as early as 1 hour after CFA injection and over at least 3 days. Synaptic LTP and behavioural mechanical allodynia have therefore the same time course.

CFA injection induces decaying metaplasticity.

Prior synaptic activity can also alter the ability of activated synapses to generate subsequent synaptic plasticity (for review see Abraham, 2008). This phenomenon, referred to as metaplasticity, manifests as modifications in the direction or degree of activity-dependent synaptic changes. In the neocortex and hippocampus, the level of postsynaptic depolarization determines whether LTP or LTD results from stimulation at a given frequency (Artola et al., 1990). Therefore, to assess metaplasticity in S1 superficial layers of CFA-injected rats, we compared the ability of vertical input-L2/3 pyramidal neuron synapses to undergo LTD and LTP using a brief afferent stimulation paired with various levels of postsynaptic depolarization

(Ngezahayo et al., 2000; Nguyen et al., *subm.*) in CFA- and NaCl-injected rats.

At 1 hour after injection (Fig. 4), pairing brief low-frequency afferent stimulation (2 Hz for 50 s) with postsynaptic depolarization to 0 mV, referred to as pairing to 0mV in the remainder of the paper, produced LTP in NaCl-injected rats ($157.8 \pm 7.4\%$ of baseline; One way ANOVA for repeated measures: $P < 0.0001$; $n=4$; $N=4$) but no synaptic change in CFA-injected rats ($98.5 \pm 2.3\%$ of baseline; One way ANOVA for repeated measures: $P=0.2076$; $n=9$; $N=8$) (Fig. 4 A). A pairing to -10mV produced LTP in NaCl-injected rats ($130.2 \pm 5.9\%$ of baseline; One way ANOVA for repeated measures: $P < 0.0001$; $n=4$; $N=4$) but LTD in CFA-injected rats ($78.0 \pm 2.8\%$ of baseline; One way ANOVA for repeated measures: $P < 0.0001$; $n=5$; $N=5$) (Fig. 4 B). A pairing to -20mV produced LTD in both NaCl-injected rats ($65.4 \pm 2.2\%$ of baseline; One way ANOVA for repeated measures: $P < 0.0001$; $n=2$; $N=2$) and CFA-injected rats ($53.4 \pm 2.8\%$ of baseline; One way ANOVA for repeated measures: $P < 0.0001$; $n=4$; $N=4$) but the magnitude of LTD was larger in CFA-injected rats than in NaCl-injected ones (LTD in CFA-injected rats vs LTD in NaCl-injected ones: One way ANOVA for repeated measures: $P < 0.0001$) (Fig. 4 C). A pairing to -30mV produced no synaptic change in NaCl-injected rats ($99.0 \pm 2.6\%$ of baseline; One way ANOVA for repeated measures: $P=0.4822$; $n=2$; $N=2$) but LTD in CFA-injected rats ($84.1 \pm 0.3\%$ of baseline; One way ANOVA for repeated measures: $P < 0.0001$; $n=6$; $N=6$) (Fig. 4 D). This clearly indicates that the direction and/or degree of activity-dependent synaptic changes are modified in CFA-injected rats compared with controls. The voltage–response function for the induction of LTD/LTP, or synaptic plasticity rule, in S1 synapses of CFA-injected rats describes a two-voltage threshold curve (Fig. 4 F), with a LTD-threshold (between -40 and -30 mV) and a LTP threshold (at 0 mV). Compared with the synaptic plasticity rule in S1 synapses of controls rats, the LTD-threshold is shifted to the left (from between -30 and -20 mV to between -40 and -30 mV) and the LTP-threshold to the right (from between -20 and -10 mV to 0 mV. Importantly, these very concomitant shifts in the LTD- and LTP-thresholds, away from each other are

characteristic of potentiated synaptic transmission (Ngezahayo et al., 2000; Nguyen et al., *subm*).

To test the hypothesis that changes in the voltage-response curve for the induction of LTD/LTP in CFA-injected rats are parallel to LTP induction, we examined how prior induction of LTP in vertical input-L2/3 pyramidal neuron synapses of NaCl-injected rats modifies their ability to subsequently undergo LTD or LTP. In this series of experiments, we assessed the effect of a test pairing to various V_m applied 10-30 min after a first, conditioning or priming, pairing to 0 mV. The voltage-response function for the induction of LTD/LTP in these potentiated synapses was superimposed with that of naïve synapses in CFA-injected rats (Fig. 4 G). These results thus confirm that CFA induced metaplastic changes are similar with those produced experimentally during LTP induction.

We performed the very same series of experiments at post-injection day 3 days (Fig. 5). Pairing to 0mV produced LTP in both NaCl-injected rats ($169.0 \pm 13.2\%$ of baseline; One way ANOVA for repeated measures: $P < 0.0001$; $n=4$; $N=4$) and CFA-injected rats ($160.4 \pm 1.8\%$ of baseline; One way ANOVA for repeated measures: $P < 0.0001$; $n=6$; $N=6$) (Fig. 5 A). A pairing to -10mV produced LTP in both NaCl-injected rats ($126.7 \pm 7.7\%$ of baseline; One way ANOVA for repeated measures: $P < 0.0001$; $n=4$; $N=4$) and in CFA-injected rats ($124.2 \pm 0.7\%$ of baseline; One way ANOVA for repeated measures: $P < 0.0001$; $n=3$; $N=3$) (Fig. 5 B). A pairing to -20mV produced LTD in both NaCl-injected rats ($67.1 \pm 0.7\%$ of baseline; One way ANOVA for repeated measures: $P < 0.0001$; $n=2$; $N=2$) and CFA-injected rats ($65.9 \pm 1.1\%$ of baseline; One way ANOVA for repeated measures: $P < 0.0001$; $n=4$; $N=4$). A pairing to -30mV produced no synaptic change in both NaCl-injected rats ($103.6 \pm 3.0\%$ of baseline; One way ANOVA for repeated measures: $P=0.9737$; $n=2$; $N=2$) and CFA-injected rats ($99.7 \pm 2.7\%$ of baseline; One way ANOVA for repeated measures: $P=0.9742$; $n=7$; $N=7$) (Fig. 5 D). Importantly, the magnitude of all these synaptic changes were the very same in CFA and NaCl-injected rats (synaptic change in CFA-injected rats vs. that in NaCl-injected ones: One way ANOVA: pairing

to 0 mV: $P=0.1916$; pairing to -10 mV: $P=0.5967$; pairing to -20 mV: $P=0.5991$; pairing to -30 mV: $P=0.7600$) (Fig. 5 A-C). Consistently, the two voltage–response functions for the induction of LTD/LTP in S1 synapses of CFA- and NaCl-injected rats were exactly superimposed (Fig. 5 F). This indicates that, though synaptic strength remained potentiated, CFA injection-induced metaplastic changes slowly decayed over 3 days (Fig. 6).

CFA injection induces LTP of intrinsic excitability of S1 L2/3 pyramidal neurons

It is now well established in various brain areas, including the cerebellum (Aizenman & Linden, 2000), hippocampal CA1 (Daoudal et al., 2002) and S1 (Nguyen et al., *subm.*), that synaptic activation also produces long-term changes in intrinsic neuronal excitability (for review see Zhang and Linden, 2003; Kourrich et al., 2015; Titley et al., 2017). We therefore investigated whether the intrinsic excitability of S1 L2/3 pyramidal neurons was also altered after CFA injection.

Intrinsic excitability was measured in current-clamp mode by injecting brief depolarizing currents (350 to 770 pA, with 30 pA increments) from a baseline potential of -70 mV. The number of depolarization-evoked action potentials (AP) was taken as a measure of neuronal excitability. Comparison of the input–output curves, relating the number of evoked APs or firing response to the injected depolarizing current, referred to as F-I curve, in CFA-injected rats ($n=54$; $N=34$) and NaCl-injected ones ($n=33$; $N=16$), at 1 hour after injection, showed that the F-I curve in CFA-injected rats was shifted to the left; more APs were elicited by depolarizing current steps after CFA injection than after NaCl injection (F-I curve in CFA-injected rats *vs.* F-I curve in controls: One way ANOVA for repeated measures: $P<0.0001$) (Fig. 7A). Interestingly, whereas the firing response increased (response to a 770-pA-step: $155.6 \pm 5.9\%$ of that in NaCl-injected rats), its gain—i.e. the slope of the F-I curve—did not change (0.0278 ± 0.0008 and 0.0280 ± 0.0007 number of AP.pA⁻¹ in CFA- and NaCl-injected rats, respectively; One way ANOVA:

$P=0.9979$). These results suggest that CFA injection induces an enduring potentiation or LTP of intrinsic excitability (LTP-IE). We then asked whether such LTP-IE was similar to that experimentally triggered by evoked synaptic activation in S1. We assessed the intrinsic excitability of postsynaptic neurons in control rats, in which we had induced LTP of vertical input-L2/3 pyramidal neuron synapses using a pairing to 0mV (see above) ($n=21$; $N=16$). As expected (see Nguyen et al., *subm.*), such synaptic activity produced LTP-IE manifest as a leftward shift in the F-I curve (F-I curve in NaCl-injected rats before *vs* after pairing to 0mV: One way ANOVA for repeated measures: $P<0.0001$) (Fig. 7A). Importantly, F-I curves in CFA-injected rats and in NaCl-injected ones after pairing to 0 mV were superimposed (One way ANOVA for repeated measures: $P=0.9491$). Altogether, these results indicate that CFA injection induces LTP-IE in L2/3 pyramidal neurons

To further examine changes in the intrinsic properties, we analyzed the properties of APs (Fig. 7). Compared with NaCl-injected rats, CFA-injected ones exhibited a ~ 2 -mV hyperpolarizing shift in the voltage threshold (Fig. 7 C) and a decreased rheobase (Fig. 7 D), AP amplitude (Fig. 7 E) and after-hyperpolarization (Fig. 7 G). Importantly, similar changes occurred after induction of LTP-IE in control rats (Fig. 7 C-G).

Given that L2/3 pyramidal neurons integrate tremendous inputs from subcortical regions and generate output signals to lamina V output neurons, we questioned whether the strategy for the information processing would be changed in neurons from CFA-injected rats. To answer this question, we investigated spike frequency adaption (SFA), which operates to filter the output signal by attenuating unnecessary firing (Benda and Herz, 2003; Pozzorini et al., 2013). To determine SFA, all interspike intervals (ISIs) of the firing responses to 770-pA-steps were calculated and normalized to the first ISIs. Despite the increase in the firing rates, there was no significant change in calculated SFA of neurons from CFA-injected rats compared with those

of controls (Fig. 7B). We concluded that CFA-induced hyperexcitability of S1 L2/3 pyramidal neurons does not manifest as changes in the strategy of information process, but only modify the gain of the firing rates.

F-I curves were also assessed at post-injection day 3 (CFA-injected rats: n=44; N=21; NaCl-injected rats: n=22; N=13). As at 1 hour after injection, F-I curves in CFA-injected rats were shifted to the left (F-I curve in CFA-injected rats vs. F-I curve in controls: One way ANOVA for repeated measures: $P < 0.0001$) (Fig. 8 A). Again, only the firing response increased (response to a 770-pA-step: $156.2 \pm 10.3\%$ of that in NaCl-injected rats) but not its gain (0.0272 ± 0.0007 and 0.0263 ± 0.0006 number of AP.pA⁻¹ in CFA- and NaCl-injected rats, respectively; One way ANOVA: $P > 0.9$). We also assessed the intrinsic excitability of postsynaptic neurons in control rats, in which we had induced LTP of vertical input-L2/3 pyramidal neuron synapses using a pairing to 0mV (n=13; N=13). Such synaptic activity produced a leftward shift in F-I curves (F-I curve in NaCl-injected rats before vs. after pairing to 0mV: One way ANOVA for repeated measures: $P > 0.9$) which was again similar to that in CFA-injected rats (One way ANOVA for repeated measures: $P > 0.9$). Importantly, F-I curves (Fig. 8 A), voltage thresholds (Fig. 8 C), rheobases (Fig. 8 D) AP amplitudes (Fig. 8 E) and after-hyperpolarizations (Fig. 8 G), at 1 hour and 3 days after CFA injection were the same, demonstrating that CFA injection had induced a LTP-IE of S1 L2/3 pyramidal neurons that lasted at least 3 days.

DISCUSSION

This study was designed to assess simultaneously several forms of plasticity—synaptic and intrinsic—and their time course in superficial S1 cortex in a rat model of facial chronic inflammatory pain. The manifestation of facial mechanical allodynia was associated, as early as 1 hour after pain onset, with, at the synaptic level, (i) LTP of excitatory synaptic transmission onto L2/3 pyramidal neurons and (ii) an inhibition to generate further LTP but a facilitation to

generate LTD (metaplasticity), and, at the neuronal level, (iii) LTP of the intrinsic excitability of postsynaptic L2/3 pyramidal neurons. Whereas both synaptic and intrinsic LTP stayed constant during the time they were assessed—3 days after inflammatory pain onset—LTP inhibition and LTD facilitation slowly decayed to control levels, consistent with a reversal of metaplastic phenomenon.

These results describe LTP of synaptic strength and intrinsic excitability in the S1 neocortex under chronic inflammatory conditions. Such plasticity might account at least in part for the L2/3 neuron hyperactivity in the S1 neocortex observed using two-photon Ca^{2+} imaging (hindpaw CFA model; Eto et al., 2011; 2012). It should occur together with a reduction in synaptic inhibition due to both (i) a shift in the activity of local inhibitory interneuron networks in favour of pyramidal neuron hyperactivity, and (ii) a reduced efficacy of synaptic inhibition. Indeed, on the one hand, local somatostatin-expressing and parvalbumin-expressing inhibitory neurons were shown to reduce their activity, while vasoactive intestinal polypeptide-expressing ones increased their activity under neuropathic pain conditions (Cichon et al., 2016; but see Eto et al., 2012). On the other hand, under chronic inflammatory pain conditions, the expression and function of KCC2 is reduced (Eto et al., 2012), resulting in a disruption in the anion homeostasis (Coull et al., 2003). Release of BDNF could be one possible trigger of such KCC2 reduction (Coull et al., 2005). Under inflammatory conditions, BDNF is upregulated in the S1 cortex, potentiating neuronal responses together with triggering pain hypersensitivity (Thibault et al., 2014).

Synaptic LTP in superficial S1 cortex

Our results demonstrate that chronic inflammatory pain triggers synaptic LTP within the S1 cortex that may underlie inflammatory pain-induced S1 hyperactivity (Eto et al., 2011; 2012). Using anatomical markers of activation, it was shown that the ACC is activated under both

neuropathic (Li et al., 2010; Chen et al., 2014) and chronic inflammatory pain conditions (Wei et al., 2001) and that synaptic transmission onto from L2/3 (Wu et al., 2005; Zhao et al. 2006; Xu et al., 2008; Li et al., 2010; Bie et al. 2011; Ning et al. 2013; Koga et al., 2015; Chen et al. 2016) as well as L5 pyramidal neurons (Chen et al., 2014) in *ex vivo* ACC slices is concomitantly potentiated.

Analysis of sEPSCs suggests that, under inflammatory conditions, synaptic LTP in S1 cortex involves exclusively a postsynaptic mechanisms. In ACC, potentiation of excitatory inputs onto ACC layer 2-3 pyramidal neurons was shown to involve both pre- and postsynaptic mechanisms in mice (Xu et al., 2008; Li et al., 2010; Koga et al., 2015) as well as rats (Shen et al. 2015) under neuropathic pain conditions, while only presynaptic mechanisms in mice (Zhao et al., 2006; Koga et al., 2015) or postsynaptic ones in rats (Bie et al., 2011) under inflammatory pain conditions. It is noteworthy that recent evidence in mice (Koga et al., 2015; Zhuo et al., 2016) suggests that the form of LTP in ACC, which is expressed by an increase in glutamate release—that is, the presynaptic form—, may specifically contribute to pain-related anxiety. It is therefore possible that such presynaptic form of LTP does not occur in the S1 cortex since this cortical area is rather responsible for the sensory aspects of pain, such as the intensity and location of the pain (Bushnell et al., 1999; Gross et al. 2007).

Of note, the magnitude of synaptic LTP after pairing to 20mV was the same in inflammatory pain and control animals. This indicates that synaptic activity can produce similarly large potentiation in potentiated synapses as in naïve ones provided that the level of postsynaptic depolarization is increased.

Metaplasticity

Our results also demonstrate that right after pain onset, the induction of LTP was inhibited and that of LTD, facilitated.

This observation is consistent with our conclusion that excitatory synapses were potentiated under inflammatory conditions. In adult hippocampal CA1, low-frequency afferent stimulation (LFS) produces little or no depression in naïve synapses but depresses these very synapses once they have been potentiated (Barrionuevo et al., 1980; Staubli and Lynch, 1990; Fujii et al., 1991; Larson et al., 1993; Wexler and Stanton, 1993; Bortolotto et al., 1994; O'Dell and Kandel, 1994; Wagner and Alger, 1995; Norris et al., 1996), suggesting that prior induction of LTP has primed the pathway to subsequent LTD induction. Interestingly, high-frequency stimulation conditioning can similarly facilitate the subsequent induction of pain-LTP in humans (Magerl et al., 2018). Direct evidence for such leftward shift in the LTD threshold in potentiated synapses was obtained in hippocampal CA1 (Ngezahayo et al., 2000) as well as the S1 cortex (Nguyen et al., *subm.*) using a pairing protocol. Similarly, that tetani, which produce LTP can subsequently induce LTD (Yang and Faber, 1991) suggests that the LTP threshold is concomitantly shifted to higher levels of depolarization in potentiated synapses. Direct evidence for a rightward shift in the LTP threshold in potentiated synapses was recently obtained in the S1 cortex (Nguyen et al., *subm.*). Therefore that, at 1 h after CFA injection, the LTD threshold was shifted to lower levels of depolarization and the LTP threshold concomitantly to higher levels of depolarization strongly suggests that excitatory synapses were potentiated under inflammatory conditions.

Our results also show that the shifts in LTD and LTP thresholds slowly decayed over 3 days. It is clear that metaplastic changes in the ability to generate synaptic plasticity are reversible. However, the reported durations of LTD facilitation (Fujii et al., 1991; Christie and

Abraham, 1992; Holland and Wagner, 1998; Wang et al., 1998) and LTP inhibition (Huang et al., 1992; Abraham and Huggett, 1997; Frey et al., 1995) ranged from minutes to hours. It has to be noted that the above metaplastic phenomenon were triggered by electrical stimulation of presynaptic afferents. Here, metaplasticity was produced by CFA-induced activity in pain pathways to S1 cortex; that is a more physiological condition.

LTP-IE

Whereas intrinsic excitability was found to be unchanged in ACC (Wu et al., 2005) or decreased in prelimbic cortex (Wang et al., 2015) L2/3 pyramidal neurons under inflammatory conditions (hindpaw CFA model), our results demonstrate that facial chronic inflammatory pain triggers LTP-IE within the S1 cortex that may also contribute to the inflammatory pain-induced S1 hyperactivity (Eto et al., 2011; 2012). First, the F-I curve was shifted to the left under inflammatory conditions, as in control rats after pairing to 0mV. Second, synaptic activation in CFA-injected rats produced a very peculiar LTD-IE–reduction in the firing response associated with a decrease in its gain–characteristic of that obtained in control animals after prior induction of LTP-IE (see Nguyen et al., *subm.*). Finally, such LTP-IE was associated with synaptic LTP.

There are many examples of synergistic synaptic and intrinsic changes in CA1 pyramidal neurons (Daoudal *et al.*, 2002; Wang *et al.*, 2003; Xu *et al.*, 2005; Campannac and Debanne, 2008; Gasselin *et al.*, 2017) and cerebellar granule (Armano et al., 2006; Rizwan *et al.*, 2016) and Purkinje cells (Belmeguenai et al., 2010; Ohtsuki et al., 2012; Shim *et al.*, 2017; but see Yang and Santamaria, 2016). Moreover, parallel frequency-dependent (Daoudal *et al.*, 2002) or spike-timing-dependent (Campannac and Debanne, 2008) synaptic and intrinsic plasticity rules were observed in hippocampal CA1. Non-synergistic (i.e. homeostatic) intrinsic plasticity has also been reported–LTD-IE with synaptic LTP–but it was in hippocampal CA1, associated with

large synaptic LTP (Fan et al., 2005; Narayanan & Johnston, 2006; Campanac et al., 2008).

It is already known that intrinsic excitability changes accompany some forms of learning and last at least 24 hr after training (Disterhoft et al., 1986; Moyer et al., 1996; Schreurs et al., 1998). We demonstrate here that enhanced excitability, as behavioral mechanical allodynia, had not returned to naive pre-pain values 3 days after pain onset, which indicates a more persistent role in pain memories.

These results demonstrate that under inflammatory conditions, excitatory synaptic transmission and intrinsic excitability are enhanced and the induction of synaptic LTD and LTP are facilitated and inhibited, respectively, in S1 superficial layers. Whereas synaptic and intrinsic LTP stay constant as behavioral mechanical allodynia, accounting, at least in part, for S1 hyperactivity during pain, metaplastic changes—i.e. LTD facilitation and LTP inhibition—slowly return to pre-pain values within 3 days. Right after pain onset, when CFA-induced activity within pain pathways is high, homeostatic metaplasticity processes—LTD facilitation and LTP inhibition—should prevent too large synaptic potentiation. On the other hand, when activity within pain pathways decreases, such homeostatic processes are no more needed and can thus return to baseline.

REFERENCES

- Abraham WC (2008) Metaplasticity: tuning synapses and networks for plasticity. *Nat Rev Neurosci.* 9:387-399.
- Abraham WC, Huggett A (1997) Induction and reversal of long-term potentiation by repeated high-frequency stimulation in rat hippocampal slices. *Hippocampus* 7:137–145.
- Agmon A, Connors BW (1991) Thalamocortical responses of mouse somatosensory (barrel) cortex in vitro. *Neuroscience* 41:365-380.
- Aizenman CD, Linden DJ (2000) Rapid, synaptically driven increases in the intrinsic excitability of cerebellar deep nuclear neurons. *Nat Neurosci* 3:109-111.
- Armano S, Rossi P, Taglietti V, D'Angelo E (2000) Long-term potentiation of intrinsic excitability at the mossy fiber-granule cell synapse of rat cerebellum. *J Neurosci.* 20:5208-5216.
- Artola A, Bröcher S, Singer W (1990) Different voltage-dependent thresholds for inducing long-term depression and long-term potentiation in slices of rat visual cortex. *Nature* 347:69 –72.
- Barrionuevo G, Schottler F, Lynch G (1980) The effects of repetitive low frequency stimulation on control and “potentiated” synaptic responses in the hippocampus. *Life Sci* 27:2385–2391.
- Basbaum AI, Bautista DM, Scherrer G, Julius D (2009) Cellular and molecular mechanisms of pain. *Cell* 139:267–284.
- Belmeguenai A, Hosy E, Bengtsson F, Pedroarena C, Piochon C, Teuling E, He Q, Ohtuski G, De Jeu MT, Elgersma Y, De Zeeuw CI, Jorntell H, Hansel C (2010) Intrinsic plasticity complements long-term potentiation in parallel fiber input gain control in cerebellar Purkinje cells. *J Neurosci* 30:13630 –13643.

- Benda J, Herz AV (2003) A universal model for spike-frequency adaptation. *Neural Comput* 15:2523–2564.
- Bie B, Brown DL, Naguib M (2011) Increased synaptic GluR1 subunits in the anterior cingulate cortex of rats with peripheral inflammation. *Eur J Pharmacol.* 653(1-3):26-31.
- Bortolotto ZA, Bashir ZI, Davies CH, Collingridge GL (1994) A molecular switch activated by metabotropic glutamate receptors regulates induction of long-term potentiation. *Nature* 368:740–743.
- Boyer N, Dallel R, Artola A, Monconduit L (2014) General trigeminospinal central sensitization and impaired descending pain inhibitory controls contribute to migraine progression. *Pain* 155(7):1196-205.
- Bushnell MC, Ceko M, Low LA (2013) Cognitive and emotional control of pain and its disruption in chronic pain. *Nat. Rev. Neurosci.* 14:502–511.
- Bushnell MC, Duncan GH, Hofbauer RK, Ha B, Chen JI, Carrier B (1999) Pain perception: is there a role for primary somatosensory cortex? *Proc. Natl. Acad. Sci. USA* 96:7705–7709.
- Campanac E, Daoudal G, Ankri N, Debanne D (2008) Downregulation of dendritic I(h) in CA1 pyramidal neurons after LTP. *J Neurosci.* 28:8635-8643.
- Campanac E, Debanne D (2008) Spike timing-dependent plasticity: a learning rule for dendritic integration in rat CA1 pyramidal neurons. *J Physiol* 586:779–793.
- Chen ZY, Shen FY, Jiang L, Zhao X, Shen XL, Zhong W, Liu S, Wang ZR, Wang YW (2016) Attenuation of Neuropathic Pain by Inhibiting Electrical Synapses in the Anterior Cingulate Cortex. *Anesthesiology* 124(1):169-183.
- Chen T, Koga K, Descalzi G, Qiu S, Wang J, Zhang LS, Zhang ZJ, He XB, Qin X, Xu FQ, Hu J, Wei F, Huganir RL, Li YQ, Zhuo M (2014) Postsynaptic potentiation of corticospinal projecting neurons in the anterior cingulate cortex after nerve injury. *Mol Pain* 10:33.

- Chiou CS, Chen CC, Tsai TC, Huang CC, Chou D, Hsu KS (2016) Alleviating Bone Cancer-induced Mechanical Hypersensitivity by Inhibiting Neuronal Activity in the Anterior Cingulate Cortex. *Anesthesiology* 125(4):779-792.
- Christie BR, Abraham WC (1992) Priming of associative long-term depression in the dentate gyrus by e⁻ frequency synaptic activity. *Neuron* 8:79–84.
- Cichon J, Blanck TJJ, Gan WB, Yang G (2017) Activation of cortical somatostatin interneurons prevents the development of neuropathic pain. *Nat Neurosci.* 20(8):1122-1132.
- Coull JA, Beggs S, Boudreau D, Boivin D, Tsuda M, Inoue K, Gravel C, Salter MW, De Koninck Y (2005) BDNF from microglia causes the shift in neuronal anion gradient underlying neuropathic pain. *Nature* 438(7070):1017-1021.
- Coull JA, Boudreau D, Bachand K, Prescott SA, Nault F, Sîk A, De Koninck P, De Koninck Y (2003) Trans-synaptic shift in anion gradient in spinal lamina I neurons as a mechanism of neuropathic pain. *Nature* 424(6951):938-942.
- Daoudal G, Hanada Y, Debanne, D (2002) Bidirectional plasticity of excitatory postsynaptic potential (EPSP)-spike coupling in CA1 hippocampal pyramidal neurons. *Proc Natl Acad Sci USA* 99:14512–14517.
- De Ridder D, De Mulder G, Menovsky T, Sunaert S, Kovacs S (2007) Electrical stimulation of auditory and somatosensory cortices for treatment of tinnitus and pain. *Prog. Brain Res.* 166: 377–388.
- Disterhoft JF, Coulter DA, Alkon DL (1986). Conditioning-specific membrane changes of rabbit hippocampal neurons measured in vitro. *Proc. Natl. Acad. Sci. USA* 83: 2733– 2737.
- Dugué GP, Dumoulin A, Triller A, Dieudonné S (2005) Target-dependent use of co-released inhibitory transmitters at central synapses. *J Neurosci* 25:6490-6498.

- Eto K, Wake H, Watanabe M, Ishibashi H, Noda M, Yanagawa Y, Nabekura J (2011) Inter-regional contribution of enhanced activity of the primary somatosensory cortex to the anterior cingulate cortex accelerates chronic pain behavior. *J Neurosci.* 31(21):7631-7636.
- Eto K, Ishibashi H, Yoshimura T, Watanabe M, Miyamoto A, Ikenaka K, Moorhouse AJ, Nabekura J (2012) Enhanced GABAergic activity in the mouse primary somatosensory cortex is insufficient to alleviate chronic pain behavior with reduced expression of neuronal potassium-chloride cotransporter. *J Neurosci.* 32(47):16552-16559.
- Fan Y, Fricker D, Brager DH, Chen X, Lu HC, Chitwood RA, Johnston D (2005) Activity-dependent decrease of excitability in rat hippocampal neurons through increases in I(h). *Nat Neurosci* 8:1542–1551.
- Flor H, Denke C, Schaefer M, Grüsser S (2001) Effect of sensory discrimination training on cortical reorganisation and phantom limb pain. *Lancet* 357: 1763–1764.
- Frey U, Schollmeier K, Reymann KG, Seidenbecher T (1995) Asymptotic hippocampal long-term potentiation in rats does not preclude additional potentiation at later phases. *Neuroscience* 67:799–807.
- Fujii S, Saito K, Miyakawa H, Ito K, Kato H (1991) Reversal of longterm potentiation (depotential) induced by tetanus stimulation of the input to CA1 neurons of guinea pig hippocampal slices. *Brain Res* 555:112–122.
- Gasselin C, Inglebert Y, Ankri N, Debanne D (2017) Plasticity of intrinsic excitability during LTD is mediated by bidirectional changes in h-channel activity. *Sci Rep* 7(1):14418.
- Gross J, Schnitzler A, Timmermann L, Ploner, M (2007) Gamma oscillations in human primary somatosensory cortex reflect pain perception. *PLoS Biol.* 5, e133.
- Gu L, Uhelski ML, Anand S, Romero-Ortega M, Kim YT, Fuchs PN, Mohanty SK (2015) Pain inhibition by optogenetic activation of specific anterior cingulate cortical neurons. *PLoS One* 10(2):e0117746.

- Huang Y-Y, Colino A, Selig DK, Malenka RC (1992) The influence of prior synaptic activity on the induction of long-term potentiation. *Science* 255:730–733.
- Holland LL, Wagner JJ (1998) Primed facilitation of homosynaptic long-term depression and depotentiation in rat hippocampus. *J Neurosci* 18:887–894.
- Koga K, Descalzi G, Chen T, Ko HG, Lu J, Li S, Son J, Kim T, Kwak C, Huganir RL, Zhao MG, Kaang BK, Collingridge GL, Zhuo M (2015) Coexistence of two forms of LTP in ACC provides a synaptic mechanism for the interactions between anxiety and chronic pain. *Neuron* 85(2):377-389.
- Kourrich S, Calu DJ, Bonci A (2015) Intrinsic plasticity: an emerging player in addiction. *Nat Rev Neurosci.* 16(3):173-184.
- Kuner R (2010) Central mechanisms of pathological pain. *Nat. Med.* 16, 1258–1266 (2010).
- Larson J, Xiao JP, Lynch G (1993) Reversal of LTP by theta frequency stimulation. *Brain Res* 600:97–102.
- Latremoliere A, Woolf CJ (2009) Central sensitization: a generator of pain hypersensitivity by central neural plasticity. *J Pain* 10(9):895-926.
- Li XY, Ko HG, Chen T, Descalzi G, Koga K, Wang H, Kim SS, Shang Y, Kwak C, Park SW, Shim J, Lee K, Collingridge GL, Kaang BK, Zhuo M (2010) Alleviating neuropathic pain hypersensitivity by inhibiting PKMzeta in the anterior cingulate cortex. *Science* 330(6009):1400-1404.
- Lotze M1, Grodd W, Birbaumer N, Erb M, Huse E, Flor H (1999) Does use of a myoelectric prosthesis prevent cortical reorganization and phantom limb pain? *Nat. Neurosci.* 2 : 501–502.
- Magerl W, Hansen N, Treede RD, Klein T (2018) The human pain system exhibits higher-order plasticity (metaplasticity). *Neurobiol Learn Mem.* 154:112-120.

- Moyer JR Jr., Thompson LT, Disterhoft JF (1996). Trace eyeblink conditioning increases CA1 excitability in a transient and learning-specific manner. *J. Neurosci.* 16: 5536–5546.
- Narayanan R, Johnston D (2007) Long-term potentiation in rat hippocampal neurons is accompanied by spatially widespread changes in intrinsic oscillatory dynamics and excitability. *Neuron* 56:1061–1075.
- Ngezahayo A, Schachner M, Artola, A (2000) Synaptic activity modulates the induction of bidirectional synaptic changes in adult mouse hippocampus. *J. Neurosci.* 20:2451–2458.
- Ning L, Ma LQ, Wang ZR, Wang YW (2013) Chronic constriction injury induced long-term changes in spontaneous membrane-potential oscillations in anterior cingulate cortical neurons in vivo. *Pain Physician* 16(5):E577-89.
- Norris CM, Korol DL, Foster TC (1996) Increased susceptibility to induction of long-term depression and long-term potentiation reversal during aging. *J Neurosci* 16:5382–5392.
- O'Dell TJ, Kandel ER (1994) Low-frequency stimulation erases LTP through an NMDA receptor-mediated activation of protein phosphatases. *Learn Mem* 1:129 –139.
- Ohtsuki G, Piochon C, Adelman JP, Hansel C (2012) SK2 channel modulation contributes to compartment-specific dendritic plasticity in cerebellar Purkinje cells. *Neuron* 75:108-120.
- Peyron R1, Schneider F, Faillenot I, Convers P, Barral FG, Garcia-Larrea L, Laurent B (2004) An fMRI study of cortical representation of mechanical allodynia in patients with neuropathic pain. *Neurology* 63, 1838–1846.
- Pozzorini C, Naud R, Mensi S, Gerstner W (2013) Temporal whitening by power-law adaptation in neocortical neurons. *Nat Neurosci* 16:942–948.
- Schreurs BG, Gusev PA, Tomsic D, Alkon DL, Shi T (1998) Intracellular correlates of acquisition and long-term memory of classical conditioning in Purkinje cell dendrites in slices of rabbit cerebellar lobule HVI. *J. Neurosci.* 18: 5498–5507.

- Sessolo M, Marcon I, Bovetti S, Losi G, Cammarota M, Ratto GM, Fellin T, Carmignoto G (2015) Parvalbumin-Positive Inhibitory Interneurons Oppose Propagation But Favor Generation of Focal Epileptiform Activity. *J Neurosci* 35:9544-9557.
- Rizwan AP, Zhan X, Zamponi GW, Turner RW (2016) Long-Term Potentiation at the Mossy Fiber-Granule Cell Relay Invokes Postsynaptic Second-Messenger Regulation of Kv4 Channels. *J Neurosci* 36:11196-11207.
- Saab CY (2012) Pain-related changes in the brain: diagnostic and therapeutic potentials. *rends Neurosci.* 35: 629–637.
- Seifert F, Maihöfner C (2009) Central mechanisms of experimental and chronic neuropathic pain: findings from functional imaging studies. *Cell. Mol. Life Sci.* 66, 375–390.
- Seminowicz DA¹, Laferriere AL, Millicamps M, Yu JS, Coderre TJ, Bushnell MC (2009) MRI structural brain changes associated with sensory and emotional function in a rat model of long-term neuropathic pain. *Neuroimage* 47:1007–1014.
- Shackman AJ¹, Salomons TV, Slagter HA, Fox AS, Winter JJ, Davidson RJ (2011) The integration of negative affect, pain and cognitive control in the cingulate cortex. *Nat. Rev. Neurosci.* 12, 154–167.
- Shen FY, Chen ZY, Zhong W, Ma LQ, Chen C, Yang ZJ, Xie WL, Wang YW (2015) Alleviation of neuropathic pain by regulating T-type calcium channels in rat anterior cingulate cortex. *Mol Pain* 11:7.
- Shim HG, Jang DC, Lee J, Chung G, Lee S, Kim YG, Jeon DE, Kim SJ (2017) Long-Term Depression of Intrinsic Excitability Accompanied by Synaptic Depression in Cerebellar Purkinje Cells. *J Neurosci* 37:5659–5669.
- Staubli U, Lynch G (1990) Stable depression of potentiated synaptic responses in the hippocampus with 1–5 Hz stimulation. *Brain Res* 513:113–118.

- Tan LL, Pelzer P, Heintz C, Tang W, Gangadharan V, Flor H, Sprengel R, Kuner T, Kuner R (2017) A pathway from midcingulate cortex to posterior insula gates nociceptive hypersensitivity. *Nat Neurosci.* 20(11):1591-1601.
- Thibault K, Lin WK, Rancillac A, Fan M, Snollaerts T, Sordoillet V, Hamon M, Smith GM, Lenkei Z, Pezet S (2014) BDNF-dependent plasticity induced by peripheral inflammation in the primary sensory and the cingulate cortex triggers cold allodynia and reveals a major role for endogenous BDNF as a tuner of the affective aspect of pain. *J Neurosci.* 34(44):14739-51.
- Titley HK, Brunel N, Hansel C (2017) Toward a Neurocentric View of Learning. *Neuron* 95(1):19-32.
- Vogt BA, Berger GR, Derbyshire SWG (2003) Structural and functional dichotomy of human midcingulate cortex. *Eur. J. Neurosci.* 18: 3134–3144.
- Vogt BA (2005) Pain and emotion interactions in subregions of the cingulate gyrus. *Nat. Rev. Neurosci.* 6: 533–544 (2005).
- Wager TD, Atlas LY, Lindquist MA, Roy M, Woo CW, Kross E (2013) An fMRI-based neurologic signature of physical pain. *N. Engl. J. Med.* 368:1388–1397.
- Wagner JJ, Alger BE (1995) GABAergic and developmental influences on homosynaptic LTD and depotentiation in rat hippocampus. *J Neurosci* 15:1577–1586.
- Wang GQ, Cen C, Li C, Cao S, Wang N, Zhou Z, Liu XM, Xu Y, Tian NX, Zhang Y, Wang J, Wang LP, Wang Y (2015) Deactivation of excitatory neurons in the prelimbic cortex via Cdk5 promotes pain sensation and anxiety. *Nat Commun.* 6:7660.
- Wang Y, Wu J, Rowan MJ, Anwyl R (1998) Role of the protein kinase C in the induction of homosynaptic long-term depression by brief low frequency stimulation in the dentate gyrus in the rat hippocampus in vitro. *J Physiol (Lond)* 513.2:467– 475?
- Wang Z, Xu NL, Wu CP, Duan S, Poo MM (2003) Bidirectional changes in spatial dendritic integration accompanying long-term synaptic modifications. *Neuron* 37:463-472.

- Wei F, Qiu CS, Kim SJ, Muglia L, Maas JW, Pineda VV, Xu HM, Chen ZF, Storm DR, Muglia LJ, Zhuo M (2002) Genetic elimination of behavioral sensitization in mice lacking calmodulin-stimulated adenylyl cyclases. *Neuron* 36(4):713-26.
- Wei F, Wang GD, Kerchner GA, Kim SJ, Xu HM, Chen ZF, Zhuo M (2001) Genetic enhancement of inflammatory pain by forebrain NR2B overexpression. *Nat Neurosci.* 4(2):164-169.
- Wexler EM, Stanton PK (1993) Priming of homosynaptic long-term depression in hippocampus by previous synaptic activity. *NeuroReport* 4:591–594.
- Wu LJ, Toyoda H, Zhao MG, Lee YS, Tang J, Ko SW, Jia YH, Shum FW, Zerbinatti CV, Bu G, Wei F, Xu TL, Muglia LJ, Chen ZF, Auberson YP, Kaang BK, Zhuo M (2005) Upregulation of forebrain NMDA NR2B receptors contributes to behavioral sensitization after inflammation. *J Neurosci.* 25(48):11107-11116.
- Xu H, Wu LJ, Wang H, Zhang X, Vadakkan KI, Kim SS, Steenland HW, Zhuo M (2008) Presynaptic and postsynaptic amplifications of neuropathic pain in the anterior cingulate cortex. *J Neurosci.* 28(29):7445-7453.
- Xu J, Kang N, Jiang L, Nedergaard M, Kang J (2005) Activity-dependent long-term potentiation of intrinsic excitability in hippocampal CA1 pyramidal neurons. *J Neurosci* 25:1750-1760.
- Yang X-D, Faber DS (1991) Initial synaptic efficacy influences induction and expression of long-term changes in transmission. *Proc Natl Acad Sci USA* 88:4299–4303.
- Yang Z, Santamaria F (2016) Purkinje cell intrinsic excitability increases after synaptic long term depression. *J Neurophysiol.* 116(3): 1208–1217.
- Zhang W, Linden DJ (2003) The other side of the engram: experience-driven changes in neuronal intrinsic excitability. *Nat Rev Neurosci.* 4(11):885-900.

- Zhao MG, Ko SW, Wu LJ, Toyoda H, Xu H, Quan J, Li J, Jia Y, Ren M, Xu ZC, Zhuo M (2006) Enhanced presynaptic neurotransmitter release in the anterior cingulate cortex of mice with chronic pain. *J Neurosci.* 26(35):8923-8930.
- Zhuo M (2016) Neural Mechanisms Underlying Anxiety-Chronic Pain Interactions. *Trends Neurosci.* 39(3):136-145.

LEGENDS TO FIGURES

Figure 1. Experimental design and behavioral testing. **A**, Schematic representation of the experimental design. Rats were acclimated to glass chambers for behavioral testing and to mechanical stimulation during 5 days before subcutaneous injection. Mechanical thresholds (using von Frey filaments) were assessed before and 1 h or 3 days after NaCl or Complete Freund Adjuvant (CFA) injection into the right vibrissa pad. Animals were then quickly decapitated and electrophysiological recordings were performed in *ex vivo* slices obtained from these animals. **B**, Paired bar histograms of mechanical thresholds measured before (left bar of each pair) and 1 hour or 3 days (right bar of each pair; 1 hour: black bars, 3 days: grey bars) subcutaneous injection of NaCl or Complete Freund Adjuvant (CFA) into the right vibrissa pad in 4 groups of rats: NaCl injection, 1 hour: N=16; CFA injection, 1 hour: N=34; NaCl injection, 3 days: N=13; CFA injection, 3 days: N=21. One way ANOVA, *** $P < 0.001$.

Figure 2. Facial inflammation is associated with LTP of synaptic transmission in superficial layers of the somatosensory cortex (S1). **A-D**, Spontaneous EPSCs recorded from rat S1 L2/3 pyramidal neurons 1 hour (left) after injection of NaCl (N=5, n=5) or CFA (N=19, n=19) or 3 days (right) after injection of NaCl (N=4, n=4) or CFA (N=17, n=17). **A**, Sample traces of spontaneous EPSCs recorded from pyramidal neurons after injection of NaCl, before (top; Naïve) and after induction of LTP (middle; LTP), or CFA (bottom; Naïve). Calibration bars: 20 msec, 50 pA and 5 msec and 20 pA. **B**, Corresponding cumulative amplitude distributions of sEPSCs recorded from naïve (empty circles) and potentiated (filled triangles) NaCl-injected rats and from naïve CFA-injected rats (1 hour: filled circles; 3 days: empty squares). Note that the two distributions, potentiated/NaCl and naïve/CFA sEPSCs, are superimposed at both 1 hour and 3 days after injection. Kolmogorov–Smirnov tests: 1 hour: Naïve CFA *versus* naïve

NaCl distributions: different $P < 0.0001$; Potentiated NaCl *versus* naïve NaCl distributions: different $P < 0.0001$; Naïve CFA *versus* Potentiated NaCl distributions: not different $P = 0.6490$; 3 days: Naïve CFA *versus* naïve NaCl distributions: different $P < 0.0001$; Potentiated NaCl *versus* naïve NaCl distributions: different $P < 0.0001$; Naïve CFA *versus* Potentiated NaCl distributions: not different $P = 0.9167$. **C, D**, Bar histograms (mean + S.E.M.) of the amplitude (**C**) and frequency (**D**) of spontaneous EPSCs recorded from pyramidal neurons in naïve synapses from NaCl- (empty bar; NaCl naïve) or CFA-injected rats (black bar; CFA naïve) and after induction of LTP from (the same) NaCl-injected rats (grey bars; NaCl LTP). One way ANOVA, ** $P < 0.01$, *** $P < 0.001$.

Figure 3. LTP of synaptic transmission in superficial layers of the somatosensory cortex (S1) is stable over the first 3 days after pain onset. **A**, Cumulative amplitude distributions of sEPSCs recorded from naïve NaCl- (1 hour and 3 days: empty circles) and CFA-injected rats (1 hour: filled circles; 3 days: empty squares). Note that the two CFA curves, at 1 hour and 3 days after injection, are superimposed. Kolmogorov–Smirnov test: NaCl 3 days *versus* NaCl 1 hour distributions: not different $P = 0.9892$; CFA 3 days *versus* CFA 1 hour distributions: not different $P = 0.6$. **B, C**, Bar histograms (mean + S.E.M.) of the amplitude (**C**) and frequency (**D**) of spontaneous EPSCs recorded from pyramidal neurons from naïve NaCl- (empty bars) and CFA-injected rats (filled bars), as indicated on the graph. One way ANOVA, ** $P < 0.01$, *** $P < 0.001$.

Figure 4. Voltage-response curves for the induction of synaptic LTD/LTP in CFA- and NaCl-injected rats, 1 hour after injection. **A–D**, Summary graphs of whole-cell recordings in which synaptic stimulation (2 Hz, 50 sec) was paired to 0mV (**A**; $n=9$, $N=8$), -10mV (**B**; $n=5$, $N=5$) -

20mV (**C**; n=4, N=4) and -30mV (**D**; n=6, N=6) in (naïve) CFA-injected rats (filled circles). In each graph, the effect in (naïve) CFA-injected rats is compared with that in naïve NaCl-injected rats (empty circles) 0mV (**A**; n=4, N=4), -10mV (**B**; n=4, N=4) -20mV (**C**; n=2, N=2) and -30mV (**D**; n=2, N=2) and in potentiated NaCl-injected rats (filled triangles) (**A**; n=3, N=3), -10mV (**B**; n=2, N=2) -20mV (**C**; n=3, N=3) and -30mV (**D**; n=2, N=2). In potentiated NaCl-injected rats, this is the effect of a second (test) pairing to the various V_m , 30 min after a first (conditioning) pairing to 0mV which had induced LTP. **A-D Insets**: Superimposed averages of 10 successive evoked EPSCs recorded before (thin trace) and 30 min after (thick trace) pairing in representative cells in CFA-injected rats. Calibration bars: 20 msec, 50 pA. **E**, Cumulative histograms showing the effect of a pairing to -40mV (n=7, N=6), -30mV (n=6, N=6, same as 1D), -20mV (n=4, N=4; same as Fig. 1C), -10mV (n=5, N=5; same as Fig. 1B), 0mV (n=9, N=8; same as Fig. 1A), +10mV (n=9, N=8), and +20mV (n=5, N=5), in every neuron (naïve) CFA-injected rats. **F**, Voltage–response function for the induction of LTD/LTP (synaptic plasticity rule) in naïve CFA- (filled circles) and NaCl-injected rats (empty circles). **G**, Voltage–response function for the induction of LTD/LTP (synaptic plasticity rule) in naïve CFA-injected rats (filled circles) and potentiated NaCl-injected rats (filled triangles). The curve in potentiated NaCl-injected rats displays the net effect of the second (test) pairing; that is, the amplitude changes are normalized to the magnitude of LTP after a single pairing to 0mV. Note that the two curves are exactly superimposed, consistent with our conclusion that synapses onto L2/3 pyramidal neurons have been potentiated, following peripheral inflammation.

Figure 5. Voltage-response curves for the induction of synaptic LTD/LTP in CFA- and NaCl-injected rats, 3 days after injection. **A–D**, Summary graphs of whole-cell recordings in which synaptic stimulation (2 Hz, 50 sec) was paired to 0mV (**A**; n=6, N=6), -10mV (**B**; n=3, N=3) -20mV (**C**; n=4, N=4) and -30mV (**D**; n=7, N=7) in (naïve) CFA-injected rats (filled circles).

In each graph, the effect in (naïve) CFA-injected rats is compared with that in naïve NaCl-injected rats (empty circles) (**A**; n=2, N=2), -10 mV (**B**; n=2, N=2) -20 mV (**C**; n=4, N=4) and -30 mV (**D**; n=3, N=3). **A-D Insets**: Superimposed averages of 10 successive evoked EPSCs recorded before (thin trace) and 30 min after (thick trace) pairing in representative cells in CFA-injected rats. Calibration bars: 20 msec, 50 pA. **E**, Cumulative histograms showing the effect of a pairing to -40mV (n=4, N=4), -30mV (n=7, N=7, same as 1D), -20mV (n=4, N=4; same as Fig. 1C), -10mV (n=3, N=3; same as Fig. 1B), 0mV (n=6, N=6; same as Fig. 1A), +10mV (n=3, N=3), and +20mV (n=3, N=3), in every neuron (naïve) CFA-injected rats. **F**, Voltage–response function for the induction of LTD/LTP (synaptic plasticity rule) in naïve CFA- (filled circles) and NaCl-injected rats (empty circles). Note that the two curves are exactly superimposed, consistent with our conclusion that metaplasticity had decayed over the 3 days.

Figure 6. Time course of synaptic metaplasticity decay. **A, B**, Comparison of the effect of pairing to 0mV (**A**) and to -30mV (**B**) at 1 hour after injection, in naïve NaCl-injected rats (n=4, N=4), potentiated NaCl-injected rats (n=2, N=2) and naïve CFA-injected rats (n=9, N=8) and at 1 day (n=2 N=2), 2 days (n=2, N=2) and 3 days (n=6, N=6) in CFA-injected rats. Note that the effect of the two pairings progressively return to control values within 3 days.

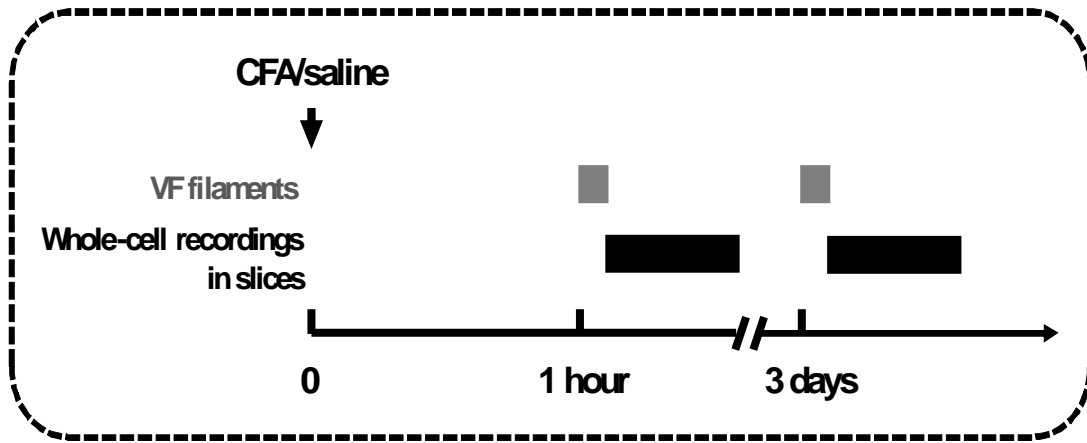
Figure 7. Facial inflammation is associated with LTP of the intrinsic excitability of L2/3 pyramidal neurons within the somatosensory cortex (S1). **A**, Averaged relationships between injected current and evoked firing rate (F-I curve) in (naïve) CFA-injected rats (filled circles; n=54 N=34), naïve NaCl-injected rats (empty circles; n=33, N=16), and potentiated NaCl-injected rats (filled triangles; n=21, N=16). Note that the F-I curve in (naïve) CFA-injected rats is shifted to the left—more action potential are elicited by depolarizing current steps—compared with that in naïve NaCl-injected rats but overlapping with that in potentiated NaCl-injected rats.

Insets, Examples of firing responses to 500, 590 and 770 pA current pulses recorded before (left) and after (middle) pairings to 0mV in a representative pyramidal neuron from a NaCl-injected rat and in a representative pyramidal neuron from a CFA-injected rat (right). Calibration bars: 100 msec, 10 mV. **B**, Normalized instantaneous frequency prior to (open symbols) in (naïve) CFA-injected rat (filled circles) and naïve NaCl-injected rats (empty circles). In **A, B**, Values are presented as mean \pm S.E.M.. One way ANOVA for repeated measures, *** $P < 0.001$. **C, D, E, F, G**, Action potential threshold (**C**), rheobase (**D**), amplitude (**E**) and duration (**F**) and after-hyperpolarization amplitude (**G**) in the same naïve NaCl-injected rats (empty circles), CFA-injected rats (filled circles) and potentiated NaCl-injected rats (filled triangles) as in **A**. Note that (naïve) CFA-injected rats exhibit the very same changes in action potential properties and after-hyperpolarization amplitude as potentiated NaCl-injected ones. In **C-G**, One way ANOVA, *** $P < 0.001$.

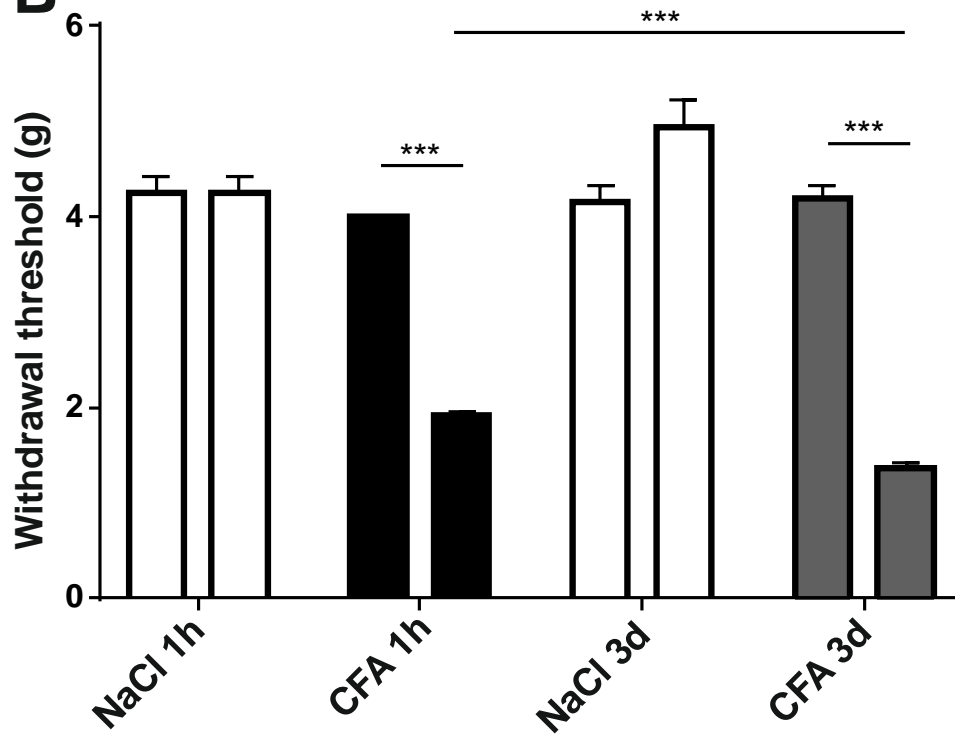
Figure 8. LTP of intrinsic excitability of S1 L2/3 pyramidal neurons is stable over the first 3 days after pain onset. **A**, Averaged relationships between injected current and evoked firing rate (F-I curve) in naïve NaCl-injected rats at 1 hour (empty circles; same as in Fig.7) and in CFA-injected rats at 1 hour (filled circles; same as in Fig.7) and 3 days after injection (filled squares; n=44 N=21). Note that the two F-I curves in CFA-injected rats are overlapping. **Insets**, Examples of firing responses to 500, 590 and 770 pA current pulses recorded in naïve NaCl-injected rats at 1 hour (left) and CFA-injected rats at 1 hour (middle) and 3 days (right). Calibration bars: 100 msec, 10 mV. **B**, Normalized instantaneous frequency prior to (open symbols) in the naïve NaCl-injected rats at 1 hour (empty circles) and the CFA-injected rats at 1 hour (filled circles) and 3 days after injection (filled squares). In **A, B**, Values are presented as mean \pm S.E.M.. One way ANOVA for repeated measures, *** $P < 0.001$. **C, D, E, F, G**, Action potential threshold (**C**), rheobase (**D**), amplitude (**E**) and duration (**F**) and after-

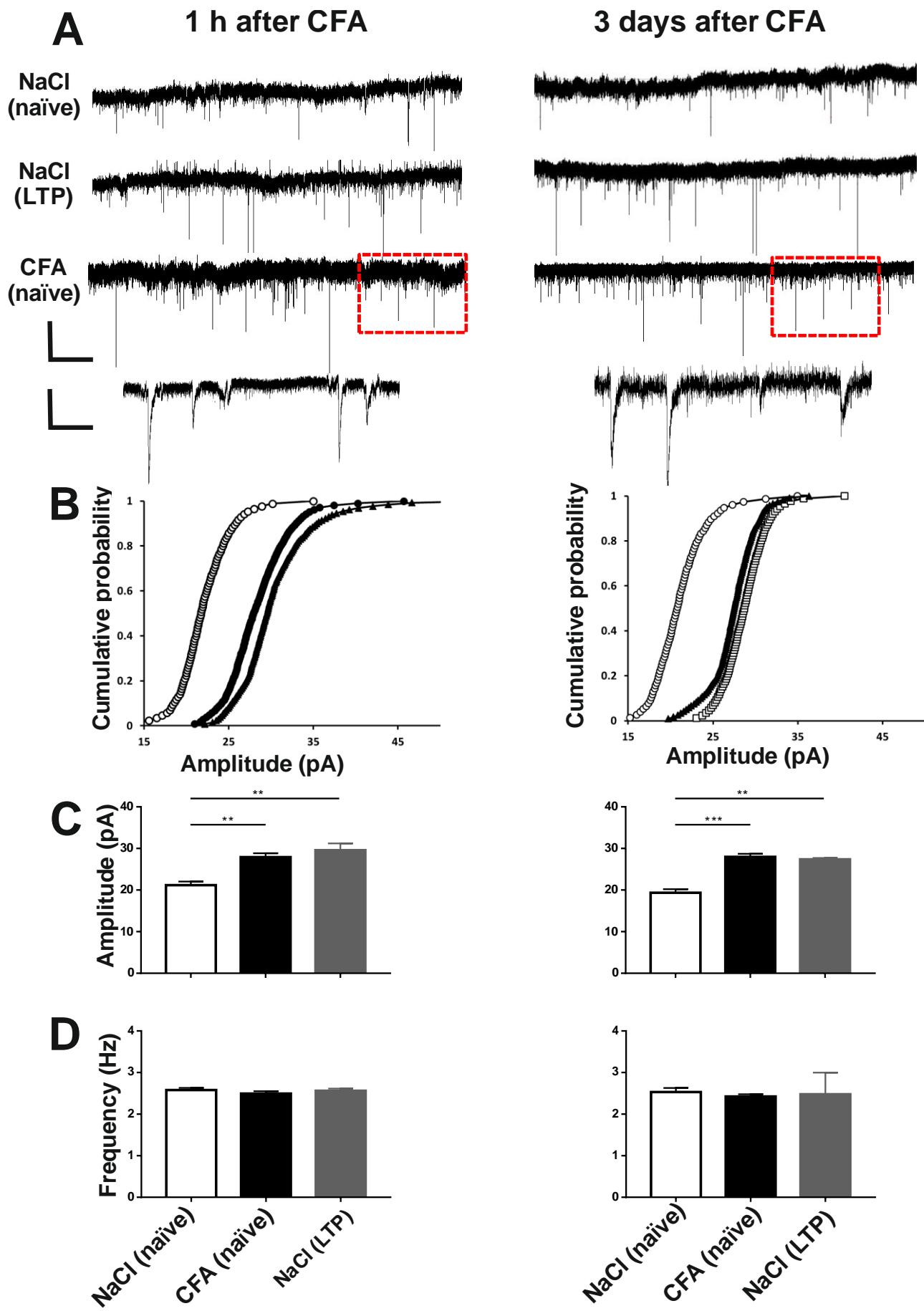
hyperpolarization amplitude (**G**) in the same naïve NaCl-injected rats at 1 hour (empty circles) and the CFA-injected rats at 1 hour (filled circles) and 3 days after injection (filled squares) as in **A**. Note that CFA-injected rats at 1 hour and 3 days exhibit the very same changes in action potential properties and after-hyperpolarization amplitude. In **C-G**, One way ANOVA: CFA 1 hour versus NaCl 1 hour: *** $P < 0.001$ and §§§ CFA 3 days versus NaCl 3 days: $P < 0.001$.

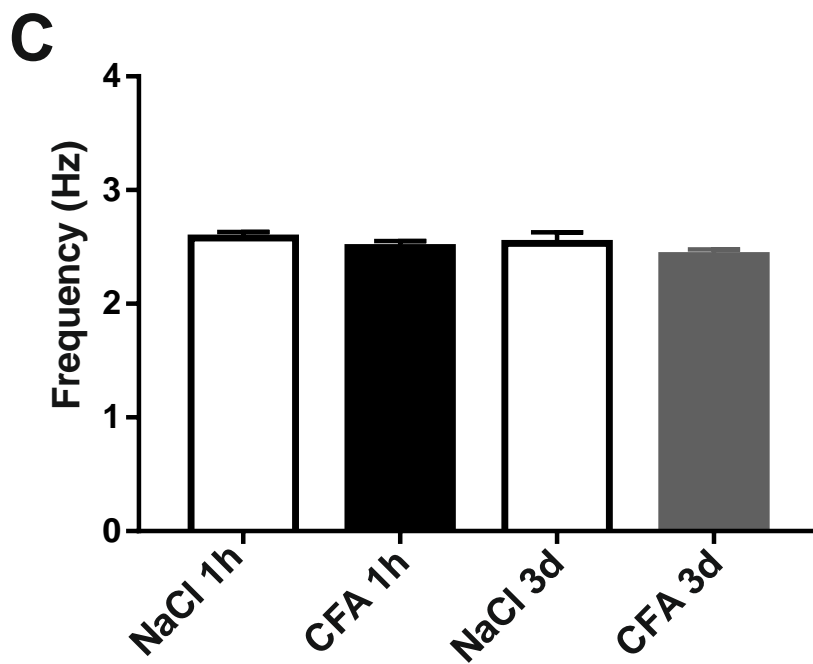
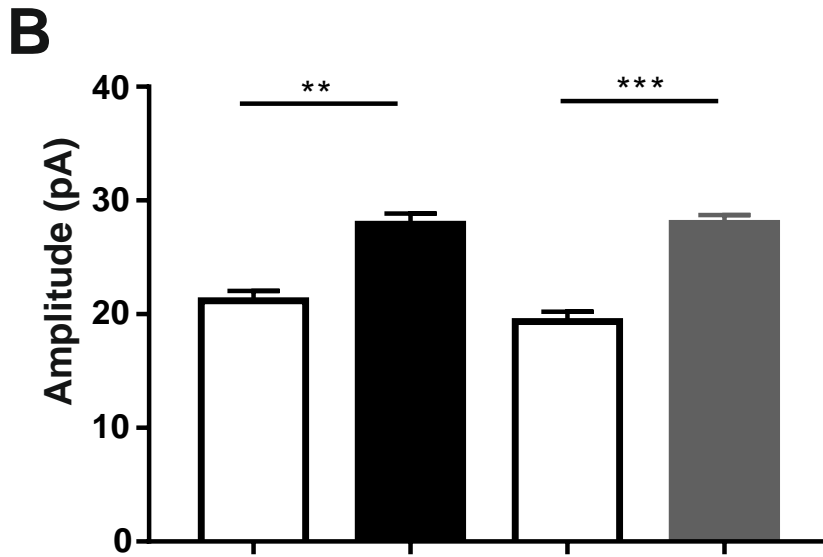
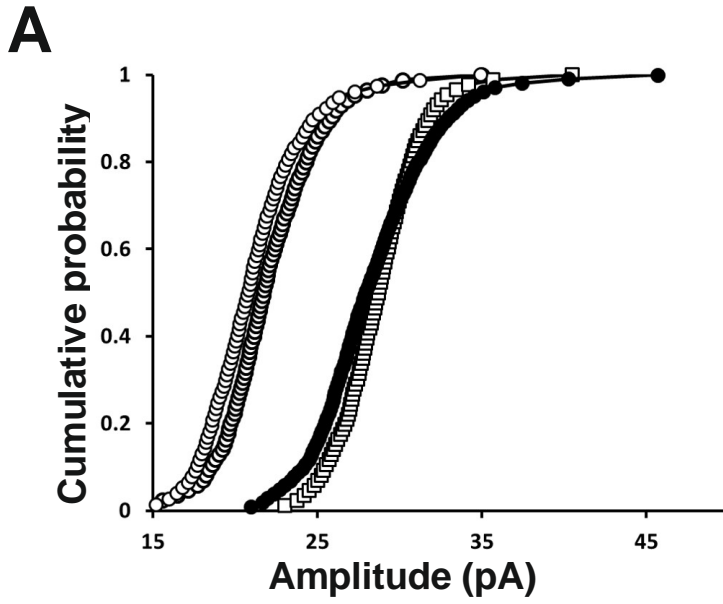
A

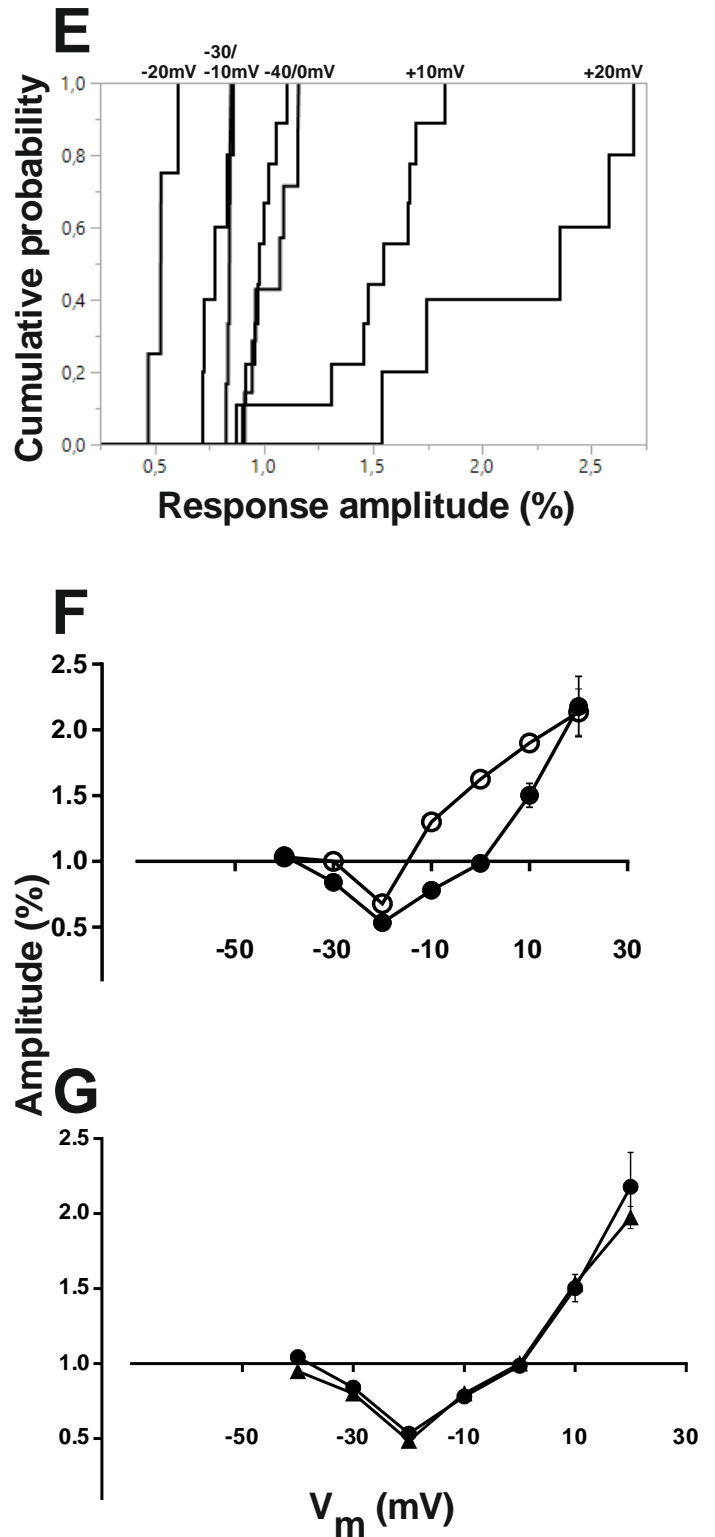
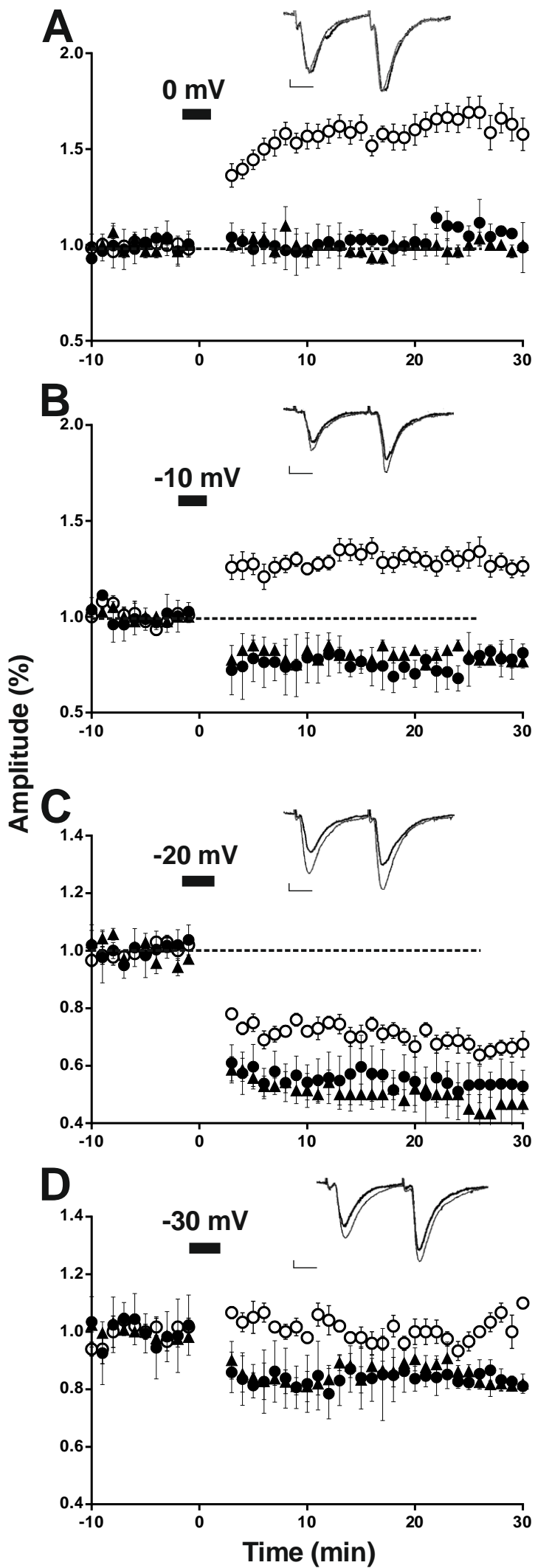


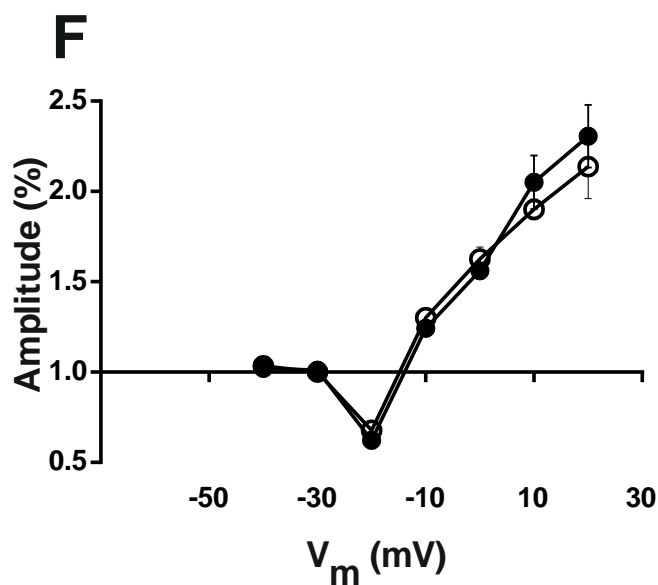
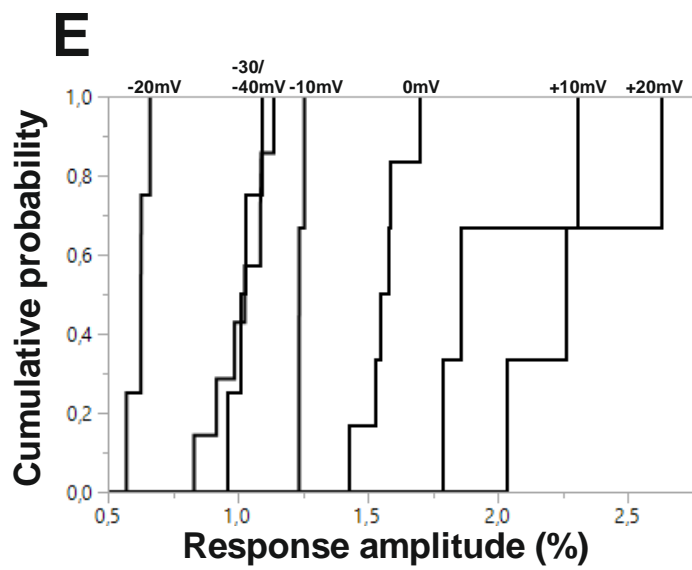
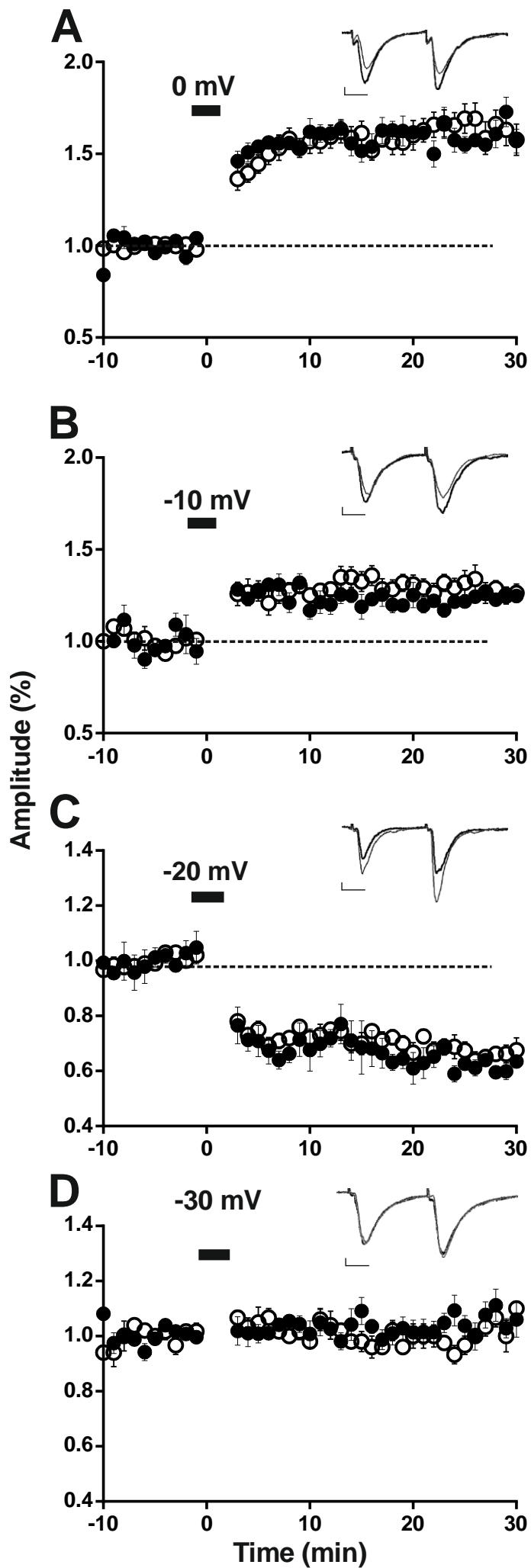
B

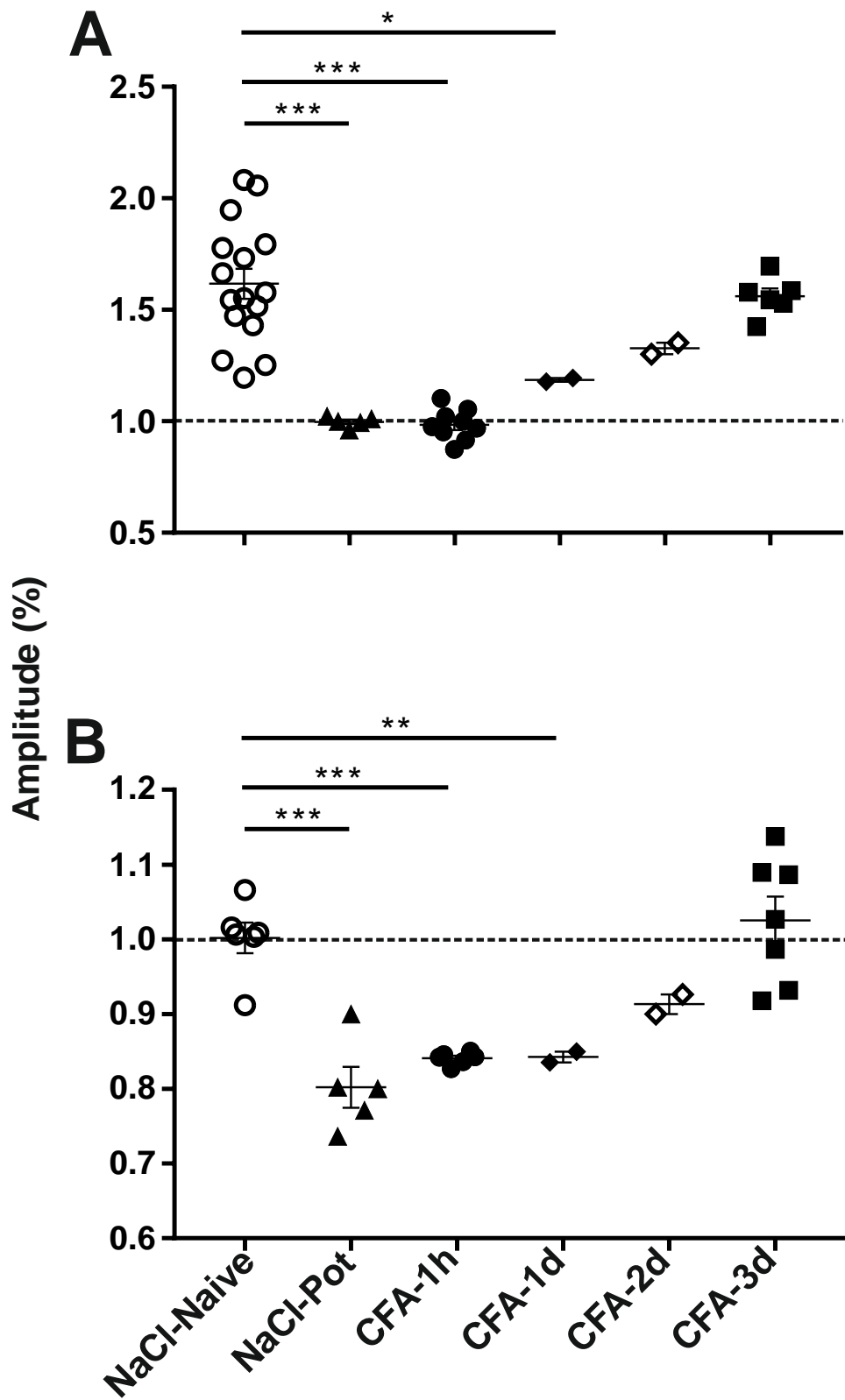


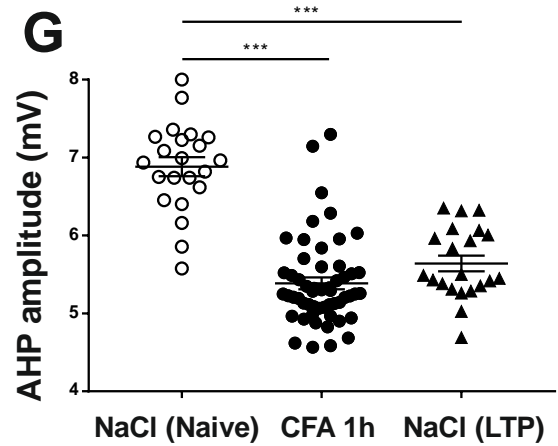
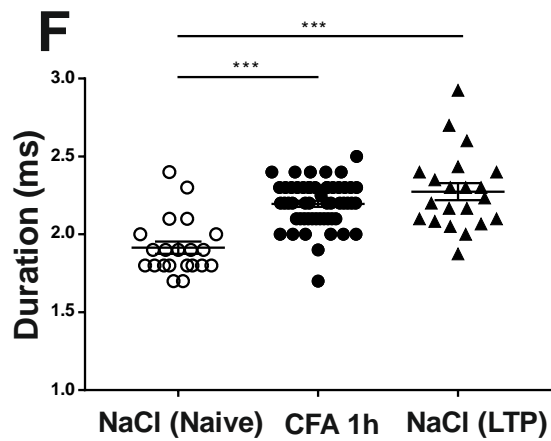
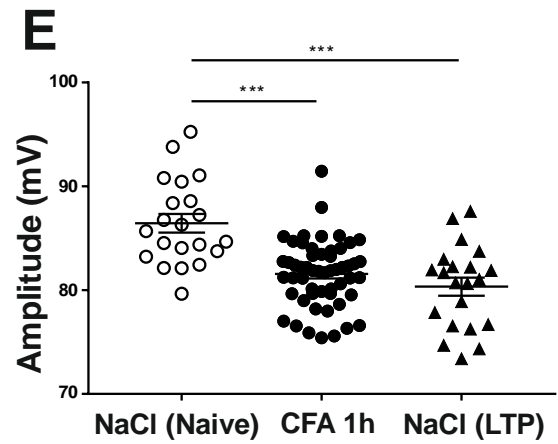
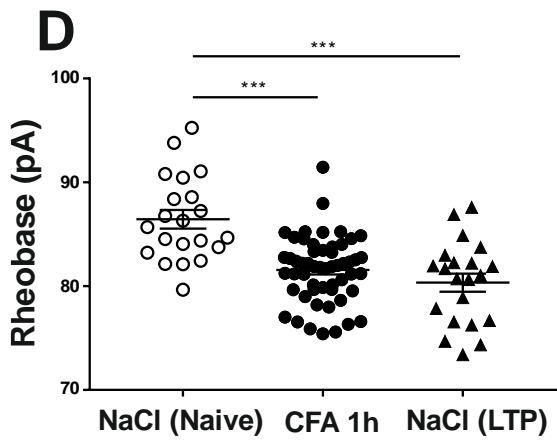
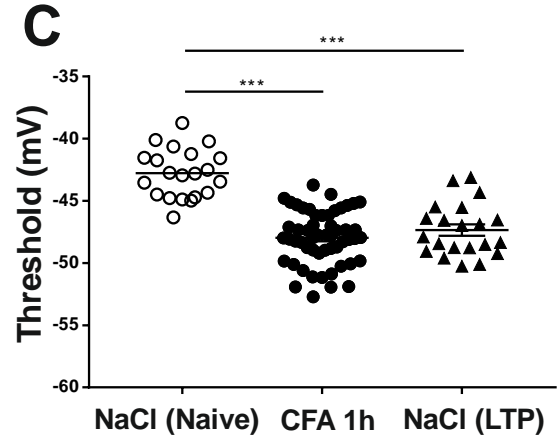
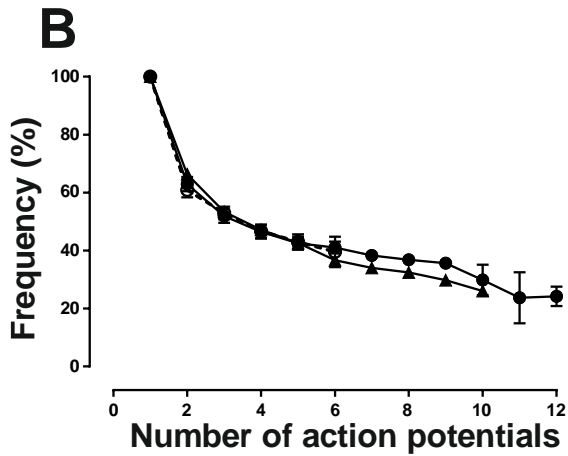
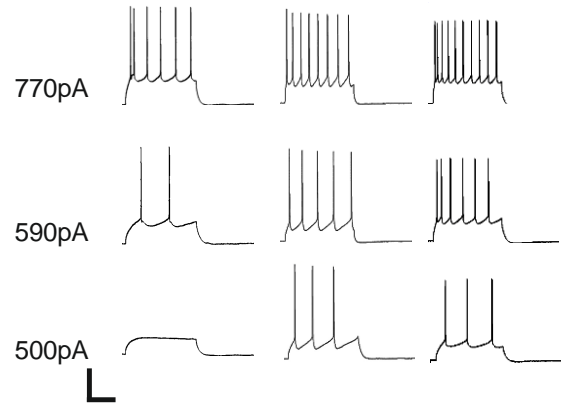
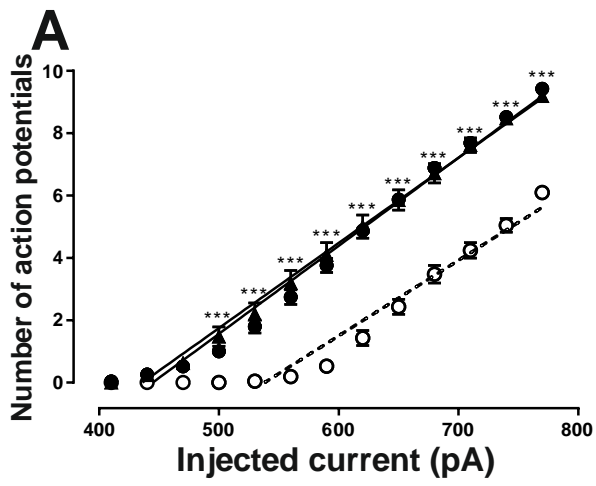


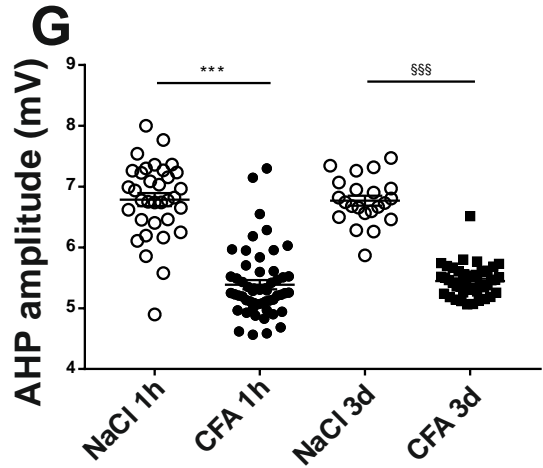
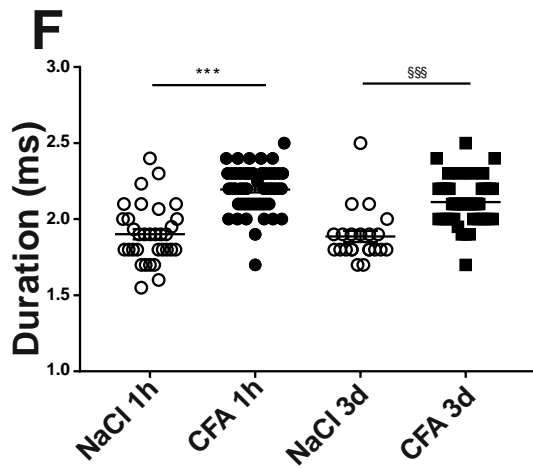
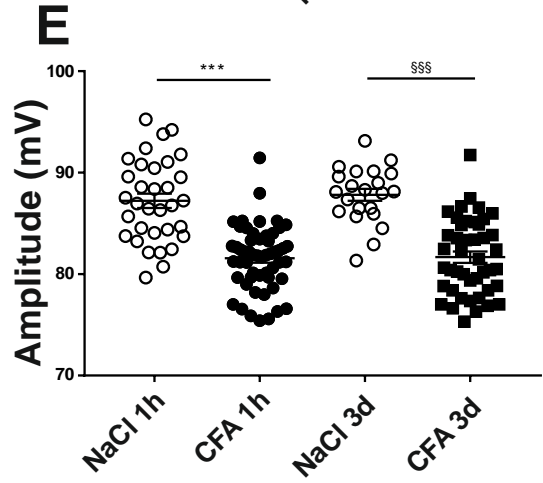
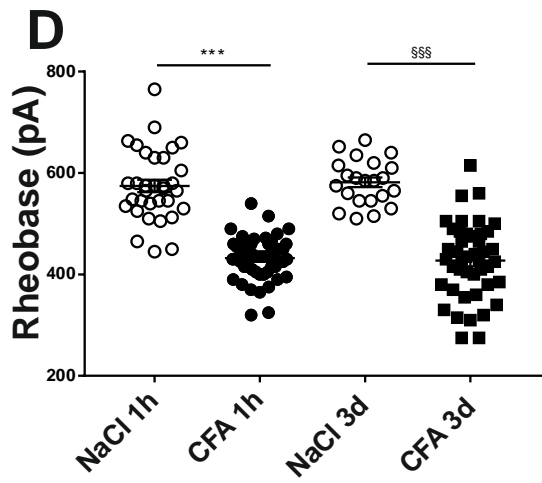
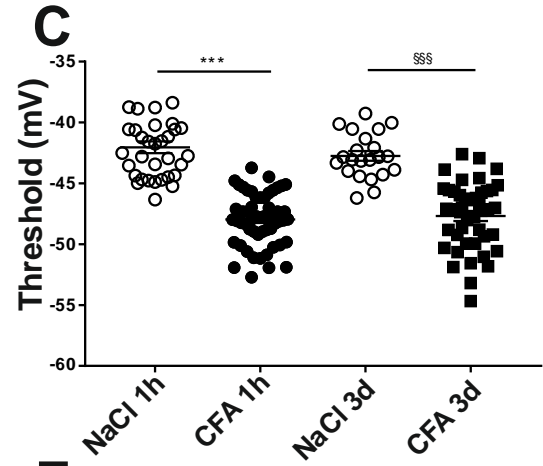
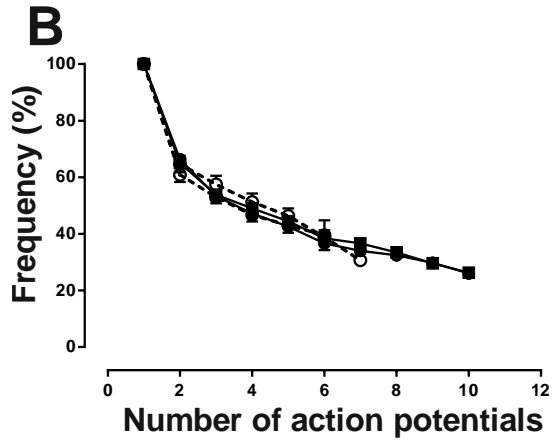
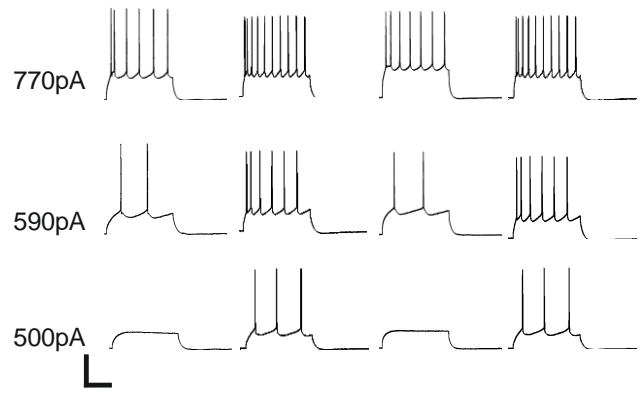
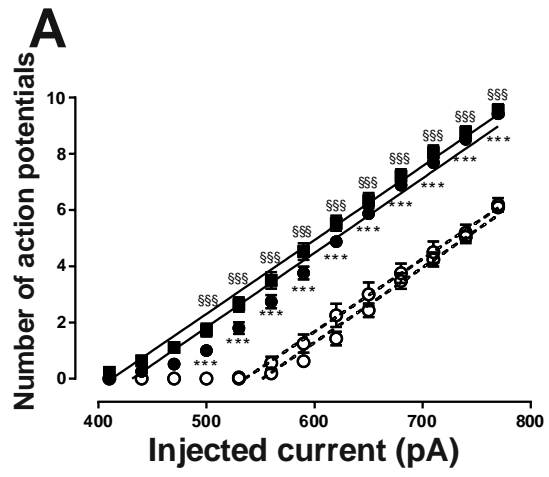












CHAPITRE 3:

RAPID DENDRITIC REMODELING IN THE RAT ADULT SOMATOSENSORY CORTEX FOLLOWING PERIPHERAL INFLAMMATION AND ITS ASSOCIATION WITH INFLAMMATORY PAIN

Rapid Dendritic Remodeling in the Adult Rat Somatosensory Cortex Following Peripheral Inflammation and Its association with Inflammatory Pain

At the end of electrophysiological recordings, neurobiotin-filled pyramidal neurons were proceeded for morphological analysis.

MATERIAL AND METHODS

Electrophysiological patch-clamp recordings

(See Chapters 1 and 2)

Immunohistological procedures

At the end of electrophysiological recordings, immunostaining of neurobiotin-filled pyramidal neurons was performed. Slices with recorded neurons were transferred in 4% paraformaldehyde in 0.1 M PBS (pH 7.4) and stored at 4°C for two days maximum. Next, fixed slices were washed with 0.05 M Tris-buffered saline (TBS), and an immunolabeling neurobiotin was carried out. Thus, slices were first incubated with Avidin DCS-rhodamine (1:200, Ref. A-2012; Vector Laboratories, Burlingame, CA, USA) for 4 h at room temperature. Subsequently, all slices were mounted on gelatinized slides in a DPX mounting medium, cover-slipped and conserved at 4°C.

Confocal imaging and image analysis

Morphological reconstruction of neurobiotin-labelled pyramidal neurons were performed from the 350- μ m parasagittal slices imaged with a Zeiss LSM 510 confocal microscope (Carl Zeiss, Hamburg, Germany). To suppress emission cross-talk, z-scanning was sequential, using oil immersion X40 objective, and images were sampled at a resolution of 1024x1024 pixels, a z-

step size of 0.38 μm . Image analyses and quantifications were performed using Fiji-ImageJ v1.51 software (<http://rsbweb.nih.gov/ij>; NIH, USA).

- Morphometric classification of pyramidal neurons

The classification of each pyramidal neuron was performed using scatter plots comparisons of morphometric parameters (Yasaka et al., 2007): medio-lateral (ML) and dorso-ventral (DV) extents (Fig. 1A). The ratios of RC to DV extents were evaluated for individual pyramidal neuron. The linear regression for each of paired comparisons was calculated to obtain the RC/DV average ratio. This ratio allowed us to separate the pyramidal neurons into two groups: vertical and horizontal.

- Morphological and structural analysis of neuronal arborisation

Three-dimensional neuronal trees of neurobiotin-labelled pyramidal neurons were reconstructed by the Simple Neurite Tracer plugin following to (Alba-Delgado et al., 2015). Neurons with extensively truncated neurites as consequence of slice preparation were excluded. Field area was calculated as the product of medio-lateral and dorso-ventral extents of neuritic arbor (Fig. 1A). The neuronal arborisation complexity was analysed using the fractal dimension approach by the box-counting method obtained from the Fractal Box count tool of Fiji-ImageJ (Fig. 1B) (Cutting and Garvin, 1987; Smith et al., 1996). A score close to 1 implied that the branches filled the space poorly, whereas a score close to 2 implied to fill the space almost entirely. A difference of 0.1 represents a doubling of complexity. The distribution of branches in the space was analysed by the Sholl analysis (Fig. 1C) (Ferreira et al., 2010; Langhammer et al., 2010). Concentric circles around the soma were traced with radii increasing of 3 μm . The individual cumulative number of interactions for each neuron was compiled and graphed as a function of radial distance from body cell. Primary, secondary, tertiary, quaternary and quinary branches were analysed (Fig. 1D) using NeuronJ plugin (Meijering et al., 2004). The number

and length of branches for each order, and the total number of nodes were counted. A branch was defined as uninterrupted projection starting at the cell body or at one branch point (node) and ending at the next node or when the projection terminates (terminal point). Quinary branches included the ramifications of fifth, sixth and subsequent orders.

Statistical analysis

All data are presented as the mean \pm S.E.M. The number (n) of animals or neurons used for each analysis is showed in the corresponding Figure. We used one-way non-repeated measures analysis of variance (ANOVA) followed by the Tukey HSD post-test. $P \leq 0.05$ was considered to be statistically significant.

RESULTS

We investigated whether CFA injection produced morphological changes in S1 L2/3 pyramidal neurons by comparing the structural morphology of pyramidal neurons, through 3D-reconstruction of neuritic arbors, recorded in *ex vivo* slices from NaCl-injected rats (n=22) and CFA-injected rats at 1 hour (n=9) and 3 days (n=10) after injection. Since there was no difference between NaCl injected rats at 1 hour and 3 days after injection, they were put together.

The morphometric classification of pyramidal neurons reveals that, whereas both vertical and horizontal pyramidal neurons were obtained at post-injection day 3, as in control rats, no horizontal neuron could be recorded from at 1 hour after CFA injection (Fig. 2).

Comparison of the morphological features of vertical pyramidal neurons in NaCl-injected rats (n=10) and CFA-injected rats 1 hour (n=7) and 3 days (n=5) reveals that vertical pyramidal neurons had undergone a strong morphological reorganization as quickly as 1 hour after the start of peripheral inflammation and mechanical allodynia (Fig. 3). The fractal dimension of vertical pyramidal neurons was decreased suggesting an inflammation-induced reduction in the

dendritic arbor complexity of these neurons. In addition, Sholl analysis identified a decrease in the number of interactions from the soma. Finally, there was a decrease in the number of branches, mostly the secondary and tertiary branches.

Importantly, both the ratio of vertical to horizontal pyramidal neurons as well as the reduction in the dendritic arbor complexity of vertical pyramidal neurons were all back to control values at post-CFA injection day 3. There was no difference in the morphological features of horizontal pyramidal neurons in control and CFA-injected rats at 3 days (Fig. 4).

These preliminary results suggest that CFA-induced facial inflammation produces a quick, strong structural reorganization of L2/3 pyramidal neurons within the S1 cortex. However, whereas mechanical allodynia is still present and synaptic transmission and intrinsic excitability still potentiated 3 days after peripheral inflammation, all these morphological changes appeared to be reversed.

REFERENCES

- Alba-Delgado C, El Khoueiry C, Peirs C, Dallel R, Artola A, Antri M (2015) Subpopulations of PKC γ interneurons within the medullary dorsal horn revealed by electrophysiologic and morphologic approach. *Pain* 156:1714–1728. CrossRef Medline
- Cutting JE, Garvin JJ (1987) Fractal curves and complexity. *Percept Psychophys* 42:365–370. CrossRef Medline.
- Ferreira TA, Iacono LL, Gross CT (2010) Serotonin receptor 1A modulates actin dynamics and restricts dendritic growth in hippocampal neurons. *Eur J Neurosci* 32:18–26. CrossRef Medline
- Meijering E, Jacob M, Sarria JC, Steiner P, Hirling H, Unser M (2004) Design and validation of a tool for neurite tracing and analysis in fluorescence microscopy images. *Cytometry A* 58:167–176. CrossRef Medline
- Smith TG Jr, Lange GD, Marks WB (1996) Fractal methods and results in cellular morphology—dimensions, lacunarity and multifractals. *J Neurosci Methods* 69:123–136. CrossRef Medline
- Yasaka, T, Kato G, Furue H, Rashid MH, Sonohata M, Tamae A, Murata Y, Masuko S, Yoshimura M (2007) Cell-type-specific excitatory and inhibitory circuits involving primary afferents in the substantia gelatinosa of the rat spinal dorsal horn in vitro. *J Physiol* 581:603–618.

LEGENDS TO FIGURES

Figure 1. Methodology for morphological analysis. *A*, Field area of neuronal arborization calculated as the product of rostrocaudal and dorsoventral extents of neuritic arbor. *B*, Fractal dimension (Df) was measured from the reconstructed pyramidal neurons (black on white) transformed in skeletonized drawings. Fractal Box count was used to determine the Df score of each pyramidal neurons, estimated as the negative slope of the logarithm of the number of non-empty box [$\log(\text{count})$] versus the logarithm of the box size of grids [$\log(\text{box size})$]. *C*, Sholl analysis of reconstructed pyramidal neurons was performed by counting the number of branches crossing concentric circles traced around the soma (radii increasing at 3.0 μm steps). *D*, Neuritic branching order corresponding to primary (magenta), secondary (yellow), tertiary (blue), and quaternary (green) branches.

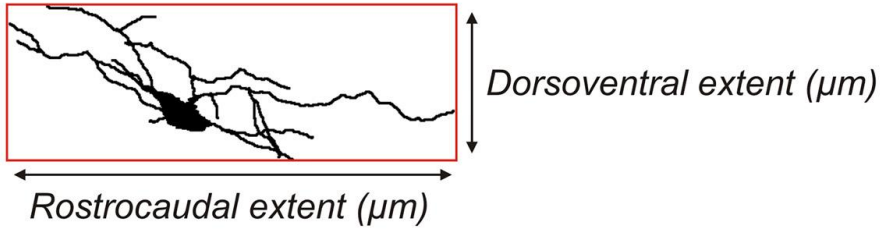
Figure 2. Morphometric analysis and morphologic classes of S1 L2/3 pyramidal neurons 1 hour and 3 days after CFA injection. *A*, Representative fluorescence image of a neurobiotin labeled L2/3 pyramidal cell in the projecting area of vibrissae in S1, contralateral to the injection side. *B*, Scatter plot analysis of dorso-ventral (DV) versus medio-lateral ML extents for S1 L2/3 pyramidal neurons. Each point represents an individual neuron. Vertical (squares), horizontal (triangles) and non-classified (circle) pyramidal neurons in control rats (n=22; 1 hour and 3 days after NaCl injection; black) and CFA-injected rats, 1 hour (n=8; green) and 3 days (n=10; blue) after injection. The line represents the ML/DV ratio which is used to distinguish vertical from horizontal pyramidal neurons. *C*, Vertical (black), horizontal (grey) and non-classified (white) pyramidal neurons in control rats and in CFA-injected rats, 1 hour and 3 days after injection. Note that in CFA-injected rats, horizontal pyramidal neurons could not be recorded from at 1 hour but only at 3 days after injection. At post-injection day 3, the ratio vertical/horizontal had recovered and was again similar to that in control rats.

Figure 3. CFA-induced facial inflammation produces reversible structural modifications in vertical S1 L2/3 pyramidal neurons. **A–G**, Morphological features of 3D-reconstructed neuritic arbors of neurobiotin labeled pyramidal neurons after subcutaneous injection into the vibrissa pad of saline (vehicle; 1 hour and 3 days; black; n=10) or CFA (2.5 mg/kg; 1 hour: green, n=7 and 3 days: blue, n=5). For bar histograms, bars represent mean + S.E.M of n neurons per group and each symbol is the value for a single neuron. There was no difference between 1 hour and 3 days post-NaCl injection; therefore, controls at 1 hour and 3 days post-NaCl were put together. **A, B**, Total field area (**A**) and fractal dimension (**B**) of pyramidal neurons in the different experimental groups. **C**, Sholl analysis curves of pyramidal neurons in control and 1 hour post-CFA groups showing the number of branching intersections as a function of path length from soma. Symbols represent mean + or - SEM of 10 and 7 pyramidal neurons in the NaCl and CFA groups, respectively. **D**, Number of neuritic branches of pyramidal neurons in the different experimental groups. **E**, Representative neuronal reconstructions showing the neuritic arborizations of pyramidal neurons, 1 hour after NaCl injection and 1 hour and 3 days after CFA injection. **F**, Number of primary, secondary, tertiary, quaternary and quinary branches of pyramidal neurons in the different experimental groups. Note that the number of dendritic branches was reduced—secondary and tertiary branches were predominantly reduced—as quickly as 1 hour after CFA injection. Importantly, all these morphological changes were reversible at post-CFA injection day 3. **G**, Curves showing the primary, secondary, tertiary, quaternary and quinary branch distribution of pyramidal neurons according to their length. Symbols represent the number of branches per 5 μm bin. * $P < 0.05$ by Tukey's HSD post-test following one-way ANOVA.

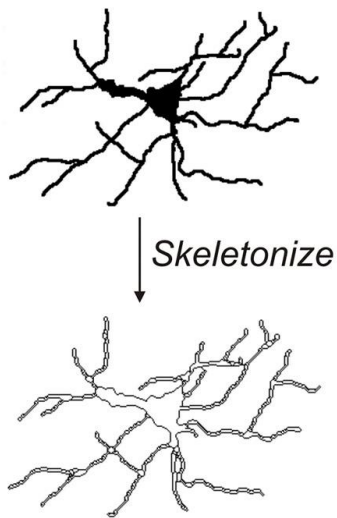
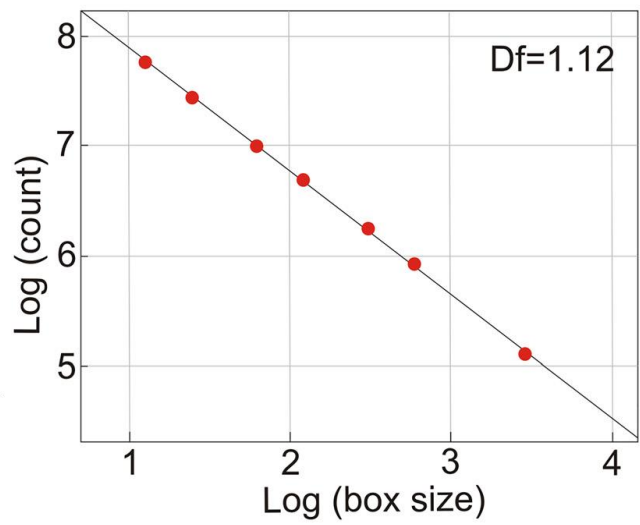
Figure 4. The morphological features of control and post-CFA injection day 3 horizontal S1 L2/3 pyramidal neurons are similar. *A–C*, Morphological features of 3D-reconstructed neuritic arbors of neurobiotin labeled pyramidal neurons after subcutaneous injection into the vibrissa pad of saline (vehicle; 1 hour and 3 days; black; n=12) or CFA (2.5 mg/kg; 3 days: blue, n=5). For bar histograms, bars represent mean + S.E.M of n neurons per group and each symbol is the value for a single neuron. There was no difference between 1 hour and 3 days post-NaCl injection; therefore, controls at 1 hour and 3 days post-NaCl have been put together. *A, B*, Total field area (*A*) and fractal dimension (*B*) of pyramidal neurons in the different experimental groups. *C*, Number of neuritic branches of pyramidal neurons in the different experimental groups. *D*, Representative neuronal reconstructions showing the neuritic arborizations of pyramidal neurons, 3 days after NaCl and CFA injection. Tukey's HSD post-test following one-way ANOVA.

A

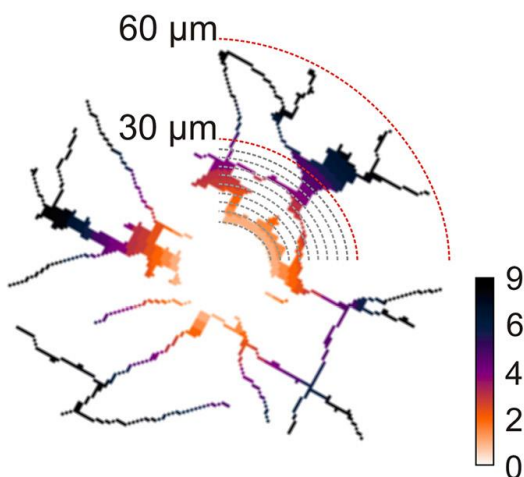
Neuritic area

**B**

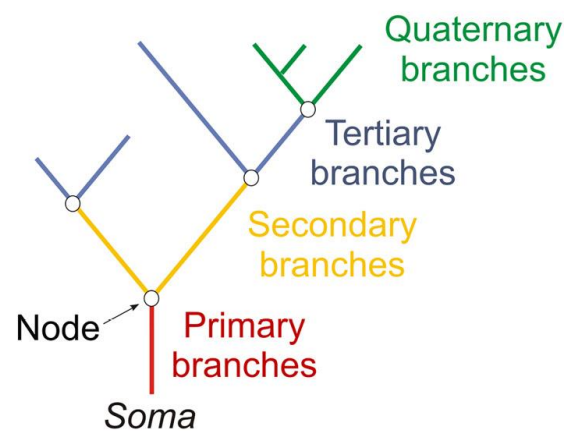
Fractal dimension

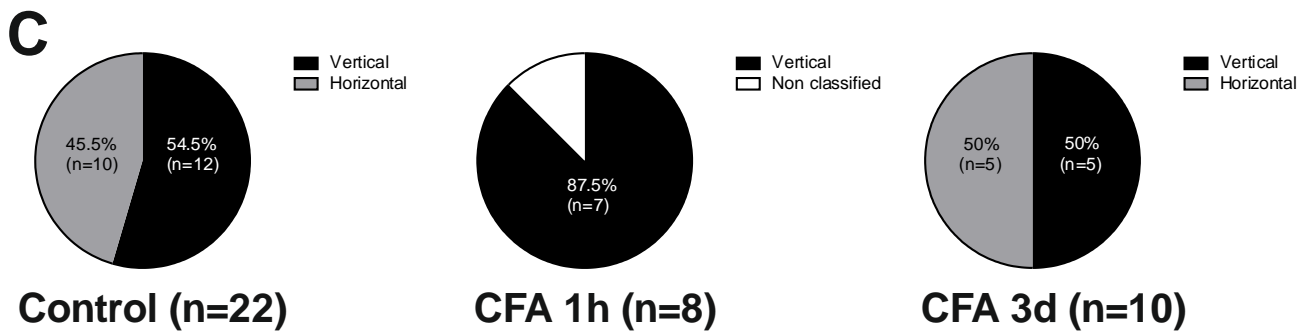
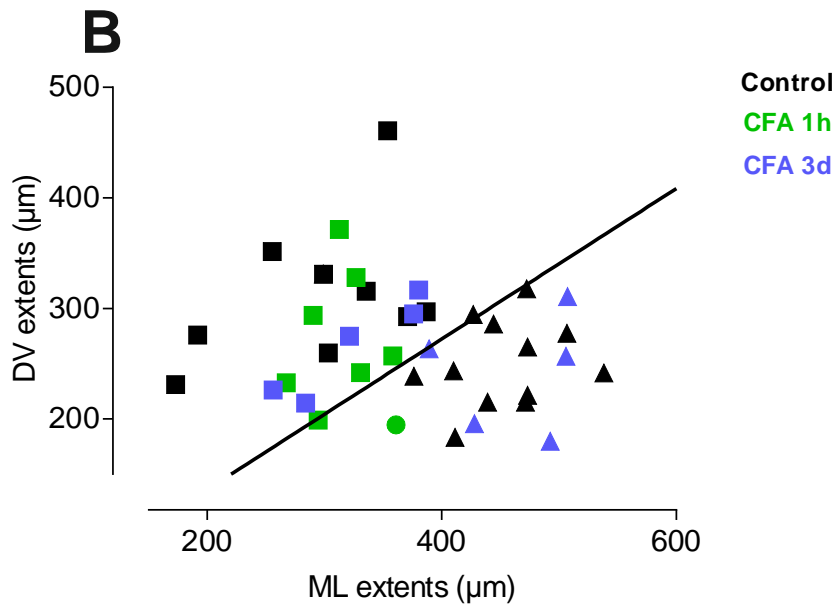
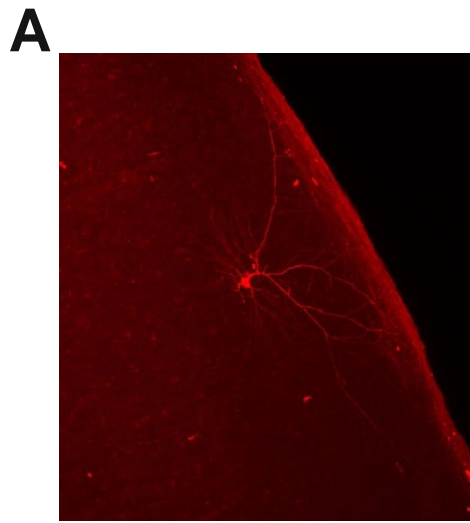
Fractal
Box count**C**

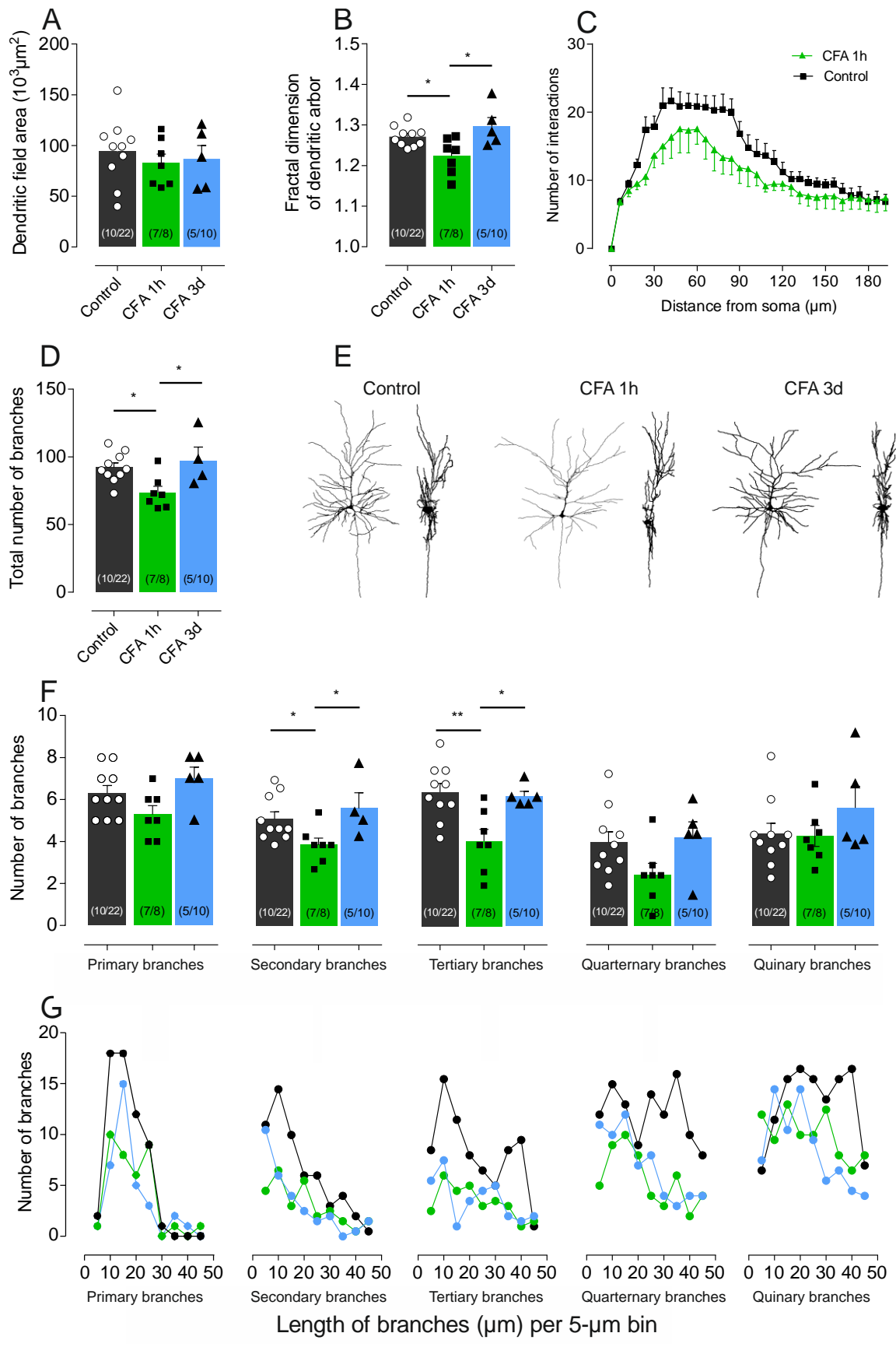
Sholl analysis

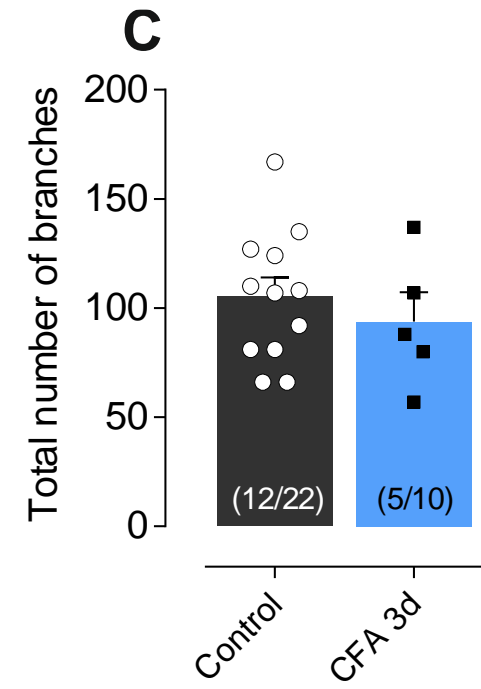
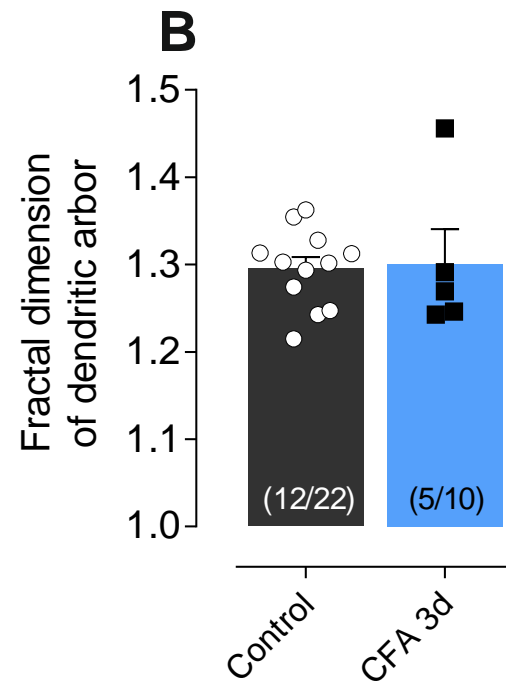
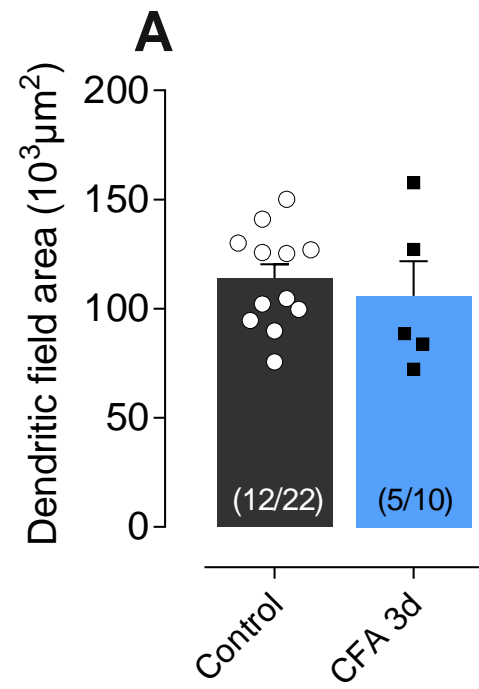
**D**

Neuritic branching order









CONCLUSION

De nombreuses données expérimentales suggèrent que la chronicisation d'une douleur met en jeu une plasticité des voies de la douleur parmi lesquelles le cortex. Une grande attention s'est portée sur l'ACC. Or, le cortex S1 est aussi impliqué dans la douleur chronique. Il est le siège d'une hyperactivité chez le patient comme chez l'animal douloureux chronique. Mais cette hyperactivité est-elle soutenue par une plasticité ? Et si oui, laquelle ?

En effet, il est maintenant clairement établi que l'activité synaptique peut déclencher simultanément de nombreux phénomènes de plasticité, incluant notamment (i) des changements bidirectionnels durables de la transmission synaptique (LTP ou LTD), (ii) des changements dans la capacité même qu'a cette transmission synaptique d'exprimer une future plasticité synaptique (méta-plasticité), (iii) des changements bidirectionnels durables de l'excitabilité neuronale (LTP-IE et LTD-IE) et (iv) une réorganisation morphologique.

Pour répondre à cette question, nous avons donc procédé en deux étapes.

Dans une première étape (Chapitre 1), nous avons recherché, en conditions contrôles, quels sont les phénomènes de plasticité déclenchés par l'activation synaptique dans les couches superficielles (2 et 3) de S1 et comment ils sont reliés entre eux. En effet, il est crucial de connaître à la fois (i) les relations entre activité synaptique et chaque type de plasticité ou règles de plasticité (synaptique, intrinsèque) et (ii) les relations entre ces différentes plasticités – i.e. les différentes règles de plasticité – pour déterminer le rôle de chaque plasticité dans l'engram, ici la mémoire douloureuse. Nous montrons qu'en règle générale, dans les couches 2/3 du cortex S1, changements synaptiques et changements neuronaux sont synergiques : LTP synaptique avec LTP-IE et LTD synaptique avec LTD-IE. Ainsi les changements d'excitabilité intrinsèque tendent à amplifier les changements synaptiques. De plus, nous révélons que les deux règles de plasticité, synaptique et intrinsèque, sont (i) superposables et (ii) varient parallèlement en fonction de l'état potentialisé ou déprimé du couple synapse/neurone postsynaptique – i.e. les méta-plasticités synaptiques et intrinsèque sont aussi synergiques.

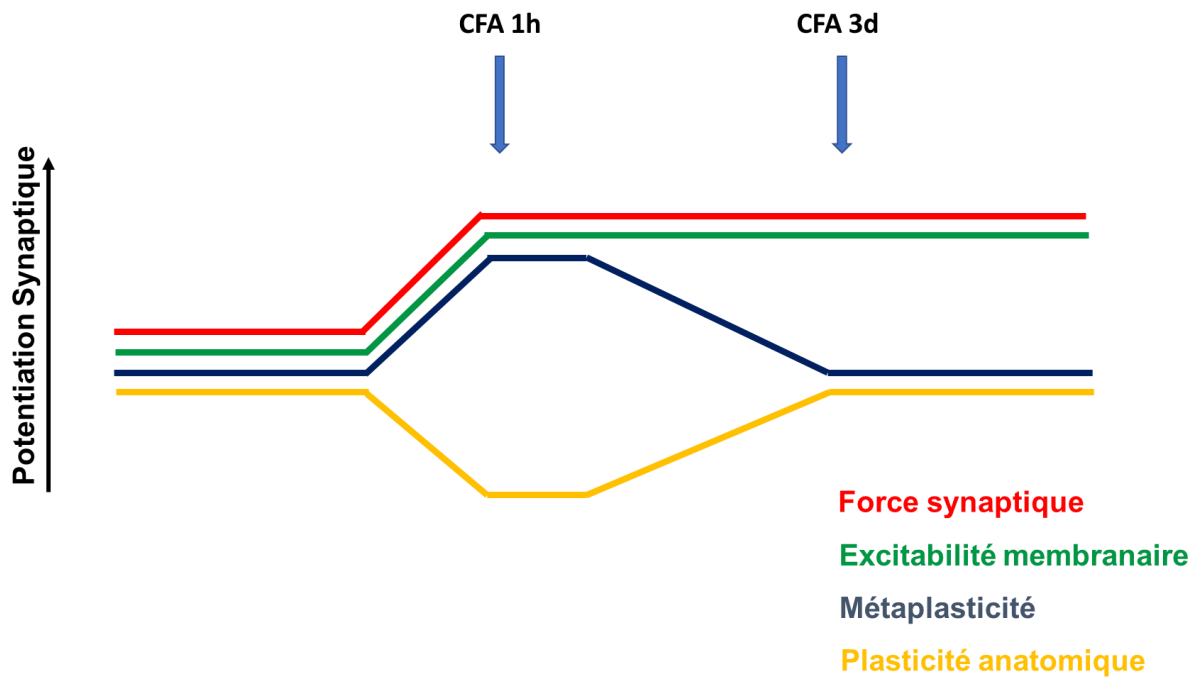
Il est intéressant de comparer ici le rôle respectif des plasticités synaptique et neuronale dans le contrôle de l'induction ultérieure d'une plasticité synaptique. Nous avons montré que s'il y a par exemple induction d'une LTP synaptique, l'induction ultérieure de la LTD est facilitée et celle de la LTP au contraire inhibée. Or cette méta-plasticité, homéostatique, est spécifique des synapses qui ont été activées ; l'induction des LTD/LTP synaptiques dans les autres synapses n'est pas modifiée (voir Ngezahayo et al., 2000 ; revue dans Abraham, 2008). La LTP synaptique s'accompagne d'une LTP-IE. Cette hyperexcitabilité, elle, facilite l'induction d'une plasticité synaptique – elle est donc synergique – dans l'ensemble des synapses sur ce neurone.

Dans une seconde étape (Chapitres 2 et 3), nous avons identifié (i) les plasticités mises en jeu dans un modèle de douleur inflammatoire chronique (modèle CFA de la face) dans les couches superficielles du cortex S1 et (ii) leur évolution en fonction du temps. Nous confirmons que cette inflammation périphérique déclenche une allodynie mécanique très importante, rapidement (dès 1 heure après le début de l'inflammation) et durablement (3 jours après). Nous montrons que cette inflammation déclenche aussi (i) une potentialisation de la transmission synaptique, (ii) une métaplasticité synaptique, compatible avec une LTP de la transmission synaptique, (iii) une hyperexcitabilité neuronale et (iv) une modification du ratio neurone pyramidal vertical/ neurone pyramidal horizontal et une réduction de la complexité de l'arbre dendritique des neurones pyramidaux. De plus ces plasticités suivent des évolutions différentes : alors que potentialisation de la transmission synaptique et hyperexcitabilité neuronale restent stables, changements métaplastiques et réduction de la complexité dendritique sont réversibles (Fig. 1) en 3 jours. Ces résultats suggèrent que seuls la LTP de la transmission excitatrice et l'hyperexcitabilité des neurones pyramidaux post-synaptiques sont associés au maintien de l'hypersensibilité mécanique. Cependant, il est possible que la réversibilité de la réduction de la complexité dendritique ne soit pas nécessairement un retour à un état *quo ante*.

Il est intéressant de remarquer ici qu'alors que la métaplasticité synaptique revient à son état basal, le neurone reste hyperexcitable à 3 jours. Donc le rôle respectif des plasticités synaptique et neuronale dans le contrôle de l'induction ultérieure d'une plasticité synaptique est non seulement différent (voir ci-dessus) mais aussi varie différemment dans le temps.

Reste la question des mécanismes de ces diverses plasticités – cibles éventuelles pour des médicaments antalgiques. Une grande attention s'est portée sur les mécanismes des modifications bidirectionnelles de la transmission synaptique (LTP et LTD ; voir les revues : Bliss et Collingridge, 1993 ; Collingridge et al., 2010 ; Hiester et al., 2018 ; dans l'ACC : Bliss et al., 2016). Par contre, on connaît peu ceux de la métaplasticité synaptique (voir Abraham, 2008). Il est important de noter que les shifts simultanés, en directions opposées des deux seuils pour l'induction de la LTD et de la LTP, imposent des contraintes aux mécanismes possibles (voir Discussion dans Ngezahayo et al., 2000). De même, s'il est clair que la plasticité intrinsèque met en jeu des canaux membranaires (voltage-, Ca^{2+} -dépendants), il n'existe pas de consensus quant au canal ou la famille de canaux mis en jeu (voir Discussion dans Chapitre 2). Cependant, nous montrons que ces changements peuvent prendre au moins deux formes, en fonction de la modification ou non du gain de la réponse neuronale, suggérant l'intervention d'au moins deux canaux différents.

Cependant, nos résultats peuvent avoir une application thérapeutique immédiate dans la conduite du traitement de la douleur chronique par stimulation électrique ou magnétique non-invasive du cerveau. En effet, ces traitements cherchent à prévenir ou à supprimer la plasticité dans les aires codant pour la douleur. Ils adaptent donc les fréquences de stimulation en conséquence. Nos résultats indiquent qu'il faut aussi adapter la fréquence des séances de stimulation à l'évolution dans le temps des processus de modulation de la plasticité. Par exemple, une stimulation qui, en conditions normales, induit une LTP (prenons par exemple un pairing à 10 mV ; voir Chapitre 1 et 2), induit une LTD juste après potentialisation synaptique/intrinsèque et à nouveau une LTP, 3 jours après.



REFERENCES

- Abraham WC (2008) Metaplasticity: tuning synapses and networks for plasticity. *Nat Rev Neurosci* 9(5):387.
- Aigner M, Robert Lukas J, Denk M, Ziya-Ghazvini F, Kaider A, Mayr R (2000) Somatotopic organization of primary afferent perikarya of the guinea-pig extraocular muscles in the trigeminal ganglion:a post-mortem DiI-tracing study. *Exp Eye Res* 70(4):411-418.
- Alba-Delgado C, Mountadem S, Mermet-Joret N, Monconduit L, Dallel R, Artola A, Antri M (2018) 5-HT_{2A} receptor-induced morphological reorganization of PKC γ -expressing interneurons gates inflammatory mechanical allodynia in rat. *J Neurosci* pii: 1294-18.
- Almeida TF, Roizenblatt S, Tufik S (2004) Afferent pain pathways:a neuroanatomical review. *Brain Res* 1000(1):40-56.
- Alvarez P, Dieb W, Hafidi A, Voisin DL, Dallel R (2008) Insular cortex representation of dynamic mechanical allodynia in trigeminal neuropathic rats. *Neurobiol Dis* 33(1): 89-95.
- Andrew D, Craig AD (2001) Spinothalamic lamina I neurons selectively sensitive to histamine:a central neural pathway for itch. *Nat Neurosci* 4(1):72-77.
- Arvidsson J, Pfaller K, Gmeiner S (1992) The ganglionic origins and central projections of primary sensory neurons innervating the upper and lower lips in the rat. *Somatosensory Motor Res* 9(3):199-209.
- Apkarian AV, Bushnell MC, Treede RD, Zubieta JK (2005) Human brain mechanisms of pain perception and regulation in health and disease. *Eur J Pain* 9:463–84.
- Attal N, Perrot S, Fermanian J, Bouhassira D (2011) The neuropathic components of chronic low back pain:a prospective multicenter study using the DN4 Questionnaire. *J Pain Off J Am Pain Soc* 12(10):1080-1087.
- Augustine JR (1985) The insular lobe in primates including humans. *Neurol Res* 7(1):2-10.
- Augustine JR (1996) Circuitry and functional aspects of the insular lobe in primates including humans. *Brain Res Rev* 22(3):229-244.
- Baron R, Binder A, Wasner G (2010) Neuropathic pain:diagnosis, pathophysiological mechanisms, and treatment. *Lancet Neurol* 9(8):807-819.
- Bennett DL, Michael GJ, Ramachandran N, Munson JB, Averill S, Yan Q, McMahon SB, Priestley JV (1998) A distinct subgroup of small DRG cells express GDNF receptor components and GDNF is protective for these neurons after nerve injury. *J Neurosci*, 18(8):3059-3072.
- Berthier M, Starkstein S, Leiguarda R (1988) Asymbolia for pain:A sensory-limbic disconnection syndrome. *Ann Neurol* 24(1):41-49.

- Besson JM, Chaouc A (1987) Peripheral and spinal mechanisms of nociception. *Physiologi Rev* 67(1):67-186.
- Beuerman RW, Tanelian DL (1979) Corneal pain evoked by thermal stimulation. *Pain* 7(1):1-14.
- Bie B, Brown DL, Naguib M (2011) Increased synaptic GluR1 subunits in the anterior cingulate cortex of rats with peripheral inflammation. *Eur J Pharmacol.* 653(1-3):26-31.
- Biemond A (1956) The conduction of pain above the level of the thalamus opticus. *Arch Neurol Psychiatry* 75:231–44.
- Bliss TV, Collingridge GL (1993) A synaptic model of memory: long-term potentiation in the hippocampus. *Nature* (361)6407:31-9.
- Bliss TV, Collingridge GL, Kaang BK1, Zhuo M (2016) Synaptic plasticity in the anterior cingulate cortex in acute and chronic pain. *Nat Rev Neurosci* 17(8):485-96.
- Borsook D (2007) Pain and motor system plasticity. *Pain*, 132(1-2):8.
- Bouhassira D, Attal N (2007) *Douleurs Neuropathiques*. Edition Arnette Groupe Liaison S.A. 2007.
- Bragin EO, Yeliseeva ZV, Vasilenko GF, Meizerov EE, Chuvain BT, Durinyan RA (1984) Cortical projections to the periaqueductal grey in the cat: a retrograde horseradish peroxidase study. *Neurosci Lett* 51:271–275.
- Bromm B, Scharein E, Vahle-Hinz C (2000) Cortex areas involved in the processing of normal and altered pain. *Progr Brain Resc* 129:289-302.
- Burstein R, Hiroyoshi Y, Amy M, Strassman M (1998) Chemical stimulation of the intracranial dura induces enhanced responses to facial stimulation in brain stem trigeminal neurons. *J Neurophysiol* 79(2):964-982.
- Burstein R, Cutrer MF, Yarnitsky D (2000) The development of cutaneous allodynia during a migraine attack clinical evidence for the sequential recruitment of spinal and supraspinal nociceptive neurons in migraine. *Brain* 123 (Pt 8):1703-1709.
- Bushnell MC, Ceko M, Low LA (2013) Cognitive and emotional control of pain and its disruption in chronic pain. *Nat Rev Neurosci* 14(7):502-11
- Bushnell MC, Duncan GH, Hofbauer RK, Ha B, Chen JI, Carrier B (1999) Pain perception: is there a role for primary somatosensory cortex? *Proc. Natl. Acad. Sci. USA* 96:7705–7709.
- Capra NF, Wax TD (1989) Distribution and central projections of primary afferent neurons that innervate the masseter muscle and mandibular periodontium: a double-label study. *J Comp Neurol* 279(3):341-352.
- Caruana F, Jezzini A, Sbriscia-Fioretti B, Rizzolatti G, Gallese V (2011) Emotional and social behaviors elicited by electrical stimulation of the insula in the macaque monkey. *Curr Biol* 21:195–9.
- Casey KL (1999) Forebrain mechanisms of nociception and pain: analysis through imaging. *Proc Natl Acad Sci U S A* 96(14):7668-7674.

- Casey KL, Minoshima S, Morrow TJ, Koeppe RA (1996) Comparison of human cerebral activation patterns during cutaneous warmth, heat pain, and deep cold pain. *J Neurophysiol* 76(1):571-581.
- Caterina MJ, Schumacher MA, Tominaga M, Rosen TA, Levine JD, Julius D (1997) The capsaicin receptor: a heat-activated ion channel in the pain pathway. *Nature* 389(6653):816-824.
- Cervero F (1994) Sensory innervation of the viscera: peripheral basis of visceral pain. *Physiol Rev*, 74(1):95-138.
- Chen T, Koga K, Descalzi G, Qiu S, Wang J, Zhang LS, Zhang ZJ, He XB, Qin X, Xu FQ, Hu J, Wei F, Haganir RL, Li YQ, Zhuo M (2014) Postsynaptic potentiation of corticospinal projecting neurons in the anterior cingulate cortex after nerve injury. *Mol Pain* 10:33.
- Chen ZY, Shen FY, Jiang L, Zhao X, Shen XL, Zhong W, Liu S, Wang ZR, Wang YW (2016) Attenuation of Neuropathic Pain by Inhibiting Electrical Synapses in the Anterior Cingulate Cortex. *Anesthesiology* 124(1):169-183.
- Chiou CS, Chen CC, Tsai TC, Huang CC, Chou D, Hsu KS (2016) Alleviating Bone Cancer-induced Mechanical Hypersensitivity by Inhibiting Neuronal Activity in the Anterior Cingulate Cortex. *Anesthesiology* 125(4):779-792.
- Chua P, Krams M, Toni I, Passingham R, Dolan R. (1999) A functional anatomy of anticipatory anxiety. *Neuroimage* 9(6):563-571.
- Cichon J, Blanck TJJ, Gan WB, Yang G (2017) Activation of cortical somatostatin interneurons prevents the development of neuropathic pain. *Nat Neurosci*. 20(8):1122-1132.
- Coghill RC, Sang CN, Maisog JM, Iadarola MJ. (1999) Pain intensity processing within the human brain: a bilateral, distributed mechanism. *J Neurophysiol* 82(4):1934-1943.
- Cometto-Muñiz JE, Cain WS (1995) Relative sensitivity of the ocular trigeminal, nasal trigeminal and olfactory systems to airborne chemicals. *Chemical Senses* 20(2):191-198.
- Collingridge GL, Peineau S, Howland JG, Wang YT (2010) Long-term depression in the CNS. *Nat Rev Neurosci* 11(7):459-73.
- Coste J, Voisin DL, Miraucourt LS, Dallel R, Luccarini P (2008) Dorsal horn NK1-expressing neurons control windup of downstream trigeminal nociceptive neurons. *Pain* 137(2):340-351.
- Costigan M, Scholz J, Woolf CJ (2009) Neuropathic pain: a maladaptive response of the nervous system to damage. *Annu Rev Neurosci* 32:1-32.
- Craig AD (2009) How do you feel—now? The anterior insula and human awareness. *Nat Rev Neurosci* 10:59–70.
- Craig AD, Kniffki KD (1985) Spinothalamic lumbosacral lamina I cells responsive to skin and muscle stimulation in the cat. *J Physiol*, 365:197-221.
- Cruccu G, Aminoff MJ, Curio G, Guerit JM, Kakigi R, Mauguiere F, Rossini PM, Treede RD, Garcia-Larrea L (2008) Recommendations for the clinical use of somatosensory-evoked potentials. *Clin Neurophysiol* 119(8):1705-1719.

- Curtis R (1992) Self-organizing processes, anxiety, and change. *J Psychot Integr* 2(4):295-319.
- Dallel R, Clavelou P, Woda A (1989) Effects of tractotomy on nociceptive reactions induced by tooth pulp stimulation in the rat. *Exp Neurol* 106(1):78-84.
- Dallel R, Dualé C, Molat JL (1998) Morphine administered in the substantia gelatinosa of the spinal trigeminal nucleus caudalis inhibits nociceptive activities in the spinal trigeminal nucleus oralis. *J Neurosci* 18(10):3529-3536.
- Dallel R, Duale C, Luccarini P, Molat JL (1999) Stimulus-function, wind-up and modulation by diffuse noxious inhibitory controls of responses of convergent neurons of the spinal trigeminal nucleus oralis. *Eur J Neurosci* 11(1):31-40.
- Damasio AR, Grabowski TJ, Bechara A, Damasio H, Ponto LL, Parvizi J, Hichwa RD (2000) Subcortical and cortical brain activity during the feeling of self-generated emotions. *Nat Neurosci* 3(10):1049-1056.
- De Ridder D, De Mulder G, Menovsky T, Sunaert S, Kovacs S (2007) Electrical stimulation of auditory and somatosensory cortices for treatment of tinnitus and pain. *Prog. Brain Res.* 166:377–388.
- Derbyshire SW, Jones AK, Gyulai F, Clark S, Townsend D, Firestone LL (1997) Pain processing during three levels of noxious stimulation produces differential patterns of central activity. *Pain* 73(3):431-445.
- Derbyshire SW, Jones AK, Creed F, Starz T, Meltzer CC, Townsend DW, Peterson AM, Firestone L (2002) Cerebral responses to noxious thermal stimulation in chronic low back pain patients and normal controls. *Neuroimage* 16(1):158-168.
- Dias R, Robbins T, Roberts A (1996) Dissociation in prefrontal cortex of affective and attentional shifts. *Nature* 380(6569):69-72.
- Diogenes A, Patwardhan AM, Jeske NA, Ruparel NB, Goffin V, Akopian AN, Hargreaves KM (2006) Prolactin modulates TRPV1 in female rat trigeminal sensory neurons. *J Neurosci* 26(31):8126-8136.
- Dong WK, Chudler EH, Sugiyama K, Roberts VJ, Hayashi T (1994) Somatosensory, multisensory, and task-related neurons in cortical area 7b (PF) of unanesthetized monkeys. *J Neurophysiol* 72(2):542-564.
- Dum RP, Levinthal DJ, Strick PL (2009) The spinothalamic system targets motor and sensory areas in the cerebral cortex of monkeys. *J Neurosci* 29:14223–14235.
- Dworkin RH et al. (2003) Advances in neuropathic pain: diagnosis, mechanisms, and treatment recommendations. *Arch Neurol* 60(11):1524-1534.
- Eisenberger NI, Lieberman MD, Williams KD (2003) Does rejection hurt? An fMRI study of social exclusion. *Science* 302:290–292.
- Eto K, Wake H, Watanabe M, Ishibashi H, Noda M, Yanagawa Y, Nabekura J (2011) Inter-regional contribution of enhanced activity of the primary somatosensory cortex to the anterior cingulate cortex accelerates chronic pain behavior. *J Neurosci.* 31(21):7631-7636.

- Eto K, Ishibashi H, Yoshimura T, Watanabe M, Miyamoto A, Ikenaka K, Moorhouse AJ, Nabekura J (2012) Enhanced GABAergic activity in the mouse primary somatosensory cortex is insufficient to alleviate chronic pain behavior with reduced expression of neuronal potassium-chloride cotransporter. *J Neurosci.* 32(47):16552-16559.
- Feindel W, Penfield W, McNaughton F (1960) The tentorial nerves and localization of intracranial pain in man. *Neurology* 10:555-563.
- Feng J, Zhang Z, Li W, Shen X, Song W, Yang C, Chang F, Longmate J, Marek C, St Amand RP, Krontiris TG, Shively JE, Sommer SS (2009) Missense mutation in the MEFV gene are associated with fibromyalgia syndrome and correlate with elevated IL-1beta plasma level. *PLoS One* 4(12):e8480.
- Flor H, Elbert T, Knecht S, Wienbruch C, Pantev C, Birbaumer N, Larbig W, Taub E (1995) Phantom-limb pain as a perceptual correlate of cortical reorganization following arm amputation. *Nature* 375(6531):482-484.
- Flor H, Denke C, Schaefer M, Grüsser S (2001) Effect of sensory discrimination training on cortical reorganisation and phantom limb pain. *Lancet* 357:1763–1764.
- Foltz EL, White Jr LE (1962) Pain “Relief” by Frontal Cingulumotomy. *J Neurosurgery* 19(2):89-100.
- Frot M, Rambaud L, Guenot M, Mauguier F (1999) Intracortical recordings of early pain-related CO₂-laser evoked potentials in the human second somatosensory (SII) area. *Clin Neurophysiol* 110:133–45.
- Frot M, Magnin M, Mauguière F, Garcia-Larrea L (2013) Cortical representation of pain in primary sensory-motor areas (S1/M1)-a study using intracortical recordings in humans. *Hum Brain Mapp* 34:2655–68.
- Garcia-Larrea L (2012) The posterior insular-opercular region and the search of a primary cortex for pain. *Neurophysiol Clin* 42:299–313.
- Garcia-Larrea L, Perchet C, Creac’h C, Convers P, Peyron R, Laurent B, Mauguière F, Magnin M (2010) Operculo-insular pain (parasyllian pain):a distinct central pain syndrome. *Brain* 133:2528–39.
- Garcia-Larrea L, Peyron R (2013) Pain matrices and neuropathic pain matrices:a review. *Pain* 154.
- Gerard MW (1923) Afferent impulses of the trigeminal nerve. The intramedullary course of the painful thermal and tactile impulses. *Arch Neurol Psychiatr* 9:306-338.
- Gonçalves DA, Dal Fabbro AL, Campos JA, Bigal ME, Speciali JG (2010) Symptoms of temporomandibular disorders in the population:an epidemiological study. *J Orofac Pain* 24(3):270-278.
- Gorsky M, Silverman S, Jr & Chinn H (1991) Clinical characteristics and management outcome in the burning mouth syndrome. An open study of 130 patients. *Oral Sur, Oral Med Oral Pathol* 72(2):192-195.
- Graham SH, Sharp FR, Dillon W (1988) Intraoral sensation in patients with brainstem lesions:role of the rostral spinal trigeminal nuclei in pons. *Neurology* 38(10):1529-1533.

- Greenspan JD, Lee RR, Lenz FA (1999) Pain sensitivity alterations as a function of lesion location in the parasyllian cortex. *PAIN* 81:273–82.
- Gross J, Schnitzler A, Timmermann L, Ploner M (2007) Gamma oscillations in human primary somatosensory cortex reflect pain perception. *PLoS Biol* 5:e133.
- Gu L, Uhelski ML, Anand S, Romero-Ortega M, Kim YT, Fuchs PN, Mohanty SK (2015) Pain inhibition by optogenetic activation of specific anterior cingulate cortical neurons. *PLoS ONE* 10:e0117746.
- Guilbaud G, Kayser V, Benoist JM, Gautron M (1986) Modifications in the responsiveness of rat ventrobasal thalamic neurons at different stages of carrageeninproduced inflammation. *Brain Res.* 385:86–98.
- Guilbaud G, Benoist JM, Jazat F, Gautron M (1990) Neuronal responsiveness in the ventrobasal thalamic complex of rats with an experimental peripheral mononeuropathy. *J. Neurophysiol.* 64:1537–1554.
- Guo A, Vulchanova L, Wang J, Li X, Elde R (1999) Immunocytochemical localization of the vanilloid receptor 1 (VR1):relationship to neuropeptides, the P2X3 purinoceptor and IB4 binding sites. *Eur J Neurosci* 11(3):946-958.
- Hagains CE, Senapati AK, Huntington PJ, He JW, Peng YB (2011) Inhibition of spinal cord dorsal horn neuronal activity by electrical stimulation of the cerebellar cortex. *J Neurophysiol* 106(5):2515-2522.
- Han S, Soleiman MT, Soden ME, Zweifel LS, Palmiter RD (2015) Elucidating an affective pain circuit that creates a threat memory. *Cell* 162, 363–374.
- Hari R, Portin K, Kettenmann B, Jousmäki V, Kopal G (1997) Right-hemisphere preponderance of responses to painful CO₂ stimulation of the human nasal mucosa. *Pain* 72(1):145-151.
- Hiester BG, Becker MI, Bowen AB, Schwartz SL and Kennedy MJ (2018) Mechanisms and Role of Dendritic Membrane Trafficking for Long-Term Potentiation. *Front. Cell. Neurosci.* 12:391.
- Hoffmann KD, Matthews MA (1990) Comparison of sympathetic neurons in orofacial and upper extremity nerves:implications for causalgia. *J Oral Maxillofacial Surg* 48(7):720-726; discussion 727.
- Howland EW, Wakai RT, Mjaanes BA, Balog JP, Cleeland CS (1995) Whole head mapping of magnetic fields following painful electric finger shock. *Brain Res Cogn Brain Res* 2(3):165-172.
- Hu JW, Sessle BJ, Raboisson P, Dallel R, Woda A (1992) Stimulation of craniofacial muscle afferents induces prolonged facilitatory effects in trigeminal nociceptive brain-stem neurones. *Pain* 48(1):53-60.
- Hu JW, Woda A, Sessle BJ (1999) Effects of pre-emptive local anaesthesia on tooth pulp deafferentation-induced neuroplastic changes in cat trigeminal brainstem neurones. *Arch Oral Biol*, 44(3):287-293.

- Hughes DI, Scott DT, Todd AJ, Riddell JS (2003) Lack of evidence for sprouting of Aβ afferents into the superficial laminae of the spinal cord dorsal horn after nerve section. *J Neurosci* 23(29):9491-9499.
- Hunt SP, Rossi J (1985) Peptide- and non-peptide-containing unmyelinated primary afferents: the parallel processing of nociceptive information. *Philos Transactions of the R Soc Lond B Biol Sci* 308(1136):283-289.
- Hunt SP, Mantyh PW (2001) The molecular dynamics of pain control. *Nat Rev Neurosci* 2(2):83-91.
- Hurt R, Ballantine HT Jr (1973) Stereotactic anterior cingulate lesions for persistent pain: a report on 68 cases. *Clin Neurosurg* 21:334-351.
- Iggo A, Andres KH (1982) Morphology of Cutaneous Receptors. *Ann Rev Neurosci* 5(1):1-31.
- Ikeda H, Heinke B, Ruscheweyh R, Sandkühler J (2003) Synaptic plasticity in spinal lamina I projection neurons that mediate hyperalgesia. *Science (New York, N.Y.)* 299(5610):1237-1240.
- Ikeda H, Stark J, Fischer H, Wagner M, Drdla R, Jäger T, Sandkühler J (2006) Synaptic amplifier of inflammatory pain in the spinal dorsal horn. *Science* 312:1659–1662.
- Ikeda R, Takahashi Y, Inoue K, Kato F (2007) NMDA receptor-independent synaptic plasticity in the central amygdala in the rat model of neuropathic pain. *Pain* 127:161–172.
- Isnard J, Magnin M, Jung J, Mauguière F, Garcia-Larrea L (2011) Does the insula tell our brain that we are in pain? *PAIN* 152:946–51.
- Jensen KB, Berna C, Loggia ML, Wasan AD, Edwards RR, Gollub RL (2012) The use of functional neuroimaging to evaluate psychological and other non-pharmacological treatments for clinical pain. *Neuroscience letters* 520(2):v156-164.
- Jensen MP (2010) A neuropsychological model of pain: research and clinical implications. *The J Pain* 11(1):2-12.
- Jones EG (2012) *The thalamus*. Springer Science & Business Media.
- Juhl GI, Jensen TS, Norholt SE, Svensson P (2008) Central Sensitization Phenomena after Third Molar Surgery: A Quantitative Sensory Testing Study. *Eur J Pain* 12(1):116-127.
- Julius D, Basbaum A I (2001) Molecular mechanisms of nociception. *Nature* 413(6852):203-210.
- Kandel E, Schwartz J, Jessell T (2000) *Principles of Neural Science*. 4th ed. New York: McGraw-Hill Professional Publishing. 1414.
- Kang SJ, Kwak C, Lee J, Sim SE, Shim J, Choi T, Collingridge GL, Zhuo M, Kaang BK (2015) Bidirectional modulation of hyperalgesia via the specific control of excitatory and inhibitory neuronal activity in the ACC. *Mol. Brain* 8:81.
- Kenshalo DR (1960) Comparison of thermal sensitivity of the forehead, lip, conjunctiva and cornea. *J Appl Physiol* 15:987-991.
- Khayyat GF, Yu UJ, King RB (1975) Response patterns to noxious and non-noxious stimuli in rostral trigeminal relay nuclei. *Brain Res* 97(1):47-60.

- Kim SK, Nabekura J (2011) Rapid synaptic remodeling in the adult somatosensory cortex following peripheral nerve injury and its association with neuropathic pain. *J Neurosci* 31(14):5477-82.
- Koga K, Descalzi G, Chen T, Ko HG, Lu J, Li S, Son J, Kim T, Kwak C, Huganir RL, Zhao MG, Kaang BK, Collingridge GL, Zhuo M (2015) Coexistence of two forms of LTP in ACC provides a synaptic mechanism for the interactions between anxiety and chronic pain. *Neuron* 85(2):377-389.
- Koltzenburg M, Scadding (2001) Neuropathic pain. *Cur Opin Neurol* 14(5):641-647.
- Kwiatk R, Barnden L, Tedman R, Jarrett R, Chew J, Rowe C, Pile K (2000) Regional cerebral blood flow in fibromyalgia: Single-photon-emission computed tomography evidence of reduction in the pontine tegmentum and thalami. *Arthritis Rheum* 43(12):2823-2833.
- Lagerström MC, Rogoz K, Abrahamsen B, Persson E, Reinius B, Nordenankar K, Olund C, Smith C, Mendez JA, Chen ZF, Wood JN, Wallén-Mackenzie A, Kullander K (2010) VGLUT2-dependent sensory neurons in the TRPV1 population regulate pain and itch. *Neuron*, 68(3):529-542.
- Lamey PJ, Lewis MA (1989) Oral medicine in practice: burning mouth syndrome. *Brit Dent J* 167(6):197-200.
- Lane RD, Reiman EM, Bradley MM, Lang PJ, Ahern GL, Davidson RJ, Schwartz GE (1997) Neuroanatomical correlates of pleasant and unpleasant emotion. *Neuropsychologia* 35(11):1437-1444.
- Latremoliere A, Woolf CJ (2009) Central sensitization: a generator of pain hypersensitivity by central neural plasticity. *J Pain* 10(9):895-926.
- Lazarov NE (2002) Comparative analysis of the chemical neuroanatomy of the mammalian trigeminal ganglion and mesencephalic trigeminal nucleus. *Pro Neurobiol* 66(1):19-59.
- Leise EM (1990) Modular construction of nervous systems: a basic principle of design for invertebrates and vertebrates. *Brain Res* 15(1):1-23.
- Lenz FA, Gracely RH, Romanoski AJ, Hope EJ, Rowland LH, Dougherty PM (1995) Stimulation in the human somatosensory thalamus can reproduce both the affective and sensory dimensions of previously experienced pain. *Nat Med* 1:910-3
- Lenz FA, Rios M, Zirh A, Chau D, Krauss G, Lesser RP (1998) Painful stimuli evoke potentials recorded over the human anterior cingulate gyrus. *J Neurophysiol* 79:2231-4.
- Lenz FA, Rios M, Chau D, Krauss GL, Zirh TA, Lesser RP (1998) Painful stimuli evoke potentials recorded from the parasylvian cortex in humans. *J Neurophysiol* 80:2077-88.
- Levy D, Strassman Andrew M (2002) Mechanical response properties of A and C primary afferent neurons innervating the rat intracranial dura. *J Neurophysiol* 88(6):3021-3031.
- Lévesque J, Eugène F, Joannette Y, Paquette V, Mensour B, Beaudoin G, Leroux JM, Bourgouin P, Beaugregard M. (2003) Neural circuitry underlying voluntary suppression of sadness. *Biol Psychiatry* 53(6):502-510.

- Li XY, Ko HG, Chen T, Descalzi G, Koga K, Wang H, Kim SS, Shang Y, Kwak C, Park SW, Shim J, Lee K, Collingridge GL, Kaang BK, Zhuo M (2010) Alleviating neuropathic pain hypersensitivity by inhibiting PKMzeta in the anterior cingulate cortex. *Science* 330(6009):1400-1404.
- Li Y, Esain V, Teng L, Xu J, Kwan W, Frost IM, Yzaguirre AD, Cai X, Cortes M, Maijenburg MW, Tober J, Dzierzak E, Orkin SH, Tan K, North TE, Speck NA (2014) Inflammatory signaling regulates embryonic hematopoietic stem and progenitor cell production. *Genes Dev* 28(23):2597-612.
- Light AR, Perl E R (1979) Spinal termination of functionally identified primary afferent neurons with slowly conducting myelinated fibers. *J Comp Neurol* 186(2):133-150.
- Liu MG, Koga K, Guo YY, Kang SJ, Collingridge GL, Kaang BK, Zhao MG, Zhuo M (2013) Long-term depression of synaptic transmission in the adult mouse insular cortex *in vitro*. *Eur. J. Neurosci.* 38:3128–3145 (2013).
- Liu MG, Kang SJ, Shi TY, Koga K, Zhang MM, Collingridge GL, Kaang BK, Zhuo M (2013) Long-term potentiation of synaptic transmission in the adult mouse insular cortex: multielectrode array recordings. *J. Neurophysiol.* 110:505–521.
- Liu Y, Abdel Samad O, Zhang L, Duan B, Tong Q, Lopes C, Ji RR, Lowell BB, Ma Q (2010) VGLUT2-dependent glutamate release from nociceptors is required to sense pain and suppress itch. *Neuron* 68(3):543-556.
- Lorente de No R (1938) Cerebral cortex:architecture, intracortical connexions, motor projections. In:Physiology of the nervous system (Fulton JF, ed):291–339. Oxford:Oxford UP
- Lorenz J, Casey K(2005) Imaging of acute versus pathological pain in humans. *Eur J Pain* 9(2):163-165.
- Lotze M, Grodd W, Birbaumer N, Erb M, Huse E, Flor H (1999) Does use of a myoelectric prosthesis prevent cortical reorganization and phantom limb pain? *Nat. Neurosci.* 2:501–502.
- Lu Y, Perl Edward R (2005) Modular organization of excitatory circuits between neurons of the spinal superficial dorsal horn (laminae I and II). *J Neurosci* 25(15):3900-3907.
- Lundy-Ekman L (2007) *Neuroscience:Fundamentals for Rehabilitation*. 3rd ed. St. Louis, MI:Saunders Elsevier. 575.
- Lynn B (1991) Silent' nociceptors in the skin. *Trends Neurosci* 14(3):95.
- Löken LS, Wessberg J, Morrison I, McGlone F, Olausson H (2009) Coding of pleasant touch by unmyelinated afferents in humans. *Nat Neurosci* 12(5):547-548.
- Ma W, Peschanski M (1998) Spinal and trigeminal projections to the parabrachial nucleus in the rat:electron-microscopic evidence of a spino-pontoamygdalian somatosensory pathway. *Somatosens. Res* 5:247–257.

- Malmberg AB, Brandon EP, Idzerda RL, Liu H, McKnight GS, Basbaum AI (1997) Diminished inflammation and nociceptive pain with preservation of neuropathic pain in mice with a targeted mutation of the type I regulatory subunit of cAMP-dependent protein kinase. *J Neurosci* 17(19):7462-7470.
- Marfurt CF (1981) The somatotopic organization of the cat trigeminal ganglion as determined by the horseradish peroxidase technique. *Anat Record* 201(1):105-118.
- Marfurt CF, Rajchert DM (1991) Trigeminal primary afferent projections to “non-trigeminal” areas of the rat central nervous system. *J Compara Neurol* 303(3):489-511.
- Matthews B (1989) Autonomic mechanisms in oral sensations. *Proc Fin Dent So* 85(4-5):365-373.
- Mazzola L, Isnard J, Mauguiere F (2006) Somatosensory and pain responses to stimulation of the second somatosensory area (SII) in humans:a comparison with SI and insular responses. *Cereb Cortex* 16:960–8.
- Mazzola L, Isnard J, Peyron R, Mauguière F (2012) Stimulation of the human cortex and the experience of pain:Wilder Penfield’s observations revisited. *Brain* 135:631–40.
- McGlone F, Vallbo AB, Olausson H, Loken L, Wessberg J (2007) Discriminative touch and emotional touch. *Can J ExpPsychol* 61(3):173-183.
- McMahon G (1998) Phantom limb pain following amputation. *Paediatric Nurs* 10(6):22-25.
- Melzack R (1999) From the gate to the neuromatrix. *Pain* 82:S121-S126.
- Melzack R,Coderre TJ, Katz J, Vaccarino AL (2001) Central neuroplasticity and pathological pain. *Annals of the New York Aca Sci* 933(1):157-174.
- Merskey H, Bogduk N (1994) Classification of Chronic Pain. IASP Task Force on Taxonomy. *Classification of Chronic Pain:Description of Chronic Pain Syndromes and Definitions of Pain Terms* Seattle:IASP Press.
- Metz AE, Yau HJ, Centeno MV, Apkarian AV, Martina M (2009) Morphological and functional reorganization of rat medial prefrontal cortex in neuropathic pain. *Proc. Natl Acad. Sci. USA* 106:2423–2428.
- Michaud K, Wolfe F (2007) Comorbidities in Rheumatoid Arthritis. *Best Pract Res Clin Rheumatol* 21(5):885-906.
- Millan (1999) The induction of pain:an integrative review. *Prog Neurobiol* 57(1):1-164.
- Mima T, Nagamine T, Nakamura K, Shibasaki H (1998) Attention modulates both primary and second somatosensory cortical activities in humans:a magnetoencephalographic study. *J Neurophysiol* 80(4):2215-2221.
- Miracourt LS, Dallel R, Voisin DL (2007) Glycine inhibitory dysfunction turns touch into pain through PKCgamma interneurons. *PloS One* 2(11):e1116.
- Miracourt LS, Moisset X, Dallel R, Voisin DL (2009) Glycine inhibitory dysfunction induces a selectively dynamic, morphine-resistant, and neurokinin 1 receptor- independent mechanical allodynia. *J Neurosci* 29(8):2519-2527.

- Mountz JM, Bradley LA, Modell JG, Alexander RW, Triana-Alexander M, Aaron LA, Stewart KE, Alarcón GS, Mountz JD. (1995) Fibromyalgia in women. Abnormalities of regional cerebral blood flow in the thalamus and the caudate nucleus are associated with low pain threshold levels. *Arthritis Rheum.* 38(7):926-938.
- Mountcastle VB (1957) Modality and topographic properties of single neurons of cat's somatic sensory cortex. *J Neurophysiol* 20(4):408-434.
- Müller LJ, Pels L, Vrensen GF (1996) Ultrastructural organization of human corneal nerves. *Invest Ophthalmol Vis Sci* 37(4):476-488.
- Nagy JI, Hunt SP (1982) Fluoride-resistant acid phosphatase-containing neurones in dorsal root ganglia are separate from those containing substance P or somatostatin. *Neurosci* 7(1):89-97.
- Nakao A, Takahashi Y, Nagase M, Ikeda R, Kato F (2012) Role of capsaicin-sensitive C-fiber afferents in neuropathic pain-induced synaptic potentiation in the nociceptive amygdala. *Mol. Pain* 8:51.
- Neugebauer V, Li W (2003) Differential sensitization of amygdala neurons to afferent inputs in a model of arthritic pain. *J Neurophysiol* 89(2):716-727.
- Neumann S, Braz JM, Skinner K, Llewellyn-Smith IJ, Basbaum AI (2008) Innocuous, not noxious, input activates PKCgamma interneurons of the spinal dorsal horn via myelinated afferent fibers. *J Neurosci* 28(32):7936-7944.
- Ngezahayo A, Schachner M, Artola A (2010) Synaptic activity modulates the induction of bidirectional synaptic changes in adult mouse hippocampus. *J Neurosci* 20(7):2451-8.
- Ning L, Ma LQ, Wang ZR, Wang YW (2013) Chronic constriction injury induced long-term changes in spontaneous membrane-potential oscillations in anterior cingulate cortical neurons in vivo. *Pain Physician* 16(5):E577-89.
- Nishimori T, Sera M, Suemune S, Yoshida A, Tsuru K, Tsuiki Y, Akisaka T, Okamoto T, Dateoka Y, Shigenaga Y (1986) The distribution of muscle primary afferents from the masseter nerve to the trigeminal sensory nuclei. *Brain Res* 372(2):375-381.
- Ohara S, Anderson WS, Lawson HC, Lee HT, Lenz FA (2006) Endogenous and exogenous modulators of potentials evoked by a painful cutaneous laser (LEPs). *Acta Neurochir Suppl* 99:77-9.
- Olausson P, Jentsch JD, Taylor JR (2003) Repeated nicotine exposure enhances reward-related learning in the rat. *Neuropsychopharmacology* 28(7):1264-1271.
- Pajot J, Pelissier T, Sierralta F, Raboisson P, Dallel R (2000) Differential effects of trigeminal tractotomy on Delta- and C-fiber-mediated nociceptive responses. *Brain Res* 863(1-2):289-292.
- Panteleev S, Sokolov AY, Amelinn KV, Ignatov YD (2005) Responses of neurons in the spinal nucleus of the trigeminal nerve to electrical stimulation of the dura mater of the rat brain. *Neurosc Behav Physiol* 35(5):555-559.
- Pearson AA (1952) Role of gelatinous substance of spinal cord in conduction of pain. *A.M.A.* 68(4):515-529.

- Pereira LC, Modesto AM, Sugai R, da Mota LA (2005) Pain sensitive cerebral areas and intracranial structures revealed at fully awake craniotomies for primary intracranial tumor resection. Communication to the 11th World Congress of the IASP. Pain Program No. 1517–P20. Sydney, Australia.
- Peirs C, Williams SP, Zhao X, Walsh CE, Gedeon JY, Cagle NE, Goldring AC, Hioki H, Liu Z, Marell PS, Seal RP (2015) Dorsal Horn Circuits for Persistent Mechanical Pain. *Neuron* 87(4):797-812.
- Perl ER (1984) Pain and nociception. In: *Handbook of physiology. The nervous system, Vol 3* (Darian-Smith I, ed):915–975.
- Petrovic P, Petersson KM, Ghatan PH, Stone-Elander S, Ingvar M (2000) Pain-related cerebral activation is altered by a distracting cognitive task. *Pain* 85(1):19-30.
- Peyron R, Laurent B, Garcia-Larrea L (2000) Functional imaging of brain responses to pain: a review and meta-analysis. *Neurophysiol Clin* 30:263-88.
- Peyron R, Garcia-Larrea L, Gregoire MC, Convers P, Lavenne F, Bonnefoi F, Mauguière F, Manet L, Barral FG, Michel D, Laurent B (2000) Parietal and cingulate processing in central pain: a positron emission tomography study. *PAIN* 84:77–87.
- Peyron R, Schneider F, Faillenot I, Convers P, Barral FG, Garcia-Larrea L, Laurent B (2004) An fMRI study of cortical representation of mechanical allodynia in patients with neuropathic pain. *Neurology* 63:1838–1846.
- Pham-Dang N, Descheemaeker A, Dallel R, Artola A (2016) Activation of medullary dorsal horn γ isoform of protein kinase C interneurons is essential to the development of both static and dynamic facial mechanical allodynia. *Eur J Neurosci* 43(6):802-810.
- Ploghaus A, Tracey I, Gati JS, Clare S, Menon RS, Matthews PM, Rawlins JN (1999) Dissociating pain from its anticipation in the human brain. *Science* 284(5422):1979-1981.
- Ploner M, Schmitz F, Freund HJ, Schnitzler A (2000) Differential organization of touch and pain in human primary somatosensory cortex. *J Neurophysiol* 83(3):1770-1776.
- Pomares FB, Faillenot I, Barral FG, Peyron R (2013) The where and the when of the BOLD response to pain in the insular cortex: discussion on amplitudes and latencies. *Neuroimage* 64:466–75.
- Porro CA, Baraldi P, Pagnoni G, Serafini M, Facchin P, Maieron M, Nichelli P (2002) Does anticipation of pain affect cortical nociceptive systems? *J Neurosci* 22(8):3206-3214.
- Price DD (2000) Psychological and neural mechanisms of the affective dimension of pain. *Science* 288:1769–1772.
- Qiu S, Chen T, Koga K, Guo YY, Xu H, Song Q, Wang JJ, Descalzi G, Kaang BK, Luo JH, Zhuo M, Zhao MG (2013) An increase in synaptic NMDA receptors in the insular cortex contributes to neuropathic pain. *Sci. Signal.* 6:ra34.
- Qiu S, Zhang M, Liu Y, Guo Y, Zhao H, Song Q, Zhao M, Huganir RL, Luo J, Xu H, Zhuo M (2014) GluA1 phosphorylation contributes to postsynaptic amplification of neuropathic pain in the insular cortex. *J. Neurosci.* 34:13505–13515.

- Raboisson P, Dallel R, Woda A (1989) Responses of neurones in the ventrobasal complex of the thalamus to orofacial noxious stimulation after large trigeminal tractotomy. *Ex Brain Res.* 77(3):569-576.
- Rainville P, Duncan GH, Price DD, Carrier B, Bushnell MC (1997) Pain affect encoded in human anterior cingulate but not somatosensory cortex. *Science* 277(5328):968-971.
- Reiman EM, Lane RD, Ahern GL, Schwartz GE, Davidson RJ, Friston KJ, Yun LS, Chen K (1997) Neuroanatomical correlates of externally and internally generated human emotion. *Am J Psychiatry* 154(7):918-925.
- Rexed B (1952) The cytoarchitectonic organization of the spinal cord in the cat. *J Comp Neurol* 96(3):414-495.
- Ribeiro-Da-Silva A, Castro-Lopes JM, Coimbra A (1986) Distribution of glomeruli with fluoride-resistant acid phosphatase (FRAP)-containing terminals in the substantia gelatinosa of the rat. *Brain Res* 377(2):323-329.
- Romo R, Hernández A, Zainos A, Lemus L, Brody CD (2002) Neuronal correlates of decision-making in secondary somatosensory cortex. *Nat Neurosci* 5(11):1217-1225.
- Rózsa AJ, Beuerman RW (1982) Density and organization of free nerve endings in the corneal epithelium of the rabbit. *Pain* 14(2):105-120.
- Ruscheweyh R, Wilder-Smith O, Drdla R, Liu XG, Sandkuhler J (2011) Long-term potentiation in spinal nociceptive pathways as a novel target for pain therapy. *Mol. Pain* 7:20.
- Saab C, Willis W (2001) Nociceptive visceral stimulation modulates the activity of cerebellar Purkinje cells. *Exp Brain Res* 140(1):122-126.
- Sandkuhler J (2007) Understanding LTP in pain pathways. *Mol. Pain* 3:9.
- Sandkuhler J, Liu X (1998) Induction of long-term potentiation at spinal synapses by noxious stimulation or nerve injury. *Eur. J. Neurosci.* 10:2476–2480.
- Schepelmann K, Ebersberger A, Pawlak M, Oppmann M, Messlinger K (1999) Response properties of trigeminal brain stem neurons with input from dura mater encephali in the rat. *Neurosci* 90(2):543-554.
- Schmelz M (2001) A neural pathway for itch. *Nat Neurosci* 4(1):9-10.
- Schmelz M, Schmidt R, Bickel A, Handwerker HO, Torebjörk HE (1997) Specific C-receptors for itch in human skin. *J Neurosci* 17(20):8003-8008.
- Schmidt R, Schmelz M, Forster C, Ringkamp M, Torebjörk E, Handwerker H (1995) Novel classes of responsive and unresponsive C nociceptors in human skin. *J Neurosci*:15(1 Pt 1):333-341.
- Seal RP, Wang X, Guan Y, Raja SN, Woodbury CJ, Basbaum AI, Edwards RH (2009) Injury-induced mechanical hypersensitivity requires C-low threshold mechanoreceptors. *Nature* 462(7273):651-655.
- Seifert F, Maihöfner C (2009) Central mechanisms of experimental and chronic neuropathic pain: findings from functional imaging studies. *Cell Mol Life Sci* 66:375–390.

- Sellmeijer J, Mathis V, Hugel S, Li XH, Song Q, Chen QY, Barthas F, Lutz PE, Karatas M, Luthi A, Veinante P, Aertsen A, Barrot M, Zhuo M, Yalcin I (2018) Hyperactivity of Anterior Cingulate Cortex Areas 24a/24b Drives Chronic Pain-Induced Anxiodepressive-like Consequences. *J Neurosci* 38(12):3102-3115.
- Seminowicz DA, Laferriere AL, Millecamps M, Yu JS,Coderre TJ, Bushnell MC (2009) MRI structural brain changes associated with sensory and emotional function in a rat model of long-term neuropathic pain. *Neuroimage* 47:1007–1014.
- Sessle BJ, Greenwood LF (1976) Inputs to trigeminal brain stem neurones from facial, oral, tooth pulp and pharyngolaryngeal tissues:I. Responses to innocuous and noxious stimuli. *Brain Res* 117(2):211-226.
- Sessle BJ, Hu JW, Yu XM (1993) Brainstem. Mechanisms of referred pain and hyperalgesia in the orofacial and temporomandibular region. In:New trends in referred pain and hyperalgesia, pain research and clinical management, edited by L. Vecchiet, D. AlbeFessard and U. Lindblom. Amsterdam:59-71.
- Sessle BJ, Yao D, Nishiura H, Yoshino K, Lee JC, Martin RE, Murray GM (2005) Properties and plasticity of the primate somatosensory and motor cortex related to orofacial sensorimotor function. *Clin Exp Pharmacol Physiol* 32(1-2):109-114.
- Shen FY, Chen ZY, Zhong W, Ma LQ, Chen C, Yang ZJ, Xie WL, Wang YW (2015) Alleviation of neuropathic pain by regulating T-type calcium channels in rat anterior cingulate cortex. *Mol Pain* 11:7.
- Sherrington CS (1906) The integrative action of the nervous system. New Haven, CT:Yale University Press.
- Shigenaga Y, Sera M, Nishimori T, Suemune S, Nishimura M, Yoshida A, Tsuru K (1988) The central projection of masticatory afferent fibers to the trigeminal sensory nuclear complex and upper cervical spinal cord. *J Comp Neurol* 268(4):489-507.
- Shyu BC, Vogt BA (2009) Short-term synaptic plasticity in the nociceptive thalamic-anterior cingulate pathway. *Mol. Pain* 5, 51.
- Siegel P, Wepsic JG (1974) Alteration of nociception by stimulation of cerebellar structures in the monkey. *Physiol Behav* 13(2):p. 189-194.
- Sikes RW, Vogt BA (1992) Nociceptive neurons in area 24 of rabbit cingulate cortex. *J Neurophysiol* 68:1720-1720.
- Silverman JD, Kruger L (1988) Lectin and neuropeptide labeling of separate populations of dorsal root ganglion neurons and associated « nociceptor » thin axons in rat testis and cornea whole-mount preparations. *Somatos Res* 5(3):259-267.
- Singer T, Seymour B, O'Doherty J, Kaube H, Dolan RJ, Frith CD (2004) Empathy for pain involves the affective but not sensory components of pain. *Science* 303(5661):1157-1162.
- Snider WD, McMahon SB (1998) Tackling pain at the source:new ideas about nociceptors. *Neuron* 20(4):629-632.

- Steiner TJ, Scher AI, Stewart WF, Kolodner K, Liberman J, Lipton RB (2003) The prevalence and disability burden of adult migraine in England and their relationships to age, gender and ethnicity. *Cephalalgia* 23(7):519-527.
- Stewart WF, Lipton RB, Celentano DD, Reed ML (1992) Prevalence of migraine headache in the United States. Relation to age, income, race, and other sociodemographic factors. *JAMA* 267(1):64-69.
- Strassman A, Raymond, SA, Burstein R (1996) Sensitization of meningeal sensory neurons and the origin of headaches. *Nature* 384(6609):560-564.
- Strassman AM, Weissner W, Williams M, Ali S, Levy D (2004) Axon diameters and intradural trajectories of the dural innervation in the rat. *J Comp Neurol* 473(3):364-376.
- Svensson P, Minoshima S, Beydoun A, Morrow TJ, Casey KL (1997) Cerebral processing of acute skin and muscle pain in humans. *J Neurophysiol* 78(1):450-460.
- Talbot JD, Marrett S, Evans AC, Meyer E, Bushnell MC, Duncan GH (1991) Multiple representations of pain in human cerebral cortex. *Science* 251:1355-8.
- Tammiala-Salonen T, Hiidenkari T, Parvinen T (1993) Burning mouth in a Finnish adult population. *Community Dent Oral Epidemiol* 21(2):67-71.
- Tan LL, Pelzer P, Heidl C, Tang W, Gangadharan V, Flor H, Sprengel R, Kuner T, Kuner R (2017) A pathway from midcingulate cortex to posterior insula gates nociceptive hypersensitivity. *Nat Neurosci*. 20(11):1591-1601.
- Tracey I, Mantyh PW (2007) The cerebral signature for pain perception and its modulation. *Neuron* 55:377-91.
- Trowbridge HO, Franks M, Korostoff E, Emling R (1980) Sensory response to thermal stimulation in human teeth. *J Endodontics* 6(1):405-412.
- Vardeh D, Wang D, Costigan M, Lazarus M, Saper CB, Woolf CJ, Fitzgerald GA, Samad TA (2009) COX2 in CNS Neural Cells mediates Mechanical Inflammatory Pain Hypersensitivity in Mice. *J Clin Invest* 119(2):287-294.
- Von Korff M, Dunn KM (2008) Chronic pain reconsidered. *Pain* 138(2):267-276.
- Wang GQ, Cen C, Li C, Cao S, Wang N, Zhou Z, Liu XM, Xu Y, Tian NX, Zhang Y, Wang J, Wang LP, Wang Y (2015) Deactivation of excitatory neurons in the prelimbic cortex via Cdk5 promotes pain sensation and anxiety. *Nat Commun* 6:7660.
- Wei F, Li P, Zhuo M (1999) Loss of synaptic depression in mammalian anterior cingulate cortex after amputation. *J Neurosci* 19:9346-9354.
- Wei F, Wang GD, Kerchner GA, Kim SJ, Xu HM, Chen ZF, Zhuo M (2001) Genetic enhancement of inflammatory pain by forebrain NR2B overexpression. *Nat Neurosci*. 4(2):164-169.
- Wei F, Qiu CS, Kim SJ, Muglia L, Maas JW, Pineda VV, Xu HM, Chen ZF, Storm DR, Muglia LJ, Zhuo M (2002) Genetic elimination of behavioral sensitization in mice lacking calmodulin-stimulated adenylyl cyclases. *Neuron* 36(4):713-26.

- Wessberg J, Olausson H, Fernström KW, Vallbo AB (2003) Receptive field properties of unmyelinated tactile afferents in the human skin. *J Neurophys*, 89(3):1567-1575.
- Wicker B, Keysers C, Plailly J, Royet JP, Gallese V, Rizzolatti G (2003) Both of us disgusted in My insula: the common neural basis of seeing and feeling disgust. *Neuron* 40:655–64.
- Wik G, Fischer H, Bragée B, Finer B, Fredrikson M (1999) Functional anatomy of hypnotic analgesia: a PET study of patients with fibromyalgia. *Eur J Pain* 3(1):p. 7-12.
- Woda A, Blanc O, Voisin DL, Coste J, Molat JL, Luccarini P (2004) Bidirectional modulation of windup by NMDA receptors in the rat spinal trigeminal nucleus. *Eur J Neurosci* 19(8):2009-2016.
- Woolf CJ, Ma Q (2007) Nociceptors--Noxious Stimulus Detectors. *Neuron* 55(3):353-364.
- Wu LJ, Toyoda H, Zhao MG, Lee YS, Tang J, Ko SW, Jia YH, Shum FW, Zerbinatti CV, Bu G, Wei F, Xu TL, Muglia LJ, Chen ZF, Auberson YP, Kaang BK, Zhuo M (2005) Upregulation of forebrain NMDA NR2B receptors contributes to behavioral sensitization after inflammation. *J Neurosci*. 25(48):11107-11116.
- Xu H, Wu LJ, Wang H, Zhang X, Vadakkan KI, Kim SS, Steenland HW, Zhuo M (2008) Presynaptic and postsynaptic amplifications of neuropathic pain in the anterior cingulate cortex. *J Neurosci*. 28(29):7445-7453.
- Yang JM, Wu SN, Chen IJ (1993) Spinal adenosine modulates capsaicin-induced depressor reflex: Involvement of adenosine A2 receptor. *Gen Pharmacol* 24(4):961-970.
- Yoshino A, Okamoto Y, Onoda K, Yoshimura S, Kunisato Y, Demoto Y, Okada G, Yamawaki S (2010) Sadness enhances the experience of pain via neural activation in the anterior cingulate cortex and amygdala: an fMRI study. *Neuroimage* 50:1194–1201.
- Zhao MG, Ko SW, Wu LJ, Toyoda H, Xu H, Quan J, Li J, Jia Y, Ren M, Xu ZC, Zhuo M (2006) Enhanced presynaptic neurotransmitter release in the anterior cingulate cortex of mice with chronic pain. *J Neurosci*. 26(35):8923-8930.
- Zhuo M (2008) Cortical excitation and chronic pain. *Trends Neurosci*. 31:199–207.
- Zhuo M (2014) Long-term potentiation in the anterior cingulate cortex and chronic pain. *Philos Trans R Soc Lond B Biol Sci* 369(1633): 20130146.
- Zhuo M (2016) Contribution of synaptic plasticity in the insular cortex to chronic pain. *Neuroscience* 338:220-229.

Abstract

Chronic neuropathic or inflammatory pain is believed to result from long-lasting synaptic and neuronal changes in pain pathways, including the primary somatosensory cortex (S1) which codes for pain intensity and location. Using *ex vivo* electrophysiological recordings from S1 layer 2/3 pyramidal neurons, we investigated pain-induced plasticity in a rat model (CFA injection) of chronic facial inflammatory pain.

We first establish the relation in basal conditions between synaptic activity and (i) bidirectional synaptic plasticity (long-term depression/potential; LTD/LTP), (ii) changes in the ability to express synaptic plasticity (metaplasticity), (iii) bidirectional changes in intrinsic neuronal excitability (LTP/LTD-IE); i.e. the rules for synaptic and intrinsic plasticity in S1 layer 2/3 pyramidal neurons.

We then investigated such plasticity processes in CFA-treated rats exhibiting facial mechanical allodynia, at 1 hour and 3 days post-injection. At 1-hour, mechanical allodynia is associated with (i) LTP of excitatory synaptic transmission, together with (ii) an inhibition to generate further LTP but a facilitation to generate LTD (metaplasticity), consistent with LTP of synaptic transmission, (iii) LTP-IE and (iv) reduced dendritic arbor complexity of S1 layer 2/3 pyramidal neurons. At 3 days, LTP and LTP-IE were still present but metaplasticity and dendritic arbor complexity had returned to control levels.

Résumé

La douleur chronique, neuropathique ou inflammatoire, résulterait de changements durables synaptiques et neuronaux dans les voies de la douleur dont le cortex somatosensoriel primaire (S1). Utilisant des enregistrements électrophysiologiques *ex vivo* de neurones pyramidaux des couches 2/3 de S1, nous avons étudié la plasticité induite dans un modèle de douleur inflammatoire chronique de la face chez le rat (injection de CFA).

Nous établissons d'abord la relation, dans les conditions normales, entre activité synaptique et (i) plasticité synaptique bidirectionnelle (long-term depression/potentiation ; LTD/LTP), (ii) changements dans la capacité d'exprimer une plasticité synaptique (méta-plasticité), (iii) changements bidirectionnels de l'excitabilité neuronale intrinsèque (LTP/LTD-IE) ; soit les règles de plasticité synaptique et intrinsèque de ces neurones.

Nous étudions alors ces plasticités chez des rats exprimant une allodynie mécanique faciale, 1 heure et 3 jours après l'injection de CFA. A 1 heure, l'allodynie mécanique est associée à (i) une LTP de la transmission synaptique excitatrice, combinée à (ii) une inhibition de l'induction de la LTP/facilitation de l'induction de la LTD (méta-plasticité), consistants avec la LTP, (iii) une LTP-IE et (iv) une réduction de la complexité de l'arbre dendritique de ces neurones. A 3 jours, LTP and LTP-IE sont toujours présentes mais méta-plasticité et complexité de l'arbre dendritique sont retournées à l'état basal.